Spring 1-1-2012

A Geochemical Characterization of Putative Biosignatures in Subseafloor Basalts

Emily J.K. Knowles
University of Colorado at Boulder, knowlese@colorado.edu

A GEOCHEMICAL CHARACTERIZATION OF PUTATIVE BIOSIGNATURES IN SUBSEAFLOOR BASALTS

By

EMILY J. K. KNOWLES
B.S. Cornell University, 2002
M.S. University of Colorado, 2007

A thesis submitted to the
Faculty of the Graduate School of the
University of Colorado in partial fulfillment
of the requirement for the degree of
Doctor of Philosophy
Department of Geological Sciences
2012

This thesis entitled:

A Geochemical Characterization of Putative Biosignatures in Subseafloor Basalts

written by

Emily J. K. Knowles

has been approved for the Department of Geological Sciences

_____

(Alexis S. Templeton, Thesis Advisor)

_____

(Hubert Staudigel, Committee Member)

_____

(Tom McCollom, Committee Member)

_____

(G. Lang Farmer, Committee Member)

Date_____

The final copy of this thesis has been examined by the signatories, and we find that both the content and the form meet acceptable presentation standards of scholarly work in the above mentioned discipline.

ABSTRACT

Emily J. K Knowles (Ph.D., Geological Sciences)

A Geochemical Characterization of Putative Biosignatures in Subseafloor Basalts

Thesis Directed by Associate Professor Alexis Templeton

The discoveries of tubular alteration features of potential biological origin in subseafloor basalt glasses, ophiolites, and ancient greenstones has important implications for increasing our understanding of global biogeochemical cycling in hard-rock systems and the evolution of life on Earth, and for exploring other planets for signs of life. Given the technological challenges in accessing the modern subseafloor and the possibility that it could take thousands of years to form these features, at this point it is not possible to observe their formation *in-situ*, nor have they been successfully modeled in the lab. Thus, we must infer the formation and preservation mechanisms of these putative biosignatures from physical and chemical clues. We have used a number of micro-analytical techniques to geochemically characterize these features at the submicron scale.

Using focused ion beam milling we prepared ultra-thin cross-sections of the tubules, which enabled high-resolution imaging and chemical analyses by transmission electron microscopy and electron-dispersive spectroscopy. These analyses revealed leached rims around the tubule margins, and partially crystalline Fe-bearing phyllosilicates infilling the tubules. In addition, we combined four different high-resolution synchrotron-based techniques, including X-ray fluorescence microprobe mapping, micro-diffraction, and absorption spectroscopy to determine the distribution and speciation of key major and trace elements. These studies revealed

consistent patterns of Ca, Mg, Ti, Fe, Mn, S, and P distributions, metal oxidation, and authigenic precipitation of secondary phases, as well as identified possible biominerals and organic material. Put together, these results have provided insight into the processes involved in tubular alteration and mineralization. The formation mechanism involves initial incongruent dissolution of the glass potentially accompanied by the authigenic precipitation of biominerals, specifically Fe-oxides and sulfate. Successive stages of fluid flow then infill the tubules with a variety of Fe- and Ti-rich minerals, with concomitant partial to complete oxidation of the redox active elements. The consistency of these results across a 100Ma suite of subseafloor samples and one ophiolite sample implies that the alteration and mineralization patterns are consistent spatially and temporally. These results also add significant evidence to the argument for the biological formation of the tubules by revealing potential signs of microbial geochemical processing.

DEDICATION

This work is dedicated to my mother, who encouraged me to always keep an open mind and instilled in me a deep appreciation and respect for the natural world. Not only did she help teach me how to question and how to think, but she also helped spark my passion for science, for which I am incredibly grateful.

CONTENTS

LIST OF TABLES

LIST OF FIGURES

CHAPTER 1

Introduction

1.1 The Subseafloor Biome and its Importance for Life on Earth and Elsewhere

The discovery of subsurface chemolithoautotrophic microorganisms fundamentally changed our understanding of planetary habitability. It was previously thought that all life on Earth ultimately derived its energy from the Sun, either directly through photosynthesis, or indirectly through the dependence on photosynthate. Even the ecological communities found in deep-sea sediments (e.g.; Parkes *et al*., 1994; Newberry *et al*., 2004; Fry *et al*., 2008) and oil reservoirs (e.g. Pederson, 1993, Stetter *et al*., 1993; Aitken *et al*., 2004) are driven by organic matter that was originally formed by surface phototrophs. The fact that microbes can live in the deep subsurface completely isolated from surface biological processes was the first real confirmation that there are metabolisms on Earth that can carry out primary production in the dark, which represented a paradigm shift in our understanding of the energetic basis of life on Earth (Gold, 1992; Pedersen, 1993; Steven and McKinley, 1995; Shock, 1997; Stevens, 1997; Edwards *et al*., 2005). Many hydrothermal vent ecosystems have now been explored in some detail, which has led to a general understanding of the primary metabolic processes operating in these systems (e.g. Lutz and Kennish, 1993; Jeanthon 2000; Luther *et al.*, 2001; Orcutt *et al*., 2011, and references therein). However, away from the relatively high-energy environments of the vents, beneath the cold ridge flanks and open seafloor, the microbial abundances and modes of living are more mysterious.

The open seafloor and subseafloor were once thought to be biological "deserts", virtually devoid of life. Over the past couple of decades it has become clear that these environments are not only viable habitats for microorganisms, but may in fact harbor a huge number of cells. (e.g. Bach and Edwards, 2003; Santelli *et al*., 2008; Orcutt *et al*., 2011; Edwards *et al*., 2012; Ménez *et al*., 2012). For example, Bach and Edwards (2003) calculated that the potential biomass

produced by a number of different possible chemolithoautotrophic metabolic processes in the subseafloor is on the order of $1x10^{12}$ g C/yr, which is comparable to the anaerobic oxidation of organic matter in some heterotrophic systems. There is additional evidence that this basalt-hosted niche may have been occupied by microorganisms globally for close to the entire history of life on Earth (Banerjee *et al*., 2006a; Staudigel *et al*., 2008; Fliegel *et al*., 2010a). However, due to numerous technical and scientific difficulties, including access to the subsurface, contamination in drilling, low cell numbers, and poor culturability, it has been challenging to get a clear understanding of who lives deep in the subsurface and how they make their living (e.g. Santelli *et al*., 2010). Most of our information about subseafloor biome is based on a limited number of measurements, potential seafloor analogs, and a theoretical evaluation of the likely metabolic processes.

One of the key clues that there is likely a prolific subseafloor biosphere is in the form of physical and chemical basalt glass alteration. The most conspicuous and abundant putative bioalteration features fit into two main categories: granular alteration and micron-scale tubules. Granular alteration is a general term for the irregular spheroidal microborings lining cracks in fresh glass, and tubular alteration describes the micron-sized channels extending asymmetrically from cracks into fresh glass. These features have been found in drill core samples from numerous ages and locations worldwide (e.g. Thorseth *et al*., 1992; Fisk *et al*., 1998; Furnes *et al*., 2001a,b, 2004; Staudigel *et al.,* 2008; Walton, 2008). Alteration features similar to those found in subseafloor drill cores have also been identified in ophiolites and greenstone belts with preserved glassy margins from numerous locations worldwide. It appears that as long as the tubules are infilled with minerals their morphologies can be preserved over millions to billions of years in the glassy margins of subseafloor basalts that have been obducted and only undergone low-grade

metamorphism. U-Pb isotopic dating of the ancient features in a few cases has shown that the biosignatures are nearly as old as the rocks themselves, the oldest dating back to ~3.5 Ga (Banerjee *et al*., 2006b, 2007; Fliegel *et al*., 2010a), which puts them amongst the oldest signs of life on Earth.

The possibility that these features are indeed biosignatures has exciting implications for the evolution of life on Earth and exploring other planets for signs of life, as well as for increasing our understanding of global geochemical cycling. If the tubules in the ancient ophiolites and greenstones were in fact formed by life then it means that the subseafloor endolithic niche has been occupied since the very earliest days of life on Earth. It is even possible that life on Earth could have originated in the subseafloor (e.g. Baross and Hoffman, 1985; Rasmussen, 2000; Summit and Baross, 2001), which may have provided a refuge from meteorite impacts and the resulting habitat instability on the surface (e.g. Maher and Stevenson, 1988; Sleep and Zahnle, 1998; Abramov and Mojzsis, 2009). In addition, it's possible that similar features could be found in the glassy margins of basalts on other planets, particularly Mars. This idea has recently gained considerable attention with the discovery of alteration features in the Martian Nakhla meteorite that are very similar to those of putative microbial origin in Earth basalts (McKay *et al*., 2006; McLoughlin *et al*., 2007).

Mars is the most Earth-like body in solar system. There is abundant evidence from Martian meteorites and orbital and surface observations that at some point in Martian history there was abundant liquid water on the surface. There is also substantial evidence for current water ice at the poles and in the shallow subsurface. This makes a strong case for abundant water ice, or even liquid water reservoirs deeper in the subsurface of Mars, in contact with basaltic bedrock or mantle (Squyers *et al*., 2004; Herkenhoff *et al*., 2004; Haskin *et al*, 2005; Poulet *et*

al., 2005; McEwen *et al*., 2007; Fairén, 2010). It's also likely that there is dissolved inorganic, or even organic carbon available. Even though the Martian atmosphere is much thinner than Earth's, it's composed of 95% carbon dioxide, and was likely much thicker in the past. Fluid flow in the subsurface would have lead to the formation of abundant carbonate minerals, and possibly complex organic compounds (Griffith and Shock, 1997; Shock, 1997). Therefore, the subsurface of Mars contains not only plenty of carbon for biosynthesis, but possibly even an organic energy source. Additional energy sources are available in the basaltic subsurface rocks, which are very similar to Earth mid-ocean ridge basalt (MORB) (Fisk and Giovannoni, 1999).

Given the hostile conditions on the surface of Mars today it is likely that any potential extant life would be limited to the subsurface or near-subsurface. It is also likely that if there were past life on Mars it would have occupied the endolithic niche at some point in its evolution, or possibly originated there (Boston *et al*., 1992; Shock, 1997; Stevens, 1997; Brack, 1999; Fisk and Giovannoni, 1999; Wierzchos and Ascaso, 2002; Banerjee *et al*., 2004, Fisk *et al*., 2006). The present Martian atmosphere has a very low oxygen content ($fO_2 \approx 10^{-5}$), however, geochemical calculations have shown that hypothetically even these low levels could potentially support aerobic chemolithoautotrophic metabolisms in locations where water interacts with minerals in low-temperature near-surface environments (Link *et al*., 2005). In other environments within the subsurface of Mars there are numerous different possible energy sources for anaerobic chemolithotrophs (e.g. Boston *et al*., 1992) or possibly anaerobic chemoorganotrophs.

The potential of a vast subseafloor biosphere intimately associated with the alteration of basalts also has important implications for global geochemistry. The fact that these features have been found in young to very old basalts from around the world indicates that the microbial

alteration of subseafloor basalts is a broadly underappreciated process, which likely has large-scale effects on geochemical cycling. Numerous laboratory and environmental studies have shown that microbial alteration of basalt glass enhances both the rate of dissolution and extent of element exchange with seawater (e.g. Staudigel *et al*., 1995, 1998; Thorseth *et al*., 1995; Bennett *et al*., 2001; Bach and Edwards, 2003). In addition, microbial alteration has been shown to produce different morphological, chemical, and mineralogical alteration products than abiotic processes (e.g. Thorseth *et al*., 1992; Staudigel *et al*., 1998; Alt and Mata, 2000; Daughney *et al*., 2004; Storrie-Lombardi and Fisk, 2004; Kruber *et al*., 2008). For example, in a laboratory experiment using a closed-loop flow-through reactor with both synthetic and natural glass grains and polished slabs, Staudigel *et al*., (1998) demonstrated that in the biotic systems alteration of the glass was significantly accelerated, producing twice the mass of secondary phases, and increasing the dissolution of Sr from the glass into seawater by a factor of 20-40 compared to the abiotic controls. These findings emphasize the importance of increasing our understanding of the microbial alteration of subseafloor basalts. The global effect on element exchange could be enormous, which would change our understanding of the recycling of elements throughout Earth history.

1.2 Microbial Alteration Features

1.2.1 *Summary of the Cumulative Evidence for Biogenicity*

Previous studies of tubular and granular alteration features in subseafloor basalts and ophiolites have provided a number of different pieces of evidence that researchers have cited for calling the features biological. First recognized, and also the most noticeable, are the physical

and morphological characteristics. The features always originate along fractures and extend asymmetrically into fresh glass regions (e.g. Furnes *et al*., 2004; Staudigel *et al*., 2008; see Figures 1, A1, B1, and B3). This implies a means of introducing microbial cells into the system via the fluids that flow through the cracks. The structures all approximately fit the appropriate size ranges, shapes, and organizational characteristics to have been produced by the boring and metabolic activities of microbial endoliths. The tubules tend to range in diameter from about 0.5 to 20 μm, and extend tens to a few hundred microns. They occur with a variety of different structural characteristics, ranging from tapered tubules, often with one or more branches, to tubules with septate divisions, and even occasionally helical structures (Thorseth *et al*., 1995; Fisk *et al*., 1998; Furnes *et al*., 2001b, 2004; Walton, 2008; McLoughlin *et al.*, 2009). In addition, the tubules are not randomly oriented, they tend to avoid plagioclase crystals and extend towards olivine (e.g. Walton, 2008), which may be used for energy or nutrient extraction.

No intact cells have yet been identified in or extracted from the bioalteration features, but there have been several objects identified in the tubules that could be remnant microbial cells. They appear roughly spheroidal and tend to be a few microns in diameter, representative of typical cell sizes for bacteria and archaea. Additional evidence that these structures are microbial in origin come from fluorescent staining tests. In several different cases the nucleic acid stains DAPI and ethidium bromide have shown putative DNA within the spherical bodies, around granular textures, and at the tips of tubules (Thorseth *et al*., 1995; Torsvik *et al*., 1998; Banerjee and Muehlenbachs, 2003). Chemical and isotopic analyses of the microbial alteration features also support their biological origins. Studies using conventional electron microprobe element mapping have shown elevated levels of carbon, nitrogen, phosphorus, and potassium within the channels relative to the surrounding glass, suggesting the presence of cellular remnants (Fisk *et*

al., 1998; Torsvik *et al*., 1998; Furnes *et al*, 2001c, 2004; Banerjee and Muehlenbachs, 2003). In addition, several different studies have shown that the carbon deposits within the bioalteration zones of basalt glass samples have low isotopic $\delta^{13}C$ values compared to carbonate in the rock interior, indicating biological fractionation (Thorseth *et al*., 1995; Torsvik *et al*., 1998; Furnes *et al*., 2001a, 2004).

1.2.2 *Potential Analogs and Proposed Model*

There are numerous examples of pits and tunnels formed by the boring and metabolic activities of endolithic microorganisms, primarily fungi and cyanobacteria, in clays, carbonate rocks, and even some silicate minerals, sometimes leading to trace fossil formation (e.g. Jongmans *et al.*, 1997; Golubic *et al.*, 2005; Smits, 2006; Cockell and Herrera, 2008). The boring activities of microbes in these various environments, especially the examples of fungi excavating tunnels in silicate minerals, provide the best analogs for the proposed mechanism of tubular and granular bioalteration in subseafloor basalt glass. Theoretically, similar processes could be carried out by any microorganism that forms filament, pilus, nanowire, or other appendage. One general model proposed for the bioalteration mechanisms that could produce tubular and granular alteration features in subseafloor basalt glass is shown in Figure 1 (Staudigel *et al.*, 2008). At this point in time technological and practical limitations have prevented either the *in situ* observations or laboratory testing necessary to either confirm or reject this model.

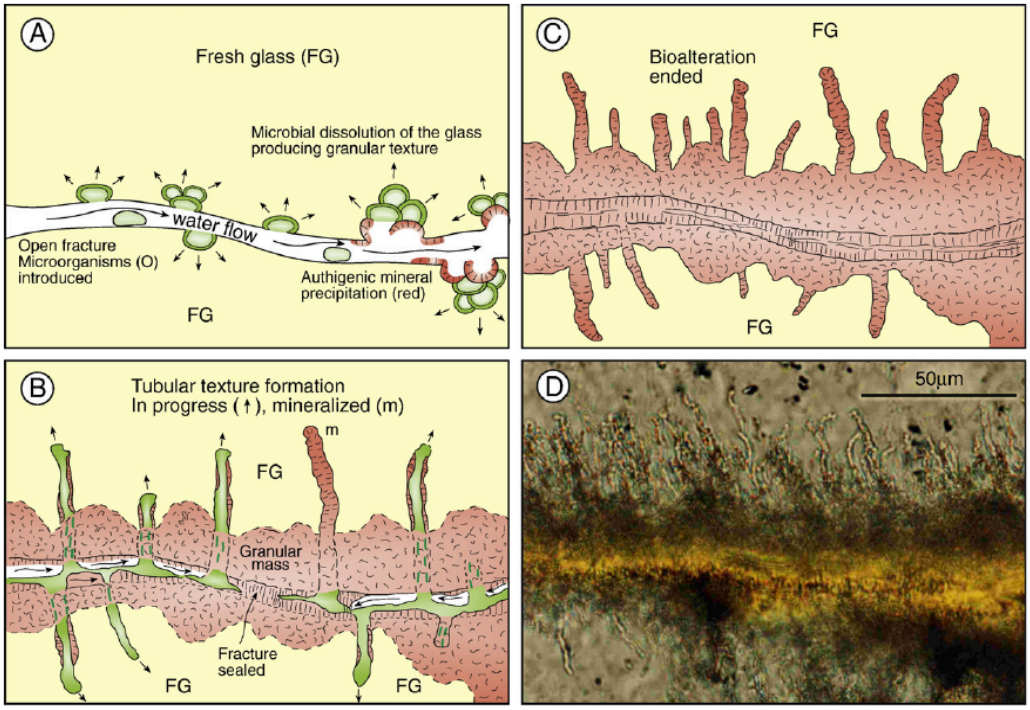

Figure 1. One model of the bioalteration process proposed by Staudigel *et al.* (2008). (A) Microbial cells colonize fresh glass surfaces and begin dissolving the matrix to produce granules. (B) Authigenic mineral deposition limits diffusion of materials to and from cells, promoting the extension of hyphal-like filaments deeper into the glass. (C) When the features are completely mineralized all biotic process cease. (D) Photomicrograph of granular and tubular alteration features in a drill core sample (396B-20R-4).

Interestingly, granular and tubular alteration features have only been found in subseafloor basalt glasses and ophiolites, and not in glasses of the same composition that are subaerial or in freshwater systems. In a study of a drill core from the Hilina Slope on the flank of Mauna Kea, Hawaii, Walton *et al*. (2008) report that they observed no alteration features in the subaerial and freshwater sections of the core, but in the submarine section the alteration features were abundant. In a separate study, Cousins *et al*. (2009) showed that tubules were abundant in the glassy margins of basalt that erupted subglacially in James Ross Island Volcanic Group in the northern Antarctic Peninsula region, but again only in the submarine sections. Few to no bioalteration features were found in the sections that had been permeated by only fresh glacial

meltwater. These observations imply that there are particular physical and chemical parameters that control the formation of bioalteration features in basalt glass, which are specific to marine conditions. At this point these parameters are poorly understood, as it is technologically difficult to constrain the fluid chemistry in the subseafloor. Continued investigations will help to increase our understanding of not only the subseafloor fluid chemistry, but also potentially provide valuable insights into the microbiology and metabolic processes operating deep in the oceanic volcanic layers.

1.3 Abiotic Basalt Alteration

Over the past several decades a number of bulk investigations have been carried out of the alteration of natural basalt samples of different ages and from numerous geographic locations (e.g. Staudigel and Hart, 1983; Furnes, 1984; Thorseth *et al*., 1991; Stroncik and Schmincke, 2001; Walton and Schiffman, 2003), as well as experimental studies of the alteration of synthetic glasses (Crovisier *et al*., 1987). These studies have provided a large amount of data and observations that have helped to paint a picture of the general process of alteration, but it has also become clear that there are many possible different alteration courses and outcomes depending on a number of factors, namely the physical and chemical characteristics of both the rock and the seawater. One general trend in the alteration process is the hydration of the glass causing dissolution and eventually replacement of the parent basalt with palagonite and secondary phases. There are several intermediates in the process of palagonization that tend to be variable in timing and extent. Incipient alteration includes dissolution, fracturing, mechanical reduction of porosity, and initial growth of authigenic minerals in pore spaces. These precipitated phases

include clays (primarily smectites, illite, and celadonite) and zeolites, commonly phillipsite and chabazite (Walton *et al*., 2005; Schramm *et al.*, 2005). This stage is followed by increased deposition of these pore-filling phases as cements in vesicles, fractures, and inter-granular spaces. The final stage is the replacement at the margins of parent minerals by palagonite and additional reductions in porosity by cementation (Walton and Schiffman, 2003). Abiotic basalt alteration tends to produce smooth alteration fronts with a sharp contact between the palagonite and any remaining fresh glass (Figure 2), in contrast to the irregular, asymmetrical nature of bioalteration features (see Figures 1, A1, B1, and B3).

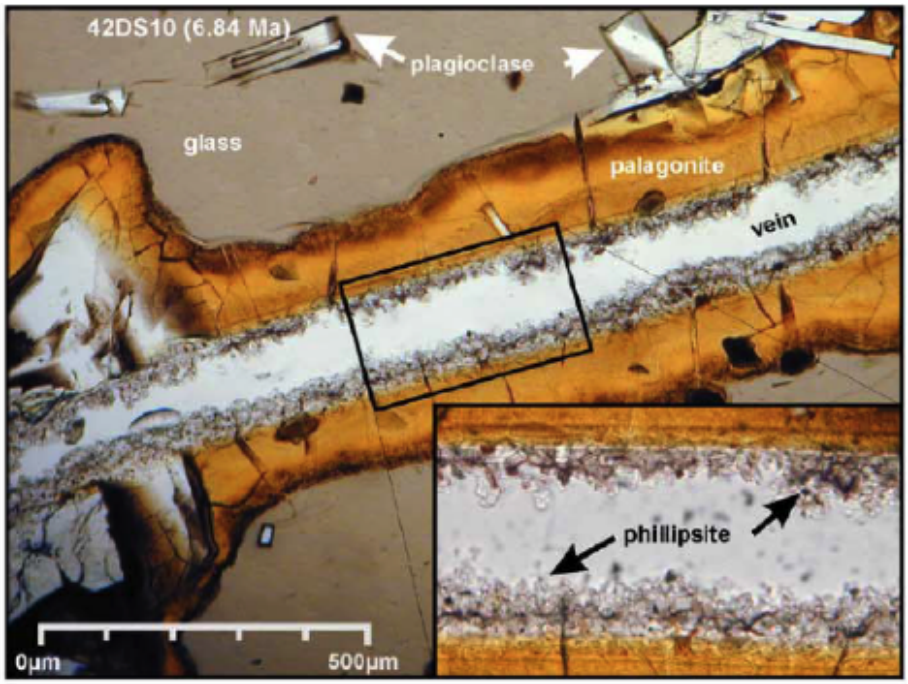

Figure 2. Photomicrograph of a thin section of altered basalt glass from the East Pacific Rise. A smooth, symmetrical palagonite rim surrounds a vein through which seawater once flowed. The inside of the vein is lined with phillipsite. (Modified from Schramm *et al*., 2005)

As dissolution of basalt glass progresses there tends to be a significant depletion of most major elements, e.g. Si, Al, Mg, Mn, Ca, Na, and P, with replacement by H_2O, CO_2 and K_2O (Staudigel and Hart, 1983; Stroncik and Schmincke, 2001; Walton *et al.*, 2005; Schramm *et al.*, 2005). The only major elements that are generally immobile are Fe, which is fully retained, and Ti, which is enriched in the palagonite. Many of the elements mobilized are re-deposited in secondary phases, primarily zeolites and smectites. The mobility of trace elements during abiotic glass alteration is not as clearly understood as the major elements. In most cases it appears that Rb, Cs, Ba, and U are taken up from seawater and incorporated in secondary minerals, similar to K (Schramm *et al*., 2005). There is also an exchange of Sr during palagonite formation: isotopic data show that a significant fraction of the basalt Sr is dissolved, while about half of that amount is replaced by seawater Sr (Staudigel and Hart, 1983). The mobility of many other trace elements varies from strong enrichments to strong depletions depending on a number of physical and chemical conditions and the secondary phases formed (Stroncik and Schmincke, 2001).

1.4 Biological Mechanisms of Silicate Mineral Dissolution

1.4.1 *Inorganic Acids*

One of the most important abiotic control on the low temperature solubility of silicate minerals is pH. Rates of mineral dissolution are lowest, and essentially independent of pH, in the circumneutral range, about 5-8. A strong change in pH of solution away from neutrality promotes proton or hydroxyl ion attack (respectively) of oxygen sites on the mineral surface. This causes the bond between the oxygen atoms and metals in the silicate matrix to become weaker, thereby increasing the rate of dissolution of the metals (Blum and Lasaga, 1988; Drever,

1994; Barker *et al.*, 1997, 1998). The most common and abundant inorganic acid in most environmental systems is carbonic acid, formed by the dissolution of CO_2 in water:

$$CO_2 + H_2O \leftrightarrow H_2CO_3$$

Carbonic acid is a weak acid; when in equilibrium with atmospheric CO_2 the pH of water only decreases to around 5.7. Acids in this pH range do not significantly enhance rates of mineral dissolution, and thus in equilibrium conditions, such as in rain or runoff, carbonic acid has little effect. The concentrations of CO_2 can be increased by orders of magnitude above atmospheric levels in pore spaces in soils and sediments where there are high levels of respiration by microorganisms and plant roots. Even these elevated concentrations of carbonic acid, however, rarely lower the pH of natural waters to below around 4.5 (Barker *et al.*, 1997), which is just about the acidity where rates of dissolution for most minerals become pH-dependent (Drever, 1994).

There are a few stronger biogenic inorganic acids that will have a more pronounced effect on mineral weathering, namely sulfuric acid and nitric acid. The main biological reaction that produces sulfuric acid is the oxidation of reduced sulfur compounds by chemolithotrophic microorganisms. Nitric acid is produced by the oxidation of reduced nitrogen compounds, such as the conversion of ammonia to nitrate by nitrifying bacteria. Sulfuric and nitric acid are both strong acids, which means that they can significantly acidify pore waters, enhancing the rate of silicate mineral dissolution far above that of carbonic acid (Sand and Bock, 1991). However, these effects also tend to be localized to small microenvironments, for example in the immediate

vicinity of the sulfate reducing or nitrifying bacteria, unlike the widespread distribution of carbonic acid in many aqueous environments.

1.4.2 *Organic Ligands*

There is abundant evidence to show that organic ligands are one of the primary biological mechanisms of silicate mineral alteration. The breakdown of larger organic molecules, chiefly by microbial fermentation, produces a number of soluble, low molecular weight organic acids, including α-ketoglutarate, acetate, citrate, formate, lactate, oxalate, propionate, pyruvate, and succinate (Welch and Ullman, 1993). While all of these acids have an effect on silicate weathering, Welch and Ullman showed that the most significant impact on plagioclase dissolution was from the polyfunctional acids oxalate, citrate, pyruvate, succinate, and 2-ketoglutarate (1993). In fact, these compounds promoted dissolution at a rate up to ten times the rate of dissolution caused inorganic acids in solutions of the same pH, and several orders of magnitude greater than the rate of dissolution in controls.

The concentration of organic ligands in environmental systems depends on the initial amount of larger organic materials, and the rates of decomposition and consumption. In any system there will be a tradeoff between the amount of low molecular weight organics produced via fermentation and consumption via respiration, with the rate of turnover being controlled by a number of environmental and biological factors. Since the rate of fermentation is directly related to the concentration of oxygen and composition and amount of organic matter present, uncontaminated groundwaters that are oxygenated tend to have very low organic acid concentrations, usually measured at a few to few tens micromolar. Organic acid concentrations

in marine sediments tend to be significantly higher than in freshwater systems, on the order of micromolar to millimolar (Sansone, 1986).

There are several different mechanisms by which organic ligands enhance mineral dissolution. First, like inorganic acids, organic acids decrease solution pH, which promotes proton attack of oxygen sites on the mineral surface. This causes the bond between the oxygen molecules and metals in the silicate matrix to become weaker, thereby increasing the rate of dissolution of the metals. In general, the rate of hydrolysis of the mineral surface controls the rate of this dissolution reaction, and thus the stronger the acid, the greater the effect. Organic ligands tend to be weak acids, but their production of protons is sufficient to effectively attack the metal-oxygen bonds and catalyze dissolution (Welch and Ullman, 1993; Barker *et al.*, 1997). Organic acids also form complexes with metals on exposed surfaces of minerals, which has a similar effect as proton attack in that it weakens the cation-oxygen bonds and promotes mineral dissolution. For example, in feldspars the rate-limiting step in dissolution is the breakdown of the aluminosilicate framework and dissolution of the Si and Al ions into solution, thus the complexing of these ions with organic acids significantly increases the rate of feldspar weathering (Lundström and Öhman, 1990; Welch and Ullman, 1993).

In addition, organic acids stimulate mineral dissolution by forming complexes with ions in solution. Schott *et al*. (2009, and references therein) have demonstrated that the solubility of minerals depends in part on the apparent saturation of metal species in the surrounding solution; when there are high concentrations of ions near the mineral surface, solubility is inhibited. Organic acids have the tendency to complex with metal ions in solution, thus lowering the saturation state and increasing rates of dissolution reactions. This effect is most pronounced

when the dissolution reactions are close to equilibrium with respect to the solution (Welch and Ullman, 1993).

Organic acids have even been shown to significantly promote the dissolution of quartz. Multiple studies have reported etch pits formed on the surfaces of quartz grains after prolonged contact with organic ligands (e.g. Bennett and Siegel, 1987; McMahon *et al.*, 1995). Quartz is very stable at low temperatures and resistant to chemical weathering, even at very low pH (~2), thus weak inorganic acids have no effect. Low molecular weight organic ligands, on the other hand, have been implicated in significantly increasing quartz weathering rates, most likely by the complexing of silica molecules (Bennett and Siegel, 1987; McMahon *et al.*, 1995). The production of organic ligands in order to promote the extraction of silica from quartz may be actively driven by the need for silica as an essential nutrient for many microorganisms, including diatoms and radiolarians for precipitation of their siliceous tests (Barker *et al.*, 1997).

One organic ligand that has been studied extensively for its effects on silicate mineral dissolution is oxalate. In natural systems, oxalate is often one of the most abundant organic ligands in solution, occasionally even reaching high enough concentrations to precipitate as oxalate salts (Johnston and Vestal, 1993). There have been many laboratory studies that have shown much higher levels of release of major ions in the presence of oxalate than in controls. These effects have been shown on plagioclase feldspars, quartz, and olivine, which implies that oxalate can bind Al, Si, Fe, and Mg (Barker *et al.*, 1997). Whether the effect of oxalate is more pronounced by increasing acidity or by acting as ligand remains unclear.

1.4.3 *Direct Effects*

In addition to the numerous indirect effects that the excretion of extracellular polysaccharides and metabolic products can have on silicate mineral dissolution, microorganisms can directly attack the surfaces of minerals by electron transfer mechanisms. Microbes are faced with a problem when using solid phase ions in minerals for electron exchange, namely the difficulty of physically transferring the electrons between mineral surfaces and the enzymes in the membrane-bound electron transport chain. The attachment of microorganisms to mineral surfaces involves initial reversible adsorption followed by irreversible attachment via extracellular polysaccharides and pili (Barker *et al.*, 1997), which essentially binds the cells very close to the surface. However, electron transfer requires more than close proximity to the donor or acceptor, there must be a mechanism of exchange between molecules of different redox potential while still maintaining charge balance. For this reason, metabolic reactions tend to be catalyzed by enzymes located either in the cytoplasm or embedded in cell membranes, where redox cascades can be created and controlled by enzyme pathways; thus, most electron donors and acceptors are transported into the cell. It is clear, however, that many different chemolithotrophic microorganisms are able to "breathe minerals" (e.g. Hernandez and Newman, 2001; Nealson *et al*., 2002), or directly use ions on solid minerals surfaces as either electron donors or acceptors.

Of particular interest is the microbial redox cycling of solid Fe and Mn in minerals, which have been studied extensively (e.g. Lovley, 1991; Nealson and Saffarini, 1994; Lovely and Chapelle, 1995; Hernandez and Newman, 2001; Nealson *et al*., 2002; Bach and Edwards, 2003; Tebo *et al*., 2004). These transition metals are abundant in the Earth and are easily converted between stable reduced (Fe^{2+} and Mn^{2+}) and oxidized forms (Fe^{3+} and Mn^{4+}) at

ambient pressures and temperatures, making them easy targets for microbial metabolic use and important players in several different biogeochemical cycles (e.g. Nealson and Saffarini, 1994). At circumneutral pHs only the reduced forms of these metals are soluble, in the oxidized form Fe- and Mn-oxide minerals rapidly precipitate. Thus, microorganisms that use Fe^{3+} and Mn^{4+} as electron acceptors must be capable of either solubilizing the oxidized metals or transferring electrons directly to the solid mineral surfaces. This first mechanism is fairly well understood. A number of different iron-reducers, such as the anaerobic bacterium *Geobacter metallireducens*, have been shown to produce specialized chelators and siderophores. Both of these molecules work by complexing and solubilizing Fe^{3+}, making it more available to the cell (Neilands, 1995). Exogenous chelators, such as humic substances, are produced by the degradation of organic matter, whereas siderophores are chelators that are made endogenously by the microorganisms. Siderophores are typically produced in large numbers and have very high affinity for iron, which has important implications for mineral dissolution. The ability of siderophores to bind strongly to iron-bearing minerals means that they can significantly enhance mineral dissolution rates (Watteau and Berthelin, 1994; Hersman *et al.*, 1996).

The use of chelators to solubilize and immobilize an electron acceptor is one solution for iron-reducing microorganisms, but in other lithotrophic metabolisms and for many iron-reducers, electrons must be transferred directly between cells and solid mineral substrates. To date, there are several known mechanisms of external electron transfer, but there are many unanswered questions and this remains an active area of research. A few of the better-studied transfer mechanisms include external electron shuttles (e.g. Newman and Kolter, 2000; Hernandez and Newman, 2001), outer-membrane proteins (e.g. Magnuson *et al*., 2000; Hernandez and Newman, 2001), and direct contact via pili or electrically conductive nanowires (Gorby *et al.*, 2006). The

effects of direct biological electron transfer mechanisms on silicate mineral weathering are less well understood, but it can be assumed that the oxidation and reduction of ions on mineral surfaces acts to weaken bonds within the structural framework, thus leading to higher rates of dissolution.

1.5 The Subseafloor Biome

1.5.1 *Subseafloor Metabolic Processes*

All life on Earth takes advantage of redox disequilibrium to fuel metabolism. Chemolithotrophs take advantage of inorganic sources of redox couples, such as directly from minerals. The highest energy environments for these organisms are those unique locations where strongly oxidizing molecules or elements and strongly reducing ones are both found, such as around hydrothermal vents. The vents are abundant sources of electron donors, such as Fe^{2+}, Mn^{2+}, H_2S, S^0, H_2, and CH_4, and the surrounding oxidized seawater is essentially an infinite reservoir of electron acceptors. In these environments microorganisms take advantage of the redox disequilibrium by catalyzing reactions that are thermodynamically favorable but kinetically hindered (Shock, 1997; McCollom and Shock, 1997; McCollom, 2000). This leads to rapid and abundant microbial primary production, which builds the basis for complex and flourishing hydrothermal vent ecosystems (e.g. Grassle, 1985; Jannasch and Mottl, 1985; Lutz and Kennish, 1993; Orcutt *et al*., 2011). However, even out on the abyssal plain there are several potential forms of redox disequilibria that can be exploited by microorganisms.

It is now understood that there is deep cycling of oxidized seawater in the basement basalt of the subseafloor (e.g. D'Hondt *et al*., 2004). Since basalts are generally composed of

highly reduced minerals, the contact with oxidized seawater in fissures and pore spaces sets up strong redox gradients, which can be exploited in metabolisms. Considering that basalt is rich in reduced iron (Fe^{2+}), manganese (Mn^{2+}), and sulfide (S^{2-}, S^{1-}) minerals, the oxidation of these elements most represents the dominant chemolithoautotrophic metabolisms active in the deep subseafloor (e.g. Bach and Edwards, 2003; D'Hondt *et al.*, 2004; Edwards *et al.*, 2005; Orcutt *et al.*, 2011). The metals and sulfide are the main electron donors while oxygen from the seawater, and to a lesser extend nitrate and sulfate, are the predominant electron acceptors. The fluid-rock interactions provide an abundant source of reduced elements in this system, but without continuous active fluid flow there may be limited availability of oxidized compounds. Therefore, these metabolisms are most likely dependent on the continued cycling of oxidized seawater, and may be electron acceptor limited (Edwards *et al.*, 2005; Jørgensen and D'Hondt, 2006).

Two additional sources of electrons that play important roles in this environment hydrogen gas (H_2) and methane (CH_4), which are produced by the alteration of minerals by highly reduced seawater such as in serpentinization reactions. If molecular oxygen is available it can be directly coupled to the oxidation of hydrogen and methane with a high energetic yields. Methane and H_2 are both common products of serpentinization reactions, which are generally understood to only occur when seawater interacts with ultramafic rocks, such as peridotites (e.g. Morita, 2000; Wetzel and Shock, 2000; Sleep *et al.*, 2004; Schulte *et al.*, 2006; McCollom and Bach, 2009). The interaction of seawater or hydrothermal fluids with rocks that have higher silica contents, such as basalts, may also produce small amounts of H_2, but the concentrations tend to be at least an order of magnitude lower than in serpentinizing systems (e.g. Wetzel and Shock, 2000; McCollom and Bach, 2009). It is possible that these H_2 concentrations are still high enough to support chemolithoautotrophic communities (e.g. Chapelle *et al.*, 2002; Stevens and

McKinley, 2005). There could also be significant influx of H_2 and CH_4 from nearby ultramafic serpentinizing systems to the basalt-hosted ecological niches.

In parts of the rocks where oxygen has been depleted there are several different potential anaerobic metabolisms. These include methanogenesis and sulfate reduction, both using hydrogen gas as an electron donor, and iron oxidation, using nitrate as the electron acceptor (Edwards *et al*., 2005). Some chemolithoautotrophs have been shown to be flexible in their metabolisms, for example *Desulfitobacterium frappieri* is capable of switching back and forth between Fe oxidation and reduction depending on the conditions (Zhang *et al*., 2009). It is also possible that whole ecosystems could be built up, starting with either input of particulate organic matter or the *in situ* production of organic acids and cellular material by chemolithoautotrophic organisms. Thus, it is possible that heterotrophic organisms could also function in the basalt. In well-oxygenated areas respiration could be active, while in anaerobic micro-niches fermentative metabolisms might be functioning (Edwards *et al*., 2012b).

The amount of energy liberated from these, or any other metabolic reactions, depends on a number of factors, the most important of which are the differences in electron potential between the electron donors and acceptors, the concentrations of the products and the reactants, pH, and temperature (e.g. Hoehler, 2004). Despite the high energy yields of several of these reactions (Table 1), the availability of carbon sources and electron acceptors is likely to be limited in the subsurface, thus it is considered a low-energy environment (Hoehler, 2004; Jørgensen and D'Hondt, 2006). Most microorganisms in the subseafloor are probably doing little more than just surviving. When considering available metabolic energy in any system, three different biological states can be defined. At high energy levels, organisms are able to store sufficient energy to grow and proliferate, while at minimal metabolic energy levels, cells are just

barely able to survive, where survival is defined as only sustaining the integrity of amino acids and nucleic acids without sufficient conservation of energy for any other cellular functions. In between these two end points is the concept of maintenance energy, where cells are able to actively metabolize, harnessing just enough energy to maintain cellular integrity and basic functions but not enough to divide (Hoehler, 2004). Numerous studies have shown the continued survival of cells in energy limited systems, with the key cellular structures reaming intact, as long as there is a minimal amount of maintenance energy available (Tijhuis *et al*., 1993; Harder, 1997; Hoehler *et al*., 2001; Hoehler, 2004; Price and Sowers, 2004).

Table 1. Common metabolisms in the subseafloor and their energetic yields

Aerobic	**Reaction**	**ΔG (kJ/mol)**
Iron Oxidation	$Fe^{2+} + ¼\ O_{2(aq)} + H^+ \rightarrow Fe^{3+} + ½\ H_2O$	–65
Manganese Oxidation	$Mn^{2+} + ½\ O_{2(aq)} + H_2O \rightarrow MnO_{2(s)} + 2H^+$	–50
Sulfide oxidation	$HS^- + 2O_2 \rightarrow SO_4^{2-} + H^+$	–750
Hydrogen oxidation	$H_2 + ½\ O_2 \rightarrow H_2$	–230
Methanotrophy	$CH_4 + 2O_2 \rightarrow HCO_3^- + H^+ + H_2O$	–750
Anaerobic		
Methanogenesis	$CO_2 + 4H_2 \rightarrow CH_4 + 2H_2O$	–130
Sulfate reduction	$SO_4^{2-} + H^+ + 4H_2 \rightarrow HS^- + 4H_2O$	–170
Anaerobic iron oxidation	$10Fe^{2+} + 2NO_3^- + 12H^+ \rightarrow 10Fe^{3+} + N_2 + 6H_2O$	–100

(from Edwards *et al*., 2005)

1.5.2 *Microbial Diversity*

Most of the seafloor basalt organisms cultured or sequenced to date have been collected from young, shallow or surface rocks on the flanks of mid ocean ridges or seamounts, or from

experimental colonization studies. Many novel sequences have been identified from seafloor basalts, indicating that they represent unique populations of endemic microorganisms, probably specifically adapted to the seafloor or sub-seafloor endolithic niches (Lysnes *et al*., 2004; Templeton *et al.*, 2005; Mason *et al*., 2007, 2009; Santelli *et al.*, 2008, 2009; Orcutt *et al*., 2011). On the surfaces of seafloor basalts microbial cells tend to be found in the form of biofilms and are clearly associated with the alteration rinds. In fact, Santelli *et al.* found that the diversity of abundance of bacteria on seafloor basalts positively correlates with the amount of alteration (2009). Phylogenetic studies of seafloor bacterial communities have shown that the dominant phyla are *Alpha*- and *Gammaproteobacteria*, with common occurrences of *Actinobacteria*, *Bacteroidetes*, *Chloroflexi*, *Firmicutes*, and *Planctomycetes* (Orcutt *et al*., 2011 and references therein).

Less is known about present or past endolithic communities in deep basalts, and whether or not these organisms are similar to those colonizing younger rocks. The problem of contamination of subseafloor drill cores and the interiors of seafloor basalts with cells from the surface waters or other sources and low biomass has made it difficult to get a clear picture of how the microbial diversity differs between these two niches (Santelli *et al*., 2010). Many studies of the subseafloor microbial community have sampled various parts of igneous outcrops, diffuse flow following deep-sea volcanic eruptions, the fluids from hydrothermal and cold springs, and the outflow from boreholes (e.g. Edwards *et al*., 2012b and references therein). In recent years renewed attention to the subseafloor biome through programs such as the Integrated Ocean Drilling Project (IODP) and the Dark Energy Biosphere Institute (DEBI) has increased funding and opportunities for geochemical and microbiological studies. One of the main tools in these studies is an integrated geochemical and microbiological sampling and monitoring station called

a Circulation Obviation Retrofit Kit (CORK). CORKs are used to plug the top of an open borehole to allow the subsurface fluids to re-equilibrate, and are fitted with down-hole samplers for fluids and cells (Figure 3). These devices have now been installed on a number of different boreholes, both old and newly drilled, and have lead to new insights into hydrological cycles in the volcanic layers, the geochemistry of pore waters, and subseafloor biome (e.g. Cowen *et al*., 2003, Cowen, 2004; Amend and Teske, 2005; Fisher *et al*., 2008; Edwards *et al*., 2011b, 2012a,b, Orcutt *et al*., 2011).

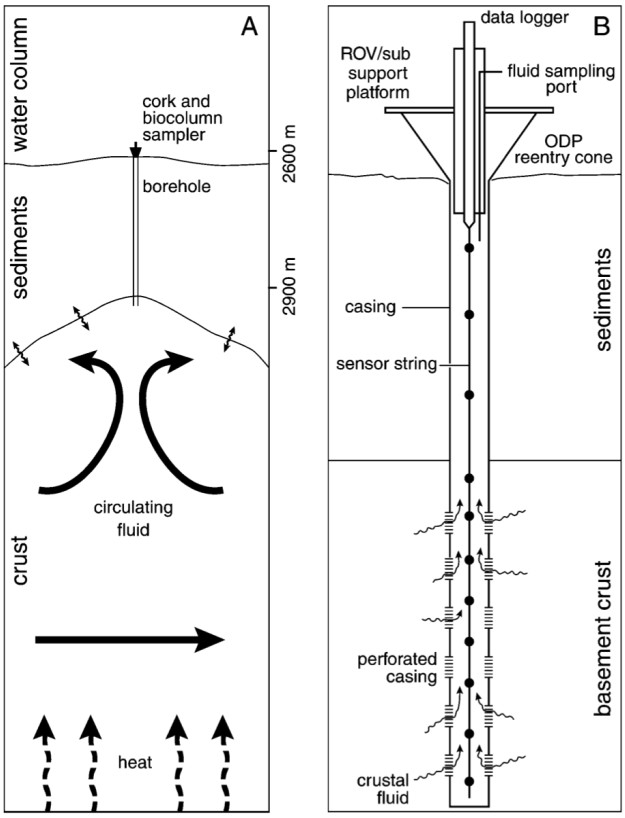

Figure 3. Schematic of an ODP borehole (A) and an early-generation CORK (B). The top of the CORK is fitted with a data logger and fluid sampling port. Multiple different sensors and sampling devices may be attached to the sensor string. (From Cowen 2004)

Sampling of fluids and microorganisms from CORKs has provided additional information about subseafloor fluid chemistry and microbial diversity, but there is still some question as to whether the fluids in the borehole accurately represent the microbiology of the basalts. In some cases the re-equilibrated basement fluid chemistry appears to be rock-derived (Cowen *et al*., 2003, Cowen, 2004), which implies that endolithic microorganisms might have been entrained and subsequently sampled in the borehole. However, rock-dwelling microbes tend to attach tightly to their substrates so as to not get displaced by fluid flow, thus they might be significantly underrepresented in the basement fluids sampled by CORK studies. To date only a few studies microbiological studies have been conducted on solid subseafloor basalt pieces, and the results of these analyses are questionable due to possible contamination (Santelli *et al*., 2010).

Taking these considerations into account it is still interesting to note that the microbial communities samples from basement fluids and solid fragments are different from those that dominate on the seafloor (Edwards *et al*., 2012b). Phylogenetic and microscopic analyses have identified organisms in basement fluids and basalt fragments that are involved in the cycling of carbon, hydrogen, and nitrogen (Cowen *et al*., 2003, Edwards *et al*., 2012b), as well as iron- and sulfur-oxidizing bacteria (Huber *et al*., 2003; Orcutt *et al*., 2011; Nigro *et al*., 2012). In one unique study of the functional genes present in samples from the gabbroic section of the subseafloor, deep beneath the basalt layers, Mason *et al*., (2010) found primarily genes encoding anaerobic respiration pathways, including sulfate, nitrate, and metal reduction, in addition to genes encoding mechanisms for the fixation of carbon and nitrogen. How similar the microbial diversity in the basalt layers is to that in the gabbro will require many more investigations of both environments.

Studies of the eukaryotic diversity of the subseafloor are even more limited than those of the bacterial and archaeal communities. One recent investigation of seafloor basalts from Vailulu'u Seamount, Samoa revealed a diverse fungal community consisting of eight different yeasts and yeast-like species (Connell *et al*., 2009). Physiological studies of these fungi showed that many of them are able to reduce ferric iron and one species was capable of oxidizing Mn^{2+}. In addition, several of the fungal strains produced siderophores to aid in the acquisition and retention of the metal species. These results have exciting implications for basalt glass bioalteration, considering that fungal boring in terrestrial silicate minerals is the best analog for tubule formation in the subseafloor.

1.6 Biosignatures

1.6.1 *Defining Biosignatures*

Biosignatures are any traces of life that cannot be produced abiotically. For present Earth life, these traces range from all of the human technological innovations to atmospheric gasses that are out of thermodynamic equilibrium, to physical and chemical modifications of the environment. For past life on Earth, biosignatures are limited to the physical and chemical clues left by the structures, behaviors, and metabolisms of organisms in the form of body, trace, molecular, and chemical fossils. Identifying unambiguous biosignatures is often a difficult task, but has important applications in studying the origin and evolution of life on Earth and in the search for life elsewhere.

Excluding more obvious recent human traces, such as satellites, cities, and radio transmissions, the most obvious and easily identifiable signs of past life in an environment are

body fossils and their imprints. There are no abiotic processes that could produce anything resembling a dinosaur skeleton or bivalve shell, and there is no question among the scientific community about their origins. Body fossils consist of mostly just the hard parts of animal skeletons and some plants. This includes bones, teeth, claws, shells, and calcareous and siliceous tests. Occasionally the softer parts of animals and plants are preserved, but these are generally rather rare and limited to preservation in unique conditions. Thus, there is a bias in the fossil record towards the hard parts of marine animals, and a dearth of fossils of soft-bodied terrestrial organisms. Due to the activity of plate tectonics, oceanic and continental crust is rapidly (in geological terms) recycled, wiping out any fossil record it contains.

The older signs of life on Earth are in the form of chemical or molecular biosignatures and morphological features. The lines between these different types of biosignatures are not strict and there are many features that fit into more than one category. Chemical and molecular biosignatures encompass a broad range of features, most of which are produced by the activities of the organisms, such as isotopes, biominerals, organic molecules, and various cellular components, as well as specificity in stoichiometry and chirality. The metabolic activities of organisms can cause significant changes in their local environments, some of which are preserved long-term. These metabolic biosignatures can be found in the form of accumulations of various elements, geochemical redox gradients or distributions, and biominerals (Hoehler and Westall, 2010).

Morphological biosignatures include biosedimentary structures, biofabrics, trace fossils (ichnofossils) and microfossils (Farmer and Des Marais, 1999; Cady *et al*., 2003; Westall, 2008). There are many different types of ichnofossils, most of which record the behavior or activities of the organisms, and are typically in the form of morphological features such as stromatolites,

burrows, borings, footprints, feeding marks, root cavities, and coprolites (fossilized dung). Similar to the body fossils of plants and animals, microfossils are morphological traces of life, only on a much smaller scale. As their name implies, microfossils are the fully or partially mineralized cells of microorganisms. In general, microorganisms consist of only cellular material, which makes fossilization rare; the exceptions include diatoms and other microbes that form siliceous or calcareous tests. The morphologies of cells and filaments are best preserved by permineralization, where minerals replace the cell walls and sometimes even organelles. The activities of endolithic organisms, namely the precipitation of silicate minerals around the cells, means they are more likely to be preserved than many other types of microbes. In addition, there are many physical trace and chemical fossils left by rock-inhabiting organisms that could potentially be preserved for far longer than the cells themselves. The identification of trace fossils and microfossils is often very difficult, especially ancient ones, and can be the subject of much controversy in the scientific community.

While there are many examples of bona fide microfossils and microbial trace fossils on Earth (e.g. Cady *et al*., 2003; Knoll *et al*, 2006; Hofmann, 2008; Westall, 2008; Allwood *et al*, 2007, 2009; Cohen *et al*., 2009; Wacey *et al*., 2011), they represent only a tiny fraction of the huge variety of microbial life forms that have existed on and within the planet throughout its history. Fossilization of microbial cells is only favorable under certain conditions, for example in anaerobic sediments, where rates of mineralization and lithification tend to be higher (Farmer, 1999). Thus, the microorganisms found in these environments are largely over-represented in the fossil record. Long-term preservation of morphological and mineralogical biosignatures requires that the rock units remain relatively unchanged by diagenetic processes, such as aqueous and oxidative alteration, compaction, and recrystallization.

There are heated debates about what is truly the oldest known microfossil on Earth. Several different controversial features have been found in the Apex chert from Western Australia, dated at ~3.5 Ga. One group of researchers argues that these morphological features are the fossilized cells of filamentous bacteria (Schopf, 1993; Schopf *et al*., 2002), while another group claims that they are abiogenic (Brasier *et al*., 2005). Less controversial are ancient stromatolites, which date back to about 3.45 Ga (Allwood *et al*., 2007, 2009). Stromatolites are large layered structures of accreted sedimentary grains formed by microbial mat communities. These structures are still produced in a few places on Earth today, which is very useful for understanding their formation and preservation. The oldest known potential eukaryotic microfossils are the 1.87 Ga impressions of filaments similar to coiled green algae (Knoll *et al*., 2006).

1.6.2 *Biominerals*

An important consideration when differentiating biological and abiotic alteration processes is that cellular metabolisms operate by exploiting redox disequilibrium in the local microenvironment. Metabolic processes take of advantage of this by catalyzing otherwise sluggish redox reactions and using the energy gained for biosynthesis and cellular functions. Chemolithoautotrophic microorganisms often leave behind clues of these metabolic processes by various forms of alteration to the local microenvironment, commonly via extraction of metabolically important elements and precipitation of minerals that either would not form or would be very slow to form abiotically. The cellular extraction of elements from the rock results in local depletions of electron sources such Fe^{2+}, Mn^{2+}, and sulfide-bearing minerals, as well producing chemical gradients from the biotic layer into the unoccupied zone. At the same time,

metabolic processes cause the increased deposition of oxidized products, such as iron and manganese oxides, clays, often in the form of nano-aggregates (e.g. Tebo et al., 1997, 2004; Fortin and Ferris, 1998; Wierzchos et al., 2003), and the build up of organic molecules, as well as other biosynthetic components, including accumulations of P, and N (Ferris *et al.,* 1987; Konhauser and Urrutia, 1999), and sometimes measureable quantities bioaccumulated of trace elements.

Biomineralization is a result of both direct catalysis of mineralization pathways, and indirect precipitation. There are a number of microorganisms that directly promote the formation of carbonate or silicate minerals for cellular structure or protection. These include microbes that form shells or tests, such as diatoms, radiolarians, foraminifera, and coccolithophores (Perry *et al*., 2007). In addition, magnetotactic bacteria intentionally form internal chains of magnetite (Fe_3O_4) crystals called magnetosomes. It is thought that these mineral structures aid the cells in navigation along physical and/or chemical gradients, particularly in microaerophilic environments (Kopp and Kirschvink, 2008). Whether or not the magnetite produced by magnetotactic bacteria can be distinguished from inorganically produced magnetite is the subject of debate (see section 5.4). Indirect pathways for biomineralization are often the result of metabolic processes, these include supersaturation of the local microenvironment via mobilization of various elements, intracellular accumulations of metabolic compounds, concentration of elements via organic compounds such as siderophores or chelating agents, and the promotion of nucleation within exopolysaccharide layers or on cell surfaces (e.g. Labrenz *et al*., 2000; Banfield *et al*., 2001; Tebo *et al*., 2004; Wierzchos *et al*., 2005; Perry *et al*., 2007; Zhang *et al*., 2009; Gadd *et al*., 2011; Couradeau *et al*., 2012).

Due to their high surface area to volume ratios and presence of charged chemical groups in the cell walls, bacterial cells are strong mineral-nucleating agents. There are numerous examples of bacterial cells becoming encrusted in metal-bearing and silicate minerals, particularly clays (e.g. Ferris *et al.*, 1987; Schultze-Lam *et al*., 1996; Fortin and Ferris, 1998; Konhauser and Urrutia, 1999; Douglas and Beveridge, 1998; Edwards *et al*., 2004), which increases their fossilization potential (Toporski *et al*., 2002; Souza-Egipsy *et al.*, 2005; Wierzchos *et al*., 2005). These bacterially nucleated minerals are often distinctive structurally and chemically from those precipitated in the same conditions abiotically. For example, in many different freshwater systems, biofilms have been shown to nucleate amorphous to poorly-ordered, fine-grained clay-like material (e.g. Konhauser and Urrutia, 1999), which is structurally distinctive from well-ordered abiotically formed clays.

1.6.3 *Criteria for Biogenicity*

Most often, biosignatures represent only a tiny part of the organism's structure, or one characteristic of its behavior, and thus are limited to inconclusive traces. When these sparse clues are the only potential signs of life the interpretation of their origins often lead to rather heated controversies in the scientific community. This was made very clear and public with the debate surrounding the claim that biosignatures had been identified in the Martian meteorite ALH84001, discovered in Allan Hills, Antarctica. In 1996, David McKay and colleagues published the results of their study of petrographic thin-sections of the meteorite that contained morphological features very similar to bacterial cells. Further potential evidence for life was in the identification of chains of highly ordered magnetite crystals, which are potential biominerals. The huge implications of these findings – as potential signs of life on Mars – sparked much

public interest and even prompted an announcement of the findings by US president Bill Clinton. However, the findings were immediately disputed by a number of reputable scientists, and to this day the interpretation of the features remains controversial.

The main reason that the unambiguous identification of biosignatures can be so difficult and so controversial is that in order for any physical or chemical trace to be interpreted as a bona fide biosignature it must be a feature that is unique to life. It is often very challenging or even impossible to rule out all abiotic processes that could have produced various features, especially when the systematics of various geological and chemical processes are poorly understood. For example, the identification of the magnetite chains in ALH84001 as possible biosignatures was prompted by the theory that only biomineralization by magnetotactic bacteria could produce such small and highly ordered crystal chains. After the announcement of this finding there were a number of studies that showed the abiotic production of similar small, highly ordered magnetite crystals under certain conditions, which then cast doubt on those in ALH84001 as biosignatures (Golden et al. 2001, 2004). Therefore, it is equally as important to study abiotic processes that produce alteration textures, minerals, chemical gradients, and morphological features that could be mistaken as biogenic, as well as the alteration and degradation of biosignatures over geological time. There are numerous examples of modern environments on Earth where microbial taphonomy, specifically permineralization, can be studied *in situ*, including some potential Mars analog environments, and many of these processes have been successfully modeled in the lab (e.g. Buick, 1990; Tazaki, 1997; Fortin and Ferris, 1998; Farmer, 1999; Westall, 1999; Schopf, 2004).

The strongest case for the biogenicity of a specific feature comes from multiple complementary lines of evidence, for example observations of cell-like morphologies combined

with the presence of organic matter, biominerals, and stable isotope patterns. In their assessment of possible biosignatures of euendolithic microorganisms in a variety of rock types, McLoughlin et al. (2007) discussed three useful criteria: "(1) a geological context that demonstrates the syngenicity and antiquity of the putative biological remains; (2) evidence of biogenic morphology and behavior; and (3) geochemical evidence for biological processing." Any single one of these criteria alone makes a weak case for a biosignature, but when all three are met for a potential microfossil or trace fossil then the case is strong for its biogenicity. The first two of these criteria have been well established for both the modern and ancient tubular alteration features in basalts. The third criterion has some support in the forms of DNA staining and microprobe element mapping, but the value and accuracy of these data have been questioned, thus this category needs more support, particularly in terms of establishing a biological mechanism of tubule formation and granular alteration.

1.7 Goals and Overview of Project

1.7.1 *Scientific Objectives*

As discussed above, recognizing life when we find it is a major scientific challenge in the study of ancient biosignatures on Earth and in astrobiology. Establishing what to look for as signs of extant life is a significant task on its own, but in many ways the question of how to recognize the fingerprints of past life on a planet is even more complex. At this point, the biogenicity of the tubular and granular alteration features in subseafloor basalts is disputed. The main issue is that at we are unable to actually watch the bioalteration processes *in situ*, model it in the lab, or even identify the organisms responsible. The biological mechanisms producing

these alteration features operate under unknown constraints of temperature and pressure, and possibly on such long time scales (hundreds to thousands of years) that we won't ever be able reproduce the processes experimentally. In addition, the techniques involved in drill core extraction tend to be destructive to biological molecules, so we haven't been able to clearly identify cells or extract DNA from granular alteration features or tubules. This means that for now we are left with inferring the formation processes from the physical and chemical clues left behind. The ability to clearly differentiate the geochemical changes that take place during both biotic and abiotic glass alteration processes, and a clear understanding of how these features change over time would help significantly to establish these features as signs of life.

In this work I carried out a detailed investigation of the geochemical fingerprints of basalt glass alteration, focusing specifically on tubular alteration features. The primary purpose of this project was to evaluate the geochemical characteristics of tubular alteration features in subseafloor basalts and ophiolites in order to strengthen the evidence for biological processing. The investigations carried out were based on the following four specific objectives:

Objective 1: Analyze the structural and textural characteristics of the tubules in order to elucidate the formation mechanisms.

Objective 2: Identify the geochemical differences between abiotic alteration and putative bioalteration by comparing the patterns of major and trace element enrichments and depletions in different alteration zones.

Objective 3: Characterize the secondary mineral phases in-filling the tubules and identify potential biominerals and organic deposits in alteration features.

Objective 4: Analyze the oxidation and coordination states of iron, manganese, titanium, and sulfur deposits in order to constrain mineralogy and identify signs of biological processing.

1.7.2 *Analytical Techniques*

All four of these objectives were achieved by utilizing a number of cutting-edge micro-analytical techniques. Focused ion beam (FIB) milling is a largely underappreciated tool in the Earth and planetary sciences (e.g. Wirth, 2004, 2009), but is unparalleled in its utility in preparation of samples for micron-scale investigations. Using FIB instruments both at the Nanomaterials Characterization Facility at the University of Colorado and with collaborator Richard Wirth at GeoForschungsZentrum in Potsdam, Germany in October 2011, I prepared several cross-sections of tubular alteration features. I was then able to image the ultra-thin sections using transmission electron microscopy (TEM) and conducted a number of additional chemical analyses. These investigations were primarily focused around Objective 1, but have also added important data for Objectives 2 and 3, as discussed in Chapter 2.

The other primary tools I used in this work are a number of different synchrotron-based X-ray analytical techniques. I was fortunate to start this project at a time when these techniques were developed enough to provide strong analytical capabilities, but were (and are) still progressing. Microprobe beamlines are constantly being pushed to focus down to smaller spot

sizes, increase their spectral resolution and detector capabilities, and simplify and improve the analytical data processing. The analysis of tubular bioalteration features in particular has presented technological challenges and pushed development at the forefront of synchrotron-based micro-spectroscopy research. Since the tubules tend to be one to several microns in diameter, the X-ray beam must be focused down to only a few microns and rastered across the image in very small step sizes to be able to resolve the fine-scale element changes and gradients and at the same time require the ability to map and collect spectra for multiple different elements and different oxidation states. The challenges presented by the analysis of these features lead to their use as a test case of the capabilities of a new micro-spectroscopy beamline at the Australian Synchrotron. I was also fortunate that I had the opportunity to co-author a review article about the power of synchrotron-based X-ray techniques in geomicrobiology with my advisor, Alexis Templeton (Templeton and Knowles, 2009). Since each beamline is designed for different techniques and has different capabilities, I ended up traveling to five different facilities in three different countries to perform my analyses. Combined, these analyses provided a huge amount of data, which helped achieve Objectives 2, 3, and 4, as discussed in detail in Chapters 3 and 4.

Put together all of these micro-analytical techniques were necessary to provide a set of data with enough detail to fully characterize the geochemistry of tubular alteration features. Unfortunately, they did not provide sufficient information to be able to completely end the debate about the biogenicity of these features. Whether or not it is even possible to answer the biogenicity question is unclear. This question and ideas for further studies are discussed at length in Chapter 5.

1.7.3 *Samples*

Granular and tubular bioalteration features have been found in drill cores and ophiolites from a wide variety of ages and locations (e.g. Staudigel *et al*., 2008, and references therein). In the older ophiolite and greenstone samples the bioalteration features tend to show significant chemical changes due to various stages of metamorphism and hydrothermal or cold aqueous alteration. Thus, tubular alteration in these samples is identified primarily by morphology. The main focus of this project was to show evidence of geochemical processing in order to more firmly establish tubular alteration features as biological in origin, thus I focused on the younger samples that are more likely to retain geochemical biosignatures. I have a broad collection of subseafloor glass samples containing tubular alteration features, provided by collaborators Nicola McLoughlin, Harald Furnes, and Hubert Staudigel. Most of my samples are from drill cores, but I also have a few young ophiolite samples from the Troodos Ophiolite in Cyprus. A comprehensive list of the samples I analyzed in this study is shown in Table 1. These samples were chosen both to represent a variety of collection locations, ages, and depths, and for the abundance and accessibility (near the surfaces of the thin section) of the tubules they contain.

Table 2. Comprehensive sample list (* meters into volcanic basement)

Sample Name	**Location**	**Type**	**Age (Ma)**	**Depth (mivb*)**
409-13	North Atlantic	Drill Core	2.3	129
896A-11R1	Cost Rica Rift	Drill Core	5.9	92
46-396B-16	Mid-Atlantic	Drill Core	10	100
46-396B-17	Mid-Atlantic	Drill Core	10	121
46-396B-20	Mid-Atlantic	Drill Core	10	140
418A-49-2	S.W. Atlantic	Drill Core	110	147
418A-43-1	S.W. Atlantic	Drill Core	110	100
418A-52-5	S.W. Atlantic	Drill Core	110	274
418A-56-5	Mid-Atlantic	Drill Core	110	312
CY-1-31	Cyprus	Ophiolite	92	N/A
CY-1-34A	Cyprus	Ophiolite	92	N/A

1.8 Synchrotron-Based X-Ray Absorption Spectroscopy

Synchrotron-based X-ray absorption spectroscopy (XAS) techniques offer a range of high-resolution analyses, which can provide detailed chemical, biological, and mineralogical information about a sample. These techniques have recently gained popularity as powerful tools in geomicrobiology (Templeton and Knowles, 2009). Since most microbial processes operate on nanometer to micron scales, geochemical and biological analyses require resolution on these scales. Many microprobe beamlines are now capable of focusing spot sizes down to 1 μm or less, depending on the focusing optics (e.g. Kirkpatrick- Baez mirrors or Fresnel zone-plates) and are constantly being pushed further.

The fine spectral resolution of most monochromators means that very specific incident energies can be selected, allowing for detailed resolution of the spectrum obtained. This enables the identification of specific oxidation and coordination states of elements of interest, sometimes quantitatively, depending on the sample and beamline setup (e.g. Lanzirotti *et al*., 2010) analyses of elements and oxidation states with absorption edges that are very close in energy. In addition, the high flux of a synchrotron X-ray source enables analyses of elements that are present in only trace amounts. For environmental samples, synchrotron-based techniques offer the ability to analyze liquids and solids of various shapes and sizes with little or no damage to the sample, which is a distinct advantage.

These techniques are based on the principle of the photoelectric effect. When an X-ray is absorbed by an atom the energy is transferred to a core-level electron, which is then ejected from the atom as a photoelectron. A higher-level core electron drops into the core hole, which causes

the emission of a fluorescent photon (Figure 4). The absorbing atom can be identified by the discrete energies at which X-ray fluorescence emission occurs.

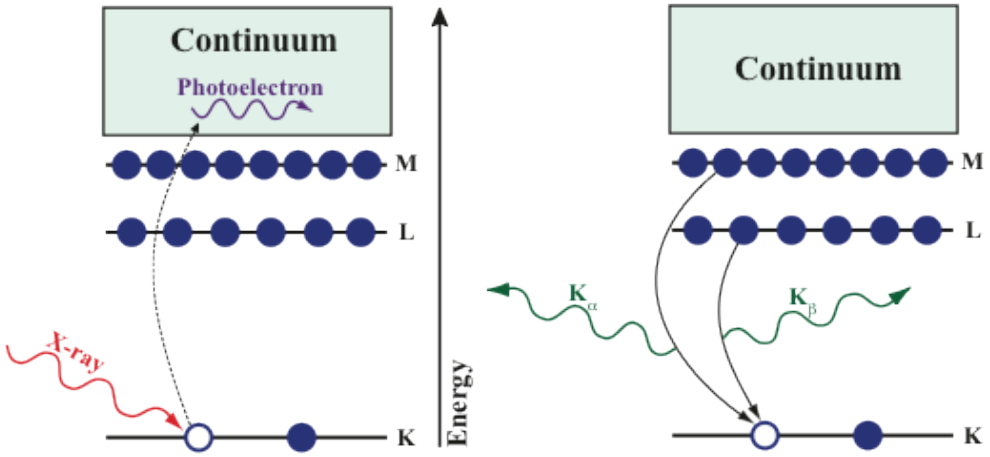

Figure 4. Cartoon of the photoelectric effect. Left: the absorption of an X-ray by an inner-shell electron causes it to be ejected as a photoelectron. Right: a higher-level electron drops into the core hole, causing the emission of a fluorescent photon (Kα and Kβ). (Figure from Matt Newville)

The experimental end-stations at synchrotron facilities are called beamlines. A typical microprobe beamline set up consists of a monochromator to select the desired energy range, focusing lenses, a sample holder, and finally a variety of detectors and cameras depending on the technique (Figure 5).

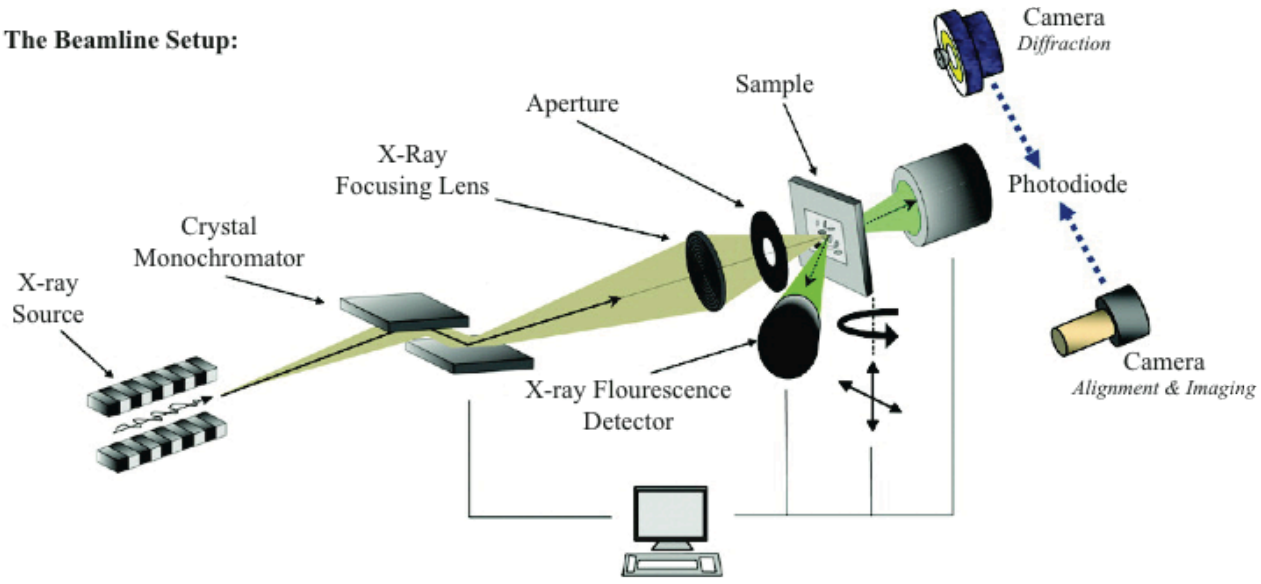

Figure 5. A typical microprobe beamline setup. X-rays produced in the accelerator ring are filtered to a specific energy or range of energies in the monochromator. The beam is then focused through a series of lenses and apertures before it hits the sample. Fluorescence detectors are oriented at 45° to the sample, while the diffraction camera is in-line with the X-ray beam. Not shown are the ion chambers: i0 is placed upstream of the sample to measure the intensity of the incident beam, i1 is placed downstream on the sample for transmission mode measurements.

The energy range of X-rays generated by various synchrotron sources is split into two different types. Soft X-ray are those with energies less than ~4 keV and are used to analyze the K absorption edges of elements with low Z numbers, typically lower than Ca, and the L absorption edges of transition elements. Since biological macromolecules are primarily made up of carbon, nitrogen, hydrogen, oxygen, phosphorus, and sulfur, analyses of cells and biological systems must be conducted on soft X-ray beamlines. Most mineral and metal analyses use hard X-rays, which have energies higher than ~4 keV.

In this work I used four main XAS techniques: hard and soft X-ray fluorescence microprobe mapping, micro X-ray absorption near-edge structure (μ-XANES) spectroscopy, and micro X-ray diffraction (μ-XRD). Microprobe element mapping is conducted by setting the

beam energy to above the absorption edge of the element of interest and then rastering the beam across the region to be mapped. In most beamline configurations the full fluorescence spectrum is collected and the different photon wavelengths are binned according to the known elemental emission energies. The fluorescence intensity for each element of interest can then be plotted for each pixel to generate elemental distribution maps. Since the absorption edge of an element varies with the oxidation state of the element, X-ray fluorescence microprobe analyses can be used to make element maps at slightly different energies to show the distributions of an element of interest in various redox states. For example, one map can be made at the absorption edge of Fe^{2+} (~7120 eV) and another map can be made at the absorption edge of Fe^{3+} (~7133 eV; this map will contain the total counts for Fe^{2+} plus Fe^{3+}). The proportions of oxidized and reduced iron can be plotted by comparing the fluorescent yields at the two different energies in any given pixel to a matrix of normalized XANES fluorescence values from Fe model compounds of known valence. The maps can then be merged in an appropriate analyses software package (such as Sam's Microprobe Analyses Kit, http://smak.sams-xrays.com) to show the variations in Fe oxidation state throughout a sample (e.g. Mayhew *et al*., 2011).

Using XANES analyses one can determine the oxidations states of elements of interest, as well as the coordination chemistry. XANES analyses are conducted by choosing a specific spot of interest and then scanning in energy from ~50 eV below the absorption edge of the element of interest to ~150eV above the edge. The interaction of the photons emitted from an excited atom with nearby atoms leads to specific details in pre-edge, absorption edge, and post-edge features of the absorption spectrum. The spectrum can then be fit with standards to determine the coordination chemistry of the element of interest, for example whether iron is bound to oxygen or sulfur. Synchrotron-based μ-XRD is very similar to conventional XRD, but

instead of bulk analyses of powdered samples, one can collected diffraction patterns from a discrete spot within a thin section. For more information about these and additional synchrotron-based X-ray techniques see Templeton and Knowles (2009).

In this work, the hard X-ray fluorescence microprobe mapping and μ-XANES analyses were conducted primarily on beamline 13-ID-C at the Advances Photon Source (APS) at Argonne National Laboratory, Chicago, IL, and a few initial studies on beamline 2-3 at the Stanford Synchrotron Radiation Lightsource (SSRL). The soft X-ray fluorescence microprobe mapping and sulfur μ-XANES spectra collection was conducted on the Phoenix beamline at the Swiss Light Source (SLS) at the Paul Scherrer Institut (PSI) in Villigen, Switzerland. The Phoenix beamline is in the pilot phase of operations, meaning that it is still undergoing evaluation and development. The requirements for as small of spot sizes as possible, mapping with multiple different energies, and the need for distinct processing capabilities help both test and push the further development of this beamline. For the micro-XRD analyses I used beamline X26A at that National Synchrotron Light Source (NSLS) at Brookhaven National Laboratory, Upton, NY. In addition, in September 2009 I had the opportunity travel to Clayton, Victoria in Australia to work on the Australian Synchrotron.

1.9 Organization of this Dissertation

This dissertation is organized into five main chapters, followed by compiled references and appendices. The first chapter introduces the motivation and main questions addressed in this work, provides a relevant literature review, describes the samples used, and explains the theory and applicability of synchrotron-based X-ray techniques. The three main body chapters (2, 3, and

4) were all written in manuscript format. Chapter 2 focuses on the coupled FIB-TEM analyses, which yielded detailed, high-resolution images of the structures and textures of the secondary phases and tubule margins and helped to initially constrain the mineralogy. This chapter has already been submitted to Chemical Geology and is currently in review. Chapter 3 covers all of the hard X-ray analyses that I conducted at a number of different synchrotron facilities, as well as additional FIB-TEM analyses. The results presented in this chapter make up the bulk of the chemical and mineralogical findings of this work, including detailed element distribution maps, μ-XANES spectra and relevant model compound fits, diffraction patterns, and additional high-resolution images. This chapter will be submitted in the next few weeks pending final revisions, and is included here in submission format. Chapter 4 discusses the soft X-ray analyses that I conducted, focusing on sulfur. These results are very complementary to and build off of the hard X-ray results discussed in Chapter 3 by providing distribution maps for several low-Z elements probing the oxidation and coordination states of sulfur. Since these three chapters are in manuscript format it was necessary to repeat some of the material in the introduction and discussion sections, particularly the descriptions of tubular alteration features and abiotic basalt alteration, thus these sections are kept fairly brief in Chapter 1. Additional data that did not fit well into the manuscripts in Chapters 2 and 3 are included in appendices A and B, respectively. The references for Chapters 2, 3, and 4 are included at the end of each manuscript, as well as in the complied references. Chapter 5 explains how all of the results fit together, discusses their importance in terms of biosignatures, and describes additional techniques and studies that could potentially provide further insight into the biogenicity of tubular alteration features.

CHAPTER 2

A Comparative Analysis of Potential Biosignatures in Basalt Glass by FIB-TEM

In review at *Chemical Geology*

Co-authors: Richard Wirth[b], and Alexis Templeton[a]

[a]Department of Geological Sciences, University of Colorado, 2200 Colorado Ave., UCB 399 Boulder, CO 80309

[b]Chemistry and Physics of Earth, GeoForschungsZentrum, Telegrafenberg C 120, D-14473 Potsdam, Germany

Abstract

Bulk analyses of fresh and altered subseafloor basalts have elucidated the large-scale geochemical fluxes that result from water-rock interactions, which ultimately affect both seawater and mantle compositions, but these analyses do not provide insights into the physical and chemical processes occurring on the scale of microorganisms. Micron-sized tubules that may represent microbial boring into basalt glass are ubiquitous throughout the seafloor and can potentially be preserved over geological time. These putative biosignatures give clues into the history of life on Earth, and may be significant for the search for life on other planets; however, their formation and mineralization are still poorly understood. We have used a combination of focused ion beam (FIB) milling and transmission electron microscopy (TEM) to analyze the textural and geochemical characteristics of tubular alteration features from four basalt glass samples representing different sample locations, collection depths, and ages, including one sample from the Cretaceous Troodos ophiolite.

High-resolution TEM imaging consistently identified platy layers of partially crystalline material in-filling the tubules. The lattice spacings and diffraction patterns showed that this material comprises a mix of two-layer and three-layer clays. Closer inspection of the contact point between the tubules and the surrounding basalt glass commonly revealed a thin leached rim around the tubules. Electron energy loss spectroscopy mapping demonstrated that these rims are depleted in everything but Si and O, which implies that they are formed by a leaching process, likely the incongruent dissolution of the glass during formation of the tubule. The in-filling material is depleted in Ca and enriched in K, and in most cases also enriched in Fe, which is consistent with their identification as Fe-bearing phyllosilicates. These observations are

consistent across the samples, which implies that the processes that form and mineralize tubular glass alteration features are similar throughout the oceanic subsurface and through time.

Keywords: Focused ion beam, TEM, tubular alteration, subseafloor, EDX, EELS

Abbreviations: Focused ion beam (FIB), transmission electron microscopy (TEM), Deep Sea Drilling Project (DSDP), Ocean Drilling Project (ODP), meters into volcanic basement (mivb), high angle annular dark-field (HAADF), energy-dispersive X-ray spectroscopy (EDX), electron energy-loss spectroscopy (EELS), low temperature alteration (LTA), mid-ocean ridge basalts (MORBs)

1. Introduction

Fluid-rock interactions at and beneath the seafloor have a significant influence on global geochemical cycling (e.g. Staudigel and Hart, 1983; Edmond et al., 1979), ultimately affecting even the composition of the mantle (Hofmann and White, 1982; Bach and Edwards, 2003). The majority of studies of ocean crust alteration have been carried out on bulk samples from the seafloor and subseafloor (e.g. Staudigel and Hart, 1983; Alt, 1995; Stroncik and Schmincke, 2002; Walton and Schiffman, 2003; Drief and Schiffman, 2004; Schramm et al., 2005; Walton et al., 2005), subglacial and shallow marine environments (e.g. Furnes, 1984; Thorseth et al., 1991), ophiolites (e.g. Stakes et al., 1984; Bednarz and Schmincke, 1989; Alt et al., 1998), and on synthetic basalt samples (e.g. Crovisier et al., 1987). These studies have shown that while the degree of alteration and specific mineral assemblages vary depending on a number of physical and chemical factors, including age of the crust, alteration temperature, porosity, lithology, and oxidation state of the fluids, there are some common trends in low-temperature seafloor basalt alteration. The overall process starts with oxidation and hydration of the silicate matrix, causing dissolution, which leads to precipitation of secondary phases in the fractures and vesicles. Initially the glassy margins are devitrified and converted to palagonite, a partially crystalline, heterogeneous, gel-like material made up of a mix of clays, zeolites, and oxides (Stroncik and Schmincke, 2002), while the groundmass tends to form alteration haloes that consist of hydrated phases and incipient secondary mineral precipitates. The most common secondary minerals include Fe-oxyhydroxides, clays (primarily smectites, illite, glauconite, and celadonite), zeolites (commonly phillipsite and chabazite), and in some cases carbonate minerals. Increased deposition of these pore-filling phases continues to replace the parent basalt and acts to cement vesicles, fractures, and inter-granular spaces, which limits fluid flow, eventually sealing off the

system. As alteration advances, the chemistry of the circulating fluid evolves, which determines the progression of the secondary minerals (Alt, 1995; 1999; Clayton and Pearce, 2000; Walton and Schiffman, 2003; Schramm et al., 2005). These alteration processes occur abiotically through the hydrolysis and dissolution of the glass, but can be significantly enhanced by the activity of microorganisms (e.g. Staudigel et al., 1995; 1998; Thorseth et al., 1995; Alt and Mata, 2000; Storrie-Lombardi and Fisk, 2004; Einen et al., 2006).

The glassy rinds of pillow basalts are particularly reactive and their weathering involves significant chemical exchange with seawater. As dissolution of the glass progresses, most major elements are depleted, including Si, Al, Mg, Mn, Ca, Na, and P, with replacement by H_2O, CO_2 and K_2O (Staudigel and Hart, 1983; Stroncik and Schmincke, 2002; Walton et al., 2005). The only major elements that are generally considered immobile are Fe, which is fully retained, and Ti, which is often enriched in the palagonite. Many of the elements mobilized are re-deposited in secondary phases, primarily zeolites and smectite clays. The mobility of trace elements during abiotic glass alteration is not as clearly understood as the major elements. In most cases it appears that Rb, Cs, Ba, and U are taken up from seawater and incorporated in secondary minerals, similar to K (Schramm et al., 2005). There is also an exchange of Sr during palagonite formation: isotopic data show that a significant fraction of the basalt Sr is released, while about half of that amount is replaced by seawater Sr (Staudigel and Hart, 1983).

While these bulk analyses have revealed many of the basaltic ocean crust alteration pathways and products, the signal of fine-scale alteration features is lost using this approach. Of particular interest are the micron-sized tubules (Fig. 1) that have been found in the glassy margins of subsurface oceanic basalts from a wide variety of locations and ages (e.g. Staudigel et al., 1995; 1998; Torsvik et al., 1998; Fisk et al., 1998; Furnes et al., 2001a,b; 2004; Banerjee et

al., 2006; Benzerara et al., 2007; Walton, 2008; McLoughlin et al., 2011; Fliegel et al., 2010b; 2011). These tubules always extend from cracks or fractures into the fresh glass, and tend to be in the size range of typical microbial cells: a few microns in diameter. They are strikingly similar to tracks left by fungal hyphae that bore into silicate minerals in terrestrial environments (Jongmans et al., 1997; Hoffland et al., 2003). Given the abundance of recent evidence for a potentially huge subseafloor microbial biosphere (e.g. Schumann et al., 2004; Rouxel et al., 2008; Mason et al., 2010; Santelli et al., 2010; Edwards et al., 2011; 2012; Orcutt et al., 2011; Ménez et al., 2012), it is possible that these tubules are formed by cryptoendolithic microorganisms. Abiotic basalt alteration tends to produce smooth alteration fronts with a sharp contact between the palagonite and any remaining fresh glass, in contrast to the irregular, asymmetrical nature of these putative bioalteration features (Fig. 1). A number of analogous tubular alteration features have been found in relatively young (~92 Ma) to ancient ophiolites, including the Euro Basalt formation of the Pilbara Craton (~3.35 Ga) in western Australia (Staudigel et al., 2006; Banerjee et al., 2007), and the Barberton Greenstone Belt (~3.4-3.5 Ga) in South Africa (Furnes et al., 2004; Banerjee et al., 2006; Fliegel et al., 2010a).

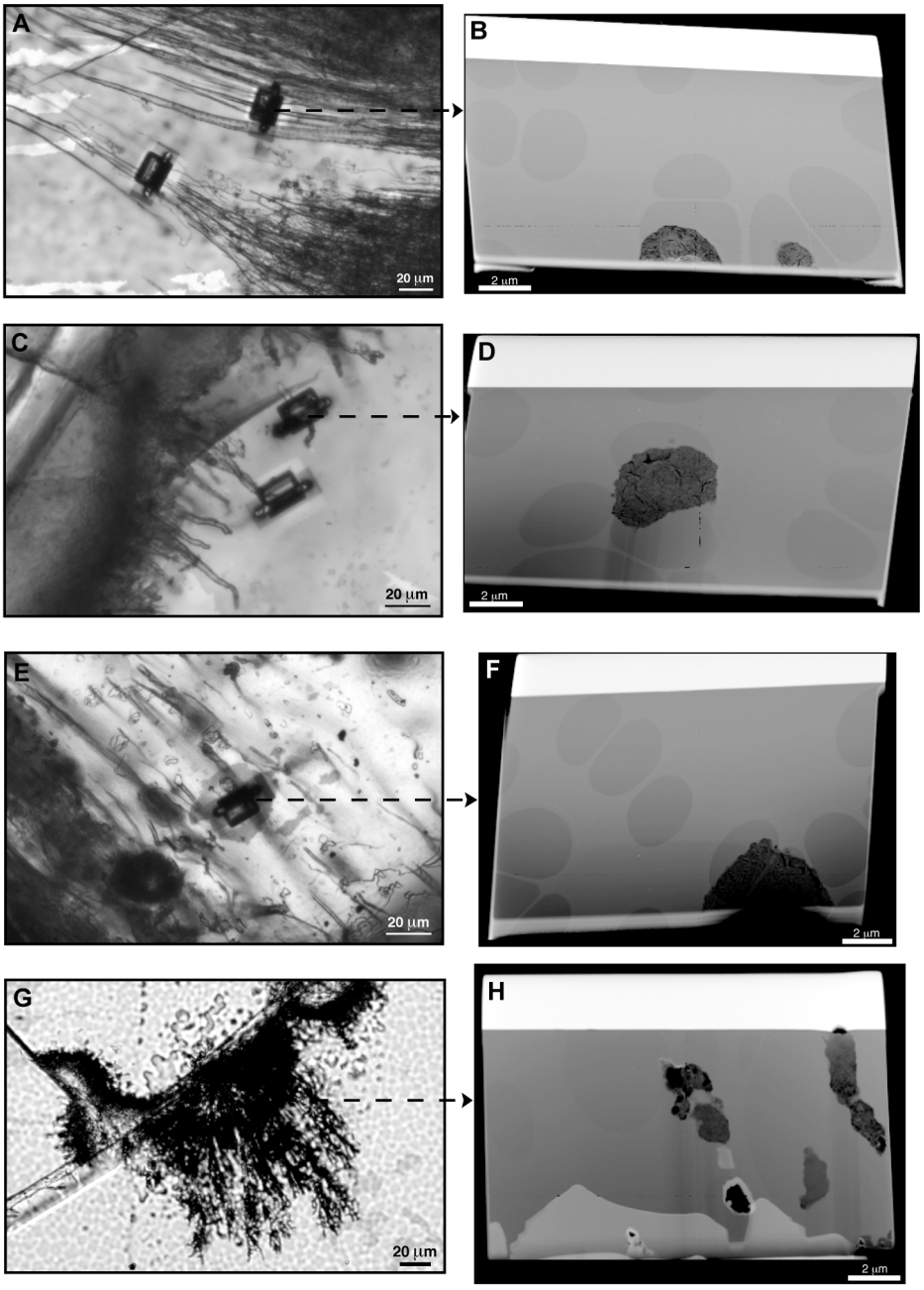

Figure 1. Thin-section photomicrographs (left) of the sample thin sections showing the locations of FIB milling. The finished FIB lamellae are shown on the right, corresponding to the milling location denoted by the arrows. The white strips on the top of the lamellae are the protective Pt layers and the white bands on the bottom are deposited Ga ions. A) and B) Sample 418A-56-5, Foil #2813. C) and D) Sample 896A-11R1, Foil #2814. E) and F) Sample CY-3-34A, Foil #2818. G) and H) Sample 46-396B-20, Foil #2996.

A clearer understanding of the formation and preservation of these potential trace fossils could yield clues into history of life on Earth, and may be significant for the search for life on other planets (McLoughlin et al., 2007). Due to technological and practical limitations, however, we are unable to observe the alteration processes that form these tubules *in situ*, and thus far no one has been able to successfully reproduce them in the lab. Therefore, we are left with only physical and chemical clues about their formation and mineralization. In order to elucidate the geochemical processes involved in this system, a detailed analysis of the micro-structural and mineralogical characteristics is required. Tubular alteration features are on the order of a few microns in diameter, thus, they must be analyzed with high-resolution on the sub-micron scale.

Transmission electron microscopy (TEM) is the ideal tool for nanometer-scale imaging and chemical analyses of Earth and extraterrestrial materials (Lee, 2010). However, standard sample preparation techniques, such as ultra-microtome sectioning, are not possible with petrographic thin-sections. In a few earlier studies researchers used epoxy to peel off the experimentally altered rinds of basalt glasses, which they were then able to cut into ultra-thin sections using a microtome (Crovisier et al., 1983; Ehret et al., 1986), but this technique is not possible with micron-sized tubules that are fully encased in glass. The standard thinning technique for TEM preparation of rocks and minerals is to use an argon ion beam to mill down a sticky wax thin section until it is electron transparent. This technique has been employed since the 1950s, and can produce sections that are decent for imaging via TEM. One previous study of tubular alteration features in subseafloor basalt glass successfully used this technique to produce the first high-resolution images of the tubules and analyze the alteration chemistry (Alt and Mata, 2000). There are, however, some major drawbacks to this sample preparation technique. First, Ar ion thinning is often rather destructive, as it requires sub-sectioning of the sample.

Second, thinning can be uneven depending on the heterogeneity of the section. Third, it is not possible to select specific regions of interest when using the Ar milling technique; the beam is rastered over the entire surface of the thin section or disk (Heaney et al., 2001). Focused ion beam (FIB) milling offers an excellent alternative. In the past several years the use of focused ion beam techniques has developed significantly in the nano-materials industry, but the application of this powerful tool to geological samples is relatively new and somewhat underappreciated (Heaney et al., 2001; Wirth, 2004; 2009; Lee, 2010). To date there are only a limited number of studies where FIB and TEM have been used to analyze basalt weathering products (Lee et al., 2003; 2007; Templeton et al., 2009). These techniques have been slowly gaining popularity in the study of microfossils, trace fossils, and potentially biogenic microstructures (Kempe et al., 2005; Benzerara et al., 2005; 2007; Bernard et al., 2007; Cavalazzi, 2007; Schiffbauer and Xiao, 2009; Lepot et al., 2011; Wacey et al., 2011; Fliegel et al., 2010b; 2011; revised version in review), but the applications have still been rather limited.

Two of these studies focused on tubular alteration features in subseafloor basalt glass samples (Benzerara et al., 2007; Fliegel et al., revised version in review) and two on ophiolites (Fliegel et al., 2010b; 2011). The results of these investigations have significantly enhanced our understanding of the structural and geochemical characteristics of tubular alteration. However, these studies focused on features from two specific sample locations. Considering the broad range of locations, ages, and depths from which tubules have been found in basaltic glasses, an expansion of the scope of samples analyzed on the micron scale would help to constrain the key processes involved in tubular alteration in general. Thus, we have extended these studies to tubular alteration features from four samples of different ages and from different alteration environments, including one Cretaceous ophiolite. By cross-comparing the structural,

mineralogical, and geochemical characteristics of tubular alteration features representing different alteration environments we show that the dissolution and precipitation processes involved in the formation of tubular alteration features are remarkably common. These results provide new insights into the mechanisms of formation and mineralization of these features, as well as their potential as biosignatures.

2. Samples and Methods

Three subseafloor samples, 418A-56-5, 896A-11R1, and 46-396B-20, were originally collected through the Deep Sea Drilling Project/Ocean Drilling Program (DSDP/ODP). Sample 418A-56-5 (section 129-132) was collected from 312.1 meters into volcanic basement (mivb) in the drill core from Hole 418A on the Bermuda Rise in the southwestern Atlantic (DSDP leg 52). This section of the core is predominantly composed of moderately phyric pillow basalts, and has been dated at ~110 Ma (Donnelly et al., 1979). The lithology of the core is further described in detail elsewhere (Donnelly et al., 1979; Alt and Honnorez, 1984; Furnes et al., 2001b). Sample 896A-11R1 (section 73-75, piece 8) was collected at ~92 mivb from Hole 896A from the Costa Rica Rift in the eastern Pacific Ocean during ODP leg 148 (Alt et al., 1993). The basement layer at this location has been dated at ~5.9 Ma, and consists of a mix of pillow lavas and massive flows (Alt et al., 2003; Torsvik et al., 1998). Sample 46-396B-20 (section 3, 108-109cm, piece 13) was collected from 140.1 mivb the during DSDP leg 46 in the mid-Atlantic. The lithology of this unit is made up of primarily porphyritic pillow basalts (Dmitriev et al., 1978).

Sample CY-1-34A is from the Cretaceous Troodos Ophiolite Complex in Cyprus, one of the best-characterized ophiolite regions in the world (Malpas et al., 1990). The ophiolite covers about one third of the area of the island and has a complete and well-exposed stratigraphy. The

complex likely formed in a supra-subduction setting, in the early stages of island arc development. In the mid-1980s a series of cores were drilled at several locations throughout the massif. One major result of these efforts was a clearer picture of the stratigraphy of the formation. The central core, which is exposed in the domical uplift near Mt. Olympus, is a plutonic complex consisting of harzburgite tectonite, gabbros, plagiogranites, and ultramafic cumulates. This layer is overlain by sheeted dikes, followed by a series of extrusive volcanic rocks, and finally sediments. The extrusive series is characterized by numerous sheet and pillow flows from a number of submarine volcanoes. The ophiolite has experienced little to no metamorphism: abundant fresh to highly-weathered glass can be found in rims of the pillow lavas and in hyaloclastites found within the extrusive series (Xenophontos and Malpas, 1987). Sample CY-1-34A is from ~410 meters below the top of drill core CY-1. The majority of this section of the ophiolite is made up of pillow basalts, and the rest is a mix of breccias and massive flows (Schmincke and Bednarz, 1990).

Focused ion beam milling and transmission electron microscopy were conducted at the German Research Center for Geosciences (GFZ) at the Helmholtz Center Potsdam, Germany. Regions of interest were identified by a combination of transmission and reflected light microscopy. The thin sections were then coated with a thin layer of carbon and the edges covered with silver paint to improve conductivity. Ultra-thin lamellae (15 x 8 x 0.150 μm) were milled using an FEI FIB2000TEM single beam (Ga^+ ion) focused ion beam instrument, operating at an accelerating voltage of 30 keV and a current of 2.2 nA. In order to protect the surface of the sample during milling a thin layer of Pt was deposited just above a tubule of interest. The final stages of thinning were carried out at low current (70 pA) in order to limit beam damage, with final thicknesses ranging from 80-100 nm. The finished lamellae were removed manually using a

micromanipulator with a light microscope, then placed on a copper TEM grid covered with a perforated carbon membrane. Details of TEM sample preparation using FIB milling can be found elsewhere (Wirth, 2004; 2009).

TEM imaging and analyses were performed using an FEI Tecnai G2 F20 X-Twin transmission electron microscope operating at 200 kV and a field emission gun as electron source. The TEM is equipped with a Fishione high angle annular dark-field (HAADF) imaging detector, a Gatan Tridiem imaging filter and electron energy-loss spectroscopy (EELS) system, and an EDAX energy dispersive X-ray (EDX) spectroscopy system. TEM bright field or dark field images were acquired as filtered images by applying a 20 eV window to the zero loss electron beam. EDX analyses were primarily conducted for qualitative comparisons of element concentrations between two different spots, but were also performed using a standard-less method (k_{AB} factors from the TIA software package), giving semi-quantitative results.

3. Results

In total we successfully cross-sectioned over a dozen tubules in four different glassy basalt samples. Figure 1 shows the locations of the FIB cuts and four of the resulting polished FIB lamellae. Given the difficulty in estimating how far beneath the surface the alteration features are, the tubules in sample 418A-56-5 Foil #2813 (Fig. 1A,B) and sample CY-1-34A Foil #2818 (Fig. 1E,F) ended up right at the bottom of the FIB lamellae, while the tubules in sample 896A-11R1 Foil #2814 (Fig. 1C,D) and Foil #2817 (Figure A1), 46-396B-20 Foil #2996 (Fig. 1 G,H), and 418A-56-5 Foil #2815 (Figure A1) were cross-sectioned near the center of the lamellae. The elongated appearance of the tubules in sample 46-396B-20 Foil #2996, particularly on the right side of the FIB lamella is likely due to cross-sectioning of these tubules lengthwise,

along the long axis of tubules, whereas in the other samples the tubules appear to have been cross-sectioned nearly perpendicular to their long axes. In general, the tubules are circular to oval in cross-section and range in diameter from approximately 0.45 to 5 μm. The protective Pt layer is visible as the thick white strip on the top of each lamella, and the white band on the bottom is caused by the re-deposition of Ga^+ ions and sputtered materials. The darker grey ovals are the holes in the perforated carbon TEM membrane on which the lamellae are resting.

The high-resolution images of the tubules show the platy nature of the in-filling material (Fig. 2). This habit is characteristic of phyllosilicates in subseafloor basalts (e.g. Giorgetti et al., 2001; Drief and Schiffman, 2004). The phyllosilicate layers are organized in clumps that are randomly oriented throughout the tubules. Larger angular features are also present, which appear to be cracks, most likely the result of dehydration during thin sectioning or FIB milling (Zhou et al., 2001). The texture of this in-filling material looks remarkably similar between the four samples analyzed (Fig. 2), with some variability in the density. In most of the samples the phyllosilicates appear to completely fill the tubules, with a smooth interface at the margins, but in a few of the tubules the in-filling material is much less densely packed, some parts even appear hollow, particularly in sample 46-396B-20 Foil #2996 (Fig. 2D).

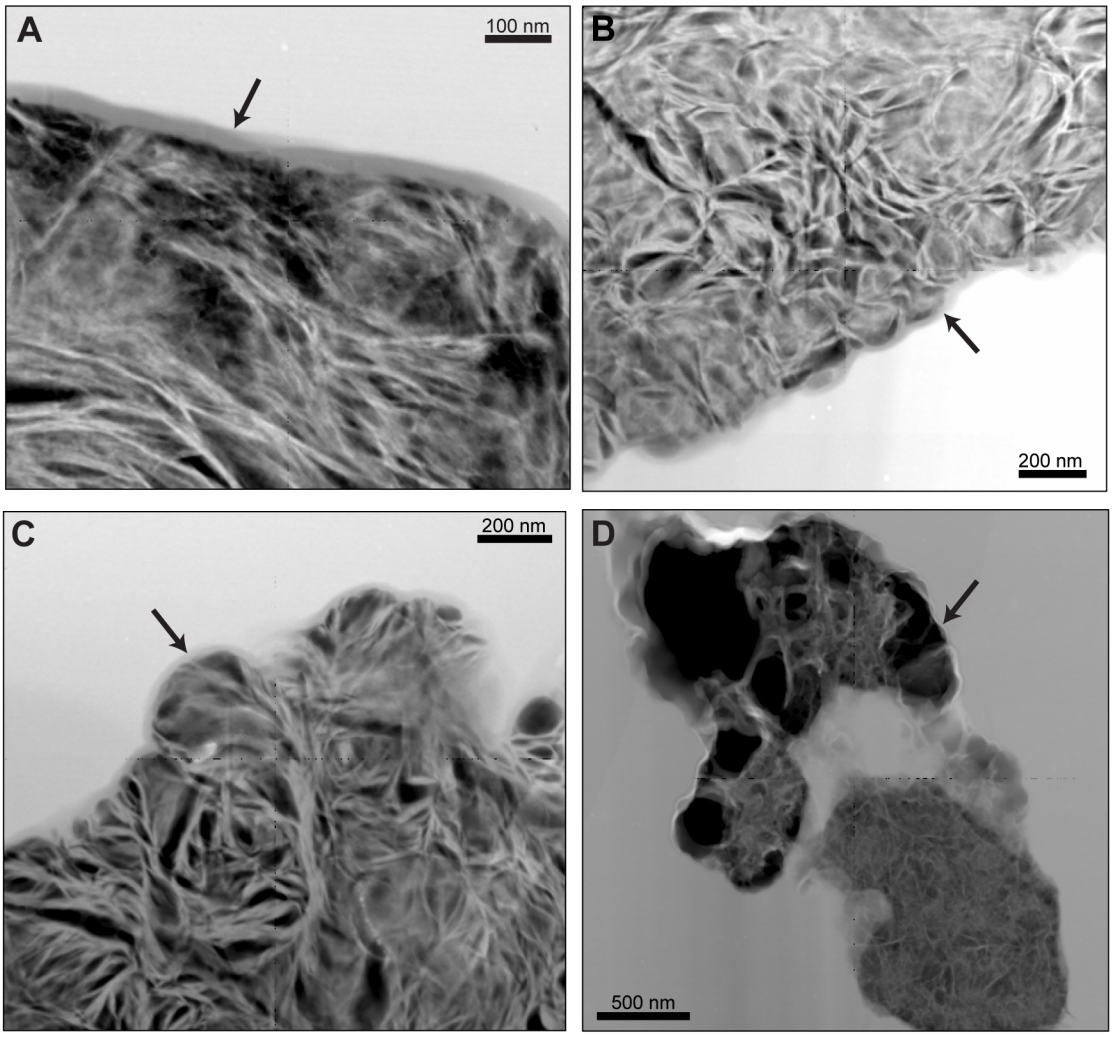

Figure 2. High-resolution high-angle angular dark field (HAADF) TEM images showing the phyllosilicates infilling the tubules and the leached rims (arrows). A) Sample 418A-56-5, Foil #2813. B) Sample 896A-11R1, Foil #2814. C) Sample CY-3-34A, Foil #2818. D) Sample 46-396B-20, Foil #2996.

At higher magnification the lattice fringes of the phyllosilicates are visible, with packets of well-ordered crystalline layers mixed with regions of amorphous material (Figures 3, A2). By measuring an intensity profile across the lattice fringes we identified two main repeated spacings of approximately 0.72 and 1.0nm, with the 1.0nm spacing more prevalent (Fig. 3G). These results fit well with a mix of poorly- to highly-ordered two-layer and three-layer clays. In addition, the electron diffraction patterns are comparable between the four samples, with four main peaks that correspond to mean d-spacings of 4.49, 3.39, 2.58, and 1.58Å (Figure A3). These results are similar to those of Benzerara *et al*. (2007), who noted lattice spacings of 4.59, 3.53, 2.66, and 2.18Å in their FIB lamellae from tubular alteration features in subseafloor basalt glasses from the Ontong Java Plateau. Benzerara *et al*. interpreted these d-spacings as indicative of nontronite. While nontronite is a probable candidate in the samples analyzed in this study, the slight variability in d-spacings both within and between samples point to a mix of 1:1 and 2:1 clays, likely a combination of smectites, micas, and kaolin-serpentine group minerals, rather than one particular species. This interpretation corresponds well with the results of the lattice spacing measurements. Numerous reports on the abiotic alteration of subseafloor basalt glasses have noted that various mixtures of saponite, nontronite, and celadonite are common as secondary minerals lining cracks and vesicles, and a major component of palagonite (e.g. Staudigel and Hart, 1983; Clayton and Pearce, 2000; Giorgetti et al., 2001; Stroncik and Schmincke, 2002; Walton and Schiffman, 2003; Drief and Schiffman, 2004), as well as the importance of mixed clays in potential bioalteration features from various drill cores (Alt and Mata, 2000; Banerjee and Muehlenbachs, 2003; Benzerara et al., 2007; Staudigel et al., 2008; Fliegel et al., in press).

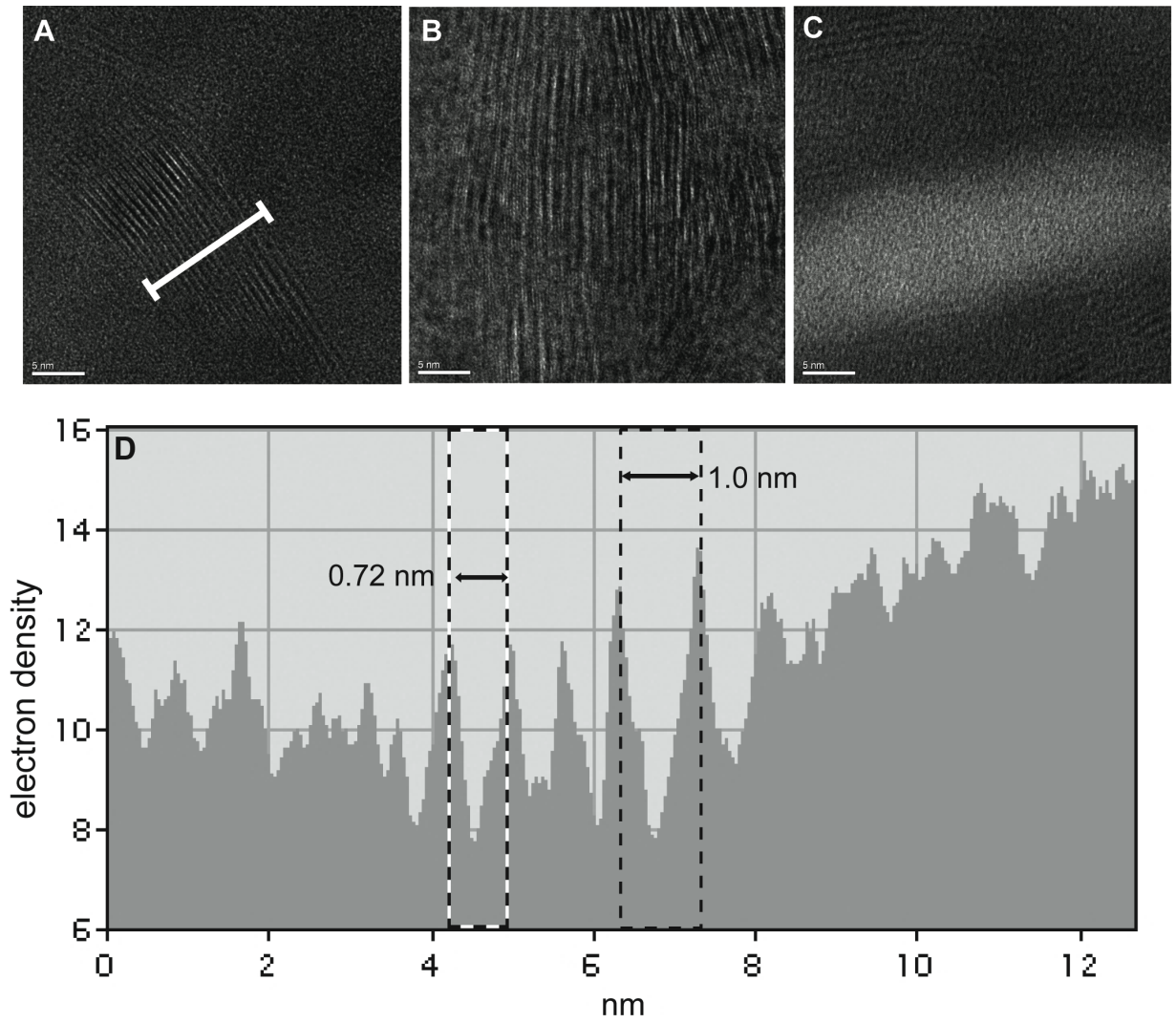

Figure 3. High-resolution images of the lattice fringes, showing the partially crystalline nature of the phyllosilicates A) Sample 896A-11R1, Foil #2814. B) Sample 418A-56-5, Foil #2813. C) Sample CY-1-34A Foil #2818. For sample 46-396B-20 Foil #2996, the phyllosilicates degraded too quickly in the electron beam to be able to acquire images of the lattice fringes, this was likely due to their decreased density. D) Intensity profile across the region shown by the white bar in image A). The peaks show the spaces between the crystal layers, which give regular d-spacings of 0.72 and 1.0 nm.

Figure 4 shows the electron energy loss spectroscopy (EELS) maps for one of the tubules cross-sectioned in sample 896A-11R1, Foil #2814. The Ca map shows a strong depletion throughout the tubule, while the Fe map shows a slight enrichment in the bulk of the tubule, but a thin line of depletion around its edge. The oxygen map shows no significant change in concentration between the tubule and the glass, but there is a clear enrichment of oxygen in a thin band around the tubule. This oxygen enrichment directly correspond with the band of Fe depletion, which shows that this is a real signal of compositional difference and not just an artifact of mapping. Closer visual inspection of the contact point between the phyllosilicates and the surrounding basalt glass reveals a thin rim around the tubule (Fig. 2). This rim is present in every tubule imaged from samples 896A-11R1, 418A-56-5, and CY-1-34A, ranging in width from approximately 20-50 nm. Sample 46-396B-20 doesn't show the same type of obvious thin rim, instead there is a more irregular perimeter around the tubules (Fig. 2). An EDX analysis of the rim of Foil #2813 from sample 418A-56-5 shows that it is strongly depleted in Mg, K, Ca, Mn, and Fe, but significantly enriched in Si compared to the glass (Fig. S1). This result, combined with the EELS maps, implies that the rims are formed by a differential leaching process, likely the incongruent dissolution of the glass during formation of the tubule (Crovisier et al., 1983; Berger et al., 1987; Benzerara et al., 2007).

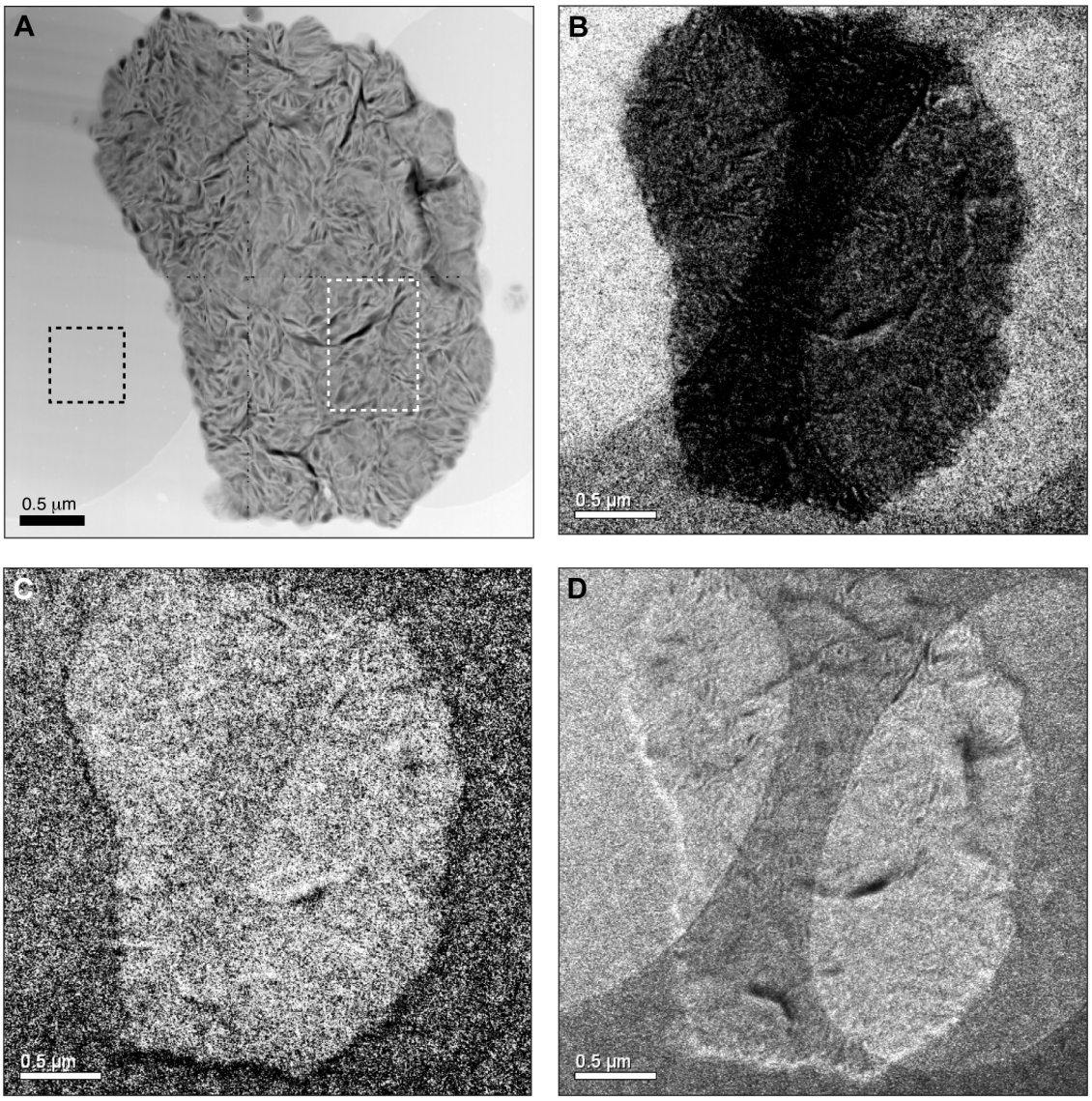

Figure 4. Energy electron loss spectroscopy (EELS) maps of the tubule in sample 896A-11R1, Foil #2814. A) HAADF TEM image of the region mapped. B) Calcium. C) Iron. D) Oxygen. The darker bar down the middle of the maps is the solid region between two holes in the lacy carbon TEM foil on which the lamella is resting. The boxes in A) show the collection locations for the EDX spectra shown in Figure 5.

Energy-dispersive X-ray spectroscopy measurements of selected volumes within the tubules and surrounding glass show that for every sample analyzed the most striking chemical changes are a strong depletion in Ca and enrichment in K (Fig. 5). For the rest of the elements analyzed the distributions show minor variability between samples. Mg, Al, and Si show little to no change in all samples. Fe is slightly enriched in the subseafloor samples, but somewhat depleted in the ophiolite sample. Overall there is little change in the concentration of Ti between the tubule-infilling material and the glass, but the low counts make the semi-quantitative analysis unreliable. These element distributions can be explained by the retention of all of the major elements in secondary phases, with the exceptions of Ca, which is lost from the system, and K, which appears to be taken up from seawater and incorporated into secondary minerals. Such patterns of element exchange are consistent with those seen in bulk studies across various seafloor alteration regimes (e.g. Staudigel and Hart, 1983; Furnes et al., 1999; Walton et al., 2005; Schramm et al., 2005).

In several of the tubules, EELS and EDX analyses revealed heterogeneously distributed carbon enrichments. EELS mapping shows that the carbon follows the same patterns as the phyllosilicate layers, indicating that the carbon and silicate phases are correlated or aligned (Fig. S2). By collecting EELS spectra of the carbon (Fig. S3) and oxygen K-edges, and the calcium L3,2-edge, and comparing them with those of carbonate, we were able to rule out the presence of carbonate in the tubules; instead, the carbon appears to be amorphous. While this hints at a possible organic origin for the carbon, a more precise determination of carbon species will require more complex spectroscopic analyses. It's possible that organic matter within the tubule acted as a template for initial phyllosilicate crystallization by providing nucleation sites, or conversely that the phyllosilicates sorbed organic matter from the circulating fluids.

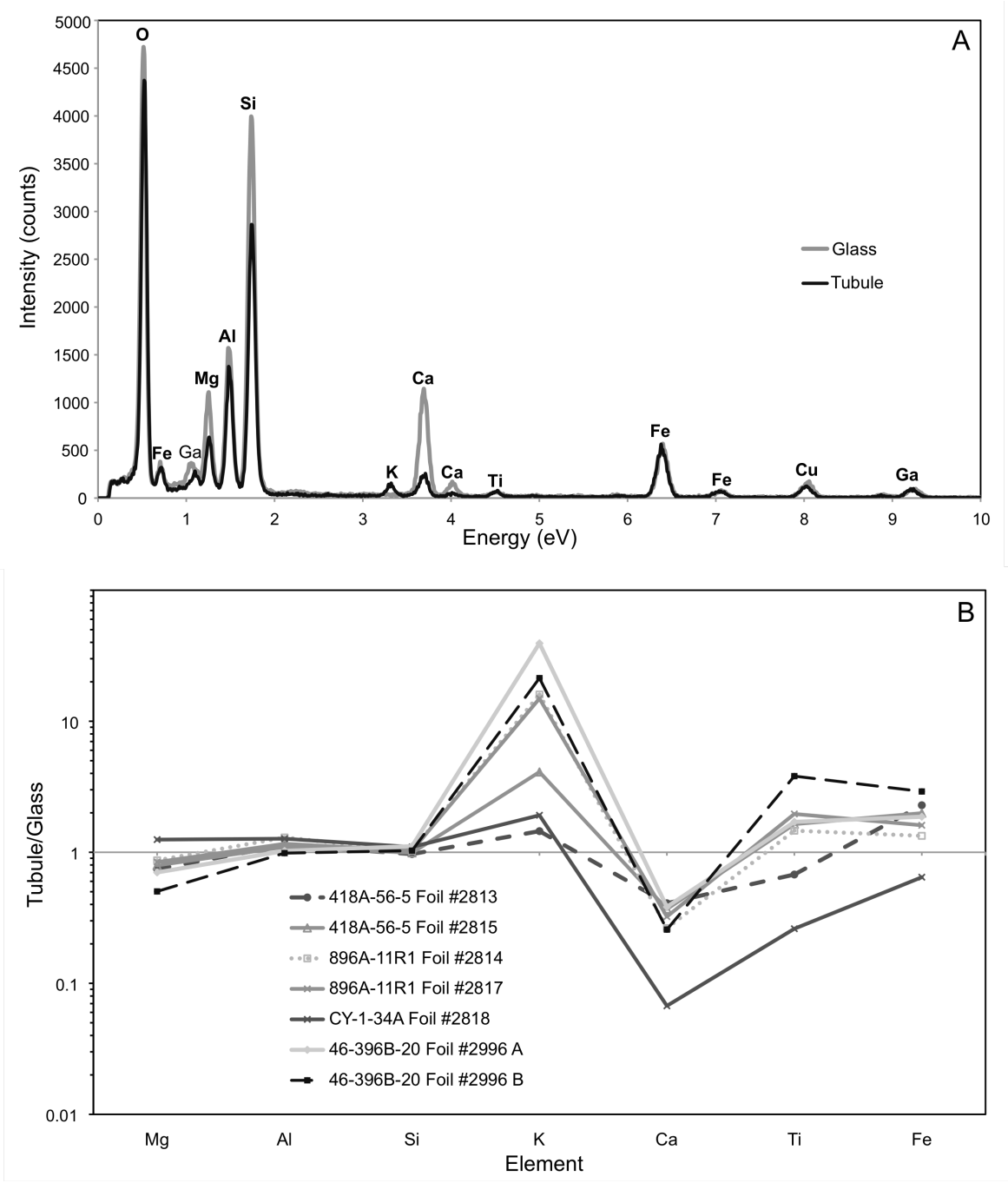

Figure 5. A) Energy-dispersive X-ray (EDX) spectra from the glass (gray) and within the tubule (black) from sample 896A-11R1 Foil #2814. The boxes in Figure 4 show the EDX spots analyzed. The Cu peak is due to the TEM grid, and the Ga peak is an artifact of FIB milling. B) Spidergram showing the changes in major element concentration relative to the glass for all four samples. For sample 46-396B-20 Foil #2996 two different datasets are shown, which correspond to the upper, less dense (A) and lower, denser (B) tubules shown in Figure 2.

4. Discussion

Put together these analyses can be used to differentiate between different stages in the tubular alteration process. Initial formation of the tubules appears to involve incongruent dissolution, where initially everything but Si and O are leached, followed by whole scale dissolution, leaving a tubule that is either hollow or partially in-filled with initial unstable phases, and a thin rim consisting of just the silicate matrix. At some point phyllosilicates infill the cavity, either through direct precipitation from supersaturated fluids in the hollow tubules, or dissolution and replacement of the initial phases in partially filled tubules. The fact that Fe is slightly enriched in subseafloor samples implies that either these phyllosilicates are somewhat Fe-rich, or that there is another Fe-bearing phase present in small amounts, mixed in with the clays. Fe oxides and hydroxides are common basalt glass alteration products, often showing strong Fe enrichments as a result of either passive accumulation or exogenous input (e.g. Alt and Honnorez, 1984; Alt, 1995; 1999; Clayton and Pearce, 2000; Schramm et al., 2005). In the tubules from the subseafloor samples the Fe enrichment is only very minor, and the ophiolite sample shows that Fe was actually slightly depleted, which implies that Fe oxides and hydroxides are not major alteration components within these samples. The predominance of Fe-bearing phyllosilicates instead of oxides within the tubules implies that the silica activity was very high within the fluids that interacted with the basalt glass. These systems are generally characterized by low water to rock ratios, thus strongly concentrating the dissolution products in the local fluids and likely supersaturating them with respect to Si, Mg, and Al.

These results are surprisingly comparable between all of the tubules analyzed in the four different samples. Chemically there are only slight differences between samples, namely in Fe concentration, with the main trends of Ca loss, retention of Mg, Al, and Si, enrichment of K

remaining constant. Visually the structural characteristics of the mineral phases in-filling the tubules are very similar, with poorly- to highly-ordered phyllosilicates infilling the tubules and thin leached rims at the contact with fresh glass. The only major structural differences are the irregular leached rim and variation in mineralization density in the tubules in sample 46-396B-20. It is possible that in this sample some of the material within the tubules was removed and that the rim was slightly damaged or destroyed during FIB milling, however this seems unlikely given that the final polishing on the FIB lamellae was done with a very gentle beam and that there are hollow spots in close proximity to densely-filled regions that do not appear damaged. It is more likely that this variation reflects differences in the timing, extent, and preservation of mineral precipitation. For the variation in mineral density there are two possible scenarios to consider: (1) the mineralization of the tubules was incomplete, leaving some spots only partially filled, or (2) the tubules were once completely in-filled with secondary phases (similar to the other three samples) but a significant amount of the mineralization, including parts of the leached rim, was lost in select locations due to later water-rock exchange. It appears that even in the hollow spots within the tubules there are thin mineral layers connecting from the margins to denser phyllosilicate packets (see lower left part of upper tubule in Fig. 2D), and the EDX analyses show that the chemistry of the phases in the denser tubules is nearly identical to that in the thinner regions (Fig. 5). This could indicate that the denser regions were the initial sites of mineral nucleation and that the phyllosilicates layers grew out into the hollows, which favors the first scenario. Without the ability to reproduce the formation and mineralization of tubules in the laboratory it is difficult, if not impossible, to determine which mineralization scenario is correct.

It is particularly interesting that the ophiolite sample, CY-1-34A, shows the same structural and general geochemical alteration patterns as the subseafloor drill core samples. Drill

hole CY-1 is located on the northern edge of the Troodos Ophiolite Complex in the Akaki River Canyon. Cutting through nearly all of the layers of the ophiolite, the exposure in this canyon and the small side canyons is excellent, revealing a cross-section of the stratigraphy. Thus, this region has been the site of extensive volcanology and geochemistry research (e.g. Bednarz and Schmincke, 1989; Malpas et al., 1990; Robinson et al., 2003; Cann and Gillis, 2004). These studies have shown that the alteration history of the ophiolite has been dynamic and variable, ranging from cold seawater to high-temperature hydrothermal alteration, and from oxygenated to anoxic fluids (Bednarz and Schmincke, 1989). In addition, both low and high-flow environments have been identified. Numerous thin sections have been made from both the drill cores and field exposures, some of which contain fresh glass with abundant tubular bioalteration features (Furnes et al., 2001a; Staudigel et al., 2008; McLoughlin et al., 2009). The drill core sample used in this study came from the region identified by Bednarz and Schmincke (1989) as the "low temperature hydrothermal alteration zone" (LTA), just below the "cold seawater alteration zone". The LTA has a mean seawater/rock ratio of ~20 and is characterized by enrichment of Na_2O and K_2O, with celadonite, smectite, and celadonite-saponite mixtures as the predominant secondary minerals (Bednarz and Schmincke, 1989). The chemistry of the circulating fluids in the LTA appears to have been affected at least somewhat by hydrothermal processes deeper in the section, however, temperatures in the LTA likely never exceeded ~170°C, which is the limit for saponite formation (Stakes and O'Neil, 1982).

While there are many close similarities, the alteration histories of the Troodos ophiolite and subseafloor samples differ in a few key aspects. In Holes 396B and 896A, alteration appears to have been controlled primarily by low-temperature (<100°C) oxidized seawater, with clays, namely saponite, as the main secondary phases, plus frequent Fe-oxyhydroxides (Böhlke et al.,

1980; Laverne et al., 1996). The basalts from Hole 418A are characterized by extensive and complex alteration histories, involving different stages of low temperature (<50°C) oxidized and anoxic fluid flow, as well as possible mixing of oxygenated seawater with cool hydrothermally-derived fluids. These various alteration stages resulted in the formation of a mix of clays (primarily smectites), chlorite, Fe-hydroxides, pyrite, zeolites, and minor calcite (Alt and Honnorez, 1984). Overall, the fluids circulating through Holes 418A, 896A, and 396B reflect a composition closer to low-temperature, oxygenated seawater than the fluids in the LTA zone of hole CY-1.

In addition, the volcanic compositions differ between the Troodos ophiolite and the subseafloor samples. The lavas making up the Troodos ophiolite are characterized by both higher silica and volatile contents, reflecting compositions more similar to island-arc volcanics than mid-ocean ridge basalts (MORBs) (Schmincke et al., 1983; Robinson et al., 1983). This fits with the assumption that the complex formed in a subduction zone (Pearce et al., 1984). In contrast, the compositions of the volcanics from Holes 418A, 896A, and 396B range from average MORB to highly depleted in incompatible elements, depending on the degree of alteration (Staudigel et al., 1989; Alt et al., 1993). Given the differences in both the host rock and circulating fluid compositions, combined with the fact that the Troodos ophiolite underwent obduction and has since been exposed to subaerial weathering conditions, it is intriguing that the textural and mineralogical characteristics of the tubular alteration features are so similar between the ophiolite and subseafloor samples. This indicates either that processes of formation and mineralization of the tubules are common throughout different alteration environments and though time, or perhaps that the tubules formed only in brief windows of the alteration histories of these samples, possibly when the physical and chemical conditions of the fluid-rock

interactions were at a similar stage. Considering the small sizes of the tubules and the lack of potential isotopes suitable for geochronology, it has not yet been possible to date the minerals in-filling the tubules. Future technique development might enable such a study, which would provide valuable insight into the timing of tubule formation.

It is interesting to note the similarities between the results of this study and those of the few previous high-resolution studies of tubular alteration features in subseafloor basalt glasses and ophiolites. Alt and Mata (2000) were the first to image tubular alteration features at high resolution. The sample they analyzed was from ODP Hole 504B, which is located 1km northwest of Hole 896A (Alt et al., 1993). By using Ar ion thinning coupled with TEM they were able to see the layering of the phyllosilicates and measure a 10Å lattice spacing. They interpreted these secondary phases as a montmorillonite-saponite mixture, interlayered with berthierine, as well as an unidentified mica, and occasional pyrite. Their EDX analyses show depletions of Ca and Na and strong enrichments of Mg, Fe, Mn, and K in the tubule interiors. The textures of the alteration zones that Alt and Mata imaged are very similar to those seen in the current study. In their images there is no narrow rim surrounding the tubules, but instead Alt and Mata identify a broad leached zone of amorphous "altered glass" surrounding the phyllosilicates with a smooth transition between the two. It's possible that this is a wide leached zone analogous to the thin rims noted in the current study, or that it reflects damage from Ar ion thinning.

In the first combined FIB/TEM study of tubular alteration features, Benzerara *et al*. (2007) analyzed tubules in drill core samples from the Ontong Java Plateau. Their results are very similar to those presented in the current study. They clearly showed thin Si-rich rims around tubules. They also identified the presence of partially crystalline secondary phases within the alteration features mixed with an amorphous matrix, and interpreted the in-filling material as

palagonite containing a mix of smectites (see above). Their EDX analyses showed the same depletion of Ca and enrichment of K within the tubules and that the secondary phases consist of primarily Si, O, Al, Mg, and Fe. The second study to use FIB/TEM in the analysis of subseafloor basalt alteration features focused on a sample from DSDP Hole 418 (sample 418A-55-4, 112-114 cm) (Fliegel et al., in press), which is complementary to sample 418A-56-5 used in the current study. Fliegel *et al*. compared the textures and chemistry of tubules with granular alteration features, which are micron-sized agglomerations of spherical globules found along cracks, often associated with tubules (Furnes et al., 2001b). Their data show thin, leached, amorphous rims and secondary mineralization by phyllosilicates in both types of alteration, with notable variation in the density of in-filling material from completely hollow to tightly packed. EDX analyses confirm that the rims are depleted in major cations and that the phyllosilicates are enriched in Fe. From these results Fliegel *et al*. were able to show that granular alteration is very similar to tubular alteration in terms of both formation mechanisms and mineralization.

Two previous studies have coupled FIB milling and TEM for the analysis of tubular alteration features in ophiolites. One study focused on samples from the 2.0 Ga Pechenga Greenstone Belt in NW Russia (Fliegel et al., 2010b). This formation has undergone low to mid-temperature metamorphism, and samples were collected from meta-volcanic glass in prehnite–pumpellyite to lower greenschist facies. In the second study Fliegel *et al*. (2011) analyzed samples from the ~443 Ma Solund-Stavfjord ophiolite complex in western Norway. The pillow basalts in this formation have undergone moderate metamorphism to greenschist facies, with most of the glass replaced by chlorite. The tubules examined in both of these studies appear broadened and significantly altered compared to those in the subseafloor basalts or Troodos ophiolite, likely due to recrystallization and phase changes during metamorphism. Thus, it does

not make sense to draw comparisons between these studies and the sample from the preserved glassy margins of the Troodos ophiolite used in this study.

5. Conclusions

These results define the common mineralogical characteristics of tubular glass alteration features and thereby help to elucidate the mechanisms of tubule formation and mineralization. However, they do not answer the question about the putative biogenicity of the tubules. The poorly- to highly-ordered clays in-filling the tubules are reminiscent of the secondary phases that replace glass during abiotic alteration. Although it is well known that microorganisms can promote the precipitation of poor-ordered clays (e.g. Ferris et al., 1987; Douglas and Beveridge, 1998; Konhauser and Urrutia, 1999), the similarities between the secondary phases in tubules and those formed in abiotic alteration experiments makes it impossible to rule out a purely abiotic origin for these secondary phases. These results, however, do not rule out the possibility of the biological formation of the tubules. It is possible that microorganisms are directly or indirectly responsible for the initial dissolution of the glass that created the tubules, either by promoting dissolution during microbial boring into the glass, or as a secondary effect of their metabolic activities. Microbial dissolution of basalt glass would likely promote the authigenic precipitation of biominerals such as Fe- and Mn-oxides and nano-particulate clays, some of which may still be constituents in the material in-filling the tubules. Over time, continued water-rock exchange likely replaced most of the initial biogenic material and the bulk of any remaining cellular material with the more stable phyllosilicate phases identified in all of the samples analyzed in this study. Until we are able to date the phases in-filling the tubules, find younger

examples of tubules, and/or form them in the lab, the potential role of microorganisms in tubular alteration of subseafloor basalt glass will remain enigmatic.

The four samples analyzed in this study, and the two from Alt and Mata and Benzerara *et al*. are from four different subseafloor drill cores and one ophiolite, were collected at different depths in the drill cores, and represent significantly different ages – spanning over 115 million years. Thus, it is remarkable that the textural and chemical characteristics of the tubules are so similar. It appears that the processes of tubule formation and mineralization are common throughout the ocean basins and have remained steady throughout a significant window of time. By examining the textural and geochemical characteristics of these features on the sub-micron scale we were able to identify the likely different stages in the tubular alteration process. The ability to identify and chemically analyze the thin leached rims around the tubules, image the structural characteristics of the in-filling material, and conduct EDX analyses at specific locations with sub-micron spot sizes required the high-resolution and fine-scale capabilities of FIB milling coupled with TEM. The application of these powerful techniques to other geochemical or geobiological systems could significantly increase our knowledge of processes functioning on the micron to sub-micron scale.

6. Acknowledgements

A sincere thank you to Anja Schreiber at GeoForschungsZentrum for technical assistance on the FIB. Thank you to Harald Furnes, Hubert Staudigel, and Nicola McLoughlin for samples and scientific input. This work was supported by a Leiv Eiriksson mobility grant from the Research Council of Norway, a NASA Earth and Space Science Fellowship, and the David and Lucile Packard Foundation.

7. References

Alt, J.C., Kinoshita, H., Stokking, L.B., et al., 1993. Site 896, in: Proceedings of the Ocean Drilling Program; Initial reports, Leg 148, Ocean Drilling Program, College Station, TX.

Alt, J.C., 1999. Very low-grade hydrothermal metamorphism of basic igneous rocks, in: Frey, M. and Robinson, D., (Eds.), Low Grade Metamorphism: Oxford, UK, Blackwell, 169-201.

Alt, J.C., 1995. Subseafloor Processes in Mid-Ocean Ridge Hydrothermal Systems, in: Humphris, S.E., Zierenberg, R.A., Mullineaux, L.S. and Thomson, R.E., (Eds.), Seafloor Hydrothermal Systems: Physical, Chemical, Biological, and Geological Interactions: American Geophysical Union Geophysical Monograph. 91, 85-114.

Alt, J.C., Davidson, G.J., Teagle, D.A.H., and Karson, J.A., 2003. Isotopic composition of gypsum in the Macquarie Island ophiolite: Implications for the sulfur cycle and the subsurface biosphere in oceanic crust. Geology. 31: 6, 549-552.

Alt, J.C., and Honnorez, J., 1984. Alteration of the upper oceanic crust, DSDP Site-417 - Mineralogy and Chemistry. Contrib Mineral Petrol. 87: 2, 149-169.

Alt, J.C., and Mata, P., 2000. On the role of microbes in the alteration of submarine basaltic glass: a TEM study. Earth Planet Sci Lett. 181: 3, 301-313.

Alt, J.C., Teagle, D.A.H., Brewer, T., III, S.W.C., and Halliday, A., 1998. Alteration and mineralization of an oceanic forearc and the ophiolite-ocean crust analogy. J Geophys Res. 103, 12365-12380.

Bach, W., and Edwards, K.J., 2003. Iron and sulfide oxidation within the basaltic ocean crust: Implications for chemolithoautotrophic microbial biomass production. Geochim Cosmochim Acta. 67: 20, 3871-3887.

Banerjee, N.R., Furnes, H., Muehlenbachs, K., Staudigel, H., and de Wit, M., 2006. Preservation of ~3.4-3.5 Ga microbial biomarkers in pillow lavas and hyaloclastites from the Barberton Greenstone Belt, South Africa. Earth Planet Sci Lett. 241: 3-4, 707-722.

Banerjee, N.R., and Muehlenbachs, K., 2003. Tuff life: Bioalteration in volcaniclastic rocks from the Ontong Java Plateau. Geochem Geophys Geosys. 4.

Banerjee, N.R., Simonetti, A., Furnes, H., Muehlenbachs, K., Staudigel, H., Heaman, L., and Van Kranendonk, M.J., 2007. Direct dating of Archean microbial ichnofossils. Geology. 35: 6, 487-490.

Bednarz, U., and Schmincke, H.U., 1989. Mass transfer during sub-seafloor alteration of the upper Troodos crust (Cyprus). Contrib Mineral Petrol. 102: 1, 93-101.

Benzerara, K., Menguy, N., Banerjee, N.R., Tyliszczak, T., Brown, G.E., and Guyot, F., 2007. Alteration of submarine basaltic glass from the Ontong Java Plateau: A STXM and TEM study. Earth Planet Sci Lett. 260: 1-2, 187-200.

Benzerara, K., Menguy, N., Guyot, F., Vanni, C., and Gillet, P., 2005. TEM study of a silicate-carbonate-microbe interface prepared by focused ion beam milling. Geochim Cosmochim Acta. 69: 6, 1413-1422.

Berger, G., Schott, J., and Loubet, M., 1987. Fundamental processes controlling the 1st stage of alteration of a basalt glass by seawater - an experimental study between 200°C and 320°C. Earth Planet Sci Lett. 84: 4, 431-445.

Bernard, S., Benzerara, K., Beyssac, O., Menguy, N., Guyot, F., Brown, G.E., and Goffe, B., 2007. Exceptional preservation of fossil plant spores in high-pressure metamorphic rocks. Earth Planet Sci Lett. 262: 1-2, 257-272.

Böhlke, J.K., Honnorez, J., and Honnorez-Guerstein, B.M., 1980. Alteration of basalts from site 396 B, DSDP: Petrographic and mineralogic studies. Contrib Mineral Petrol. 73: 4, 341-364.

Cann, J., and Gillis, K., 2004, Hydrothermal insights from the Troodos ophiolite, Cyprus, in: Davis, E.E. and Elderfield, H., (Eds.), Hydrogeology of the Oceanic Lithosphere: Cambridge, UK, Cambridge University Press.

Cavalazzi, B., 2007. Chemotrophic filamentous microfossils from the Hollard Mound (Devonian, Morocco) as investigated by focused ion beam. Astrobiology. 7, 402-415.

Clayton, T., and Pearce, R.B., 2000. Alteration mineralogy of Cretaceous basalt from ODP Site 1001, Leg 165 (Caribbean Sea). Clay Miner. 35: 4, 719-733.

Crovisier, J.L., Honnorez, J., and Eberhart, J.P., 1987. Dissolution of Basaltic Glass in Seawater - Mechanism and Rate. Geochim Cosmochim Acta. 51: 11, 2977-2990.

Crovisier, J.L., Thomassin, J.H., Juteau, T., Eberhart, J.P., Touray, J.C., and Baillif, P., 1983. Experimental Seawater Basaltic Glass Interaction at 50°C - Study of Early Developed Phases by Electron Microscopy and X-Ray Photoelectron Spectrometry. Geochim Cosmochim Acta. 47: 3, 377-387.

Dmitriev, L., Heirtzler, J., Kirkpatrick, J., Matthews, D., Petersen, N., et al., 1978. Initial Reports of the Deep Sea Drilling Project, vol. 46, Ocean Drilling Program, College Station, TX.

Donnelly, T., Francheteau, J., Bryan, W., Robinson, P.T., Flower, M.F.J., and Salisbury, M., 1979. Initial Reports of the Deep Sea Drilling Project, vol. 51, 52, 53. Ocean Drilling Program, College Station, TX.

Douglas, S., and Beveridge, T.J., 1998. Mineral formation by bacteria in natural microbial communities. FEMS Microbiol Ecol. 26: 2, 79-88.

Drief, A., and Schiffman, P., 2004. Very low-temperature alteration of sideromelane in hyaloclastites and hyalotuffs from Kilauea and Mauna Kea volcanoes: Implications for the mechanism of palagonite formation. Clays Clay Miner. 52: 5, 622-634.

Edmond, J.M., Measures, C., McDuff, R.E., et al., 1979. Ridge crest hydrothermal activity and the balances of the major and minor elements in the ocean - Galapagos data. Earth Planet Sci Lett. 46: 1, 1-18.

Edwards, K.J., Becker, K., and Colwell, F., 2012. The deep, dark energy biosphere: intraterrestrial life on Earth. Ann Rev Earth Planet Sci. 40: 1, 551-568.

Edwards, K.J., Wheat, C.G., and Sylvan, J.B., 2011. Under the sea: microbial life in volcanic oceanic crust. Nat Rev Microbiol. 9: 10, 703-712.

Ehret, G., Crovisier, J.L., and Eberhart, J.P., 1986. A new method for studying leached glasses: Analytical electron microscopy on ultramicrotomic thin sections. J Non Cryst Solids. 86: 1-2, 72-79.

Einen, J., Kruber, C., Øvreås, L., Thorseth, I.H., and Torsvik, T., 2006. Microbial colonization and alteration of basaltic glass. Biogeosci Disc. 3: 2, 273-307.

Ferris, F.G., Fyfe, W.S., and Beveridge, T.J., 1987. Bacteria as Nucleation Sites for Authigenic Minerals in a Metal-Contaminated Lake Sediment. Chem Geol. 63: 3-4, 225-232.

Fisk, M.R., Giovannoni, S.J., and Thorseth, I.H., 1998. Alteration of oceanic volcanic glass: Textural evidence of microbial activity. Science. 281: 5379, 978-980.

Fliegel, D., Knowles, E., Wirth, R., Templeton, A., Staudigel, H., Muehlenbachs, K., and Furnes, H., (in press). Characterization of alteration textures in Cretaceous oceanic crust from the N-Atlantic (DSDP Hole 418) by spatially-resolved spectroscopy. Geochim Cosmochim Acta.

Fliegel, D., Kosler, J., McLoughlin, N., Simonetti, A., de Wit, M.J., Wirth, R., and Furnes, H., 2010a. In-situ dating of the Earth's oldest trace fossil at 3.34 Ga. Earth Planet Sci Lett. 299: 3-4, 290-298.

Fliegel, D., Wirth, R., Simonetti, A., Furnes, H., Staudigel, H., Hanski, E., and Muehlenbachs, K., 2010b. Septate-tubular textures in 2.0-Ga pillow lavas from the Pechenga Greenstone Belt: a nano-spectroscopic approach to investigate their biogenicity. Geobiology. 8: 5, 372-390.

Fliegel, D., Wirth, R., Simonetti, A., Schreiber, A., Furnes, H., and Muehlenbachs, K., 2011. Tubular textures in pillow lavas from a Caledonian west Norwegian ophiolite: A combined TEM, LA-ICP-MS, and STXM study. Geochem Geophys Geosys. 12.

Furnes, H., 1984. Chemical changes during progressive subaerial palagonitization of a subglacial olivine tholeiite hyaloclastite - a microprobe study. Chem Geol. 43: 3-4, 271-285.

Furnes, H., Banerjee, N.R., Muehlenbachs, K., Staudigel, H., and de Wit, M., 2004. Early life recorded in Archean pillow lavas: Science. 304: 5670, 578-581.

Furnes, H., Muehlenbachs, K., Tumyr, O., Torsvik, T., and Thorseth, I.H., 1999. Depth of active bio-alteration in the ocean crust: Costa Rica Rift (Hole 504B). Terra Nova. 11: 5, 228-233.

Furnes, H., Muehlenbachs, K., Tumyr, O., Torsvik, T., and Xenophontos, C., 2001a. Biogenic alteration of volcanic glass from the Troodos ophiolite, Cyprus. J Geol Soc. 158, 75-82.

Furnes, H., Staudigel, H., Thorseth, I.H., Torsvik, T., Muehlenbachs, K., and Tumyr, O., 2001b. Bioalteration of basaltic glass in the oceanic crust. Geochem Geophys Geosys. 2.

Giorgetti, G., Marescotti, P., Cabella, R., and Lucchetti, G., 2001. Clay mineral mixtures as alteration products in pillow basalts from the eastern flank of Juan de Fuca Ridge: a TEM-AEM study. Clay Miner. 36: 1, 75-91.

Heaney, P.J., Vicenzi, E.P., Giannuzzi, L.A., and Livi, K.J.T., 2001. Focused ion beam milling: A method of site-specific sample extraction for microanalysis of Earth and planetary materials. Am Mineral. 86: 9, 1094-1099.

Hoffland, E., Giesler, R., Jongmans, A.G., and van Breemen, N., 2003. Feldspar tunneling by fungi along natural productivity gradients. Ecosystems. 6: 8, 739-746.

Hofmann, A.W., and White, W.M., 1982. Mantle plumes from ancient oceanic crust. Earth Planet Sci Lett. 57: 2, 421-436.

Jongmans, A.G., Van Breemen, N., Lundström, U.S., et al., 1997. Rock eating fungi. Nature. 389, 682-683.

Kempe, A., Wirth, R., Altermann, W., Stark, R.W., Schopf, J.W., and Heckl, W.A., 2005. Focused ion beam preparation and in situ nanoscopic study of Precambrian acritarchs. Precambrian Research. 140: 1-2, 36-54.

Konhauser, K.O., and Urrutia, M.M., 1999. Bacterial clay authigenesis: a common biogeochemical process. Chem Geol. 161, 399-413.

Laverne, C., Belarouchi, A., and Honnorez, J., 1996. Alteration mineralogy and chemistry of the upper oceanic crust from Hole 896A, Costa Rica Rift, in: Proceedings of the Ocean Drilling Program, Scientific Results, Ocean Drilling Program, College Station, TX, 151-170.

Lee, M.R., 2010. Transmission electron microscopy (TEM) of Earth and planetary materials: A review. Mineralogical Magazine. 74: 1, 1-27.

Lee, M.R., Bland, P.A., and Graham, G., 2003. Preparation of TEM samples by focused ion beam (FIB) techniques: applications to the study of clays and phyllosilicates in meteorites. Mineralogical Magazine. 67: 3, 581-592.

Lee, M.R., Brown, D.J., Smith, C.L., Hodson, M.E., Mackenzie, M., and Hellmann, R., 2007. Characterization of mineral surfaces using FIB and TEM: A case study of naturally weathered alkali feldspars. Am Mineral. 92: 8-9, 1383-1394.

Lepot, K., Benzerara, K., and Philippot, P., 2011. Biogenic versus metamorphic origins of diverse microtubes in 2.7 Gyr old volcanic ashes: Multi-scale investigations. Earth Planet Sci Lett. 312, 37-47.

Malpas, J., Moores, E.M., Panayiotou, A., and Xenophontos, C., 1990. Ophiolites: Oceanic Crustal Analogs. Proceedings of the Symposium 'Troodos 1987': Nicosia, Cyprus, The Geological Survey Department, Ministry of Agriculture and Natural Resources.

Mason, O.U., Nakagawa, T., Rosner, M., et al., 2010. First investigation of the microbiology of the deepest layer of ocean crust. PLoS One. 5: 11, e15399.

McLoughlin, N., Brasier, M.D., Wacey, D., Green, O.R., and Perry, R.S., 2007. On biogenicity criteria for endolithic microborings on early earth and beyond. Astrobiology. 7: 1, 10-26.

McLoughlin, N., Furnes, H., Banerjee, N.R., Muehlenbachs, K., and Staudigel, H., 2009. Ichnotaxonomy of microbial trace fossils in volcanic glass. J Geol Soc, London. 166, 159-169.

McLoughlin, N., Wacey, D., Kruber, C., Kilburn, M.R., Thorseth, I.H., and Pedersen, R.B., 2011. A combined TEM and NanoSIMS study of endolithic microfossils in altered seafloor basalt. Chem Geol. 289, 154-162.

Ménez, B., Pasini, V., and Brunelli, D., 2012. Life in the hydrated suboceanic mantle. Nature Geosci. 5: 2, 133-137.

Orcutt, B.N., Sylvan, J.B., Knab, N.J., and Edwards, K.J., 2011. Microbial ecology of the dark ocean above, at, and below the seafloor. Microbiol Mol Biol Rev. 75: 2, 361-422.

Pearce, J.A., Lippard, S.J., and Roberts, S., 1984. Characteristics and tectonic significance of supra-subduction zone ophiolites, in: Kokelaar, B.P. and Howells, M.F., (Eds.), Marginal Basin Geology: Volcanic and Associated Sedimentary and Tectonic Processes in Modern and Ancient Marginal Basins: London, UK, Geological Society London, 77-94.

Robinson, P.T., Melson, W.G., Ohearn, T., and Schmincke, H.U., 1983. Volcanic glass compositions of the Troodos Ophiolite, Cyprus. Geology. 11: 7, 400-404.

Robinson, P.T., Malpas, J., and Xenophontos, C., 2003. The Troodos Massif of Cyprus: Its role in the evolution of the ophiolite concept. Geological Society of America Special Papers. 373, 295-308.

Rouxel, O., Ono, S.H., Alt, J., Rumble, D., and Ludden, J., 2008. Sulfur isotope evidence for microbial sulfate reduction in altered oceanic basalts at ODP Site 801. Earth Planet Sci Lett. 268, 110-123.

Santelli, C.M., Banerjee, N., Bach, W., and Edwards, K.J., 2010. Tapping the subsurface ocean crust biosphere: low biomass and drilling-related contamination calls for improved quality controls. Geomicrobiol J. 27: 2, 158-169.

Schiffbauer, J.D., and Xiao, S.H., 2009. Novel application of focused ion beam electron microscopy (FIB-EM) in preparation and analysis of microfossil ultrastructures: a new view of complexity in early eukaryotic organisms. PALAIOS. 24, 616-626.

Schmincke, H.U., Rautenschlein, M., Robinson, P.T., and Mehegan, J.M., 1983. Troodos extrusive series of Cyprus: A comparison with oceanic crust. Geology. 11: 7, 405-409.

Schmincke, H., and Bednarz, U., 1990. Pillow, sheet flow and breccia flow volcanics and volcano-tectonic hydrothermal cycles in the Extrusive Series of the northeastern Troodos ophiolite (Cyprus), in: Malpas, J., Moores, E.M., Panayiotou, A. and Xenophontos, C., (Eds.), Ophiolites: Oceanic Crustal Analogs. Proceedings of the Symposium 'Troodos 1987': Nicosia, Cyprus, The Geological Survey Department, Ministry of Agriculture and Natural Resources, 185-206.

Schramm, B., Devey, C.W., Gillis, K.M., and Lackschewitz, K., 2005. Quantitative assessment of chemical and mineralogical changes due to progressive low-temperature alteration of East Pacific Rise basalts from 0 to 9 Ma. Chem Geol. 218, 281-313.

Schumann, G., Manz, W., Reitner, J., and Lustrino, M., 2004. Ancient fungal life in North Pacific Eocene oceanic crust. Geomicrobiol J. 21: 4, 241-246.

Stakes, D.S., and O'Neil, J.R., 1982. Mineralogy and stable isotope geochemistry of hydrothermally altered oceanic rocks. Earth Planet Sci Lett. 57: 2, 285-304.

Stakes, D.S., Taylor, H.P., and Fisher, R.L., 1984. Oxygen-isotope and geochemical characterization of hydrothermal alteration in ophiolite complexes and modern oceanic crust. Geological Society, London, Special Publications. 13: 1, 199-214.

Staudigel, H., Chastain, R.A., Yayanos, A., and Bourcier, W., 1995. Biologically mediated dissolution of glass: Chem Geol. 126: 2, 147-154.

Staudigel, H., Furnes, H., McLoughlin, N., Banerjee, N.R., Connell, L.B., and Templeton, A., 2008. 3.5 billion years of glass bioalteration: Volcanic rocks as a basis for microbial life? Earth-Sci Rev. 89, 156-176.

Staudigel, H., and Hart, S.R., 1983. Alteration of basaltic glass - mechanisms and significance for the oceanic-crust seawater budget. Geochim Cosmochim Acta. 47: 3, 337-350.

Staudigel, H., Hart, S.R., Schmincke, H.U., and Smith, B.M., 1989. Cretaceous ocean crust at DSDP Site-417 and Site-418 - Carbon uptake from weathering versus loss by magmatic outgassing. Geochim Cosmochim Acta. 53: 11, 3091-3094.

Staudigel, H., Yayanos, A., Chastain, R., et al., 1998. Biologically mediated dissolution of volcanic glass in seawater. Earth Planet Sci Lett. 164, 233-244.

Staudigel, H., Furnes, H., Banerjee, N.R., Dilek, Y., and Muehlenbachs, K., 2006. Microbes and volcanoes. A tale from the oceans, ophiolites, and greenstone belts: GSA Today. 16: 10, 4-10.

Storrie-Lombardi, M.C., and Fisk, M.R., 2004. Elemental abundance distributions in suboceanic basalt glass: Evidence of biogenic alteration. Geochem Geophys Geosys. 5.

Stroncik, N.A., and Schmincke, H.U., 2002. Palagonite - a review. Int J Earth Sci. 91, 680-697.

Templeton, A.S., Knowles, E.J., Eldridge, D.L., et al., 2009. A seafloor microbial biome hosted within incipient ferromanganese crusts. Nature Geosci. 2: 12, 872-876.

Thorseth, I.H., Fumes, H., and Tumyr, O., 1995. Textural and chemical effects of bacterial-activity on basaltic glass - an experimental approach. Chem Geol. 119, 139-160.

Thorseth, I.H., Furnes, H., and Tumyr, O., 1991. A textural and chemical study of Icelandic palagonite of varied composition and its bearing on the mechanism of the glass-palagonite transformation. Geochim Cosmochim Acta. 55: 3, 731-749.

Torsvik, T., Furnes, H., Muehlenbachs, K., Thorseth, I.H., and Tumyr, O., 1998. Evidence for microbial activity at the glass-alteration interface in oceanic basalts. Earth Planet Sci Lett. 162, 165-176.

Wacey, D., Kilburn, M.R., Saunders, M., Cliff, J., and Brasier, M.D., 2011. Microfossils of sulphur-metabolizing cells in 3.4-billion-year-old rocks of Western Australia. Nature Geosci. 4, 698–702.

Walton, A.W., 2008. Microtubules in basalt glass from Hawaii Scientific Drilling Project #2 phase 1 core and Hilina slope, Hawaii: evidence of the occurrence and behavior of endolithic microorganisms. Geobiology. 6: 4, 351-364.

Walton, A.W., and Schiffman, P., 2003. Alteration of hyaloclastites in the HSDP 2 Phase 1 Drill Core - 1. Description and paragenesis. Geochem Geophys Geosys. 4.

Walton, A.W., Schiffman, P., and Macpherson, G.L., 2005. Alteration of hyaloclastites in the HSDP 2 Phase 1 Drill Core: 2. Mass balance of the conversion of sideromelane to palagonite and chabazite. Geochem Geophys Geosys. 6.

Wirth, R., 2009. Focused Ion Beam (FIB) combined with SEM and TEM: Advanced analytical tools for studies of chemical composition, microstructure and crystal structure in geomaterials on a nanometre scale. Chem Geol. 261: 3-4, 217-229.

Wirth, R., 2004. Focused Ion Beam (FIB): A novel technology for advanced application of micro- and nanoanalysis in geosciences and applied mineralogy. Eur J Mineral. 16: 6, 863-876.

Xenophontos, C., and Malpas, J.G., 1987. Sheeted dikes and their relationships to pillow lavas and plagiogranite, in: Xenophontos, C. and Malpas, J.G., (Eds.), Ophiolites and oceanic lithosphere: field excursion guidebook: Nicosia, Cyprus, Geological Survey Department, p.80-87.

Zhou, W.M., Peacor, D.R., Alt, J.C., Van der Voo, R., and Kao, L.S., 2001. TEM study of the alteration of interstitial glass in MORB by inorganic processes. Chem Geol. 174, 365-376.

8. Supplementary Figures

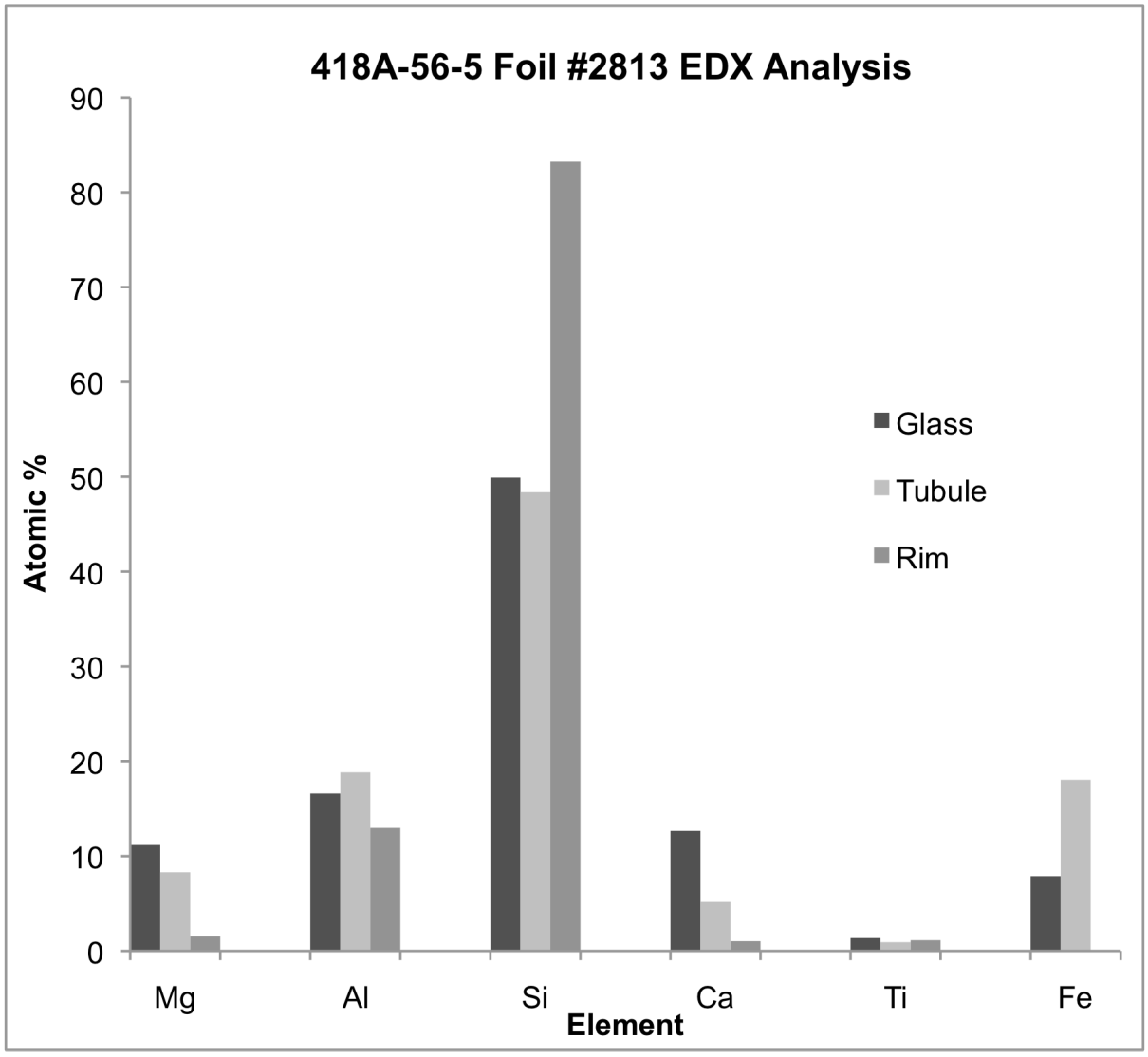

Figure S1. Results of EDX semi-quantitative analyses on three different spots in sample 418A-56-5 Foil #2813. The basalt glass is shown in dark gray, the tubule interior in light gray, and the rim in mid-gray.

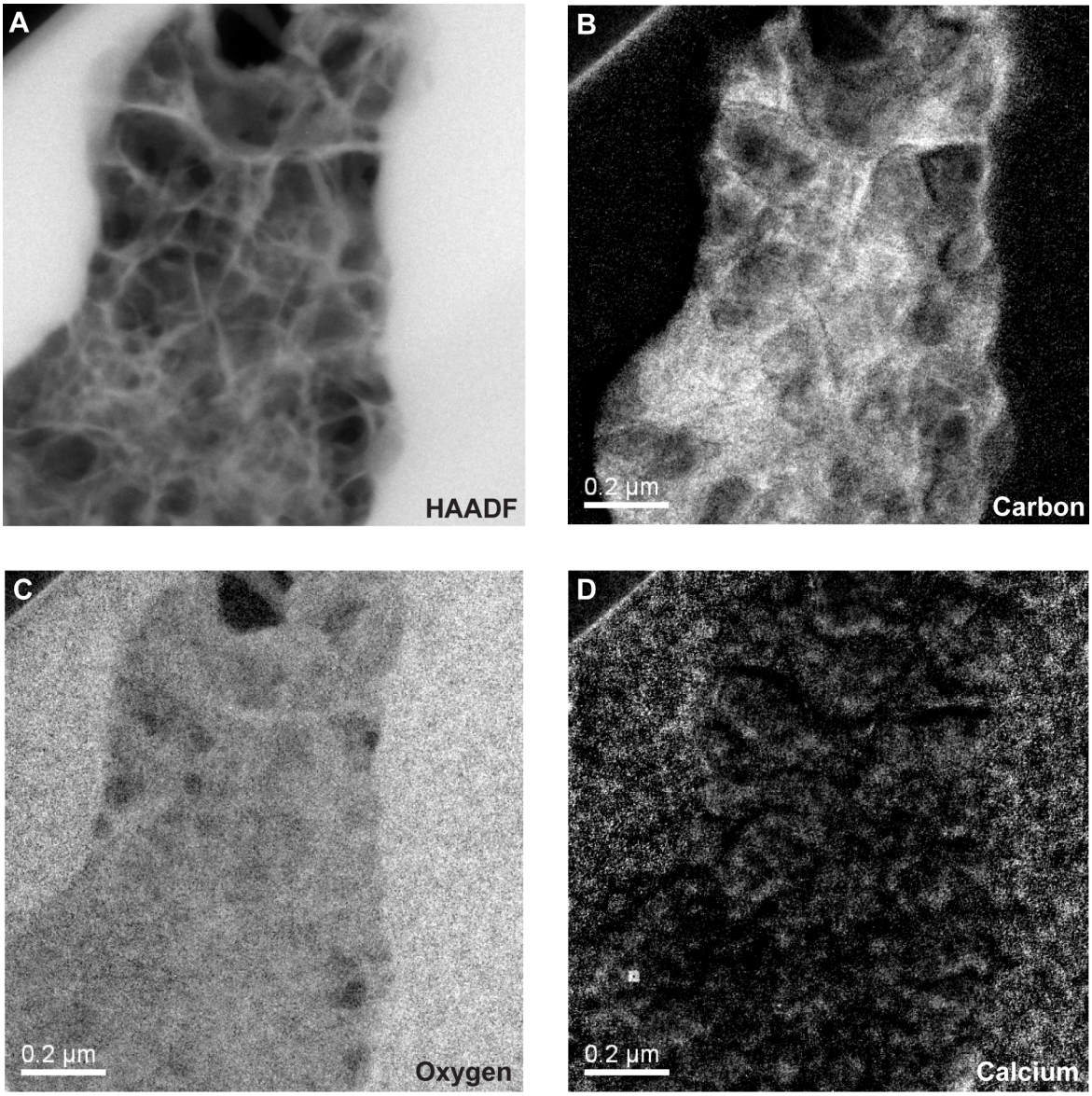

Figure S2. Photomicrograph and EELS maps of the lower part of the tubule on the far right of the foil (see Fig. 1) from sample 46-396B-20 Foil #2996. A) HAADF image of map area. B) Carbon. C) Oxygen. D) Calcium.

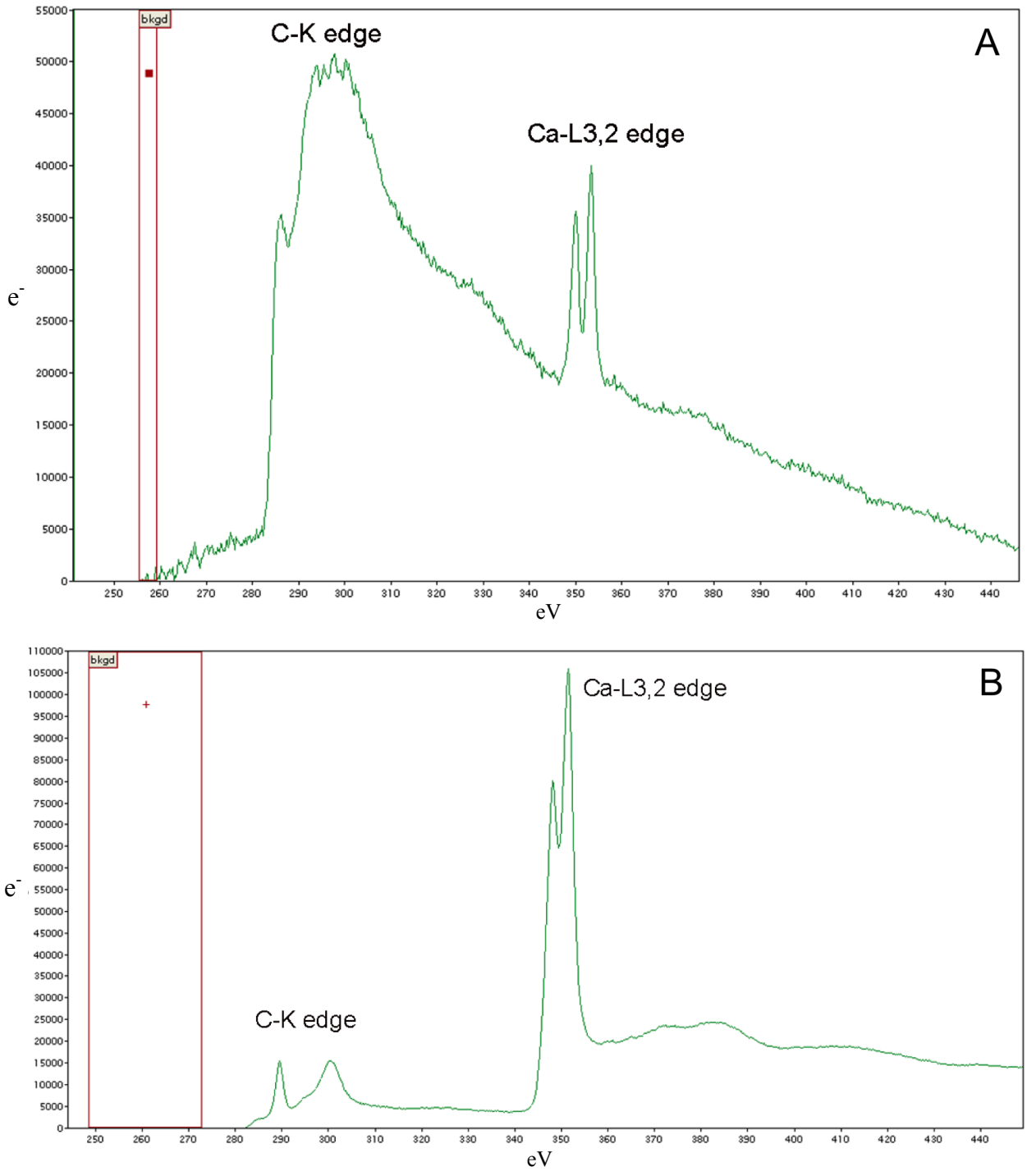

Figure S3. EELS spectra showing the C K-edge and the Ca L3,2-edge collected from the interior of a tubule in sample 46-396B-20 Foil #2996 (A), and a carbonate mineral standard for reference (B). Note the distinct differences in the shapes and sizes of the C K-edges between the sample and the standard.

CHAPTER 3

Geochemical Characterization of Putative Biosignatures in Subseafloor Basalt Glass

Abstract

Through the efforts of international collaborations such as the Integrated Ocean Drilling Program (IODP), we have seen clues that subseafloor basalts may currently host a huge quantity of active microbial cells and contain biosignatures of ancient life in the form of physical and chemical basalt glass alteration. This has exciting implications for increasing our understanding of global geochemical cycling and the evolution of life on Earth, as well as for exploring other planets for signs of life. However, the technological challenges involved in observing the formation and mineralization of these alteration features *in situ*, or reproducing these processes in the laboratory, means that we are left with interpreting the physical and chemical traces left behind. We have used a number of high-resolution methods to probe the geochemical and mineralogical characteristics of several tubular alteration features in basalt glasses obtained from subseafloor drill cores. The sample suite used in this study covers a range of different collection locations and ages, spanning over 100 million years, thus enabling a comparative analysis of the formation and mineralization of tubular alteration features throughout the ocean basins and throughout time. By combining three different synchrotron-based X-ray techniques – X-ray fluorescence microprobe mapping, XANES spectroscopy, and μ-XRD – with focused ion beam milling and electron microscopy, we have spatially resolved the oxidation state of Fe, as well as the major and trace element distributions, determined the coordination chemistry of Fe, Mn and Ti at the micron-scale, and constrained the secondary minerals that infill these features. The primary phases in-filling the alteration regions are Fe^{3+}-bearing silicates, with secondary Fe- and Ti-oxides, and a partially oxidized Mn-silicate phase. The secondary mineralogies of the palagonite and tubules are very similar, but differ from the phases in-filling the cracks. These results show that the mineralization of the tubular regions involves multiple successive stages of

fluid flow, causing complex patterns of mineral dissolution and precipitation and potentially shifting the system from biologically-dominated to abiotic. Most or all of the initial phases that precipitated during formation of the tubules, such as potential biominerals, or cellular material was replaced or overprinted by later secondary mineralization.

1. Introduction

The oceanic subsurface represents the largest unexplored biosphere on Earth. Within the past few years the evidence has been mounting that these environments harbor significant biomass, representing whole new clades of microorganisms (e.g. Mason *et al*., 2007, 2009, Santelli *et al*., 2008, 2009; Edwards *et al*., 2011, 2012; Orcutt *et al*., 2011). There are also clues that the oceanic subsurface may have been inhabited throughout the history of life on Earth in the form of mineralized tubules and granular features in altered basalt glasses that appear to be biological in origin (Staudigel *et al*., 1995, 2008; Torsvik *et al*., 1998; Fisk *et al*., 1998; Furnes *et al*., 2001b,c, 2004; Benzerara *et al.*, 2007; Walton, 2008; McLoughlin *et al*., 2009; Fliegel *et al*., 2010b, 2011). These potential biosignatures are abundant in relatively young subseafloor glasses, and similar features have been found in ancient rocks, including the Pilbara Craton in western Australia (Staudigel *et al*., 2006, Banerjee *et al*., 2007), and the Barberton Greenstone Belt in South Africa (Furnes *et al*., 2004, Banerjee *et al*., 2006; Fliegel *et al*., 2010a). The possibility that these features are indeed biosignatures has important implications for global geochemical cycling and the evolution of life on Earth, as well as for exploring other planets for signs of life.

The ubiquity of putative bioalteration structures indicates that the microbial alteration of subseafloor basalts has until recently been a widely underappreciated process. Numerous studies have shown that silicate dissolution and exchange of elements with seawater is greatly enhanced by the activities of endolithic microbial cells living on and within basalt glasses (e.g. Staudigel *et al*., 1995, 1998, Thorseth *et al*., 1995; Alt and Mata, 2000; Daughney *et al*., 2004; Storrie-Lombardi and Fisk, 2004; Einen *et al*., 2006; Kruber *et al*., 2008), which makes increasing our understanding of the microbial and abiotic alteration of subseafloor basalts an important consideration for geologists and oceanographers. The global effect on element exchange could

be enormous; for example, the biotic dissolution of glass has been shown to enhance the mobilization rate of Sr in basalt glass by a factor of at least 20 times that of abiotic alteration (Staudigel *et al*., 1998). Thus, increased knowledge of the geochemical processes involved in both biotic and abiotic low-temperature subseafloor basalt alteration could change our understanding of the recycling of elements throughout Earth history.

The potential of these features as biosignatures also has important relevance to the field of astrobiology. The tubules in the Archean rocks have been directly dated to be nearly as old as the eruptive age of the rocks themselves, and thus they might in fact represent the oldest biosignatures on Earth (Furnes *et al*., 2004, Staudigel *et al*., 2006, Banerjee *et al*., 2006, 2007, Fliegel *et al*., 2010a). In addition, given the hostile conditions on the surface of Mars today it is likely that the only possible habitat for extant life is in the basalt-hosted subsurface. It is also likely that if there were past life on Mars it would have occupied the endolithic niche at some point in its evolution, or possibly even originated there (Fisk and Giovannoni, 1999; Wierzchos and Ascaso, 2002; Banerjee *et al*., 2004; Fisk *et al*., 2006, McLoughlin *et al*., 2007). It has even been suggested that life could have been seeded on Earth by a meteorite containing endolithic organisms (e.g. Arrhenius, 1903; Melosh, 1988; Brack, 1999; Clark, 2001; Stöffler *et al.*, 2007). Thus, the potential of tubular and granular alteration features in subseafloor basalt glasses and ophiolites as biosignatures is important in the search for extraterrestrial life in our solar system. However, recognizing a true biosignature is a major scientific challenge, even here on Earth.

There are a number of different pieces of evidence that have been cited in support of the biogenicity of granular and tubular alteration features. These lines of evidence are extensively reviewed elsewhere (e.g. Furnes *et al*., 2001c; Staudigel *et al*., 2008, and references therein) and will only be briefly summarized here. These structures were first identified as potential signs of

bioalteration by their morphologies: the features match the appropriate size ranges, shapes, and organizational characteristics to have been produced by the boring of microbial endoliths. They always originate along fractures and extend asymmetrically into the glass, which implies a mode of introduction for the cells. While no intact cells have been identified in or extracted from the basalts, there have numerous objects identified in the alteration regions that could be the remnants of microbial cells (Thorseth *et al*., 1995; Torsvik, 1998; Banerjee and Muehlenbachs, 2003). These appear roughly spheroidal and tend to be a few microns in diameter, comparable to average cell sizes for bacteria and archaea. Some tubules are characterized by segmentation or helical structures, which is typical of bacterial morphology (Fisk *et al*. 1998; Furnes *et al*., 2001c; Staudigel *et al*., 2008; McLoughlin *et al*., 2009). In addition, elevated levels of carbon, nitrogen, phosphorus, and potassium within the channels may suggest the presence of cellular remnants (Fisk *et al*., 1998; Torsvik *et al*., 1998; Furnes *et al*, 2001c, 2004; Banerjee and Muehlenbachs, 2003; Fliegel *et al*., 2010, 2011, in press; Preston *et al*., 2011; Knowles *et al*., in review). The carbon deposits are particularly interesting as several studies have shown that the carbon is not associated with Ca or Mg, which indicates that it is not contained in carbonate minerals (Furnes *et al*., 2001c; Benzerara *et al.*, 2007; Fliegel *et al*., in press; Knowles *et al*., in review). In addition, the carbon deposits in the glassy pillow rims have low $\delta^{13}C$ values compared to carbonates in the crystalline interiors, which could indicate potential biological fractionation (Thorseth *et al*., 1995; Torsvik *et al*., 1998; Furnes *et al*., 2001a, 2004; Fliegel *et al*., 2010).

Given the logistical and technological challenges, we cannot actually observe the bioalteration processes *in situ* in the subseafloor. The ability to sample subseafloor fluids from open drill holes with limited contamination has advanced significantly in the past several years,

which has lead to a significant increase in our understanding of subseafloor microbiology (e.g. Edwards *et al*., 2012 and references therein), but observing microbial and geochemical processes that occur within the subseafloor basalt, or even cleanly sampling them is still very challenging. Thus far it has not been possible to clearly identify whole cells or extract DNA from granular features or tubules. It is likely that cell counts in these low-energy environments were low to start with, and that much of the organic matter has been degraded over time. It is also challenging to measure the past physical and chemical characteristics of the fluids that flowed through the cracks from which these features form, which is important for understanding the mineralization processes. In addition, efforts to reproduce subseafloor conditions in the lab and induce formation of alteration features, or even identify the organisms responsible have been unproductive. It has been difficult to constrain the conditions under which the potential biological mechanisms producing these alteration features operate, and it's possible that they work on such long time scales (hundreds to thousands of years) that we may never be able reproduce the formation processes experimentally. This means that for now we are left with interpreting the geochemical clues preserved within the tubules. A better understanding of the geochemical characteristics of these alteration features will help to elucidate the mechanisms of their formation, mineralization, and preservation.

The tubular and granular features are up to a few microns in diameter, and it may be possible that chemical gradients or boundaries are present within the features on the sub-micron scale. Thus, it is on this scale that the features must be analyzed. There have only been a few previous studies that have used high-resolution techniques to show the nanoscale structures and chemical distributions within the tubular alteration features in subseafloor basalt glass (Alt and Mata, 2000; Benzerara *et al*., 2007, Staudigel *et al*., 2008; Fliegel *et al*., 2010, 2011, in press;

McLoughlin *et al*., 2011; Knowles *et al*., in review). Benzerara *et al*. (2007) were the first to use focused ion beam (FIB) milling combined with transmission electron microscopy (TEM) and scanning transmission X-ray microscopy (STXM) to image and analyze the chemical characteristics of tubular alteration features in a sample from the Ontong Java Plateau (122 Ma). They identified the presence of partially crystalline secondary phases within the alteration features mixed with an amorphous matrix, and interpreted the in-filling material as palagonite – an amorphous or fine-grained mixture of clays of variable crystallinity, iron oxy-hydroxides, and zeolites. Using energy-dispersive X-ray spectroscopy (EDX) they showed that the in-filling materials consist of primarily Si, O, Al, Mg, and Fe, with a depletion of Ca and enrichment of K. Fliegel *et al*., (in press) and Knowles *et al*. (in review) used similar techniques to probe a whole suite of samples from a variety of locations, ages, and alteration environments. Combined, these results revealed the nanoscale textures of these features, including micron-scale amorphous alteration rims around the tubules and granules, more signs of organic carbon, and a predominance of phyllosilicates in filling the features. In addition, these previous studies have indicated that the mechanisms of formation and mineralization of the tubules are common across different alteration regimes and through a large span in time. However, no previous studies have examined the micron-scale changes in redox chemistry, element distributions, and specific mineralogies associated with tubular alteration.

One important consideration when evaluating the potential of a geological feature as a biosignature is whether or not there is any evidence of metabolic processing. Cellular metabolisms operate by exploiting redox disequilibrium in the local microenvironment. Metabolic processes take of advantage of this by catalyzing otherwise sluggish redox reactions and using the energy gained for biosynthesis and cellular functions. Chemolithoautotrophic

microorganisms often leave behind clues of these metabolic processes by various forms of alteration to the local microenvironment, commonly via extraction of metabolically important elements and precipitation of minerals that either would not form or would be very slow to form abiotically. The cellular extraction of elements from the rock results in local depletions of electron sources such Fe^{2+}, Mn^{2+}, and sulfide-bearing minerals, as well producing chemical gradients from the biotic layer into the unoccupied zone. At the same time these metabolic processes cause the build up of organic molecules and other biosynthetic components, including accumulations of P, and N (Ferris *et al.,* 1987; Konhauser and Urrutia, 1999), and sometimes measureable quantities of bioaccumulated trace elements. In addition, there are many different types of biominerals produced either directly by microbial metabolic processes, or indirectly from metabolic byproducts and cellular materials. These include poorly-ordered, nano-aggregated clays (e.g. Fortin and Ferris, 1998; Fortin *et al*., 1998; Wierzchos et al., 2003), magnesium and iron carbonates, various iron oxides and hydroxides, including maghemite, magnetite, hematite, ferrihydrite, and goethite, (e.g. Brown *et al*., 1994; Konhauser, 1997; Fisk and Giovannoni, 1999; Banfield *et al*., 2001; Toner *et al*., 2009; Zhang *et al*., 2009), and Mn-oxides (e.g. Tebo *et al*., 1994).

In order to identify potential signs of metabolic processing it is necessary to analyze a feature on the micron- to sub-micron scale with redox-sensitive techniques. In the current study, we used three different synchrotron-based X-ray techniques, combined with focused ion beam (FIB) milling and transmission electron microscopy (TEM) in order to probe the geochemical characteristics of tubular bioalteration features and surrounding fluid alteration zones. Our analyses focused on Ca and the transition metals Fe, Mn, and Ti, as well as the trace elements Cu, Ni, and Zn. We first conducted X-ray fluorescence microprobe mapping of each region of

interest at three different x-ray incidence energies around the iron absorption edge (7120-7133 eV) in order to generate Ca, Ti, Mn, Fe^{2+}, Fe^{3+}, and total Fe maps, and then mapped the same region at 10keV to determine the co-distribution of trace elements. We then collected multiple spot-specific Fe, Mn, and Ti μ-XANES spectra and micro-diffraction patterns within each mapped region in order to compare the Fe, Mn and Ti chemistry and mineralogy between fresh glass, tubular alteration, palagonite, and crack-filling materials. This study significantly expands the scope of previous studies both in terms of the geochemical data obtained and by including a number of samples from a variety of locations and of different ages. The results of this comparative analysis paint a picture of complex alteration histories characterized by multiple episodes of oxidative low-temperature, and hydrothermal fluid flow altering and overprinting previous mineralogies.

2. Methods

Samples

Table 1 shows the name, location, age, and depth of the samples used in this study. All of the samples were originally obtained from drill cores from the Deep Sea Drilling Project (DSDP) and Ocean Drilling Program (ODP). Sample 896A-11R1, from the Costa Rica Rift, is the only one from the Pacific Ocean, and was drilled during leg ODP 148 (Alt *et al.*, 1993). Hole 396B, from the mid-Atlantic, was drilled during DSDP leg 46 (Dmitriev *et al.*, 1978), and Hole 418A, in the southwestern Atlantic, was drilled during DSDP leg 52 (Robinson *et al*, 1979). For more information on the sample sites and core descriptions see Furnes *et al.* (2001c) and references therein.

Table 1. Sample details

Sample	Location	Age (Ma)	Depth (mbsf)*
896A-11R1	Costa Rica Rift	5.9	90
46-396B-16	Mid-Atlantic	10	100
46-396B-20	Mid-Atlantic	10	140
418A-56-5	Southwest Atlantic	110	312
418A-49-2	Southwest Atlantic	110	147
418A-43-1	Southwest Atlantic	110	100

*meters below sea floor

X-ray Fluorescence Microprobe Mapping and Micro X-ray Absorption Near-Edge Structure (μ-XANES) Spectroscopy

X-ray microprobe and microspectroscopy analyses were conducted on the insertion device beamline 13-IDC at the Advanced Photon Source (APS) at Argonne National Laboratory, Chicago. The incident energy was selected using a Si 111 monochromator and the beam was focused to ~ 2.5 x 2.5μm using Kirkpatrick-Baez mirrors, resulting in a flux of ~10^{11} photons/s. For X-ray microprobe element mapping, the beam was rastered across the area of interest with a step size of 1.0μm, and full fluorescence spectra were collected using a four-element vortex silicon drift detector (SDD). Each region of interest was mapped at 7120, 7126, and 7133 eV for Ca, Mn, Ti, and Fe fluorescence yield, and was re-mapped at 10,000 eV to also detect Cu, Cr and Zn distributions. The windowed fluorescence counts for each element were deadtime corrected and normalized to the incident count rate at the ion chamber upstream of the sample. The

proportions of Fe^{2+} versus Fe^{3+} in any given pixel were determined using a matrix of normalized XANES fluorescence values from three different standards: Zabargad Olivine (100% Fe^{2+}), Dyar Hematite (100% Fe^{3+}), and National Museum of Natural History Magnetite (66.7% Fe^{3+}). The maps were plotted and analyzed using Sam's Microprobe Analyses Kit (http://smak.sams-xrays.com/). The oxidation state maps were generated by simultaneously fitting the fluorescence yield values for each pixel of each map using the normalized fluorescence values of three different Fe standards analyzed by Fe K-edge XANES spectroscopy (Mayhew *et al.* 2011).

For the μ-XANES analyses the detector was calibrated using the absorption edges of an Fe^0 foil (7112.0 eV) and a Ti foil (4966.0 eV). All scans were collected from 80 eV below to 150 eV above the absorption edge of the element of interest. XANES spectra were normalized using Athena, part of the IFEFFIT software package (http://cars9.uchicago.edu/ifeffit/).

Fe and Ti μ-XANES Linear Combination Fitting

Normalized Fe and Ti μ-XANES spectra were fit to model compound databases using the least squares fitting module of Sam's Interface for XAS Package, or SIXPack (http://sixpack.sams-xrays.com/). The Fe model compound database was compiled and narrowed down to relevant end-member compounds from each mineral group as described elsewhere (Mayhew *et al*., 2011). The Ti model compound database was compiled from a mix of spectra collected as part of the current study, as well as obtained from previous studies (Berry *et al*., 2007; Pearce *et al.*, submitted). All model compounds were calibrated in energy to the relevant Fe or Ti foil edge. The SIXPack least squares fitting module has several different options for fitting algorithms, for this study we used the CycleFit routine. This algorithm works by iteratively fitting the spectrum for each model compound to the experimental spectrum and

computing an R-value for the fit. This process is cyclic, each time adding in the component from the previous cycle that gave a fit with the lowest R-value. The cycles were terminated when no additional component improved the total R-value by at least 10%. For most of the experimental spectra the number of components necessary to complete the fitting process was between 2 and 5. The fit range used for the Fe XANES spectra was 7110-7150eV, and for the Ti XANES the range used was 4965-5015eV.

X-ray Micro-Diffraction

X-ray micro-diffraction analyses were conducted on the bending magnet beamline X26A at the National Synchrotron Light Source (NSLS) at Brookhaven National Laboratories (BNL). The incident energy used was 17478.8 eV, which was chosen to match the energy of a molybdenum source on a conventional powder diffraction instrument in order to facilitate data processing. The beam was focused to ~5 x 8 μm and the energy was tuned using a Si (111) channel-cut monochromator. The diffraction detector used was a Rayonix SX-165 CCD and the counting time for each pattern collected was 120s. The samples were all standard thin sections mounted on glass slides, thus there was significant scattering of the beam as it was transmitted through the slide. There was also significant scattering of the beam from the basalt glass surrounding the alteration features. In order to account for these scattering signals, for each sample at least one spot was collected in a region of fresh basalt glass and the diffraction pattern from this spot was subtracted from the patterns collected from alteration spots. The diffraction spots analyzed were chosen to correlate with the spots for the μ-XANES spectra collected previously at the APS. The patterns were normalized and integrated using the Fit2D program

(http://www.esrf.eu/computing/scientific/FIT2D/index.html). Fitting of the integrated patterns was performed using the program Jade, version 9, from Materials Data Inc. (MDI).

Focused Ion Beam (FIB) and Transmission Electron Microscopy (TEM)

Focused ion beam (FIB) milling was used to prepare an ultra-thin lamella (50-100 nm thick) of a cross-section of a tubule in sample 418A-49-2. This sample is very similar to the other two samples from Hole 418A used in this study, but was not analyzed using the synchrotron-based techniques discussed above. FIB milling was conducted on an FEI Nova 600i dual beam instrument at the Nanomaterials Characterization Facility (NCF) at the University of Colorado, Boulder. The sample was first coated with a thin layer (~5 nm) of carbon in order to limit charging. Prior to milling, a layer of Pt was deposited over the region of interest in order to protect the surface from damage from the ion beam. Milling was performed using a current of 6.5nA and an accelerating voltage of 5.0kV. The lamella was removed from the sample using a micromanipulator, then attached to a copper TEM grid, where it was further thinned using a current of 28pA. Final polishing of the lamella was conducted with a beam current of 9.7pA. The lamella was imaged on a Phillips (FEI) CM200 TEM at the Colorado School of Mines.

3. Results

Major and Trace Element Maps

Transmitted and reflected light photomicrographs of sample 896A-11R1 and the corresponding element maps for total Fe, Mn, Ca, Ti, Cu, and Fe oxidation state are shown in Figure 1. The calcium distribution exhibits a sharp boundary between the fresh glass and the

depleted altered regions, which clearly outlines the tubules. This sample shows a significant enrichment (1.5-2x net fluorescence count) in total Fe in the crack, palagonite, and tubular alteration features in comparison with the fresh glass in the upper right, with the crack showing the strongest concentration of Fe. The oxidation state map shows that Fe in the enriched alteration zones is in the oxidized state, with a clear contrast shown with the ferrous Fe in the fresh glass. Manganese shows a similar pattern to Fe, with a strong enrichment in the crack and slightly less, but still significant enrichments in the palagonite and tubular regions. The titanium distribution shows a different pattern, where the palagonite and tubules are enriched with respect to the fresh glass, but no enrichment in the crack. Copper shows a similar distribution to titanium, where the palagonite and tubules are enriched but not the crack. Some of the tubules are clearly delineated by the Cu enrichments within them.

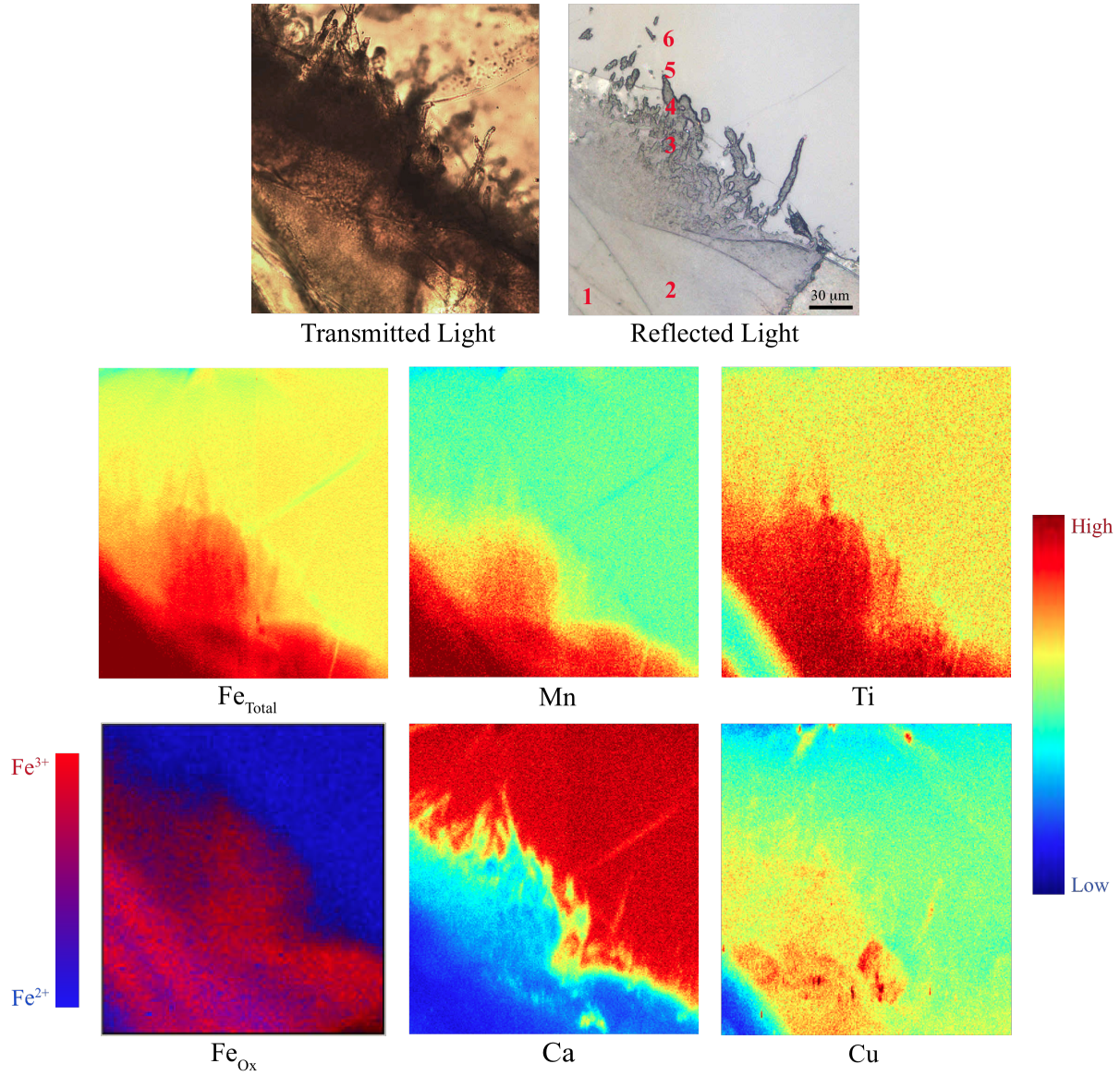

Figure 1. Upper: Transmitted and reflected light photomicrographs of an alteration region in a thin section from sample 896A-11R1. A crack can be seen in the lower left corner, along which a thick palagonite layer has formed. Extending from the palagonite into the fresh glass towards the upper right corner are several tubular alteration features. Lower: Element maps corresponding to the area shown in the photomicrographs. The colorscale for the relative intensities of the individual element maps is shown on the right, where blue corresponds to lower concentration and red to higher. The colorscale for the Fe oxidation state map is show to the left of the map, where blue indicates Fe^{2+} and red shows Fe^{3+}. The images and maps are all shown at the same magnification. The locations of the spots where µ-XANES spectra (Fig. 3) were collected are shown on the reflected light image.

Sample 418A-56-5 shows somewhat different element distribution patterns (Fig. 2). In this sample total Fe is enriched in the center of the crack and in a few discrete spots along the edges of the crack, but slightly depleted in the palagonite and tubular alteration regions. As with sample 896A-11R1, the Fe in the crack, palagonite, and tubules is in the oxidized form. Mn is also depleted in the altered regions and crack, showing a similar distribution to Ca. The Ti and Cu patterns are similar to sample 896A-11R1, with both showing enrichments in the palagonite and tubules, but not in the crack, with the exception of a few discrete hot spots.

Thin section photomicrographs and the corresponding element maps for sample 46-396B-20 are shown in Figure 3. This field of view contains three distinctly different types of alteration: (1) the thin crack running diagonally through the center, (2) the yellow semi-circular palagonite zone in the lower left corner, and (3) the tubules extending from several places along the crack. This sample shows depletions in total Fe in the crack, palagonite, and tubules, but a strong Fe^{3+} signal in these areas. Ca and Mn are also depleted throughout the alteration regions and crack. Ti is enriched only in the tubules and appears to be slightly depleted in the palagonite, while Cu is enriched in the crack, palagonite and tubular region.

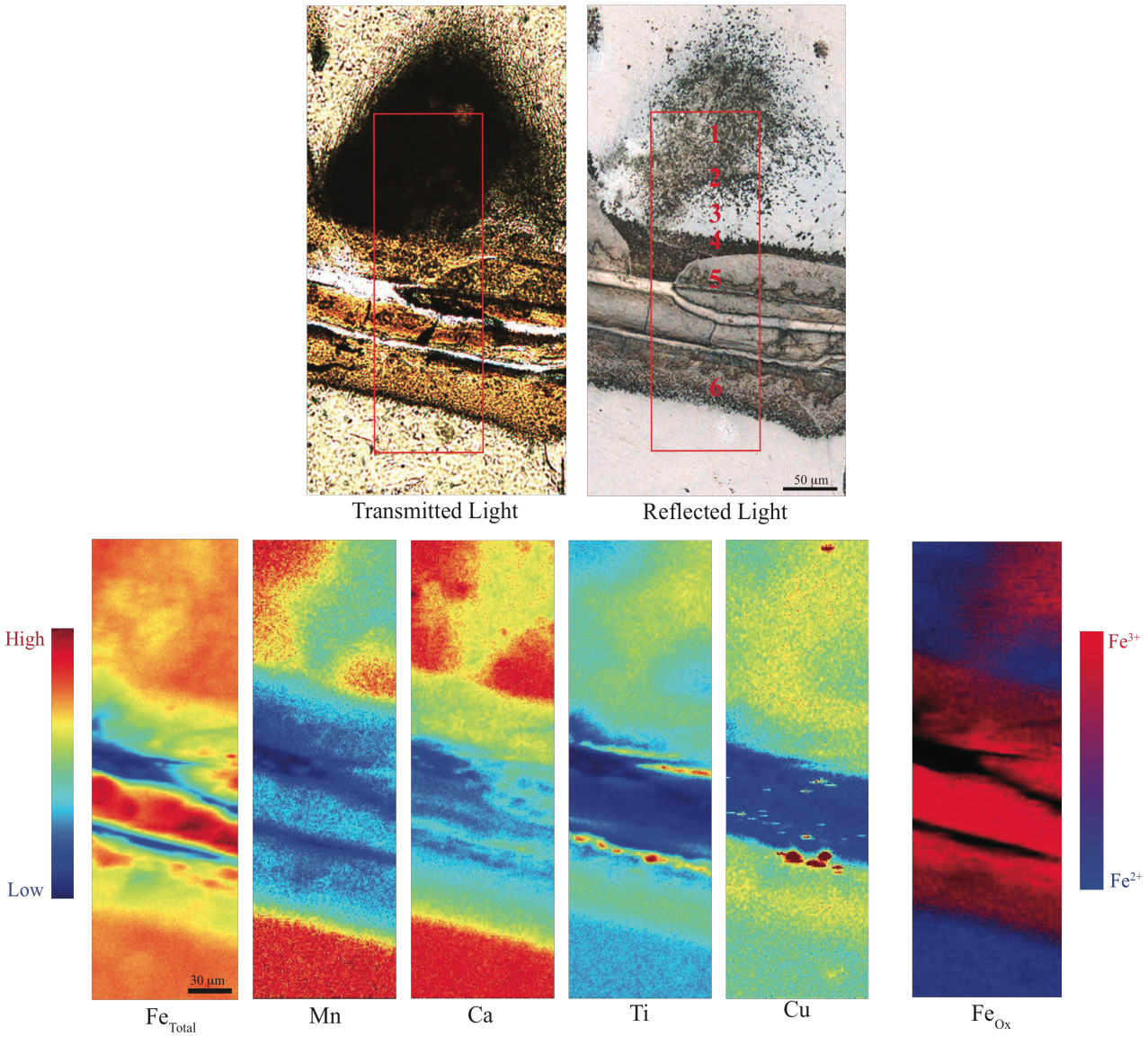

Figure 2. Upper: Transmitted and reflected light photomicrographs of an alteration region in a thin section from sample 418A-56-5. Thick palagonite layers border the crack that runs through the center of the images, and a layer of crack-filling material can be seen in the middle. A large, dense clump of tubules extends from the palagonite on top of the crack. Lower: Element maps corresponding the area outlined by the red box in the photomicrographs. The colorscale for the relative intensities of the individual element maps is shown on the left, where blue corresponds to lower concentration and red to higher. The colorscale for the Fe oxidation state maps is shown on the right.

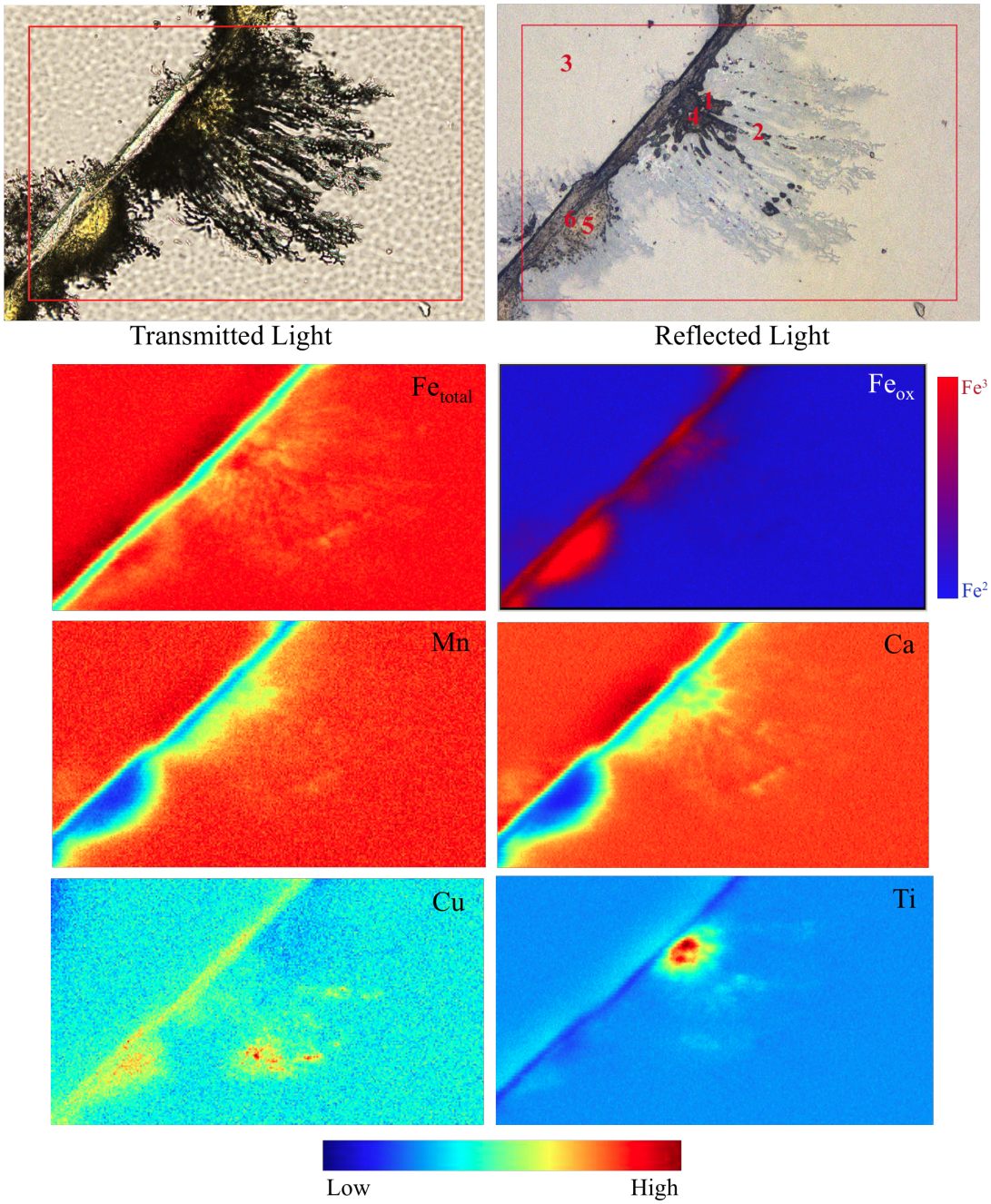

Figure 3. Upper: Transmitted and reflected light photomicrographs of an alteration region in a thin section from sample 46-396B-20. A large clump of tubules extends from the central crack, with several smaller clumps nearby. In the lower left corner a yellow zone of palagonite is visible to the right of the crack. The center of the large tubule region also appears to contain some palagonite. The Fe μ-XANES spots analyzed are shown on the reflected light image. Lower: Element maps corresponding the area outlined by the red box in the photomicrographs. The colorscale for the relative intensities of the individual element maps is shown on the bottom, where blue corresponds to lower concentration and red to higher. The colorscale for the Fe oxidation state map is shown on the right.

Fe μ-XANES Analyses

The Fe μ-XANES spectra for spots 1-6 in sample 896A-11R1 and the reference spectra used to produce the best fits for comparison are shown in Figure 4. The locations of the μ-XANES spectra are shown on the reflected light image in Figure 1. The shape and position of both the main and pre-edge peaks give information about the oxidation and coordination state of the (Bajt *et al.*, 1994; Delaney *et al*., 1998; Petit *et al*., 2001; Wilke *et al.,* 2001; Berry *et al*., 2003). The main peak positions for spots 5 and 6 are at ~7127eV, and correlate well with the spectrum for basalt, showing that the Fe at these spots is reduced. The shape of the pre-edge peak for spot 6 is very similar to that of basalt and it's position indicates that the iron is fully reduced at this spot. The main peak for spot 4 is broadened, which shows that at this spot the spectrum contains a mixture of species. The pre-edge peak for spot 4 appears to be a mix of the pre-edges for spots 1 and 6, again indicating a mixture of ferric and ferrous iron. The main and pre-edge peak positions for spots 1-3 are shifted to higher energies, implying that they are regions of oxidized iron, however, it appears that there is still some mixed ferrous iron signal at these spots as well. The peaks for these spots are all at about 7131eV, while the main peaks for ferrihydrite and smectite (both containing Fe^{3+}) are all at approximately 7133eV, which shows that the iron at spots 1-3 is mostly ferric. This pattern of oxidized iron in the alteration regions and reduced iron in the glass is common to all of the samples analyzed.

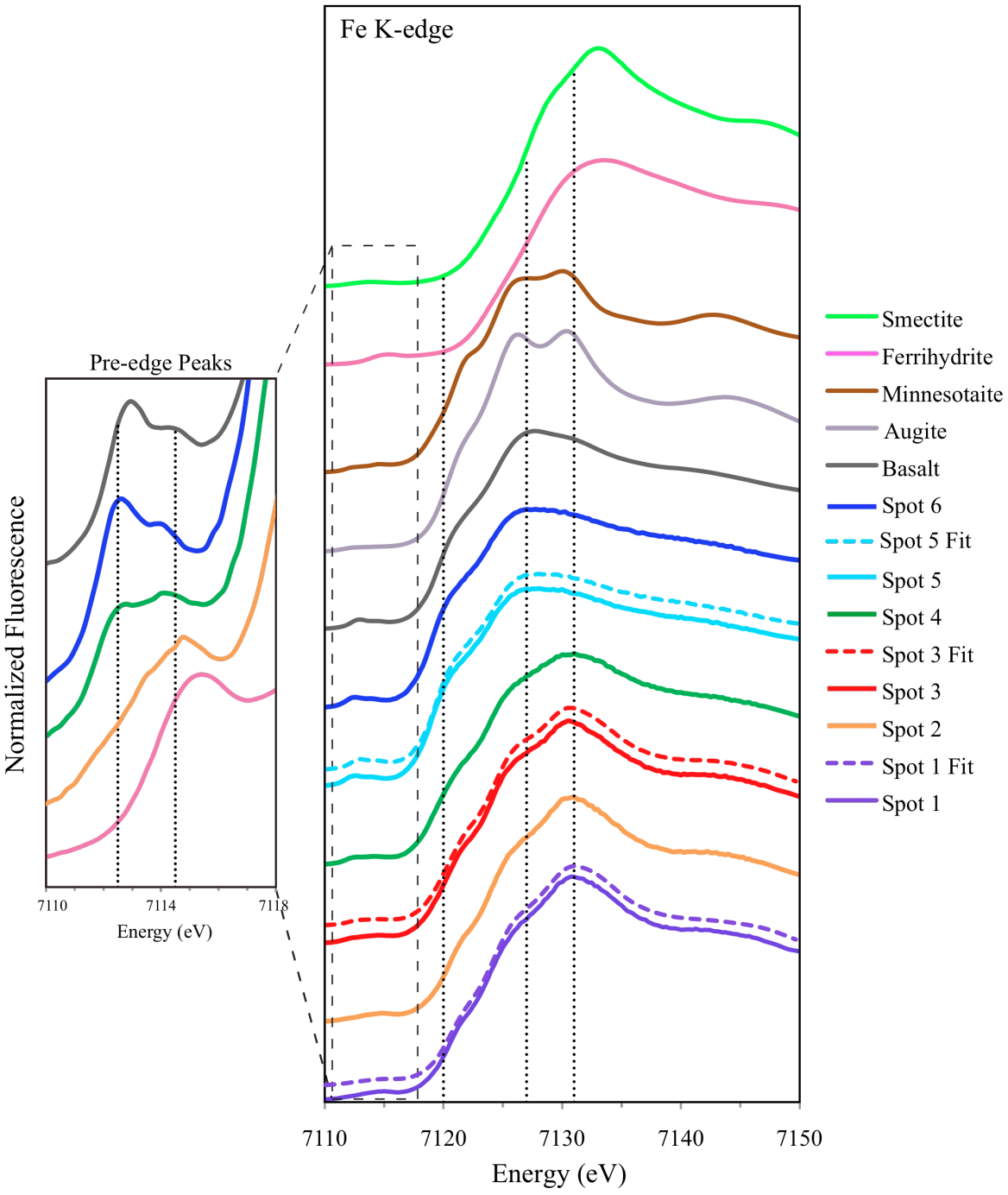

Figure 4. Fe K-edge μ-XANES spectra for spots 1-6 from sample 896A-11R1, corresponding to the locations shown in Figure 1. Left: Pre-edge peaks for spots 2 (orange), 4 (green), and 6 (blue), as well as ferrihydrite (pink) and basalt (gray) for reference. Two reference lines are shown at 7112.5 and 7114.5eV. Right: Full μ-XANES spectra for spots 1-6, the linear combination fits for spots 1, 3, and 5, and the most relevant model compound spectra (see Table 2). Three reference lines are shown at 7120, 7127, and 7131eV. Spectra are offset vertically for visual clarity.

While the position of the absorption edge of the XANES spectra is controlled by the oxidation state of the absorbing atom, the structure of the spectrum is determined by the bonding characteristics and nature of the neighboring atoms (Delaney *et al*., 1998; Berry *et al*., 2003; O'Day *et al*., 2004; Wilke *et al*., 2004; Cottrell *et al*., 2009). When photoelectrons are emitted from the absorbing atom they can be scattered by the neighboring atoms, which then modulates the absorption coefficient of the absorbing atom (Stöhr, 1992). Table 2 shows the best fit for each Fe μ-XANES spectrum collected from the spots in the alteration regions. Only those compounds that account for 10% or more of the fit are shown, as the rest are considered to be below a robust detection limit. For every μ-XANES spot analyzed in tubules, palagonite, and crack-filling material, the fitting was carried out using the model compound library and the spectrum for the basalt glass spot from the same sample (Table 2). This was to test what fraction of each spectrum can be made up by the signal from fresh glass, as it is assumed that even though the spot sizes were generally on the order of two microns and centered in the region of interest, some fluorescence from the glass could be picked up from beneath or nearby the alteration regions. The results show that many of the fits from the alteration regions did include a significant fraction of glass (up to 50%). In terms of both number of occurrences and fit fraction, the primary component in the fits of the Fe μ-XANES from all of the alteration regions is smectite. Of secondary importance in the fits are mixed Fe-oxides, augite, antigorite, and minnesotaite.

Table 2. Results of linear combination cycle fitting for Fe XANES

Sample	XANES Spot	Spot Type	Model Compound	Fraction	R-Value
896A-11R1	1	Crack	Augite	0.30	1.98E-05
			Smectite	0.23	
			Lizardite	0.22	
	2	Palagonite	Smectite	0.49	5.23E-05
			Augite	0.46	
	3	Tubular	Smectite	0.38	1.93E-05
			Augite	0.23	
			Glass	0.23	
	4	Tubular	Basalt	0.49	4.40E-05
			Glass	0.14	
			Smectite	0.14	
	5	Tubular/Glass	Glass	0.98	8.23E-06
46-396B-16	1	Palagonite	Fe-oxides*	0.45	8.19E-05
			Smectite	0.39	
			Olivine	0.11	
	2	Tubular	Fe-oxides*	0.41	2.54E-05
			Glass	0.37	
			Smectite	0.27	
46-396B-20	1	Tubular	Glass	0.52	2.39E-05
			Smectite	0.32	
	2	Tubular/Glass	Glass	0.93	9.75E-06
	4	Tubular	Glass	0.49	2.44E-05
			Smectite	0.23	
			Green Rust	0.18	
			Chamosite	0.12	
	5	Palagonite	Smectite	0.58	3.01E-05
			Greenalite	0.22	
			$Fe^{3+}PO_4$	0.15	
418A-56-5	2	Palagonite	Augite	0.28	2.52E-05
			Glass	0.23	
			Smectite	0.19	
			Antigorite	0.15	
			Minnesotaite	0.10	
	3	Crack	Smectite	0.62	3.11E-05
			Antigorite	0.20	
			Augite	0.14	
	4	Crack	Antigorite	0.39	9.48E-05
			Smectite	0.27	
			Ferrihydrite	0.16	
			Minnesotaite	0.13	
	5	Crack	Saponite	0.36	3.58E-05
			Antigorite	0.32	
			Smectite	0.25	
			Minnesotaite	0.12	
	6	Tubular	Augite	0.27	1.76E-05
			Glass	0.25	
			Smectite	0.19	
			Antigorite	0.11	

Ti μ-XANES Analyses

The titanium μ-XANES spectra were more difficult to fit using the linear combination algorithm than the Fe μ-XANES spectra. This is most likely a sign that there are relevant model compounds missing from the library used. However, the fits are still telling about the nature of the local coordination environment surrounding Ti, and thus about the possible Ti-bearing minerals present in the alteration features and palagonite. While Ti can be in two different oxidation states (+3 and +4), most natural Ti-bearing phases include only Ti^{4+}, thus the XANES spectra are much more useful for understanding the chemical coordination of the Ti, which is shown by the pre-edge peak position and intensity (Dingwell *et al*., 1994; Farges and Brown, 1997). The Ti μ-XANES spectra collected from the same spots as the Fe μ-XANES in sample 896A-11R1 are shown in Figure 5, along with a selection of significant reference spectra, and a spectrum from sample 100-BGB-08, which is from the Barberton Greenstone Belt, South Africa (Furnes *et al*., 2004, Banerjee *et al*., 2006; Fliegel *et al*., 2010a). The differences in structures of these spectra are subtle, but important.

When Ti is tetrahedrally coordinated, such as in TiO_4, the pre-edge peak is strong and located at approximately 4969.5eV. The pre-edge peak of forsterite clearly shows this $^{[4]}$Ti structure. The pre-edge peak decreases in intensity and shifts slightly to higher energy, to ~4970.5eV for 5-coordinated Ti, such as in the $(^{[5]}TiO)O_4$ square pyramid. For $^{[6]}$Ti, in octahedral coordination, the peak tends to be even smaller, often not much more than a small bump, and located between ~4971 and 4972eV (Farges and Brown, 1997). The spectra for titanomagnetite, Ti-andradite, clinohumite, ilmenite, and titanite all show this $^{[6]}$Ti structure. When comparing the heights and locations of the pre-edge peaks of the 896A-11R1 Ti μ-XANES spectra to each other and to the reference line at 4970.5eV (Fig. 5), it appears that Ti in

spots 5 and 6 are 5-coordinated. The pre-edge peaks for spots 1-4 are shifted to higher energy and are slightly decreased in intensity, thus either representing $^{[6]}$Ti or possibly a mix of $^{[5]}$Ti and $^{[6]}$Ti. The spectrum for spot 6, which represents fresh glass, was used as a model compound in the linear combination fits for all of the other μ-XANES spots. This glass spectrum comprises a significant component in spots 3 (~25%), 4 (~45%), and 5 (~98%), while the spectra for spots 1 and 2 represent only Ti in alteration minerals, and not a mixing ratio with glass. In addition to glass, the primary components (representing a fit fraction of greater than 20%) that came up Ti μ-XANES fits for spots within the tubular alteration regions are titanomagnetite, ilmenite, Ti-andradite, and pyrophanite. The palagonite fits give titanomagnetite, pyrophanite, and neptunite as the primary components, and for the Ti μ-XANES spots in the crack the main components are titanomagnetite, neptunite, anatase, and Ti-andradite (data not shown).

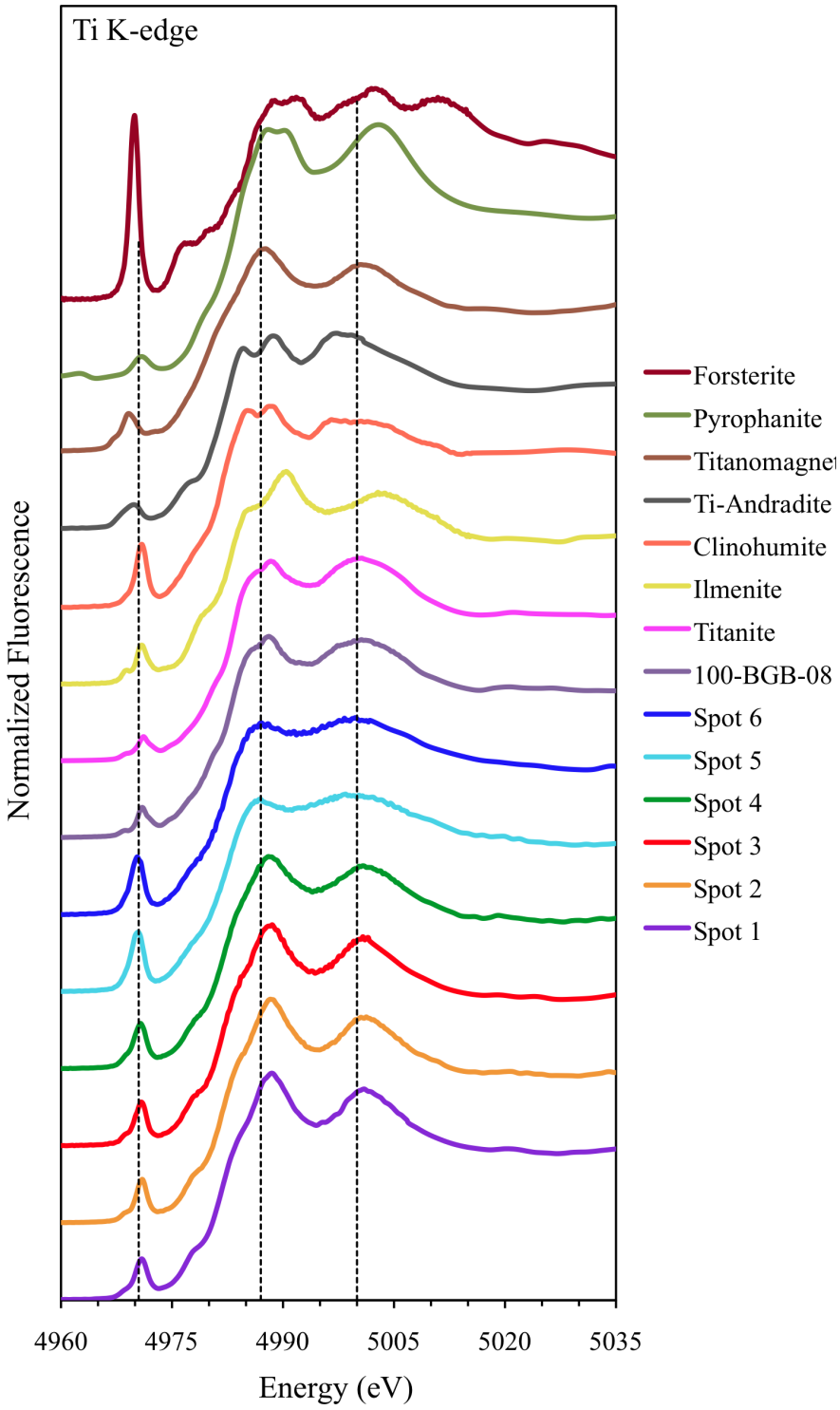

Figure 5. Ti K-edge μ-XANES spectra for spots 1-6 from sample 896A-11R1, one spectrum from sample 100-BGB-08, and the most relevant model compound spectra. Three reference lines are shown at 4970.5, 4987, and 5000eV. Spectra are offset vertically for visual clarity.

Mn μ-XANES Analyses

No full reference compound library was available for linear combination fitting of the Mn μ-XANES spectra; instead a visual comparison of the peak positions and shapes was used to qualitatively evaluate the spectra. In most of the samples analyzed Mn was depleted throughout the alteration regions and the Mn μ-XANES spectra are essentially identical to the Mn^{2+} spectrum of basalt glass. Mn enriched in the alteration regions and varies in oxidation and coordination only in sample 896A-11R1. As shown in Figure 6, the spectra for spots 1, 2, and 3 across the crack, palagonite and tubular alteration have two main peaks of nearly equal intensity. At spot 4 the higher energy peak is diminished, and it disappears in spot 5, giving the characteristic spectrum of basalt glass. The two-humped spectra for the alteration regions are similar to the spectrum for richterite ($Na(Ca,Na)(Mg,Fe)_5Si_8O_{22}(OH)_2$), an amphibole group silicate mineral in which Mn substitutes for Mg and Fe (Chalmin *et al*., 2009). The average valence of Mn in this type of richterite is 2.5, thus the two main peaks in the spectra result from the mixed Mn^{2+}/Mn^{3+} signal. The close match between the spectra from the alteration regions in sample 896A-11R1 and richterite implies that the Mn in these regions is partially oxidized to Mn^{3+} and coordinated with silica.

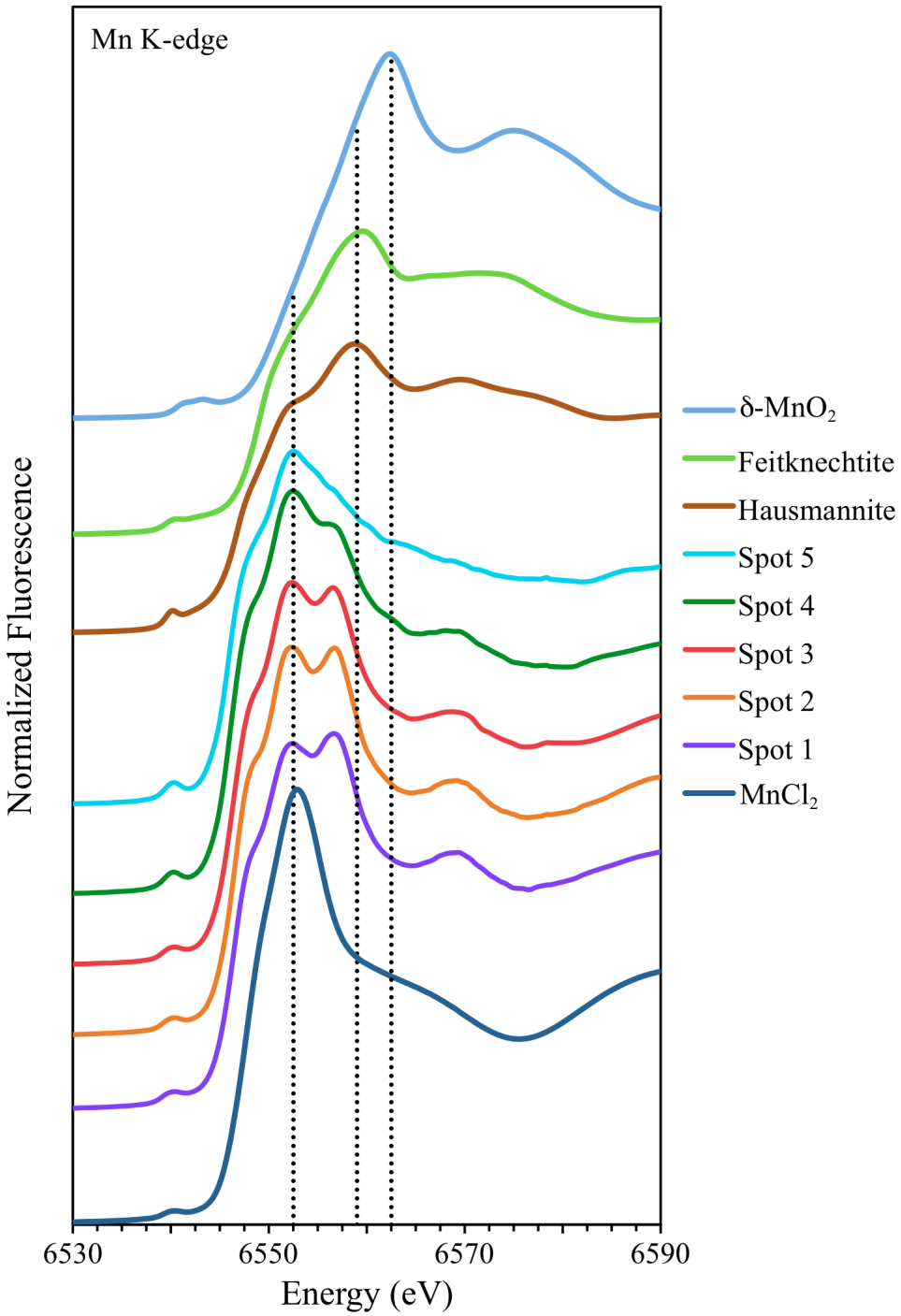

Figure 6. Mn K-edge μ-XANES spectra for spots 1-5 from sample 896A-11R1, corresponding to the locations shown in Figure 1 (spot 6 was not analyzed for Mn XANES), and the most relevant model compound spectra. Three reference lines are shown at 6552.5, 6558.5, and 6562eV. Spectra are offset vertically for visual clarity.

TEM Imaging

A TEM photomicrograph of a FIB lamella from sample 418A-49-2 and a high-resolution view of the material infilling the cross-sectioned tubule are shown in Figure 7A,B. The platy appearance of the tubule interior is characteristic of phyllosilicates, and the lattice fringes are clearly visible in the high-resolution image. The crystallinity of the phyllosilicates is evident in the ordered layering in the darker regions, while the lighter regions are an amorphous matrix, as seen previously in other TEM studies of tubular alteration (Fliegel *et al*., in press, Knowles *et al*., in review). While it was not possible to collect a diffraction pattern from the phyllosilicates, a visual measurement of the lattice fringes gives a d-spacing of 8-10Å. This value correlates well with the d-spacing for a two-layer clay.

X-ray Micro-Diffraction

Synchrotron-based X-ray micro-diffraction is another powerful tool for high-resolution analyses of mineral chemistry and structure. The ability to collect a diffraction pattern from specific location on a with a spot size of only a few microns means that heterogeneous environmental samples can be analyzed without destruction or the loss of spatial resolution that comes with grinding the sample for powder diffraction. This means that minor phases can be identified in specific locations, whereas their signals would be lost in bulk powder diffraction analyses. The drawback of this technique is that for each spot analyzed, often only a single reflection angle is seen, which makes the spectral fitting difficult. The integrated diffraction pattern from spot 4 on sample 896A-11R1 and best-fit curve are shown in Figure 7C. The components used in the fit are saponite, nontronite, vermiculite, faujasite, and clinopyroxene. The most prominent peak in the pattern, at ~2.77°, gives a d-spacing of 14.7Å, which is a typical

spacing for 2:1 clays. This peak is present in the diffraction patterns collected from the alteration regions in every sample analyzed, with little variability in 2θ (2.69-2.86°; data not shown), showing that 2:1 clays are ubiquitous.

Figure 7 (following page). A) TEM photomicrograph of a FIB lamella milled from sample 418A-49-2. One large tubule can be seen extending from the surface of the lamella down and to the left, and several smaller tubular features are visible below the large tubule and to its upper right (arrows). The bright lines in the large tubule are holes in the lamella. B) High-resolution image of a region within one of the smaller tubules in the upper right corner of the lamella. The crystallinity of the phyllosilicates in-filling the tubule can be seen by the ordered layers of the darker phase. A brighter phase can also be seen, which appears to be an amorphous matrix. C) Micro-diffraction pattern from spot 4 on sample 896A-11R1 (black line) and fit (red line). The components used in the fit are saponite, nontronite, vermiculite, faujasite, and clinopyroxene.

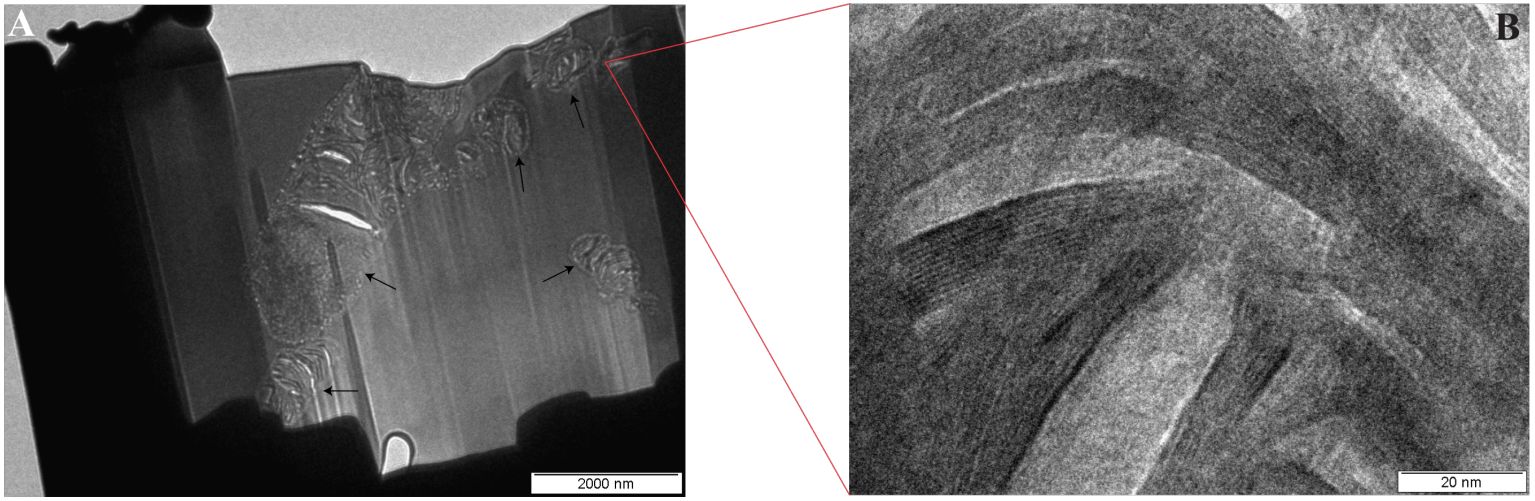
A
2000 nm
B
20 nm

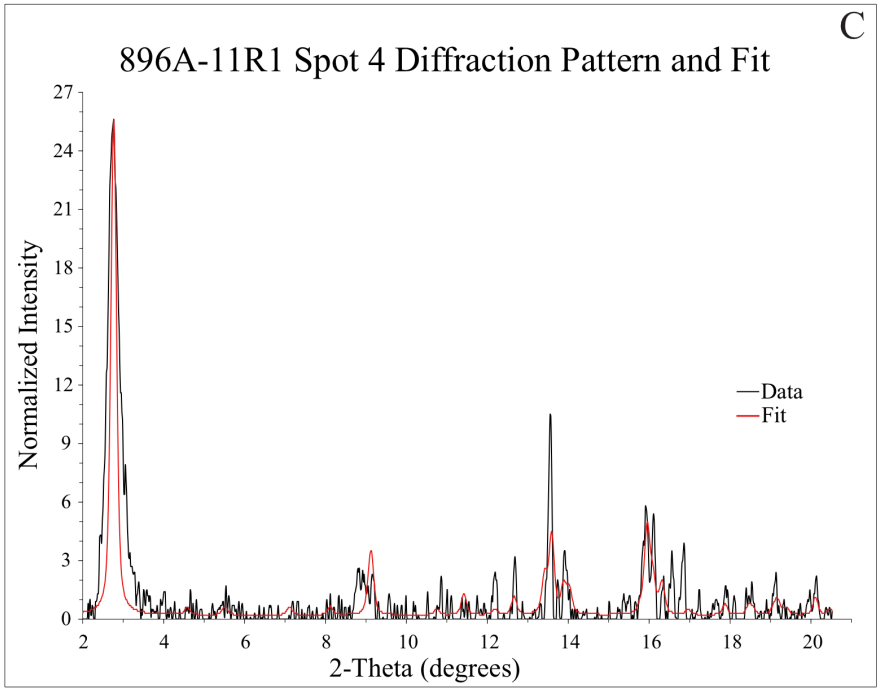
C
896A-11R1 Spot 4 Diffraction Pattern and Fit
Normalized Intensity
2-Theta (degrees)
Data
Fit
0
3
6
9
12
15
18
21
24
27
2
4
6
8
10
12
14
16
18
20

4. Discussion

Using a suite of high-resolution techniques, we were able to analyze the element distributions, coordination chemistry, and mineralogy of numerous micron-scale tubular alteration features from subseafloor basalt glass samples. The element maps show that in all of the samples analyzed the crack, palagonite, and tubular alteration regions are significantly depleted in Ca (Figs. 1,2,3). This means that either Ca is selectively extracted from the glass, or more likely that the initial formation of the tubules is a dissolution process, where the silicate matrix is broken down and most of the major elements are mobilized. The second explanation is supported by the fact that both Fe^{2+} and Mn^{2+} are also depleted in the alteration regions. This is consistent with bulk analyses of altered subseafloor basalt glasses, which show that there is significant exchange between the glass and seawater, causing depletions in Si, Al, Mg, Mn, Ca, Na, and P, and enrichments in H_2O, CO_2 and K_2O in secondary phases (e.g. Staudigel and Hart, 1983; Stroncik and Schmincke, 2002; Walton et al., 2005). Fe and Ti are usually considered immobile, as they are either fully retained or even enriched in secondary phases.

The multiple energy X-ray fluorescence maps show that the distribution of total Fe varies between samples, but all of the samples mapped show depletions in reduced Fe in the alteration regions and enrichment in oxidized Fe, which was confirmed by the Fe μ-XANES results. This implies that either the Fe^{2+} liberated from the glass during dissolution becomes oxidized and precipitates in the alteration regions and the crack or that there is an exogenous source of oxidized Fe introduced into the alteration features, or possibly a combination of the two scenarios. Only one sample (896A-11R1) showed enrichments of total Fe in the alteration regions (Fig. 1). Most of the samples analyzed also show that Mn is depleted in the alteration

regions and crack, again with 896A-11R1 being the only exception. In the Mn depleted samples, the Mn counts are too low to determine the speciation of the residual Mn spectroscopically. In 896A-11R1, the μ-XANES analyses show that the Mn enriched in this sample is partially oxidized to Mn^{3+} (Figure 5). Thus the Mn distribution and speciation exhibits a similar pattern to Fe: depletion of the reduced form from the glass and deposition of the oxidized ion.

The enrichments in Fe and Mn in sample 896A-11R1 imply that there are exogenous inputs of these elements. However, these enrichments could also be explained by differences in density between the fresh glass (sideromelane) and the alteration areas. Sideromelane has an average density of ~2.75g/cm^3, and the density of palagonite ranges from ~1.90 to 2.10 g/cm^3 (Hay and Iijima, 1968). Thus, the incident X-ray beam penetrates further in the alteration regions, interacting with a larger volume of material and thus yielding stronger fluorescence intensities than the nearby fresh glass, when in fact the actual number of Fe or Mn atoms could be the same. In heterogeneous environmental samples it is difficult to quantify beam penetration depth or account for self-absorption effects, making absolute quantification of individual elements inaccurate at best (Lanzirotti *et al*., 2010). With a thin sample an ion chamber downstream of the sample can be used to monitor variability in sample density or thickness, but standard petrographic thin sections on glass slides are too think for the beam (at 7133eV, the Fe K-edge) to fully penetrate, especially with Fe-rich samples, so correcting for variability in absorbance is not possible. This makes it difficult, if not impossible to distinguish between true total Fe and Mn enrichments and matrix effects. It is interesting to note, however, that only sample 896A-11R1 showed enrichments in Fe and Mn. Given the similar nature of the secondary phases in all of the samples analyzed and the fact that all of the samples analyzed were standard petrographic thin sections we would expect to see similar density differences between samples.

Since only this one sample shows these enrichments it is likely that this is a real signal of exogenous Fe and Mn input.

It is possible that the Mn enrichment in sample 896A-11R1 is a result of the specific Mn mineralogy. This is the only sample in this study that shows partial oxidation of Mn and coordination with silica. Mn is generally considered a mobile element during the interaction of seawater with basalt (e.g. Staudigel and Hart, 1983; Stroncik and Schmincke, 2002), so its retention requires immediate oxidation and precipitation as Mn(IV)-oxides. A number of studies of the alteration of seafloor and subseafloor basalts have revealed the importance of Mn(IV)-oxides as products of chemolithoautrophic enzymatic activities (e.g. Tebo *et al*., 2004; Edwards *et al*., 2005; Templeton *et al*., 2005), and the potential of Mn(IV)-oxides as biosignatures (Thorseth *et al*., 2003; Kim *et al*., 2011, McLoughlin *et al*., 2011), but they do not include examples of microbial Mn(II,III)-silicate formation. Perhaps at some stage in the alteration history of this sample the fluids in the crack were more oxidizing than in other samples, causing the dissolved Mn^{2+} to partially oxidize, complex with Si, and precipitate. Richterite is found in contact metamorphic zones and metasomatic deposits (Dawson and Smith, 1982), therefore it is also possible that the formation of a Mn-silicate phase similar to richterite is the result of hydrothermal fluid flow.

In samples 896A-11R1 and 418A-56-5 the Ti distributions match those of Cu, both showing enrichments in the palagonite and tubules, but not in the crack (Figs. 1 and 2). Sample 46-396B-20 shows a different pattern, with Cu enriched in the crack, palagonite, and part of the tubular region, and Ti only enriched in the tubules and depleted in the palagonite and crack. These patterns show the variability in the timing and physical and chemical characteristics of the fluids moving through the cracks. Cu is mobilized by the interaction of hydrothermal fluids with

basalt, often precipitating in sulfides (Humphris and Thompson, 1978; Seewald and Seyfried, 1990). In the subseafloor Cu is mobilized by hydrothermal activity in "reaction zones", such as along ridge axes or deep in the basement; the fluids then transport the Cu (as well as Fe, Zn, and Mn) up through the cracks and fissures where it is re-deposited in secondary phases as the fluids cool (Seewald and Seyfried, 1990; Alt, 1995). The input of these hydrothermal fluids during or immediately following tubule formation could explain the Cu enrichments seen throughout the alteration regions and several of the cracks, and is consistent with the potential exogenous input of Fe and Mn in some samples. In samples 896A-11R1 and 418A-56-5 the cracks may have once been enriched in Cu, but later fluid flow replaced the Cu-bearing phases with oxidized Fe-silicates. The central crack in the photomicrograph in sample 46-396B-20 (Fig. 3) is quite a bit narrower than in the rest of the samples, which means that it may have become sealed off quicker, while still retaining the Cu-bearing phases. Determining whether or not the Cu is complexed with sulfur will require further investigation of the Cu speciation. In contrast, Ti is considered immobile or only slightly mobile under both low-temperature and hydrothermal conditions (Van Baleen, 1993). Bulk studies of whole alteration rims have shown that during the alteration of basalt glass Ti is passively accumulated during palagonite formation (e.g. Staudigel and Hart, 1983; Eggleton *et al*., 1987; Zhou and Fyfe 1989; Stroncik and Schmincke, 2002). Passive enrichment can explain the Ti accumulations in the palagonite areas in samples 896A-11R1 and 418A-56-5, and could also account for the Ti enrichments in the tubules. Cracks tend to form by mechanical forces, such as pressure or shrinking during cooling, and not by dissolution, therefore Ti would not be passively accumulated in the crack unless it was mobilized from nearby alteration regions.

Fe and Ti μ-XANES analyses give more insight into the possible mineral phases present in these samples. The structure of a XANES spectrum is affected by both the oxidation state of the absorbing atom, which determines the location of the absorption edge, and the nature of the surrounding atoms. The position of the absorption edge of the oxidized ion of a particular element is shifted to higher energy than the reduced ion of that element (Stöhr, 1992). Numerous studies of both environmental and lab-based samples have used XANES analyses to determine the oxidation state and coordination of elements of interest, with a strong focus on metals such as Mn, Cr, U, Se, As, and particularly Fe (e.g. Bajt *et al*, 1994; Delaney *et al*., 1998; Dyar *et al*., 1998, 2002; Farges *et al*., 2005; Manceau *et al*., 2005; Cottrell *et al*., 2009; Wilke *et al*., 2001, 2004; Templeton *et al*., 2009, and references therein). In this study the Fe μ-XANES spectra were iteratively fit using an extensive database of model compounds (Mayhew *et al*., 2011). The spectral fitting algorithm outputs the best-fit curve using a combination of the different model compounds, and computes the R-value for the fit, however the interpretation of the fits must be approached with more of a qualitative perspective than quantitative. The structure of the XANES spectra gives information about both the nature and bonding of the neighboring atoms, but it is not possible to use XANES fitting to quantitatively differentiate molecules with similar bonding order, such as minerals that are closely related structurally. Therefore, the μ-XANES fits are more telling of groups of minerals than diagnostic of a specific mineral (O'Day *et al*., 2004).

The linear combination fits for the Fe μ-XANES spectra from the alteration regions often included the glass spectrum from the same sample as a significant component (Table 2), which implies that the fluorescence from these spots includes some signal from the nearby glass. In several samples augite was also a significant component in the fits of spectra from the alteration regions. Pyroxenes are common components of basalt, and can be present as microcrystalline

phases in the glass matrix, thus it is assumed that augite comprised part of the fits in order to account for at least part of the mixed signal from the unaltered glass. The same explanation applies to the olivine invoked in the fit for sample 46-396B-16 spot 1.

It is interesting to note that, with the exception of sample 46-396B-16, the primary components in the Fe μ-XANES fits and several of the main secondary components are Fe-bearing phyllosilicates, while the Fe-oxides were only minor secondary components (Table 2). Fe-oxides and hydroxides are often considered the most common alteration products of basalt glasses in oxygenated environments (e.g. Alt and Honnorez, 1984; Alt, 1995; 1999; Clayton and Pearce, 2000; Schramm et al., 2005), and yet in only one sample are they primary components in the fits from the palagonite and tubular alteration regions. One explanation for this observation is that the fluids in the crack were in fact oxidizing and also had very high silica activities, thus leading to the authigenic precipitation of Fe^{3+}-bearing silicates. This explanation is consistent with the dissolution of glass in a system with a low water-to-rock ratio, such as within the tubules and nearby small cracks. As shown in Figure 3, the absorption edges of the Fe μ-XANES spectra from the alteration regions clearly demonstrate that in all cases the Fe is in the oxidized form, which is also supported by the Fe oxidation state maps (Figs. 1 and 2). By comparing the absorption edges of many of the model compounds used the fits, it is clear that many of them also contain ferric iron, including the smectite and kaolin-serpentine group minerals, even though these minerals are often dominated by ferrous iron. The pre-edge peaks of the smectite and antigorite model compounds required for the fits are shifted significantly further to the right (~7113.8 and 7114.3eV, respectively), than the pre-edge for basalt (~7112.9eV; data not shown). This suggests that the oxidation state of Fe in these compounds in the database is strongly dominated by Fe(III).

The occurrence of the kaolin-serpentine and talc group minerals antigorite, minnesotaite, greenalite, and lizardite in the Fe μ-XANES fits is interesting. These minerals are primarily formed by the low-temperature metamorphic alteration of ultramafic rocks (Moody, 1976; Mével, 2003) and are not normally found in altered tholeiitic basalt glasses. Given the nature of XANES fitting, the inclusion of these minerals as significant components in the results does not necessarily indicate that they are in fact present in the samples, only that there is at least one component with similar chemistry and bonding. Thus, these results show that Fe^{3+}-bearing 2-layer phyllosilicates similar to the serpentine-group minerals are important components in these two samples, in addition to the ferric 3-layer clays and talc. This result is supported by the presence of three different 2:1 clays and clinopyroxene in the micro-diffraction fit for sample 896A-11R1 (Figure 7C), and the identification of a three-layer clay by TEM imaging (Figure 7B). These findings agree well with those of Fliegel *et al*., (in press) and Knowles *et al.* (in review), who also used FIB milling combined with TEM to show the presence of Fe^{3+}-bearing phyllosilicates consistent with a mix of smectites and serpentine-group minerals in tubular alteration features.

The Ti μ-XANES analyses also give interesting insights into the chemical nature of Ti in these samples. A visual comparison of the pre-edge peaks shows that the Ti in the glass (Fig. 6, spots 5 and 6) appears to be 5-coordinated, while the Ti in the crack, palagonite, and tubules is 6-coordinated, or a mix of $^{[5]}$Ti and $^{[6]}$Ti. Previous studies of natural and synthetic glasses showed that the Ti coordination can be quite variable, depending on the chemical composition and crystallinity of the glass (e.g. Dingwell *et al*., 1994; Farges and Brown, 1997; Farges, 1999; Romano, 2000; Henderson *et al*., 2002). There is some consensus, however, that amorphous silicates are usually 5-coordinated or mixed $^{[5]}$Ti and $^{[6]}$Ti and that the coordination number

increases with higher Ti content and increased crystallinity. The current results are consistent with these observations, with the spectra for spots 5 and 6 showing the characteristic structure of amorphous glass, and those for spot 1-4 showing the more crystalline nature of the secondary phases.

The Ti μ-XANES linear combination fits show that the Ti-bearing phases in the alteration regions and crack are quite different from those in the glass. The main components in the glass fits are Ti-bearing silicates, while those in the tubules are predominantly oxides (data not shown). The primary components in the palagonite and crack are a mix of silicates and oxides, with very little overlap with those in the glass. It is interesting to note that titanite does not comprise a significant component in any of the tubular regions analyzed. In fact, out of all of the Ti μ-XANES fits, titanite occurred only once in a tubule, with a maximum fit fraction of ~30%. Based on a number of different geochemical analyses, titanite is considered to be the primary phase that mineralizes the ancient tubular alteration features in ophiolites and greenstones (Furnes *et al.*, 2004, 2007, Banerjee *et al*., 2006, 2007, McLoughlin *et al.*, 2009; Fliegel *et al*., 2011), and possibly in the subseafloor (Izawa *et al*., 2010). It has been proposed that the Ti is passively accumulated during dissolution of the basalt glass and that titanite crystallizes relatively early in the alteration process, which is vital for the preservation of tubules during alteration and obduction of the ophiolites (Banerjee *et al*., 2007, Furnes *et al*. 2007, McLoughlin *et al*., 2009, Izawa *et al*., 2010). A Ti μ-XANES spectrum from the Barberton Greenstone Belt is shown in Figure 6 for comparison. This spectrum was collected from a tubule in sample 100-BGB-08 on the same beamline and with the same configuration as the Ti μ-XANES spectra from all of the samples used in this study. A visual comparison demonstrates that the Barberton spectrum is in fact very similar to the spectrum for titanite, but differs in a few key structural

characteristics from the 896A-11R1 spectra. These structural differences in the Ti μ-XANES spectra indicate that the Ti in the subseafloor samples is not in the form of titanite. This raises several questions about titanite mineralization, such as at what point during the weathering and/or metamorphic maturity of the ophiolites does the primary Ti-bearing phase become titanite, and how does this process happen. These are key questions for understanding the preservation potential of these features as biosignatures and their answers will require further studies.

This study focused on the mineralogy of Fe, Mn, and Ti, but it is important to bear in mind that there are possible minor phases in the alteration regions that do not contain any of these elements and therefore would not be characterized in the micro-XRF or μ-XANES analyses. For example, aluminosilicates, such as zeolites, do not generally include significant quantities of Fe, Mn, or Ti in their structures, and yet zeolites are known as common components of palagonite (Stroncik and Schmincke, 2002). While the μ-XANES analyses wouldn't identify many aluminosilicates, the best fits for several of the micro-diffraction patterns did include zeolites, namely faujasite (Fig. 7). The identification of the full suite of minor secondary phases in the alteration regions would require additional studies using complementary soft X-ray techniques to examine the concentrations of Si, Al, Mg, Na, and other low-Z elements of potential mineralogical or biological importance.

In order to reveal potential geochemical signs of microbial metabolic activity, it is important to compare the chemical or mineralogical differences between palagonite zones and tubular alteration regions. A large number of different studies have been carried out over the past several decades of the low-temperature aqueous alteration of basalt glass (e.g. Alt, 1995; Staudigel and Hart, 1983; Crovisier *et al*., 1987; Stroncik and Schmincke, 2001, 2002; Walton

and Schiffman, 2003, Walton *et al*., 2005; Schramm *et al*., 2005). While these results have shown that the alteration products can be vary substantially, the general process of basalt alteration starts with the hydration of the glass, causing dissolution and eventually replacement of the parent basalt with palagonite. Abiotic basalt alteration tends to produce smooth alteration fronts with a sharp contact between the palagonite and any remaining fresh glass, in contrast to the irregular, asymmetrical nature of putative bioalteration features (e.g. Furnes et al. 2001c). The current results show that although the patterns of element distributions vary somewhat between samples (for example total Fe and Mn enrichment or depletion), in general the tubular alteration regions show the same distributions as the palagonite (Figs. 1 and 2). The Fe and Ti μ-XANES analyses also show the similarity between the chemistries of the tubular and palagonite regions. This can be seen by comparing the structures of the spectra for spot 2 with those for spots 3 and 4 in Figs. 3 and 4. In addition, the Fe and Ti μ-XANES linear combination fits give similar results for the palagonite and tubular regions (Table 2 and Table S1). This implies that the mineralization of the tubules and palagonite is similar in character. It is likely that at some point after formation and mineralization of the tubules and subsequent palagonitization of the surrounding glass, continued fluid flow through the nearby crack replaced any initial potentially less-stable phases with predominantly Fe^{3+}-bearing phyllosilicates and Ti-oxides.

Some characteristics of the crack-filling material are similar to the palagonite and tubular regions, such as the enrichments in oxidized iron and depletion in Ca, but there are noticeable differences, namely the lack of Ti and Cu enrichments. The fact that the minerals present in the crack are different than those in the palagonite points to variability in the timing and extent of fluid flow through the crack, as well as its physical and chemical characteristics (composition, temperature, pH, Eh). It is likely that there were multiple successive stages of fluid flow through

the cracks, with one suite of alteration characteristics overprinting or erasing the previous. The first stage is the formation of the tubules through incongruent dissolution, possibly followed by congruent dissolution (Benzerara *et al*., 2007; Fliegel *et al*., in press; Knowles *et al*., in review). This process would occur coeval with the authigenic precipitation of secondary phases such as Fe-oxyhydroxides and poorly-ordered clays, or possibly biominerals, depending on the role of microorganisms. As fluids continue to percolate through the cracks, the fresh glass along the walls becomes palagonitized, along with any areas along the bases of the tubules that are not densely in-filled. This palagonitization process may involve replacement of some of the phases initially precipitated in the tubules with more stable secondary phases, such as higher-ordered clays and zeolites. The encroachment of palagonite along the crack walls and up the base of the tubules can be seen in nearly all of the samples analyzed (Figs. 1,2,3). Throughout this process there appears to be episodes of hydrothermal input, which deposits Cu-bearing minerals in the alteration regions and cracks, some of which is later removed by further low-temperature fluid flow. These processes will continue until the crack is sealed by secondary phases. Thus, it is reasonable to assume that the majority of the initial mineral signature of tubule formation, and any signs of potential biominerals or cellular materials were overprinted by these successive stages.

5. Conclusions

Combining synchrotron-based X-ray element mapping with micro-spectroscopy, FIB-TEM, and micro-diffraction is a powerful way to probe the geochemical characteristics of micron-scale features at high resolution. These techniques are particularly useful for analyzing

the oxidation states of elements that could be of interest biologically. The X-ray microprobe maps show the distributions of several elements and the oxidation states of Fe and Mn, while the μ-XANES spectra provide information on the specific oxidation and coordination chemistries of elements of interest, and the TEM and X-ray micro-diffraction gives more detail about the mineralogy. Combined, the results of these microanalyses show the predominance of Fe^{3+}-silicates in the alteration regions, with mixed Fe-oxides, Ti-oxides, and at least one partially oxidized Mn-silicate. This study was the first to analyze the titanium and manganese mineralogy with micron-scale. The results show that while Ti is significantly enriched in the alteration regions (tubules and palagonite) of all of the samples analyzed, titanite is clearly not the primary phase in the alteration zones of younger subseafloor samples. In most of the samples analyzed Mn was depleted in the alteration regions, and the remaining Mn is in the reduced form, with similar coordination to the basalt glass. In one sample (896A-11R1) the Mn is partially oxidized and coordinated with silica, similar to the mineral richterite.

Putting these results together it becomes clear that the authigenic minerals filling the tubular alteration features in subseafloor basalts formed through multiple successive stages of alteration. While there are possibly some minerals preserved in the tubules that precipitated during initial formation, most of the secondary phases we examined are not products of or related to the original dissolution process that formed the tubules. If there was ever any geochemical evidence of biological processing by endolithic microorganisms within the tubules the majority of it has been replaced by authigenic phases formed during low temperature and hydrothermal fluid flow, and in some cases possibly low-grade metamorphism. These phases only help to preserve the morphology of the features and do not provide any clues about potential biological mechanisms of dissolution or metabolic processes.

Although these data do not present insights into the mechanism of formation of the tubules and whether or not the process is biological, these results do help increase our understanding of the overall geochemical processes involved in the mineralization and preservation of these potential morphological biosignatures. The presence of more stable phases, such as Fe-bearing phyllosilicates and Ti-oxides within the tubules may limit further fluid flow, thus helping to preserve the tubular morphology over geological time. The ages of the samples analyzed in this study span over 100 million years, and yet each sample shows similar geochemical characteristics, which implies that the formation of the tubules, secondary mineralization, and closing off of the system occurs fairly quickly (hundreds of thousands to a few million years). Once the cracks are sealed the final secondary phases remain relatively unchanged for tens to hundreds of millions of years, unless the basalts are subjected to mid- to high-grade metamorphism. In terms of identifying and interpreting biosignatures, this is an important finding, as it is necessary to characterize both the biological and the abiotic mineralization processes in order understand how biosignatures are formed, altered, and erased.

6. Acknowledgements

Many thanks to beamline scientists Matt Newville at the Advanced Photon Source and Antonio Lanzirotti and William Rao at the National Synchrotron Light source for their beamline assistance. We appreciate Nicola McLoughlin and Harald Furnes at the University of Bergen, Norway for sharing their samples as well as their advice and insight, and Lisa Mayhew and Elizabeth Swanner at the University of Colorado for the use of their Fe XANES model compound library. We would also like to acknowledge Andrew Berry (Imperial College,

London) and Carolyn Pearce (PNNL Science Focus Area (SFA), Subsurface Biogeochemical Research (SBR) program, U.S. Department of Energy (DOE)) for use of their Ti XANES spectra. Use of the Advanced Photon Source, an Office of Science User Facility operated for the U.S. Department of Energy (DOE) Office of Science by Argonne National Laboratory, was supported by the U.S. DOE under Contract No. DE-AC02-06CH11357. A portion of this work was performed at Beamline X26A, National Synchrotron Light Source (NSLS), Brookhaven National Laboratory. X26A is supported by the Department of Energy (DOE) - Geosciences (DE-FG02-92ER14244 to The University of Chicago - CARS) and DOE - Office of Biological and Environmental Research, Environmental Remediation Sciences Div. (DE-FC09-96-SR18546 to the University of Kentucky). Use of the NSLS was supported by DOE under Contract No. DE-AC02-98CH10886. This work was supported by a NASA Earth and Space Science Fellowship and the David and Lucile Packard Foundation.

7. References

Alt, J.C. (1995) Subseafloor Processes in Mid-Ocean Ridge Hydrothermal Systems. In *Seafloor Hydrothermal Systems: Physical, Chemical, Biological, and Geological Interactions*. Humphris, S.E., Zierenberg, R.A., Mullineaux, L.S., and Thomson, R.E. (eds): American Geophysical Union, pp. 85-114.

Alt, J.C. (1999) Very low-grade hydrothermal metamorphism of basic igneous rocks. In *Low Grade Metamorphism*. Frey, M., and Robinson, D. (eds). Oxford, UK: Blackwell, pp. 169-201.

Alt, J.C., and Honnorez, J. (1984) Alteration of the Upper Oceanic-Crust, DSDP Site-417 - Mineralogy and Chemistry. *Contributions to Mineralogy and Petrology* 87: 149-169.

Alt, J.C., Kinoshita, H., Stokking, L.B., Allerton, S., Bach, W., Becker, K. et al. (1993) Site 896. In *Proceedings of the Ocean Drilling Program; Initial reports, Leg 148*. College Station, TX: Ocean Drilling Program, p. 352.

Alt, J.C., and Mata, P. (2000) On the role of microbes in the alteration of submarine basaltic glass: a TEM study. *Earth and Planetary Science Letters* 181: 301-313.

Arrhenius, S. (1903) Die Verbreitung des Lebens im Weltenraum. *Die Umschau* 7: 481-485.

Bajt, S., Sutton, S.R., and Delaney, J.S. (1994) X-ray microprobe analysis of iron oxidation-states in silicates and oxides using x-ray-absorption near-edge structure (XANES). *Geochimica et Cosmochimica Acta* 58: 5209-5214.

Banerjee, N.R., Furnes, H., Muehlenbachs, K., and Staudigel, H. (2004) Microbial alteration of volcanic glass in modern and ancient oceanic crust as a proxy for studies of extraterrestrial material [abstract 1248]. *In 35th Lunar and Planetary Science Conference Abstracts* LPI Contribution No. 1197, Lunar and Planetary Institute, Houston, Texas.

Banerjee, N.R., Furnes, H., Muehlenbachs, K., Staudigel, H., and de Wit, M. (2006) Preservation of ~3.4-3.5 Ga microbial biomarkers in pillow lavas and hyaloclastites from the Barberton Greenstone Belt, South Africa. *Earth and Planetary Science Letters* 241: 707-722.

Banerjee, N.R., and Muehlenbachs, K. (2003) Tuff life: Bioalteration in volcaniclastic rocks from the Ontong Java Plateau. *Geochemistry Geophysics Geosystems* 4.

Banerjee, N.R., Simonetti, A., Furnes, H., Muehlenbachs, K., Staudigel, H., Heaman, L., and Van Kranendonk, M.J. (2007) Direct dating of Archean microbial ichnofossils. *Geology* 35: 487-490.

Banfield, J.F., Moreau, J.W., Chan, C.S., Welch, S.A., and Little, B. (2001) Mineralogical Biosignatures and the search for life on Mars. *Astrobiology* 1: 447.

Benzerara, K., Menguy, N., Banerjee, N.R., Tyliszczak, T., Brown, G.E., and Guyot, F. (2007) Alteration of submarine basaltic glass from the Ontong Java Plateau: A STXM and TEM study. *Earth and Planetary Science Letters* 260: 187-200.

Berry, A.J., O'Neill, H. St. C., Jayasuriya, K.D., Campbell, S.J., and Foran, G.J. (2003) XANES calibrations for the oxidation state of iron in a silicate glass. *American Mineralogist* 88: 967-977.

Berry, A.J., Walker, A.M., Hermann, J., O'Neill, H.S., Foran, G.J., and Gale, J.D. (2007) Titanium substitution mechanisms in forsterite. *Chemical Geology* 242: 176-186.

Brown, D.A., Kamineni, D.C., Sawicki, J.A., and Beveridge, T.J. (1994) Minerals associated with biofilms occurring on exposed rock in a granitic underground research laboratory. *Applied and Environmental Microbiology* 60: 3182-3191.

Chalmin, E., Farges, F., and Brown, G. (2009) A pre-edge analysis of Mn K-edge XANES spectra to help determine the speciation of manganese in minerals and glasses. *Contributions to Mineralogy and Petrology* 157: 111-126.

Clark, B.C. (2001) Planetary interchange of bioactive material: probability factors and implications. *Origins of Life and Evolution of Biospheres* 31: 185-197.

Clayton, T., and Pearce, R.B. (2000) Alteration mineralogy of Cretaceous basalt from ODP Site 1001, Leg 165 (Caribbean Sea). *Clay Minerals* 35: 719-733.

Cottrell, E., Kelley, K.A., Lanzirotti, A., and Fischer, R.A. (2009) High-precision determination of iron oxidation state in silicate glasses using XANES. *Chemical Geology* 268: 167-179.

Crovisier, J.L., Honnorez, J., and Eberhart, J.P. (1987) Dissolution of basaltic glass in seawater - mechanism and rate. *Geochimica et Cosmochimica Acta* 51: 2977-2990.

Daughney, C.J., Rioux, J.P., Fortin, D., and Pichler, T. (2004) Laboratory investigation of the role of bacteria in the weathering of basalt near deep sea hydrothermal vents. *Geomicrobiology Journal* 21: 21-31.

Dawson, J.B., and Smith, J.V. (1982) Upper-mantle amphiboles - a review. *Mineralogical Magazine* 45: 35-46.

Delaney, J.S., Dyar, M.D., Sutton, S.R., and Bajt, S. (1998) Redox ratios with relevant resolution: Solving an old problem by using the synchrotron microXANES probe. *Geology* 26: 139-142.

Dingwell, D.B., Paris, E., Seifert, F., Mottana, A., and Romano, C. (1994) X-Ray-Absorption Study of Ti-Bearing Silicate-Glasses. *Physics and Chemistry of Minerals* 21: 501-509.

Dmitriev, L., Heirtzler, J., and al., e. (1978) Initial Reports of the Deep Sea Drilling Project 46. Washington, DC.: US Government Printing Office.

Dyar, M.D., Delaney, J.S., Sutton, S.R., and Schaefer, M.W. (1998) Fe3+ distribution in oxidized olivine: A synchrotron micro-XANES study. *American Mineralogist* 83: 1361-1365.

Edwards, K., Fisher, A., and Wheat, C.G. (2012) The deep subsurface biosphere in igneous ocean crust: frontier habitats for microbiological exploration. *Frontiers in Microbiology* 3.

Edwards, K.J., Bach, W., and McCollom, T.M. (2005) Geomicrobiology in oceanography: microbe-mineral interactions at and below the seafloor. *Trends in Microbiology* 13: 449-456.

Edwards, K.J., Wheat, C.G., and Sylvan, J.B. (2011) Under the sea: microbial life in volcanic oceanic crust. *Nature Reviews Microbiology* 9: 703-712.

Eggleton, R.A., Foudoulis, C., and Varkevisser, D. (1987) Weathering of basalt: changes in Rock chemistry and mineralogy. *Clays and Clay Minerals* 35: 161-169.

Einen, J., Kruber, C., Øvreås, L., Thorseth, I.H., and Torsvik, T. (2006) Microbial colonization and alteration of basaltic glass. *Biogeosciences Discussions* 3: 273-307.

Farges, F. (1999) A Ti K-edge EXAFS study of the medium range environment around Ti in oxide glasses. *Journal of Non-Crystalline Solids* 244: 25-33.

Farges, F., and Brown, G.E. (1997) Coordination chemistry of titanium(IV) in silicate glasses and melts .4. XANES studies of synthetic and natural volcanic glasses and tektites at ambient temperature and pressure. *Geochimica et Cosmochimica Acta* 61: 1863-1870.

Farges, F., Rossano, S., Lefrere, Y., Wilke, M., and Brown, G.E. (2005) Iron in silicate glasses: a systematic analysis of pre-edge, XANES and EXAFS features. *Physica Scripta* T115: 957-959.

Ferris, F.G., Fyfe, W.S., and Beveridge, T.J. (1987) Bacteria as nucleation sites for authigenic minerals in a metal-contaminated lake sediment. *Chemical Geology* 63: 225-232.

Fisk, M.R., and Giovannoni, S.J. (1999) Sources of nutrients and energy for a deep biosphere on Mars. *Journal of Geophysical Research-Planets* 104: 11805-11815.

Fisk, M.R., Giovannoni, S.J., and Thorseth, I.H. (1998) Alteration of oceanic volcanic glass: Textural evidence of microbial activity. *Science* 281: 978-980.

Fisk, M.R., Popa, R., Mason, O.U., Storrie-Lombardi, M.C., and Vicenzi, E.P. (2006) Iron-magnesium silicate bioweathering on Earth (and Mars?). *Astrobiology* 6: 48-68.

Fliegel, D., Knowles, E., Wirth, R., Templeton, A., Staudigel, H., Muehlenbachs, K., and Furnes, H. (in press) Characterization of alteration textures in Cretaceous oceanic crust from the N-Atlantic (DSDP Hole 418A) by spatially-resolved spectroscopy.

Fliegel, D., Kosler, J., McLoughlin, N., Simonetti, A., de Wit, M.J., Wirth, R., and Furnes, H. (2010) In-situ dating of the Earth's oldest trace fossil at 3.34 Ga. *Earth and Planetary Science Letters* 299: 290-298.

Fliegel, D., Wirth, R., Simonetti, A., Furnes, H., Staudigel, H., Hanski, E., and Muehlenbachs, K. (2010) Septate-tubular textures in 2.0-Ga pillow lavas from the Pechenga Greenstone Belt: a nano-spectroscopic approach to investigate their biogenicity. *Geobiology* 8: 372-390.

Fliegel, D., Wirth, R., Simonetti, A., Schreiber, A., Furnes, H., and Muehlenbachs, K. (2011) Tubular textures in pillow lavas from a Caledonian west Norwegian ophiolite: A combined TEM, LA-ICP-MS, and STXM study. *Geochemistry Geophysics Geosystems* 12.

Fortin, D., and Ferris, F.G. (1998) Precipitation of iron, silica, and sulfate on bacterial cell surfaces. *Geomicrobiology Journal* 15: 309-324.

Fortin, D., Ferris, F.G., and Scott, S.D. (1998) Formation of Fe-silicates and Fe-oxides on bacterial surfaces in samples collected near hydrothermal vents on the Southern Explorer Ridge in the northeast Pacific Ocean. *American Mineralogist* 83: 1399-1408.

Furnes, H., Banerjee, N.R., Muehlenbachs, K., Staudigel, H., and de Wit, M. (2004) Early life recorded in Archean pillow lavas. *Science* 304: 578-581.

Furnes, H., Banerjee, N.R., Staudigel, H., Muehlenbachs, K., McLoughlin, N., De Wit, M., and Van Kranendonk, M. (2007) Comparing petrographic signatures of bioalteration in recent to Mesoarchean pillow lavas: Tracing subsurface life in oceanic igneous rocks. *Precambrain Research*: 156-176.

Furnes, H., Muehlenbachs, K., Torsvik, T., Thorseth, I.H., and Tumyr, O. (2001) Microbial fractionation of carbon isotopes in altered basaltic glass from the Atlantic Ocean, Lau Basin and Costa Rica Rift. *Chemical Geology* 173: 313-330.

Furnes, H., Muehlenbachs, K., Tumyr, O., Torsvik, T., and Xenophontos, C. (2001) Biogenic alteration of volcanic glass from the Troodos ophiolite, Cyprus. *Journal of the Geological Society* 158: 75-82.

Furnes, H., Staudigel, H., Thorseth, I.H., Torsvik, T., Muehlenbachs, K., and Tumyr, O. (2001) Bioalteration of basaltic glass in the oceanic crust. *Geochemistry Geophysics Geosystems* 2

Hay, R.L., and Iijima, A. (1968) Nature and origin of palagonite tuffs of the Honolulu Group on Oahu, Hawaii. In *Studies in Volcanology - A Memoir in Honor of Howel Williams*. Boulder, CO: Geological Society of America, pp. 331-376.

Henderson, G.S., Liu, X., and Fleet, M.E. (2002) A Ti L-edge X-ray absorption study of Ti-silicate glasses. *Physics and Chemistry of Minerals* 29: 32-42.

Humphris, S.E., and Thompson, G. (1978) Trace element mobility during hydrothermal alteration of oceanic basalts. *Geochimica et Cosmochimica Acta* 42: 127-136.

Izawa, M.R.M., Banerjee, N.R., Flemming, R.L., and Bridge, N.J. (2010) Preservation of microbial ichnofossils in basaltic glass by titanite mineralization. *Canadian Mineralogist* 48: 1255-1265.

Kim, S.S., Bargar, J.R., Nealson, K.H., Flood, B.E., Kirschvink, J.L., Raub, T.D. et al. (2011) Searching for biosignatures using electron paramagnetic resonance (EPR) analysis of manganese oxides. *Astrobiology* 11: 775-786.

Knowles, E., Wirth, R., and Templeton, A. (in review) A comparative analysis of potential biosignatures in basalt glass by FIB-TEM.

Konhauser, K.O. (1997) Bacterial iron biomineralisation in nature. *FEMS Microbiology Reviews* 20: 315-326.

Konhauser, K.O., and Urrutia, M.M. (1999) Bacterial clay authigenesis: a common biogeochemical process. *Chemical Geology* 161: 399-413.

Kruber, C., Thorseth, I.H., and Pedersen, R.B. (2008) Seafloor alteration of basaltic glass: Textures, geochemistry, and endolithic microorganisms. *Geochemistry Geophysics Geosystems* 9.

Lanzirotti, A., Tappero, R., and Schulze, D.G. (2010) Practical Application of Synchrotron-Based Hard X-Ray Microprobes in Soil Sciences. In *Developments in Soil Science*. Singh, B., and Gräfe, M. (eds): Elsevier, pp. 27-72.

Manceau, A., Tommaseo, C., Rihs, S., Geoffroy, N., Chateigner, D., Schlegel, M. et al. (2005) Natural speciation of Mn, Ni, and Zn at the micrometer scale in a clayey paddy soil using X-ray fluorescence, absorption, and diffraction. *Geochimica et Cosmochimica Acta* 69: 4007-4034.

Mason, O.U., Di Meo-Savoie, C.A., Van Nostrand, J.D., Zhou, J.Z., Fisk, M.R., and Giovannoni, S.J. (2009) Prokaryotic diversity, distribution, and insights into their role in biogeochemical cycling in marine basalts. *ISME Journal* 3: 231-242.

Mason, O.U., Stingl, U., Wilhelm, L.J., Moeseneder, M.M., Di Meo-Savoie, C.A., Fisk, M.R., and Giovannoni, S.J. (2007) The phylogeny of endolithic microbes associated with marine basalts. *Environmental Microbiology* 9: 2539-2550.

Mayhew, L.E., Webb, S.M., and Templeton, A.S. (2011) Microscale imaging and identification of Fe speciation and distribution during fluid-mineral reactions under highly reducing conditions. *Environmental Science & Technology* 45: 4468-4474.

McLoughlin, N., Brasier, M.D., Wacey, D., Green, O.R., and Perry, R.S. (2007) On biogenicity criteria for endolithic microborings on early earth and beyond. *Astrobiology* 7: 10-26.

McLoughlin, N., Furnes, H., Banerjee, N.R., Muehlenbachs, K., and Staudigel, H. (2009) Ichnotaxonomy of microbial trace fossils in volcanic glass. *Journal of the Geological Society, London* 166: 159-169.

McLoughlin, N., Wacey, D., Kruber, C., Kilburn, M.R., Thorseth, I.H., and Pedersen, R.B. (2011) A combined TEM and NanoSIMS study of endolithic microfossils in altered seafloor basalt. *Chemical Geology* 189: 154-162.

Melosh, H.J. (1988) The rocky road to panspermia. *Nature* 332: 687-688.

Mével, C. (2003) Serpentinization of abyssal peridotites at mid-ocean ridges. *Comptes Rendus Geoscience* 335: 825-852.

Moody, J.B. (1976) Serpentinization - Review. *Lithos* 9: 125-138.

O'Day, P.A., Rivera, N., Jr., Root, R., and Carroll, S.A. (2004) X-ray absorption spectroscopic study of Fe reference compounds for the analysis of natural sediments. *American Mineralogist* 89: 572-585.

Orcutt, B.N., Sylvan, J.B., Knab, N.J., and Edwards, K.J. (2011) Microbial ecology of the dark ocean above, at, and below the seafloor. *Microbiology and Molecular Biology Reviews* 75: 361-422.

Petit, P.E., Farges, F., Wilke, M., and Sole, V.A. (2001) Determination of the iron oxidation state in Earth materials using XANES pre-edge information. *Journal of Synchrotron Radiation* 8: 952-954.

Preston, L.J., Izawa, M.R.M., and Banerjee, N.R. (2011) Infrared spectroscopic characterization of organic matter associated with microbial bioalteration textures in basaltic glass. *Astrobiology* 11: 585-599.

Robinson, P.T., Flower, M.F.J., Swanson, D.A., and Staudigel, H. (1979) Lithology and eruptive stratigraphy of Cretaceous oceanic crust, western Atlantic Ocean. In *Inital Reports DSDP LI, LII, LIII*. Donnelly, T., Francheteau, J., Bryan, W., Robinson, P., Flower, M., and Salisbury, M. (eds). College Station, TX: Ocean Drilling Program, pp. 1535-1555.

Romano, C., Paris, E., Poe, B.T., Giuli, G., Dingwell, D.B., and Mottana, A. (2000) Effect of aluminum on Ti-coordination in silicate glasses: A XANES study. *American Mineralogist* 85: 108-117.

Santelli, C.M., Edgcomb, V.P., Bach, W., and Edwards, K. (2009) The diversity and abundance of bacteria inhabiting seafloor lavas positively correlate with rock alteration. *Environmental Microbiology* 11: 86-98.

Santelli, C.M., Orcutt, B.N., Banning, E., Bach, W., Moyer, C.L., Sogin, M.L. et al. (2008) Abundance and diversity of microbial life in ocean crust. *Nature* 453: 653-657.

Schramm, B., Devey, C.W., Gillis, K.M., and Lackschewitz, K. (2005) Quantitative assessment of chemical and mineralogical changes due to progressive low-temperature alteration of East Pacific Rise basalts from 0 to 9 Ma. *Chemical Geology* 218: 281-313.

Seewald, J.S., and Seyfried, W.E. (1990) The effect of temperature on metal mobility in subseafloor hydrothermal systems - constraints from basalt alteration experiments. *Earth and Planetary Science Letters* 101: 388-403.

Staudigel, H., Chastain, R.A., Yayanos, A., and Bourcier, W. (1995) Biologically mediated dissolution of glass. *Chemical Geology* 126: 147-154.

Staudigel, H., Furnes, H., Banerjee, N.R., Dilek, Y., and Muehlenbachs, K. (2006) Microbes and volcanoes: A tale from the oceans, ophiolites, and greenstone belts. *GSA Today* 16: 4-10.

Staudigel, H., Furnes, H., McLoughlin, N., Banerjee, N.R., Connell, L.B., and Templeton, A. (2008) 3.5 billion years of glass bioalteration: Volcanic rocks as a basis for microbial life? *Earth-Science Reviews* 89: 156-176.

Staudigel, H., and Hart, S.R. (1983) Alteration of basaltic glass - mechanisms and significance for the oceanic-crust seawater budget. *Geochimica et Cosmochimica Acta* 47: 337-350.

Staudigel, H., Yayanos, A., Chastain, R., Davies, G., Verdurmen, E.A.T., Schiffman, P. et al. (1998) Biologically mediated dissolution of volcanic glass in seawater. *Earth and Planetary Science Letters* 164: 233-244.

Stöffler, D., Horneck, G., Ott, S., Hornemann, U., Cockell, C.S., Moeller, R. et al. (2007) Experimental evidence for the potential impact ejection of viable microorganisms from Mars and Mars-like planets. *Icarus* 186: 585-588.

Stöhr, J. (1992) *NEXAFS Spectroscopy*. New York: Springer-Verlag.

Storrie-Lombardi, M.C., and Fisk, M.R. (2004) Elemental abundance distributions in suboceanic basalt glass: Evidence of biogenic alteration. *Geochemistry Geophysics Geosystems* 5.

Stroncik, N.A., and Schmincke, H.U. (2001) Evolution of palagonite: Crystallization, chemical changes, and element budget. *Geochemistry Geophysics Geosystems* 2.

Stroncik, N.A., and Schmincke, H.U. (2002) Palagonite - a review. *International Journal of Earth Sciences* 91: 680-697.

Tebo, B.M., Bargar, J.R., Clement, B.G., Dick, G.J., Murray, K.J., Parker, D. et al. (2004) Biogenic manganese oxides: Properties and mechanisms of formation. *Annual Review of Earth and Planetary Sciences* 32: 287-328.

Templeton, A.S., and Knowles, E.J. (2009) Microbial transformations of minerals and metals: Recent Advances in Geomicrobiology Derived from Synchrotron-Based X-ray Spectroscopy and X-ray Microscopy. *Annual Review of Earth and Planetary Sciences* 37: 367-391.

Templeton, A.S., Staudigel, H., and Tebo, B.M. (2005) Diverse Mn(II)-oxidizing bacteria isolated from submarine basalts at Loihi Seamount. *Geomicrobiology Journal* 22: 127-139.

Thorseth, I.H., Pedersen, R.B., and Christie, D.M. (2003) Microbial alteration of 0-30-Ma seafloor and sub-seafloor basaltic glasses from the Australian Antarctic Discordance. *Earth and Planetary Science Letters* 215: 237-247.

Thorseth, I.H., Torsvik, T., Furnes, H., and Muehlenbachs, K. (1995) Microbes play an important role in the alteration of oceanic crust. *Chemical Geology* 126: 137-146.

Toner, B.M., Santelli, C.M., Marcus, M.A., Wirth, R., Chan, C.S., McCollom, T. et al. (2009) Biogenic iron oxyhydroxide formation at mid-ocean ridge hydrothermal vents: Juan de Fuca Ridge. *Geochimica et Cosmochimica Acta* 73: 388-403.

Torsvik, T., Furnes, H., Muehlenbachs, K., Thorseth, I.H., and Tumyr, O. (1998) Evidence for microbial activity at the glass-alteration interface in oceanic basalts. *Earth and Planetary Science Letters* 162: 165-176.

Van Baleen, M.R. (1993) Titanium mobility in metamorphic systems: a review. *Chemical Geology* 110: 233-249.

Walton, A.W. (2008) Microtubules in basalt glass from Hawaii Scientific Drilling Project #2 phase 1 core and Hilina slope, Hawaii: evidence of the occurrence and behavior of endolithic microorganisms. *Geobiology* 6: 351-364.

Walton, A.W., and Schiffman, P. (2003) Alteration of hyaloclastites in the HSDP 2 Phase 1 Drill Core - 1. Description and paragenesis. *Geochemistry Geophysics Geosystems* 4.

Walton, A.W., Schiffman, P., and Macpherson, G.L. (2005) Alteration of hyaloclastites in the HSDP 2 Phase 1 Drill Core: 2. Mass balance of the conversion of sideromelane to palagonite and chabazite. *Geochemistry Geophysics Geosystems* 6.

Wierzchos, J., and Ascaso, C. (2002) Microbial fossil record of rocks from the Ross Desert, Antarctica: implications in the search for past life in Mars. *International Journal of Astrobiology* 1: 51-59.

Wierzchos, J., Ascaso, C., Sancho, L.G., and Green, A. (2003) Iron-rich diagenetic minerals are biomarkers of microbial activity in Antarctic rocks. *Geomicrobiology Journal* 20: 15-24.

Wilke, M., Farges, F., Petit, P.E., Brown, G.E., and Martin, F. (2001) Oxidation state and coordination of Fe in minerals: An Fe K-XANES spectroscopic study. *American Mineralogist* 86: 714-730.

Wilke, M., Partzsch, G.M., Bernhardt, R., and Lattard, D. (2004) Determination of the iron oxidation state in basaltic glasses using XANES at the K-edge. *Chemical Geology* 213: 71-87.

Zhang, G., Dong, H., Jiang, H., Kukkadapu, R.K., Kim, J., Eberl, D., and Xu, Z. (2009) Biomineralization associated with microbial reduction of Fe3+ and oxidation of Fe2+ in solid minerals. *American Mineralogist* 94: 1049-1058.

Zhou, Z., and Fyfe, W.S. (1989) Palagonitization of basaltic glass from DSDP site-335, leg-37 - textures, chemical-composition, and mechanism of formation. *American Mineralogist* 74: 1045-1053.

CHAPTER 4

Examining the potential biogenicity of tubular alteration features in basalt glass using synchrotron-based soft X-ray techniques

Abstract

Tubular alteration features have been observed in relatively modern subseafloor basalts and in ophiolites that date back to the earliest records of life on Earth, and thus offer a prime opportunity to study the potential biogenicity of one of the most commonly observed putative biosignatures. Technological and practical limitations prevent *in situ* observations of tubular alteration in the subseafloor; therefore in order to understand the formation and mineralization mechanisms of these features we must study their geochemical characteristics. Sulfur plays an important role in several different types of microbial metabolisms, and these processes can cause significant changes in the chemistry and distribution of sulfur in the subseafloor. Sulfur metabolisms often result in the accumulation of various sulfur species both intracellularly and extracellularly in granules, including thiosulfate, tetrathionate, and sulfite, and S^0. Some of these sulfur species can be used as fingerprints of the microorganisms that were present, and add significantly to the evidence for biological processing in a system. Therefore, determining the distribution and speciation of sulfur-bearing phases may provide one of the most robust elemental biosignatures in these alteration features.

Using synchrotron-based soft X-ray microprobe fluorescence mapping combined with X-ray micro-spectroscopy analyses we mapped the distributions of Si, Al, Mg, O, Cl, P, and S, and probed the oxidation state of S at key spots of interest with in the fresh basalt glass, tubules, palagonite, and cracks. The current soft X-ray results build upon previous hard X-ray analyses to provide a more complete picture of the geochemical characteristics of tubular alteration features. Our mapping results show variability in the distributions of secondary phases both within an alteration region in a single sample and between samples, and distinct deposits of P and S within

the tubules. The μ-XANES analyses revealed dominance of S^{6+} in the tubules and palagonite, the origin of which has yet to be determined. These results hint at the possibility that there are remnants of biological geochemical processing in the form of sulfur-bearing biominerals and organic matter within the tubules.

1. Introduction

The study of the interactions of microorganisms with their environments is a key area in Earth and planetary science research. The questions of what metabolic processes microorganisms use in geochemical systems and what traces of their existence they leave behind have important implications not only for our understanding of the history and evolution of life on Earth, but also for our search for life on other planets. One particularly interesting environment in which these questions can be addressed is the subseafloor. There are currently a number of different efforts underway to study what types of microorganisms live within the oceanic crust, how they are able to survive there, and the biological mechanisms of rock weathering (e.g. Edwards *et al*., 2012 and references therein). Ancient and modern volcanic glasses contain numerous alteration features that may be indicative of the biological activities of endolithic microorganisms. One of the most intriguing features – mineralized micron-scale tubules – may be amongst the best microfossils preserved through the past 3.5 billion years, and may record the ubiquitous development of a deep ocean biosphere (e.g. Furnes *et al*., 2004; Banerjee *et al*., 2006; Staudigel *et al*., 2006, 2008; Fliegel *et al*., 2010).

In previous studies we used a number of different synchrotron-based hard X-ray (incident energies >4 keV) techniques to examine the distributions of Ca, Ti, total Fe, Fe^{2+} versus Fe^{3+}, Mn, and Cu, as well as the specific mineralogies of Fe and Ti in and around tubular alteration features, palagonite, and crack-filling materials (Staudigel *et al*., 2008; Fliegel *et al*., in press; Knowles *et al*., submitted). These investigations showed that the primary phases infilling the alteration regions are Fe^{3+}-bearing silicates with minor Fe- and Ti-oxides and zeolites, and that the mineralization of the tubular regions is characterized by complex patterns of dissolution and

precipitation. The hard X-ray techniques limit the analyses to higher Z elements (Ca and higher), thus excluding Si, Al, and Mg, which are all major elements in basalt glass and of potential geochemical significance, as well as elements of potential biological importance, such as P and S.

In this paper we report the results of complementary soft X-ray analyses on the same suite of samples as the hard X-ray analyses, particularly focusing on sulfur, in order to more fully characterize the geochemistry of the alteration features and identify possible geochemical biosignatures. Using soft X-ray microprobe fluorescence mapping we mapped the distributions of a number of elements of geochemical and biological relevance within the tubules, including Si, Al, Mg, O, Cl, P, and S. In addition we collected numerous micro X-ray absorption near-edge structure (μ-XANES) spectra from the alteration regions and fresh glass in each sample in order to investigate the changes in sulfur oxidation states. These analyses identified discrete enrichments of P and S^{6+} in the tubules and palagonite and revealed variable patterns in distributions of secondary phases on the micron scale both within and between samples. This is the first time that soft X-ray techniques have been used in the analysis of tubular alteration features and to the best of our knowledge the first time that that soft and hard X-ray techniques have been combined for a thorough micro-scale geochemical analysis of any putative biosignature.

1.1 *The Significance of Sulfur*

Submarine basalt glasses form by rapid quenching, resulting in little degassing of volatiles, thus they tend to retain the sulfur contents of the parent magmas, the majority of which are saturated with respect to sulfur prior to eruption. The sulfur concentrations of unaltered

oceanic basalt glasses are generally correlated with the Fe concentrations and range from ~700 to 2500ppm (Mathez, 1976; Wallace and Carmichael, 1992). Sulfur concentrations in altered subseafloor basalts show significant spatial variation, reflecting both vertical and horizontal differences in the permeability of the basalt (Bach and Edwards, 2003). The primary abiotic process that affects sulfur speciation and distribution during low-temperature basalt-seawater interaction is the dissolution of primary sulfides; the sulfur is then either lost from the system as the aqueous sulfate ion or re-deposited as secondary sulfides, primarily pyrite (Andrews, 1979; Alt and Honnorez, 1984; Alt, 1995; Bach and Edwards, 2003). In oxidizing conditions up to ~90% of the sulfur in primary sulfides is oxidized and lost from the system (Bach and Edwards, 2003). In reducing conditions more of the sulfur is retained in secondary sulfides. Secondary pyrite can also be formed by microbial sulfate reduction, and there is some evidence that the biological process may play a significant role in the authigenic precipitation of sulfides in the subseafloor (Rouxel *et al*., 2008).

At temperatures above ~350°C the solubility of S in aqueous solutions increases significantly (Seewald and Seyfried, 1990). Bulk studies of subseafloor drill cores have revealed notable increases in the mobilization of sulfur as a result of hydrothermal activity. High temperature fluid-rock interactions in the lower sheeted dikes of the oceanic subsurface mobilizes S as primary sulfide minerals are broken down. When these fluids are channeled through faults or along rift zones they can form seafloor hydrothermal vents and their associated massive sulfide deposits. Without channeling these fluids diffuse through the dikes, depositing sulfides in cracks and fissures as they cool and reduce the sulfate in seawater. In the sheeted dikes the heating of down-welling seawater in so-called “recharge zones” causes the precipitation of anhydrite (Alt, 1995), but anhydrite is rare in the upper basalt zone (Andrews, 1979; Alt *et al*.,

2003). In these layers, the primary forms of secondary sulfur are in the form of pyrite and microbially formed sulfate deposits.

Where oxidized seawater interacts with the reduced basalt in the subseafloor sulfide oxidation is expected to be an important microbial metabolism (Bach and Edwards, 2003, Edwards *et al*., 2005; Orcutt *et al*., 2011). Microorganisms can oxidize the reduced sulfur in basalt glass by using the sulfide as an electron donor and O_2 or NO_3^- in seawater as electron acceptors. These metabolic processes take a number of steps involving the production of several different intermediate sulfur species, such as thiosulfate, tetrathionate, and sulfite, as well as S^0, which is stored both intracellularly and extracellularly in sulfur granules. *In situ* X-ray absorption near edge structure (XANES) analyses of elemental sulfur granules in both environmental samples and laboratory cultures have revealed that the sulfur is frequently in the form of cyclooctasulfur (S_8), but can also be found as polymeric and organic sulfur chains (Pickering *et al*., 2001; Prange *et al.*, 2002a; Engel *et al*., 2007; Lee *et al.,* 2007). Under reducing conditions, sulfate reduction is likely to be a common metabolism in the subseafloor, where H_2 is the electron donor (Edwards *et al*., 2005; Orcutt *et al*., 2011). Isotopic evidence of microbial sulfate reduction in altered subseafloor basalts (Rouxel *et al*., 2008) implies that this metabolic process is widespread. The production of reduced sulfur species can lead to sulfur-metal complexes precipitating on or near cell surfaces, such as pyrite, FeS_2 (Konhauser, 2007). In addition, sulfur is one of the main biological elements, playing a key role in many proteins, thus it often accumulates where cells are (or were once) present. Soft X-ray microprobe mapping and XANES analyses of sulfur speciation has been used in the analysis of both recent and ancient microfossils (Phillipot *et al*., 2003; Foriel *et al*., 2004; Lemelle *et al.*, 2008). Both of these

studies mapped the sulfur distributions to show accumulations within putative cells and used XANES analyses to show the presence of organic sulfur compounds.

Three earlier studies of tubular alteration features used electron microprobes to map the distributions of S and other low-Z elements from in samples from a subseafloor drill core (Banerjee and Muehlenbachs, 2003) and two different ophiolite complexes (Furnes *et al*., 2002; Furnes *et al*., 2005). These studies all showed small, discrete S enrichments within the tubules, or near their margins, often associated with iron (Banerjee and Muehlenbachs, 2003; Furnes *et al*., 2002), or carbon enrichments (Furnes *et al*., 2005). However, in all of these studies the S counts were very low, making the map difficult to interpret. An electron microprobe offers excellent resolution, with spots sizes in the 100-200 nm range, but the detection limits for low concentration elements are constrained by the maximum intensity of incident electron beam. While the spot sizes tend to be slightly larger on most synchrotron-based X-ray microprobe beamlines (~1.5-5 μm), the incident beam fluxes are orders of magnitude higher, which considerably improves the signal-to-noise ratio for low concentration elements. In addition, the ability to finely tune the energy of the incident X-ray beam and scan through the near-edge region allows for the analysis of the speciation of sulfur, particularly different oxidation states of interest (Pickering *et al*., 1998, 2001; Phillipot *et al*., 2003; Templeton and Knowles, 2009; Lanzirotti *et al*., 2010).

2. Methods

2.1 *Samples*

All of the samples used in this study were originally obtained from drill cores from the Deep Sea Drilling Project (DSDP) and Ocean Drilling Program (ODP). Sample 46-396B-20 (section 3, 108-109cm, piece 13) was collected from 140.1 meters into volcanic basement (mivb) the during DSDP leg 46 in the mid-Atlantic. The lithology of this unit is made up of predominantly porphyritic pillow basalts (Dmitriev et al., 1978). Sample 418A-56-5 (section 129-132) was collected from 312.1 mivb in the drill core from Hole 418A on the Bermuda Rise in the southwestern Atlantic (DSDP leg 52). This section of the core is primarily composed of moderately phyric pillow basalts, and has been dated at ~110 Ma (Donnelly et al., 1979). The lithology of the core is further described in detail elsewhere (Donnelly et al., 1979; Alt and Honnorez, 1984; Furnes et al., 2001b). Sample 896A-11R1 (section 73-75, piece 8) was collected at ~286 mivb from Hole 896A from the Costa Rica Rift in the eastern Pacific Ocean during ODP leg 148 (Alt et al., 1993). The basement layer at this location has been dated at ~5.9 Ma, and consists of a mix of pillow lavas and massive flows (Alt et al., 1993; Torsvik et al., 1998). Sample CY-1-31 is from drill core CY-1 from the Cretaceous Troodos Ophiolite Complex in Cyprus (Malpas et al., 1990).

2.2 *Analytical Techniques*

X-ray microprobe and micro-spectroscopy analyses were conducted on the undulator source Phoenix X07MA/B beamline at the Swiss Light Source (SLS), part of the Paul Scherrer Institut (PSI) in Villigen, Switzerland. The incident energy was selected using a Si (111) monochromator and the beam was focused to ~ 3.8 x 2.5 μm using Kirkpatrick-Baez mirrors, resulting in a flux of ~10^{11} photons/s. For X-ray microprobe element mapping, the beam was rastered across the area of interest with step sizes of 3-5 μm. Each region of interest was mapped

at 2500 eV and full fluorescence spectra were collected using a four-element vortex silicon drift detector (SDD). The windowed fluorescence counts for each element were deadtime corrected and normalized to the incident count rate at the ion chamber upstream of the sample. The maps were plotted and analyzed using Sam's Microprobe Analyses Kit (http://smak.sams-xrays.com/). For the micro X-ray absorption near edge structure (μ-XANES) analyses the detector was calibrated using the absorption edges of $CaSO_4 \cdot 2H_2O$ and Na-thiosulfate standard model compounds.

The XANES spectra of the model compounds were collected on the wiggler source Beamline 4-3 at the Stanford Synchrotron Radiation Lightsource (SSRL) in Menlo Park, California, U.S.A. This beamline utilizes a Rh-plated Si mirror with an Si (111) crystal monochromator. An internal Na-thiosulfate standard was used to calibrate the monochromator to the leading thiosulfate edge (2472.02 eV). This standard calibration was performed after roughly every 5 to 7 sample runs. The spectra were collected in fluorescence mode using one of two detectors: either (1) a PIPS detector enclosed with the sample mount in an aluminum box under constant helium flow with sulfur-free polypropylene film windows to allow transmittance of the X-ray beam, or (2) a Vortex detector enclosed with the sample mount within a sealed plastic bag with a liquid-He cryostream flowing onto the face of the sample (T ≅ 100 K at the sample face). Model compounds were prepared for analysis by brushing a thin layer of powdered compound onto sulfur-free mylar tape. All XANES spectra were normalized using Athena, part of the IFEFFIT software package (http://cars9.uchicago.edu/ifeffit/)

3. Results and Discussion

3.1 *X-ray Fluorescence Microprobe Mapping*

A comparison of the element distributions in the alteration regions to those in the fresh glass shows the geochemical changes that take place during alteration. In all of the samples analyzed Si, O, Mg, and Cl are depleted within the tubules compared to the nearby fresh glass, with some variability around their edges (Figures 1, 2, S1, and S2). In sample CY-1-31 (Figure S2) there are three Mg hot spots that appear to be microphenocrysts in the glass, likely olivine (white spots in reflected light image, Figure S2), and there are some O and Cl enrichments around the edges of the tubules. In sample 896A-11R1 (Figure S1) the area at the base of the tubules (overlapping with the palagonite zone) appears to be generally enriched in O and depleted in Cl, and while a few tubules are outlined by depletions of these elements the resolution is too poor in the O and Cl maps to clearly define most of the tubules. The depletions are much more distinct in samples 46-396B-20 (Figure 1) and 418A-56-5 (Figure 2), where the lower element concentrations clearly outline the tubules. Al is enriched in the tubules in all of the samples except for 46-396B-20, which shows an Al depletion. The P distributions in all of the tubule regions are characterized by general depletions with a few hot spots where P is strongly enriched.

The palagonite zones show slightly different element distributions than the tubules and more variability both within and between samples. This is likely due to the different stages of palagonite development between the samples, which does not appear to be correlated with age. Samples 418A-56-5 and 896A-11R1 both have large palagonite layers flanking wide cracks, while sample 46-396B-20 only has a few small palagonite zones along a very narrow crack, and

sample CY-1-31 does not appear to contain any palagonite. All three palagonite zones are depleted in Mg, but the distributions of Si, O, and Cl vary. The smaller palagonite clumps in sample 46-396B-20 (blue arrows in Figure 1) are depleted in Si and Cl, enriched in Al, and show little change in O. The palagonite layers lining both cracks in sample 418A-56-5 (Figure 2) are generally enriched in Si, O, and Al, and depleted in Cl. In the thick palagonite zone in sample 896A-11R1 (Figure S1) Si and Cl are generally depleted, while O and Al are enriched.

All of the samples show enrichments of S in the tubules, either in discrete hot spots (samples CY-1-31 and 418A-56-5) or generally throughout the tubules (samples 46-396B-20 and 896A-11R1). In sample 46-396B-20 both the tubule region and one of the palagonite zones (μ-XANES spots 6 and 7; Figure 1) are strongly enriched in sulfur, with the maximum enrichment (~500%) occurring in the center of the large tubule clump, which is mixed with palagonite. In contrast, the leftmost palagonite zone in this sample (μ-XANES spot 8) is depleted in sulfur. The tubule region in sample 418A-56-5 (Figure 2) is generally depleted in S, but shows several spots of S enrichment, some of which appear to correlate with the P hot spots. There are also several strong S enrichments in the thin bands on either side of the main layer of crack-filling material. The sulfur distribution in sample CY-1-31 is also similar to the P distribution, with general slight depletions throughout the tubules and several S hot spots. In sample 896A-11R1 sulfur is enriched throughout most of the tubules and strongly enriched along the thin crack in the lower right-hand corner.

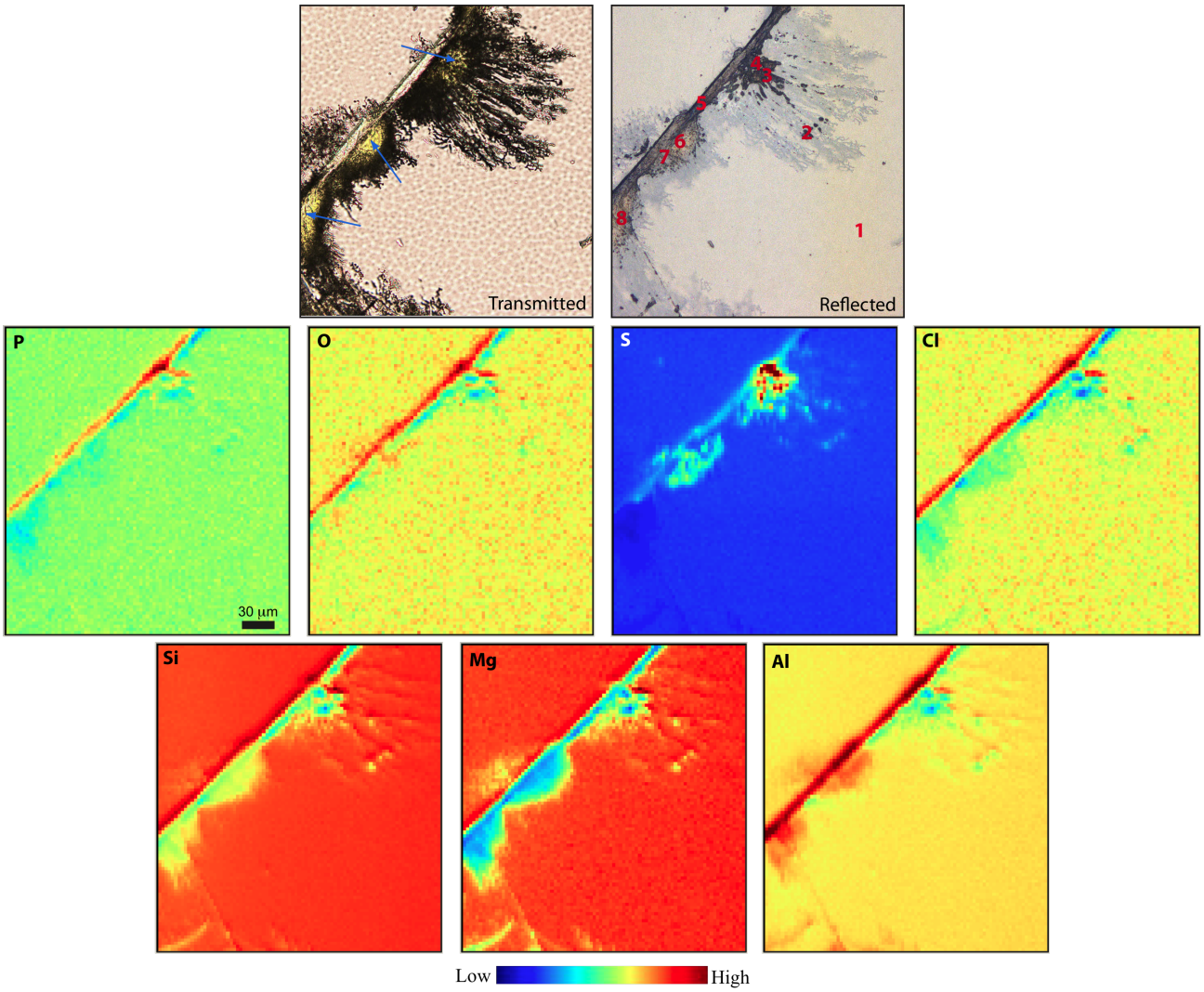

Figure 1. Top: Transmitted (left) and reflected (right) light photomicrographs of an alteration region in a thin section from sample 46-396B-20. A crack can be seen running diagonally across the field of view, from with extends a large clump of tubules, with several tubule regions nearby. The blue arrows in the transmitted light image point out the two yellow palagonite zones along the crack to the left, and the small amount of palagonite in the middle of the large tubule clump. The S µ-XANES spots analyzed are shown in red on the reflected light image. Middle and Bottom: Element maps corresponding to the field of view in the photomicrographs. The scale bar on the P map is 30µm and applies to all of the maps and the photomicrographs. The colorscale for the relative intensities of the individual element maps is shown on the bottom, where blue corresponds to lower concentration and red to higher.

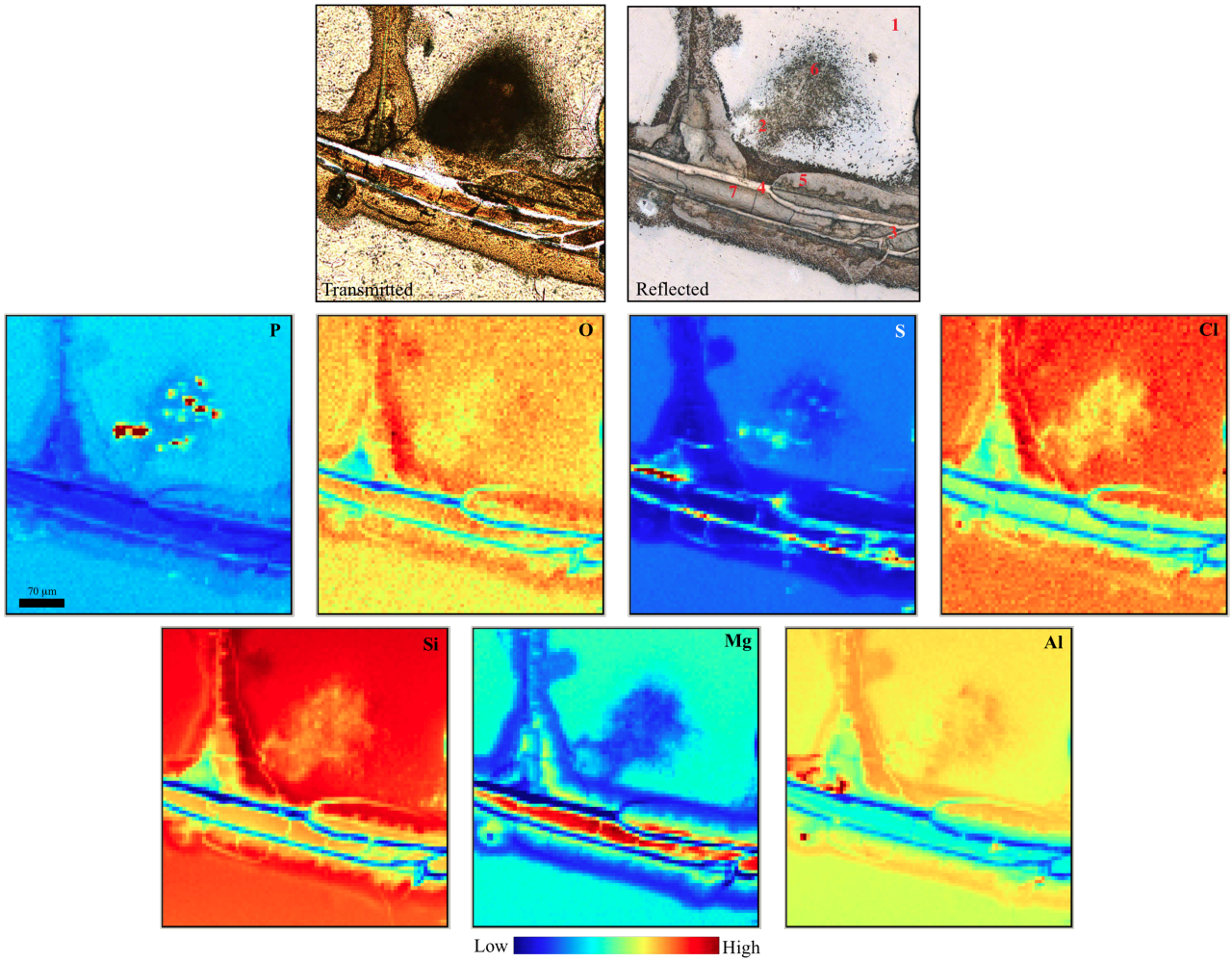

Figure 2. Top: Transmitted (left) and reflected (right) light photomicrographs of an alteration region in a thin section from sample 418A-56-5. The large central crack in this image has a thick band of crack-filling material flanked by two thinner bands, and is bordered by thick palagonite layers. On the upper part of the central crack a large, dense clump of tubules extends from the edge of the palagonite. The S μ-XANES spots analyzed are shown in red on the reflected light image. Middle and Bottom: Element maps corresponding to the field of view in the photomicrographs. The scale bar on the P map is 70μm and applies to all of the maps and the photomicrographs. The colorscale for the relative intensities of the individual element maps is shown on the left, where blue corresponds to lower concentration and red to higher.

Bulk analyses of altered subseafloor basalt glasses have demonstrated that secondary phases tend to be generally depleted in Si, Al, Mg, Mn, Ca, Na, and P, and enriched in H_2O, CO_2 and K_2O compared to the fresh glass (e.g. Staudigel and Hart, 1983; Stroncik and Schmincke, 2002; Walton et al., 2005). The most commonly observed secondary phases are Fe-oxyhydroxides, smectite, illite and kaolin-group clays, and a variety of zeolites (Alt and Honnorez, 1984; Clayton and Pearce, 2000; Drief and Schiffman, 2004; Schramm *et al*., 2005, Walton *et al.*, 2005; Knowles *et al.*, submitted). In the current results, the differences in the concentrations of Si, Al, and Mg in the alteration regions both within and between samples can be attributed to various distributions of these common secondary minerals. Oxides, clays, and zeolites are most likely present in all of the alteration regions, but vary in proportion as a result of differences in the physical and chemical characteristics of the seawater that interacted with the rocks, the extent of alteration, and any potential biological activity.

In a detailed study of basalt glass alteration products in a drill core as a part of the Hawaii Scientific Drilling Project Walton *et al*., (2005) analyzed the compositions of fresh glass, palagonite, chabazite, phillipsite, and smectite using an electron microprobe. These results showed that compared to the fresh glass the chabazite and phillipsite are significantly depleted in Mg and Al with little to change in Si concentrations, while the smectite is enriched in Mg and slightly depleted in Al and Si (Walton *et al*., 2005). These results can be applied to the interpretation of the variable elemental distributions in the alteration regions shown in the current results. Locations where Si shows no change or slight decreases, Mg is depleted, and Al is enriched likely contain a higher concentration of zeolites and/or two-layer clays that contain no interlayer Mg, such as kaolinite. These phases occur in the base of the tubules and palagonite regions of sample 896A-11R1, the tubules in sample 418A-56-5 and CY-1-31, and the

palagonite in sample 46-396B-20. There are also several areas that are depleted in Si and Al, with little to no changes in Mg; these locations are likely dominated by smectites. This includes the main parts of the tubules and the crack-filling material in sample 896A-11R1, the tubules in sample 46-396B-20, and the crack-filling material in sample 418A-56-5.

Phosphorus is generally depleted throughout the alteration regions with several distinct hot spots where P is strongly enriched (up to ~600%). Electron microprobe studies of putative bioalteration features in both subseafloor basalts and ophiolites have also noted P enrichments, often associated with C, N, and K enrichments and Ca depletions (Torsvik *et al*., 1998; Furnes *et al.*, 2002; Banerjee and Muehlenbachs, 2003; Furnes *et al*., 2008). Phosphorus is only found in trace concentrations in both seawater and basalts, and is generally strongly depleted in palagonite and secondary minerals (e.g. Stroncik and Schmincke, 2002; Schramm *et al*., 2005; Walton *et al*., 2005). These observations lead previous researchers to conclude that the P enrichments, and associated C, N, and K within the tubules can be attributed to the presence of organic matter. However, this is not conclusive evidence that the tubules were formed by microorganisms; if there was continuous fluid flow within the cracks then the organic matter could have adsorbed to the surfaces of secondary minerals, such as clays, long after the original formation of the tubules. In sample 46-396B-20 (Figure 1) the crack is also enriched in P, implying either deposits of organic matter or an unidentified P-rich mineral phase in the crack. The distribution and speciation of carbon was not analyzed in this study, but two previous studies that used focused ion beam milling (FIB) coupled with transmission electron microscopy (TEM) and associated electron energy loss spectroscopy (EELS) showed carbon enrichments, likely in the form of organic matter, in a sample 896A-11R1 and a different sample from Hole 418 (Fliegel *et al*., in

press; Knowles *et al*., in review). Confirmation of the presence of potential organic matter within the tubules mapped in the current study will require further investigations.

3.2 *Micro X-ray Absorption Near-Edge Structure (μ-XANES) Spectroscopy*

The S μ-XANES spectra collected from the basalt glass in both sample 46-396B-20 (spot 1, Figure 3) and 418A-56-5 (spot 1, Figure 4) show that the sulfur is primarily reduced. These spectra are characterized by a small peak close to the S^{2-} peak (2470.4 eV), a broad hump between ~2470 and 2480 eV, and only a small increase in fluorescence intensity at the location of the S^{6+} peak (2482.6eV). This is a typical spectrum for mid-ocean ridge or ocean island reduced basalt glass, where the 2470.4 eV peak and the broad hump are indicative of sulfide, as seen in the bornite (Cu_5FeS_4) spectrum, with a minor sulfate peak (e.g. Fleet 2005; Jugo *et al*., 2010; Wilke *et al*., 2011). A number of studies have shown that both reduced (S^{2-}) and oxidized (S^{6+}) forms of sulfur can be found in glassy rims, but that sulfate generally comprise less than 25% of the total sulfur and is often only present in trace amounts (Wallace and Carmichael, 1994, Jugo *et al*., 2010). The majority of the sulfur is in the form of sulfide globules primarily comprised of pyrrhotite, pentlandite, and mixed Cu-Fe-S phases (Mathez, 1976).

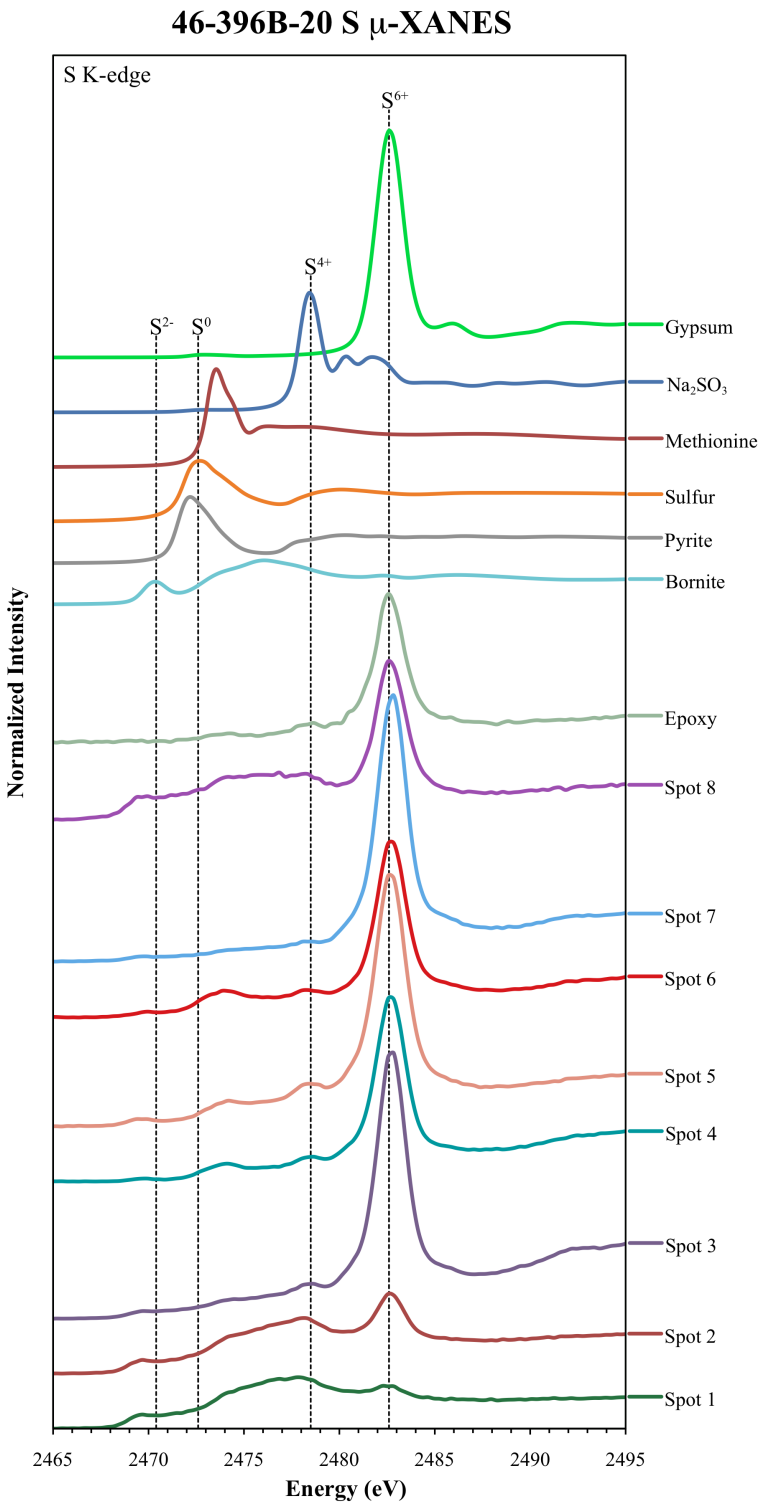

Figure 3. S K-edge μ-XANES spectra for spots 1-8 and epoxy from sample 46-396B-20, and several model compounds for reference. The locations of the spots are shown in the reflected light image in Figure 1. The spectra are offset vertically for visual clarity. Four reference lines are shown at 2470.4, 2472.6, 2478.5, and 2482.6eV, corresponding to the peak maxima for S^{2-}, S^{0}, S^{4+}, and S^{6+}, respectively.

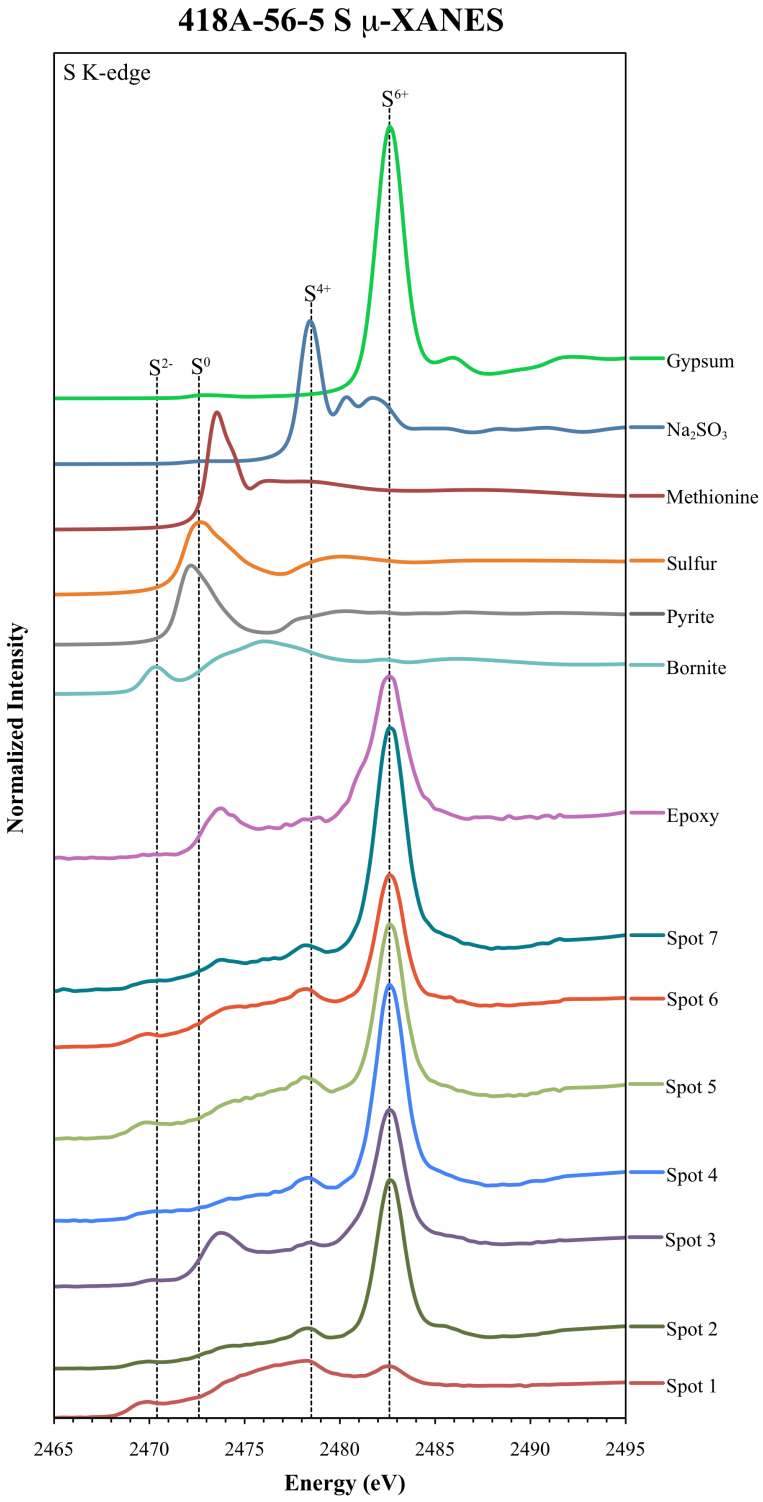

Figure 4. S K-edge μ-XANES spectra for spots 1-7 and epoxy from sample 418A-56-5, and several model compounds for reference. The locations of the spots are shown in the reflected light image in Figure 2. The spectra are offset vertically for visual clarity. Four reference lines are shown at 2470.4, 2472.6, 2478.5, and 2482.6eV, corresponding to the peak maxima for S^{2-}, S^{0}, S^{4+}, and S^{6+}, respectively.

The S μ-XANES spectra collected from the alteration regions and cracks for both sample 46-396B-20 (spot 2-8, Figure 3) and 418A-56-5 (spot 2-7, Figure 4) show the predominance of oxidized sulfur (6+) in the palagonite and the tubules. At spot 2 in sample 46-396B-20 the structure of the spectrum looks similar to that of the basalt glass (spot 1), but the sulfate (S^{6+}) peak is more pronounced, indicating that the fluorescence signal at this spot is a mix of basalt glass and alteration products. At spot 8 in this sample, which is in the middle of one of the palagonite zones, the sulfate peak is much more pronounced than at spot 2, but the rest of the spectrum is also similar to that of basalt glass, with a broad hump between 2472.6 and 2480 eV and the small peak at ~2469.5 eV. The element distribution maps for sample 46-396B-20 demonstrate that compared to the basalt glass, spot 2 only has a slight S enrichment, and at spot 8 the S is depleted (Figure 1), which agrees well with the μ-XANES results showing that these spots represent mixed signals with the reduced S in the glass. In both samples 46-396B-20 and 418A-56-5 the spectra collected from the alteration regions no longer have the broad hump characteristic of the glass and instead have much more pronounced S^{6+} peaks.

These general spectral patterns, the characteristic reduced S peaks in the basalt glass and the prominent S^{6+} peak in the alteration regions, were also seen in μ-XANES spectra from samples 896A-11R1 and CY-1-31 (Figure S3 and S4). The dominance of oxidized S in the alteration regions indicates that sulfate is abundant, while sulfides are either very low in concentration or absent altogether. Considering that during the low-temperature alteration of basalt the primary form of secondary sulfur is pyrite, the presence of almost entirely oxidized sulfur-bearing phases in the S enrichments in the tubules and palagonite could potentially be a sign of microbial sulfide oxidation within the cracks and tubules, leading to accumulations of sulfate.

Several of the spectra collected from the tubules and palagonite in all of the samples also have small peaks at ~2469.5, 2473.5, and 2478.5 eV. The peak at ~2473.5 eV correlates well with that of the reduced S in organic matter, as seen by the correlation with the main peak for methionine (e.g. Rompel *et al*., 1998; Fleet, 2005). This peak is fairly pronounced in sample 418A-56-5 at spot 5 (Figure 4), which is in the middle of the crack-filling material, and also in the epoxy for this sample, which is composed of organic compounds. However, the 2473.5 eV peak is not present in the epoxy in sample 46-396B-20, indicating a different epoxy composition, specifically one lacking the thiol groups present in methionine (Rompel *et al*., 1998).

3.3 *Ruling out Potential Epoxy Contamination*

The full X-ray fluorescence (XRF) spectra collected from spot 6 and the epoxy on the edge of the thin section for sample 418A-56-5 show the relative intensities of the peaks of interest (Figure 5). The epoxy spectrum can be considered a background signal for the sample. The intensities of all of the peaks in the epoxy spectrum were so much lower than from the tubules that it was necessary to plot them on a log scale in order to show them on the same plot. The epoxy contains small amounts of O and Al, and slightly more S and Cl. The peak intensities for these four elements are much higher in the tubule spot, indicating that the tubules contain significantly higher concentrations of these elements than could be accounted for by contamination with epoxy. The spectrum for the tubule spot also shows strong Si and Mg peaks and weaker Na and Fe L-edge peaks, all of which aren't present in the epoxy spectrum. This particular spot in sample 418A-56-5 didn't correlate with a P hotspot, thus the P peak is not present in the XRF spectrum.

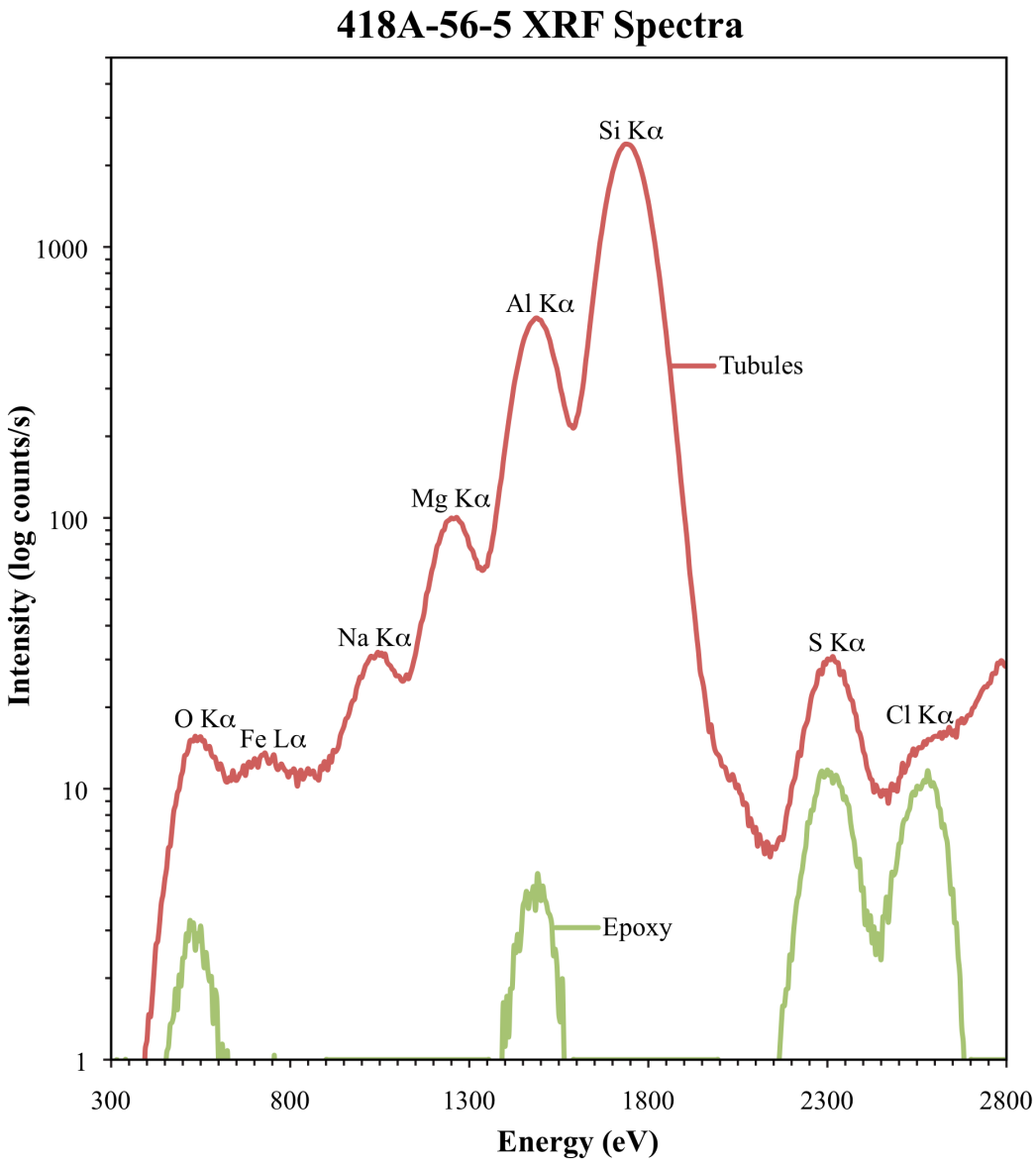

Figure 5. XRF spectra collected from spot 6 (red), which is in the middle of tubules, and the epoxy (green) from sample 418A-56-5 (Figure 2). The intensity is shown on a log scale in order to show all of the relevant peaks on the same graph.

Since the preparation of standard petrographic thin sections involves gluing the rock fragments onto the slides with epoxy it is theoretically possible that some of the epoxy may have leaked through cracks and contaminated the samples. In both sample 46-396B-20 and 418A-56-5 the μ-XANES the S^{6+} peak dominates spectra for the epoxy. The epoxy spectrum for sample 418A-56-5 also includes a smaller peak at ~2473.5 eV, which is present in some of the alteration regions, as discussed above. However, it is unlikely that the epoxy is the source of the oxidized sulfur in the alteration regions. As shown in the full XRF spectra (Figure 3), the maximum intensity for the S peak in the tubules (~31count/s) is more than twice the intensity of the S peak in the epoxy (~13 count/s). The epoxy also contains about as much Cl as S, whereas the tubules contain much less Cl than S (Figure 3). When comparing the Cl distributions in the element maps for all four samples analyzed (Figures 1, 2, S1, and S2) they are not correlated with the S distributions in the alteration regions, as would be expected if the epoxy were a significant component. Thus, there is probably little to no epoxy contamination in the tubules or palagonite. The only sample that shows a significant Cl signal in the crack is 46-396B-20. It is possible that this could represent epoxy, but it could also indicate the presence of chloride minerals, such as halite in the crack-filling material.

4. Conclusions and Recommendations

Combining synchrotron-based hard and soft X-ray fluorescence microprobe mapping and micro-spectroscopy is a powerful way to analyze the chemistry and distributions of a large suite of elements in micron-scale features. Such analyses elucidate both the mineral distributions and variations at scales relevant to endolithic microbial processes, and identify potential chemical

biosignatures. The current results demonstrate that while oxides, clays, and zeolites are common secondary alteration products in the tubules, cracks, and palagonite, their distributions are variable between samples and within a single sample across scales of only a few microns. The identification of phosphorus enrichments within the tubules suggests that presence of organic matter. These results also revealed numerous sulfur enrichment hot spots within the tubules, where the accumulated sulfur is in the S^{6+} form, likely within a sulfate phase, which suggests microbial metabolic processing. Additional micron-scale analyses focusing on the chemical nature of the P and S in the enrichments hot spots, and any potential carbon in these samples are necessary to understand the nature of the oxidized sulfur and confirm whether or not there is in fact organic matter in the alteration regions.

One common technique employed in the analysis of the coordination and specific mineralogy of an element of interest is to use quantitative linear combination algorithms to fit an experimental XANES spectrum against a database of model compound spectra (e.g. Prange *et al*., 2002a,b; Fleet, 2005; Lee *et al*., 2007). However, this technique can be difficult with elements present in multiple oxidation states, such as sulfur (Hullebusch *et al*., 2009; Wilke *et al*., 2011). In the current study we used a beamline in the pilot phase of operation and were unable to collect μ-XANES spectra with the structural detail necessary to perform high quality quantitative fits. Instead we present a qualitative comparison of the experimental spectra to several model compound spectra, focusing more on the oxidation states of sulfur present in the samples than the specific chemical coordination. Further in-depth analyses of the sulfur hotspots in these samples should include collection of μ-XANES spectra with very high spectral and spatial resolution.

An additional technique that could potentially provide valuable chemical information is synchrotron-based scanning transmission X-ray microscopy (STXM). Spot sizes on STXM beamlines can be focused down to ~30 nm, enabling the collection of very high-resolution quantitative soft X-ray element maps and fluorescence spectra. STXM is particularly useful for mapping the distribution of potential cellular material and collecting near-edge X-ray absorption fine structure (NEXAFS) spectra, which can be very instrumental in the identification functional groups in organic molecules (Templeton and Knowles, 2009). Recent applications of this technique to studies in geomicrobiology and paleontology have lead to important insights into biomineralization (e.g. Benzerara *et al*., 2011; Miot, J., *et al.* 2011; Couradeau *et al*. 2012) and microfossils (e.g. Benzerara *et al*., 2006; Galvez *et al*. 2012). STXM analyses of tubular alteration features could potentially reveal the chemical coordination of P within the tubules, map the distribution of carbon, and identify whether or not the P and C are bound in organic matter.

The confirmation of the presence of organic sulfur in the tubules would add significantly to the argument for the biogenicity of the tubules, however, most of the sulfur appears to be in the form of sulfate. Sensitive isotopic analyses using nano-scale secondary ion mass spectroscopy (NanoSIMS) could potentially help in understanding the source of the sulfate. NanoSIMS has been used successfully in a handful of studies of biosignatures and microfossils to both map element distributions and analyze isotopic fractionations (e.g. Oehler *et al.,* 2006, 2008; Fletcher *et al.,* 2008; Wacey *et al.,* 2008; McLoughlin *et al*., 2011). In previous studies of both young and ancient tubular and granular alteration features, carbon isotopic analyses have shown significantly lower $\delta^{13}C$ values in the bioalteration features than in carbonates in the surrounding glass (Furnes *et al.*, 2001a; Banerjee *et al.*, 2006). In one study of multiple sulfur

isotopes in pyrite in subseafloor basalts from ODP Hole 801 in the western Pacific, Rouxel *et al.* found compelling evidence for microbial sulfate reduction playing a significant role in basalt alteration (2008), but thus far no one has studied the sulfur isotopes within tubular alteration features. Evidence of chemolithoautotrophic geochemical processing in these features would be greatly supported by evidence of biological sulfur isotope fractionation. However, the results of NanoSIMS investigations of the $\Delta^{34}S$ values for sulfate in tubular alteration features could be difficult to interpret. There have been few studies of the isotopic fractionation associated with the oxidation of sulfide in the subseafloor, either biological or abiotic. Laboratory and field investigations in other systems indicate that the biological oxidation of H_2S to S^0 and other intermediate compounds, and the oxidation of S^0 to SO_4^{2-} are accompanied by only small isotopic fractionations (e.g. Canfield, 2001; Zerkle *et al*., 2009; Balci *et al*., 2012). The abiotic formation of anhydrite from seawater results in negligible isotopic fractionations, generally retaining the S isotope ratios of seawater (Alt *et al*., 1985). Thus, differentiating the biological formation of sulfate minerals from abiotic precipitation from seawater could be challenging.

The current results provide intriguing hints of the presence of organic matter and microbially produced sulfate in tubular alteration features. Building on these findings with additional micro-analytical techniques could potentially provide the evidence necessary to demonstrate that microorganisms once occupied the tubules and engaged in chemolithoautotrophic metabolic processing. Such a discovery would help not only to expand our understanding of the subseafloor biome, but also significantly strengthen the case for the classification of tubular alteration features as biosignatures.

5. Acknowledgements

We would like to thanks Thomas Huthwelker at the Swiss Light Source for his assistance with analyses, Hubert Staudigel at Scripps Institute of Oceanography and Harald Furnes at the University of Bergen, Norway for sharing their samples, and Graham Lau for assisting with analyses and providing sulfur model compound spectra.

6. References

Alt, J.C., Saltzman, E.S., and Price, D.A. (1985) Anhydrite in hydrothermally altered basalts: Deep Sea Drilling Project Hole 504B, Leg 83. In *Initial Reports of the Deep Sea Drilling Project Vol. 83*. U.S. Government Printing Office, pp. 283–288.

Alt, J.C. (1995) Subseafloor Processes in Mid-Ocean Ridge Hydrothermal Systems. In *Seafloor Hydrothermal Systems: Physical, Chemical, Biological, and Geological Interactions*. Humphris, S.E., Zierenberg, R.A., Mullineaux, L.S., and Thomson, R.E. (eds): American Geophysical Union, pp. 85-114.

Alt, J.C., and Honnorez, J. (1984) Alteration of the upper oceanic-crust, DSDP Site-417 - Mineralogy and chemistry. *Contributions to Mineralogy and Petrology* 87: 149-169.

Alt, J.C., Kinoshita, H., Stokking, L.B., Allerton, S., Bach, W., Becker, K. et al. (1993) Site 896. In *Proceedings of the Ocean Drilling Program; Initial reports, Leg 148*. College Station, TX: Ocean Drilling Program, p. 352.

Andrews, A.J. (1979) Effect of low-temperature seawater-basalt interaction on the distribution of sulfur in oceanic-crust, layer-2. *Earth and Planetary Science Letters* 46: 68-80.

Bach, W., and Edwards, K.J. (2003) Iron and sulfide oxidation within the basaltic ocean crust: Implications for chemolithoautotrophic microbial biomass production. *Geochimica et Cosmochimica Acta* 67: 3871-3887.

Balci, N., Mayer, B., Shanks Iii, W.C., and Mandernack, K.W. (2012) Oxygen and sulfur isotope systematics of sulfate produced during abiotic and bacterial oxidation of sphalerite and elemental sulfur. *Geochimica et Cosmochimica Acta* 77: 335-351.

Banerjee, N.R., Furnes, H., Muehlenbachs, K., Staudigel, H., and de Wit, M. (2006) Preservation of ~3.4-3.5 Ga microbial biomarkers in pillow lavas and hyaloclastites from the Barberton Greenstone Belt, South Africa. *Earth and Planetary Science Letters* 241: 707-722.

Banerjee, N.R., and Muehlenbachs, K. (2003) Tuff life: Bioalteration in volcaniclastic rocks from the Ontong Java Plateau. *Geochemistry Geophysics Geosystems* 4: doi:10.1029/2002GC000470.

Benzerara, K., Menguy, N., Lopez-Garcia, P., Yoon, T.H., Kazmierczak, J., Tyliszczak, T. et al. (2006) Nanoscale detection of organic signatures in carbonate microbialites. *Proceedings of the National Academy of Sciences of the United States of America* 103: 9440-9445.

Benzerara, K., Miot, J., Morin, G., Ona-Nguema, G., Skouri-Panet, F., and Ferard, C. (2011) Significance, mechanisms and environmental implications of microbial biomineralization. *Comptes Rendus Geoscience* 343: 160-167.

Canfield, D.E. (2001) Biogeochemistry of sulfur isotopes. *Reviews in Mineralogy and Geochemistry* 43: 607-636.

Clayton, T., and Pearce, R.B. (2000) Alteration mineralogy of Cretaceous basalt from ODP Site 1001, Leg 165 (Caribbean Sea). *Clay Minerals* 35: 719-733.

Couradeau, E., Benzerara, K., Gerard, E., Moreira, D., Bernard, S., Brown, G.E., and Lopez-Garcia, P. (2012) An early-branching microbialite cyanobacterium forms intracellular carbonates. *Science* 336: 459-462.

Dmitriev, L., and Heirtzler, J., et al. (1978) Initial Reports of the Deep Sea Drilling Project 46. Washington, DC.: US Government Printing Office.

Donnelly, T., Francheteau, J., Bryan, W., Robinson, P.T., Flower, M.F.J., and Salisbury, M. (1979) Initial Reports of the Deep Sea Drilling Project, v. 51, 52, 53. Washington: U.S. Government Printing Office, pp. 1535-1555.

Drief, A., and Schiffman, P. (2004) Very low-temperature alteration of sideromelane in hyaloclastites and hyalotuffs from Kilauea and Mauna Kea volcanoes: Implications for the mechanism of palagonite formation. *Clays and Clay Minerals* 52: 622-634.

Edwards, K.J., Bach, W., and McCollom, T.M. (2005) Geomicrobiology in oceanography: microbe-mineral interactions at and below the seafloor. *Trends in Microbiology* 13: 449-456.

Engel, A.S., Lichtenberg, H., Prange, A., and Hormes, J. (2007) Speciation of sulfur from filamentous microbial mats from sulfidic cave springs using X-ray absorption near-edge spectroscopy. *FEMS Microbiology Letters* 269: 54-62.

Fleet, M.E. (2005) XANES spectroscopy of sulfur in Earth materials. *The Canadian Mineralogist* 43: 1811-1838.

Fletcher, I.R., Kilburn, M.R., and Rasmussen, B. (2008) NanoSIMS μ-scale in situ measurement of C-13/C-12 in early Precambrian organic matter, with permil precision. *International Journal of Mass Spectrometry* 278: 59-68.

Fliegel, D., Knowles, E., Wirth, R., Templeton, A., Staudigel, H., Muehlenbachs, K., and Furnes, H. (in press) Characterization of alteration textures in Cretaceous oceanic crust from the N-Atlantic (DSDP Hole 418A) by spatially-resolved spectroscopy.

Fliegel, D., Kosler, J., McLoughlin, N., Simonetti, A., de Wit, M.J., Wirth, R., and Furnes, H. (2010) In-situ dating of the Earth's oldest trace fossil at 3.34 Ga. *Earth and Planetary Science Letters* 299: 290-298.

Foriel, J., Philippot, P., Susini, J., Dumas, P., Somogyi, A., Salome, M. et al. (2004) High-resolution imaging of sulfur oxidation states, trace elements, and organic molecules distribution in individual microfossils and contemporary microbial filaments. *Geochimica et Cosmochimica Acta* 68: 1561-1569.

Furnes, H., Banerjee, N.R., Muehlenbachs, K., and Kontinen, A. (2005) Preservation of biosignatures in metaglassy volcanic rocks from the Jormua ophiolite complex, Finland. *Precambrian Research* 136: 125-137.

Furnes, H., Banerjee, N.R., Muehlenbachs, K., Staudigel, H., and de Wit, M. (2004) Early life recorded in Archean pillow lavas. *Science* 304: 578-581.

Furnes, H., McLoughlin, N., Muehlenbachs, K., Banerjee, N.R., Staudigel, H., Dilek, Y. et al. (2008) Oceanic Pillow Lavas and Hyaloclastites as Habitats for Microbial Life Through Time - A Review. In *Links Between Geological Processes, Microbial Activities & Evolution of Life*. Dilek, Y., Furnes, H., and Muehlenbachs, K. (eds): Springer.

Furnes, H., Muehlenbachs, K., Torsvik, T., Thorseth, I.H., and Tumyr, O. (2001) Microbial fractionation of carbon isotopes in altered basaltic glass from the Atlantic Ocean, Lau Basin and Costa Rica Rift. *Chemical Geology* 173: 313-330.

Furnes, H., Muehlenbachs, K., Torsvik, T., Tumyr, O., and Shi, L. (2002) Biosignatures in metabasaltic glass of a Caledonian ophiolite, west Norway. *Geological Magazine* 139: 601-608.

Furnes, H., Staudigel, H., Thorseth, I.H., Torsvik, T., Muehlenbachs, K., and Tumyr, O. (2001) Bioalteration of basaltic glass in the oceanic crust. *Geochemistry Geophysics Geosystems* 2: doi:10.1029/2000GC000150.

Galvez, M.E., Beyssac, O., Benzerara, K., Bernard, S., Menguy, N., Cox, S.C. et al. (2012) Morphological preservation of carbonaceous plant fossils in blueschist metamorphic rocks from New Zealand. *Geobiology* 10: 118-129.

Hullebusch, E. van., Rossano, S., Farges, F., Lenz, M., Labanowski, J., Lagarde, O. et al. (2009) Sulfur K-edge XANES spectroscopy as a tool for understanding sulfur chemical state in anaerobic granular sludge. In *14th International Conference on X-Ray Absorption Fine Structure (XAFS14)*: Journal of Physics: Conference Series, pp. 1-4.

Jugo, P.J., Wilke, M., and Botcharnikov, R.E. (2010) Sulfur K-edge XANES analysis of natural and synthetic basaltic glasses: Implications for S speciation and S content as function of oxygen fugacity. *Geochimica et Cosmochimica Acta* 74: 5926-5938.

Knowles, E., Staudigel, H., and Templeton, A. (submitted) Geochemical characterization of putative biosignatures in subseafloor basalt glass.

Knowles, E., Wirth, R., and Templeton, A. (in review) A comparative analysis of potential biosignatures in basalt glass by FIB-TEM.

Konhauser, K. (2007) *Introduction to Geomicrobiology*. Malden, MA: Blackwell Publishing.

Lanzirotti, A., Tappero, R., and Schulze, D.G. (2010) Practical Application of Synchrotron-Based Hard X-Ray Microprobes in Soil Sciences. In *Developments in Soil Science*. Singh, B., and Gräfe, M. (eds): Elsevier, pp. 27-72.

Lee, Y.J., Prange, A., Lichtenberg, H., Rohde, M., Dashti, M., and Wiegel, J. (2007) In situ analysis of sulfur species in sulfur globules produced from thiosulfate by Thermoanaerobacter sulfurigignens and Thermoanaerobacterium thermosulfurigenes. *Journal of Bacteriology* 189: 7525-7529.

Lemelle, L., Labrot, P., Salome, M., Simionovici, A., Viso, M., and Westall, F. (2008) In situ imaging of organic sulfur in 700-800 My-old Neoproterozoic microfossils using X-ray spectromicroscopy at the SK-edge. *Organic Geochemistry* 39: 188-202.

Malpas, J., Moores, E.M., Panayiotou, A., and Xenophontos, C. (1990) *Ophiolites: Oceanic Crustal Analogs. Proceedings of the Symposium 'Troodos 1987'*. Nicosia, Cyprus: The Geological Survey Department, Ministry of Agriculture and Natural Resources.

Mathez, E.A. (1976) Sulfur Solubility and Magmatic Sulfides in Submarine Basalt Glass. *Journal of Geophysical Research* 81: 4269-4276.

McLoughlin, N., Wacey, D., Kruber, C., Kilburn, M.R., Thorseth, I.H., and Pedersen, R.B. (2011) A combined TEM and NanoSIMS study of endolithic microfossils in altered seafloor basalt. *Chemical Geology* 289: 154-162.

Miot, J., Maclellan, K., Benzerara, K., and Boisset, N. (2011) Preservation of protein globules and peptidoglycan in the mineralized cell wall of nitrate-reducing, iron(II)-oxidizing bacteria: a cryo-electron microscopy study. *Geobiology* 9: 459-470.

Oehler, D.Z., Robert, F., Chaussidon, M., and Gibson, E.K. (2008) Bona fide biosignatures: Insights from combined NanoSIMS-SIMS. *Geochimica et Cosmochimica Acta* 72: A698-A698.

Oehler, D.Z., Robert, F., Mostefaoui, S., Meibom, A., Selo, M., and McKay, D.S. (2006) Chemical mapping of Proterozoic organic matter at submicron spatial resolution. *Astrobiology* 6: 838-850.

Orcutt, B.N., Sylvan, J.B., Knab, N.J., and Edwards, K.J. (2011) Microbial Ecology of the Dark Ocean above, at, and below the Seafloor. *Microbiology and Molecular Biology Reviews* 75: 361-422.

Philippot, P., Foriel, J., Susini, J., Khodja, H., Grassineau, N., and Fouquet, Y. (2003) High-resolution imaging of transition metal and sulfur-redox distribution in individual microfossils. *Journal De Physique IV* 104: 381-384.

Pickering, I.J., George, G.N., Yu, E.Y., Brune, D.C., Tuschak, C., Overmann, J. et al. (2001) Analysis of sulfur biochemistry of sulfur bacteria using X-ray absorption spectroscopy. *Biochemistry* 40: 8138-8145.

Prange, A., Chauvistre, R., Modrow, H., Hormes, J., Truper, H.G., and Dahl, C. (2002) Quantitative speciation of sulfur in bacterial sulfur globules: X-ray absorption spectroscopy reveals at least three different species of sulfur. *Microbiology-SGM* 148: 267-276.

Prange, A., Dahl, C., Truper, H.G., Behnke, M., Hahn, J., Modrow, H., and Hormes, J. (2002) Investigation of S-H bonds in biologically important compounds by sulfur K-edge X-ray absorption spectroscopy. *European Physical Journal D* 20: 589-596.

Rompel, A., Cinco, R.M., Latimer, M.J., McDermott, A.E., Guiles, R.D., Quintanilha, A. et al. (1998) Sulfur K-edge X-ray absorption spectroscopy: A spectroscopic tool to examine the redox state of S-containing metabolites in vivo. *Proceedings of the National Academy of Sciences of the United States of America* 95: 6122-6127.

Rouxel, O., Ono, S.H., Alt, J., Rumble, D., and Ludden, J. (2008) Sulfur isotope evidence for microbial sulfate reduction in altered oceanic basalts at ODP Site 801. *Earth and Planetary Science Letters* 268: 110-123.

Schramm, B., Devey, C.W., Gillis, K.M., and Lackschewitz, K. (2005) Quantitative assessment of chemical and mineralogical changes due to progressive low-temperature alteration of East Pacific Rise basalts from 0 to 9 Ma. *Chemical Geology* 218: 281-313.

Seewald, J.S., and Seyfried, W.E. (1990) The effect of temperature on metal mobility in subseafloor hydrothermal systems: constraints from basalt alteration experiments. *Earth and Planetary Science Letters* 101: 388-403.

Staudigel, H., Furnes, H., Banerjee, N.R., Dilek, Y., and Muehlenbachs, K. (2006) Microbes and volcanoes: A tale from the oceans, ophiolites, and greenstone belts. *GSA Today* 16: 4-10.

Staudigel, H., Furnes, H., McLoughlin, N., Banerjee, N.R., Connell, L.B., and Templeton, A. (2008) 3.5 billion years of glass bioalteration: Volcanic rocks as a basis for microbial life? *Earth-Science Reviews* 89: 156-176.

Staudigel, H., and Hart, S.R. (1983) Alteration of Basaltic Glass - Mechanisms and Significance for the Oceanic-Crust Seawater Budget. *Geochimica et Cosmochimica Acta* 47: 337-350.

Stroncik, N.A., and Schmincke, H.U. (2002) Palagonite - a review. *International Journal of Earth Sciences* 91: 680-697.

Templeton, A.S., and Knowles, E.J. (2009) Microbial transformations of minerals and metals: Recent Advances in Geomicrobiology Derived from Synchrotron-Based X-ray Spectroscopy and X-ray Microscopy. *Annual Review of Earth and Planetary Sciences* 37: 367-391.

Torsvik, T., Furnes, H., Muehlenbachs, K., Thorseth, I.H., and Tumyr, O. (1998) Evidence for microbial activity at the glass-alteration interface in oceanic basalts. *Earth and Planetary Science Letters* 162: 165-176.

Wacey, D., Kilburn, M.R., McLoughlin, N., Parnell, J., Stoakes, C.A., Grovenor, C.R.M., and Brasier, M.D. (2008) Use of NanoSIMS in the search for early life on Earth: ambient inclusion trails in a c. 3400 Ma sandstone. *Journal of the Geological Society* 165: 43-53.

Wallace, P., and Carmichael, I.S.E. (1992) Sulfur in basaltic magmas. *Geochimica et Cosmochimica Acta* 56: 1863-1874.

Wallace, P.J., and Carmichael, I.S.E. (1994) S-speciation in submarine basaltic glasses as determined by measurements of S K-alpha X-ray wavelength shifts. *American Mineralogist* 79: 161-167.

Walton, A.W., Schiffman, P., and Macpherson, G.L. (2005) Alteration of hyaloclastites in the HSDP 2 Phase 1 Drill Core: 2. Mass balance of the conversion of sideromelane to palagonite and chabazite. *Geochemistry Geophysics Geosystems* 6.

Wilke, M., Klimm, K., and Kohn, S.C. (2011) Spectroscopic Studies on Sulfur Speciation in Synthetic and Natural Glasses. In *Sulfur in Magmas and Melts: Its Importance for Natural and Technical Processes*. Chantilly: Mineralogical Society of America, pp. 41-78.

Zerkle, A.L., Farquhar, J., Johnston, D.T., Cox, R.P., and Canfield, D.E. (2009) Fractionation of multiple sulfur isotopes during phototrophic oxidation of sulfide and elemental sulfur by a green sulfur bacterium. *Geochimica et Cosmochimica Acta* 73: 291-306.

7. Supplementary Figures

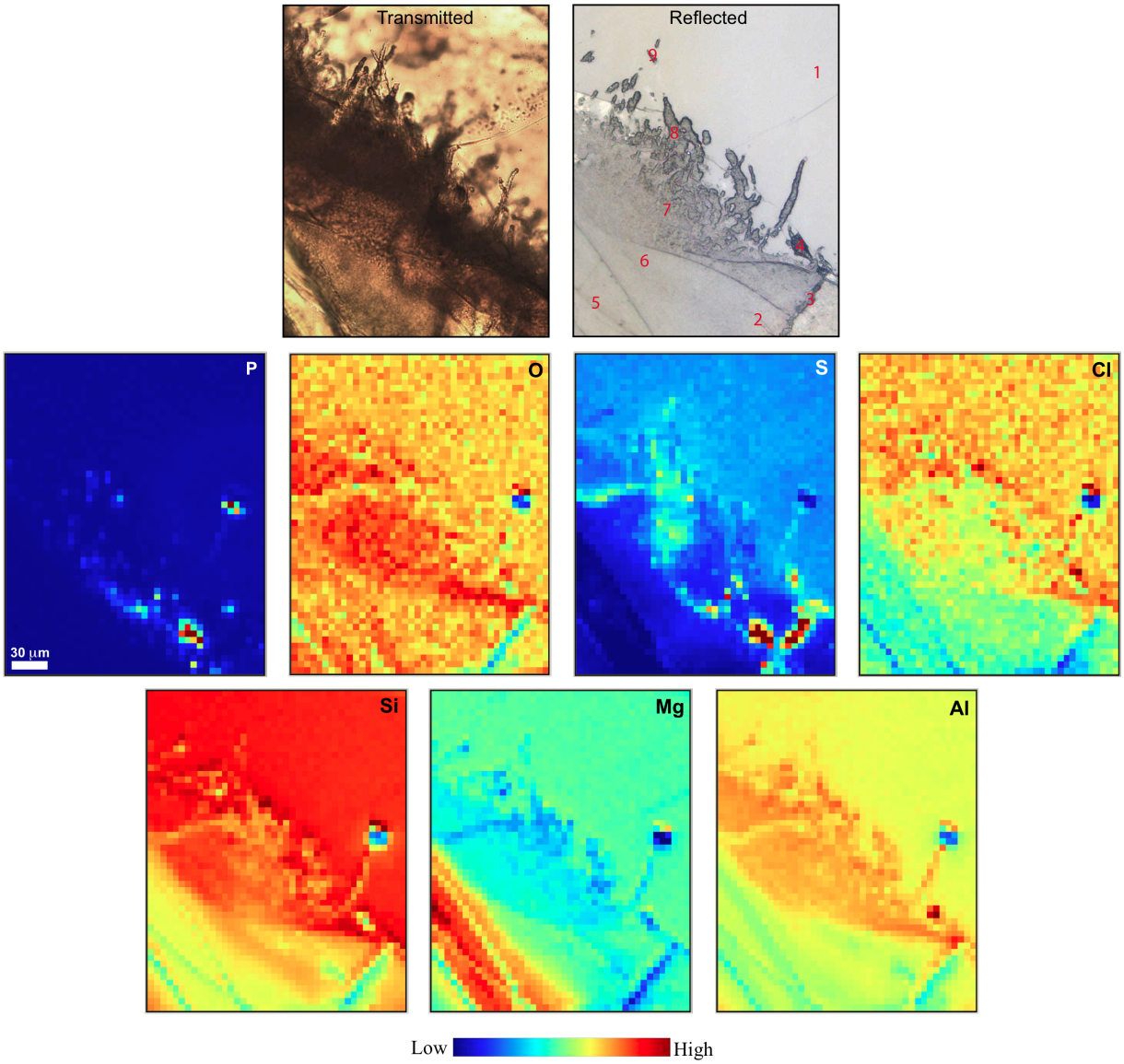

Figure S1. Top: Transmitted (left) and reflected (right) light photomicrographs of an alteration region in a thin section from sample 896A-11R1. A thick palagonite zone has formed along the main crack, which is visible in the lower left corner. Several tubules extend from the edge of the palagonite zone. Another thin crack is visible in the lower right-hand corner. At the tip of the large tubule on the right is a hole where a focused ion beam (FIB) foil was milled out (not shown in photomicrographs). The S µ-XANES spots analyzed are shown in red on the reflected light image. Middle and Bottom: Element maps corresponding field of view in the photomicrographs. The colorscale for the relative intensities of the individual element maps is shown on the bottom, where blue corresponds to lower concentration and red to higher. The scale bar on the P map is 30µm and applies to all of the maps and the photomicrographs.

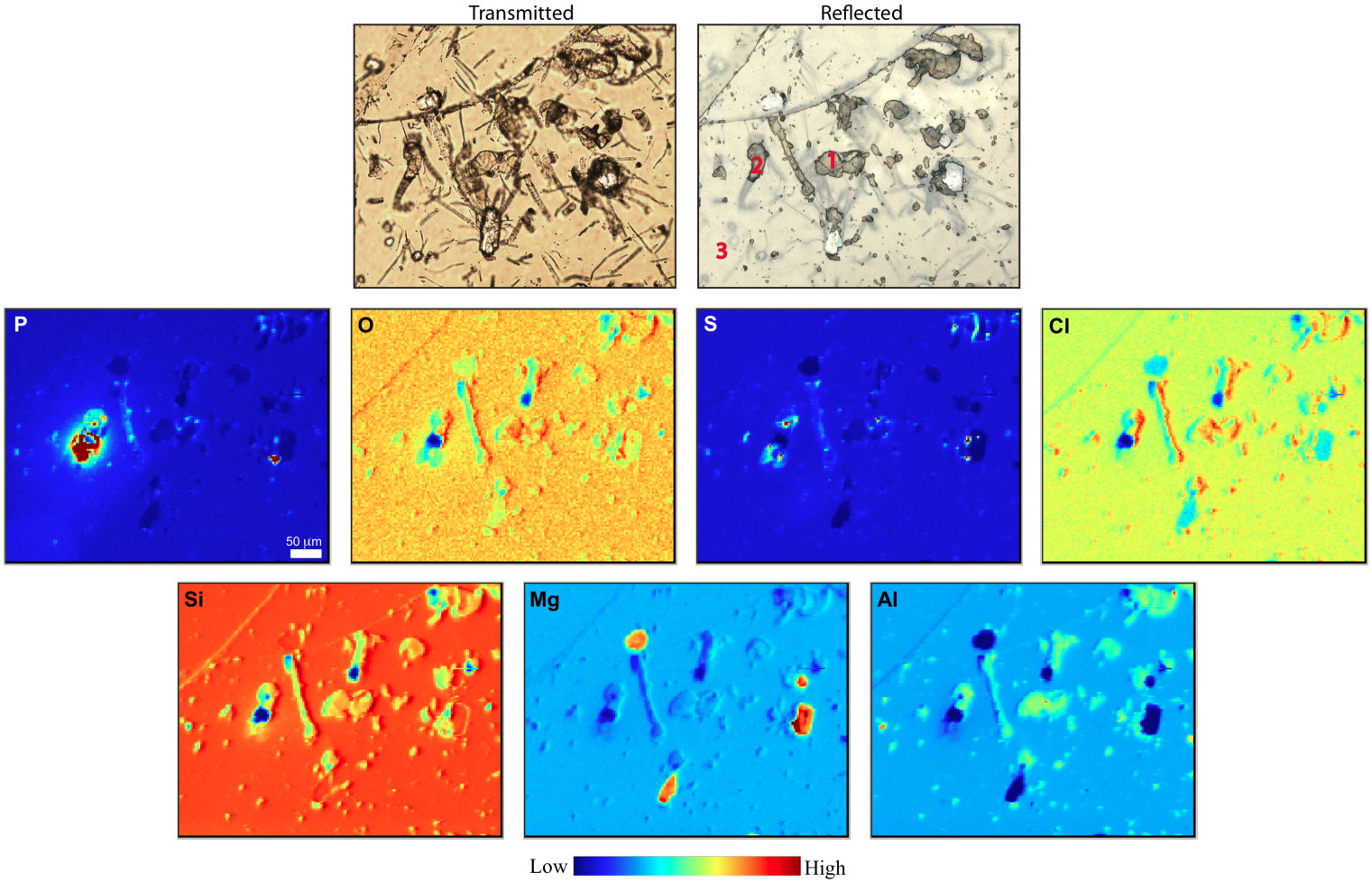

Figure S2. Top: Transmitted (left) and reflected (right) light photomicrographs of an alteration region in a thin section from sample CY-1-31. A thin crack can be seen running through the upper part of the image, from which extend several tubules. There are several more tubules visible throughout the field of view, which likely originally extended from cracks that were ground away during thin section preparation. The S µ-XANES spots analyzed are shown in red on the reflected light image. Middle and Bottom: Element maps corresponding field of view in the photomicrographs. The colorscale for the relative intensities of the individual element maps is shown on the bottom, where blue corresponds to lower concentration and red to higher. The scale bar on the P map is 50µm and applies to all of the maps and the photomicrographs.

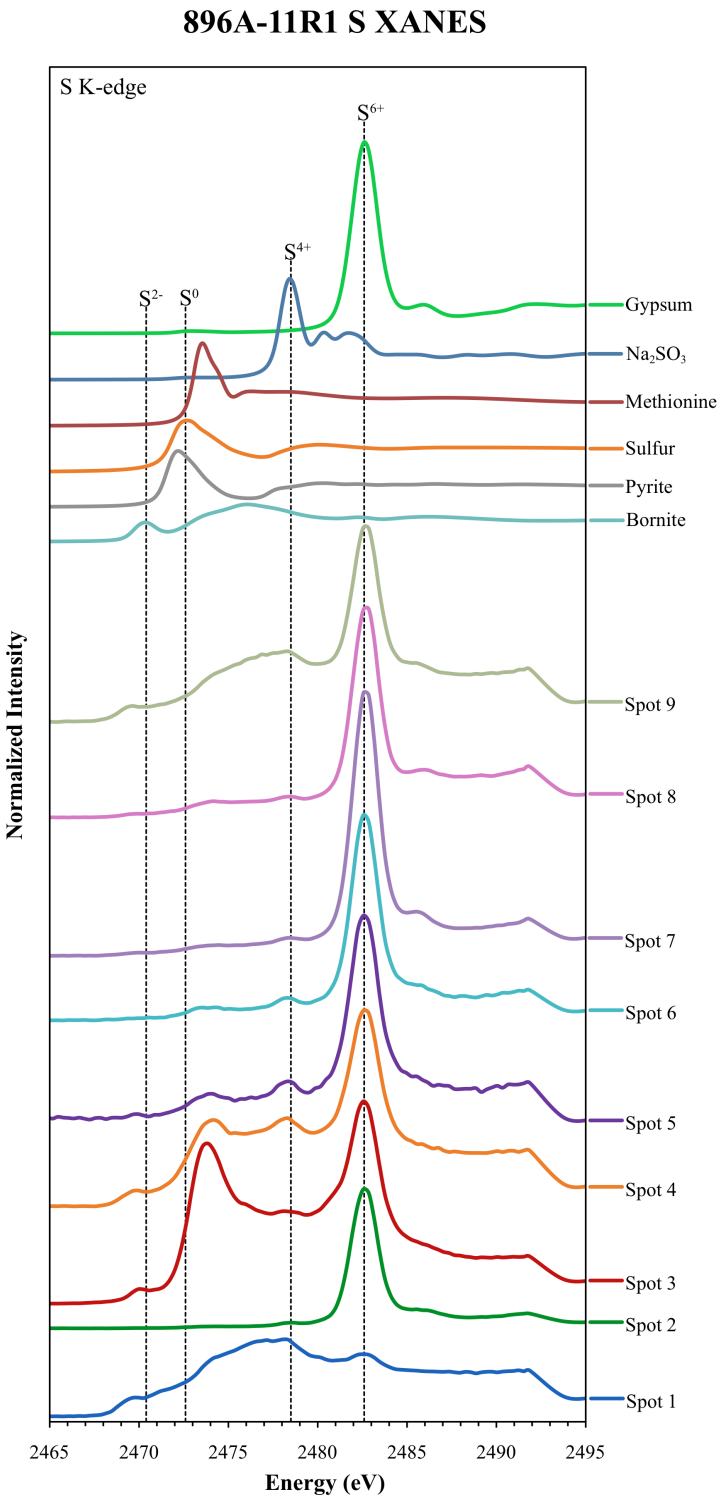

Figure S3. S K-edge μ-XANES spectra for spots 1-9 from sample 896A-11R1 and several model compounds for reference. The locations of the spots are shown in the reflected light image in Figure S1. The spectra are offset vertically for visual clarity. Four reference lines are shown at 2470.4, 2472.6, 2478.5, and 2482.6eV, corresponding to the peak maxima for S^{2-}, S^{0}, S^{4+}, and S^{6+}, respectively.

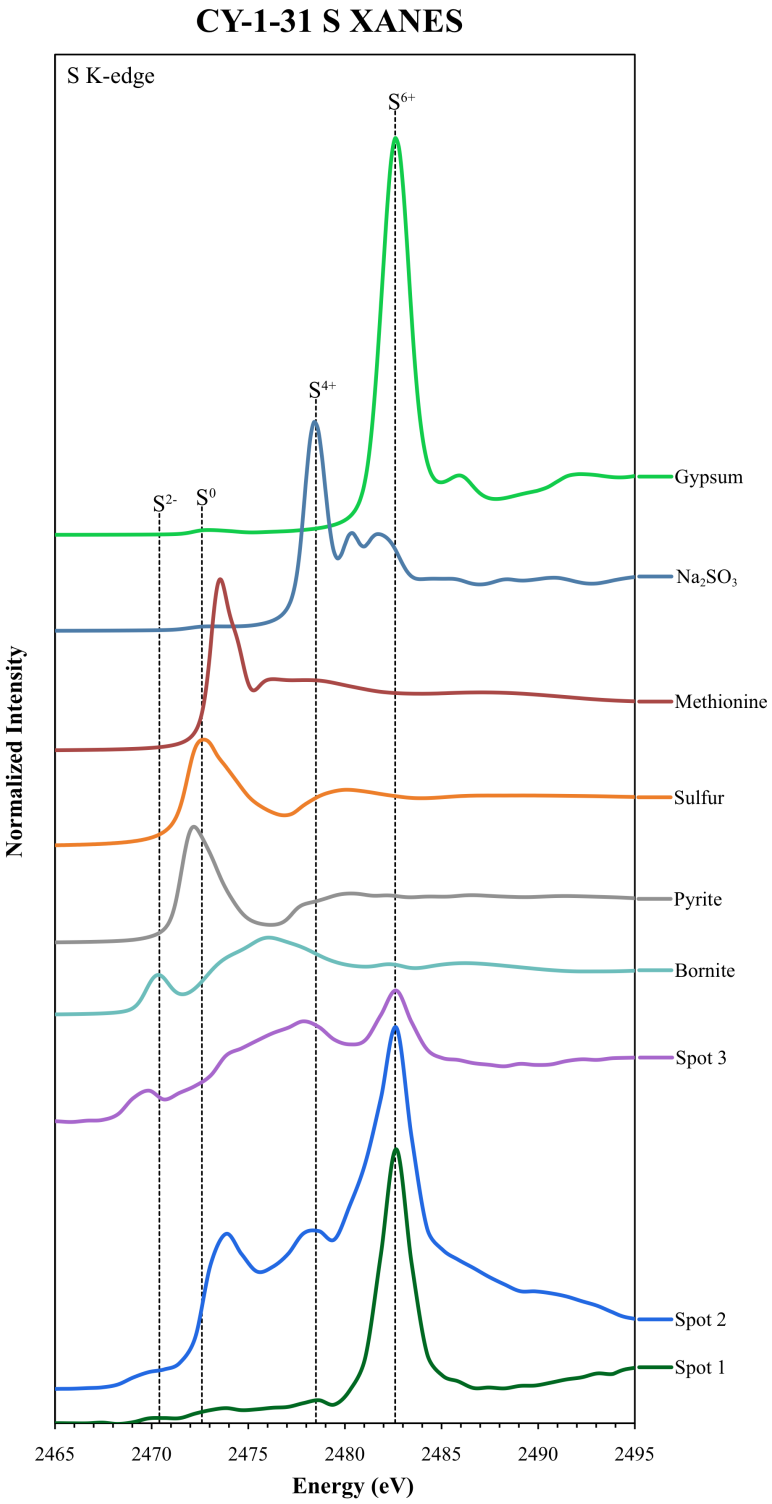

Figure S4. S K-edge μ-XANES spectra for spots 1-3 from sample CY-1-31 and several model compounds for reference. The locations of the spots are shown in the reflected light image in Figure S2. The spectra are offset vertically for visual clarity. Four reference lines are shown at 2470.4, 2472.6, 2478.5, and 2482.6eV, corresponding to the peak maxima for S^{2-}, S^{0}, S^{4+}, and S^{6+}, respectively.

CHAPTER 5

Conclusions, Insights, and Further Thoughts

5.1 Conclusions

5.1.1 *General Patterns of Tubule Formation and Mineralization*

In combination, the four main objectives of this work were to analyze different aspects of the micron-scale geochemical characteristics of tubular alteration in the hopes of strengthen the evidence for biological processing. This body of work reports the results of how each of those objectives were achieved using three main sets of techniques: focused ion beam milling coupled with transmission electron microscopy, synchrotron-based hard X-ray analyses, and synchrotron-based soft X-ray analyses. Each of these techniques produced a unique dataset, leading to different geochemical and biological insights, as detailed in the conclusions section of each main chapter, and briefly summarized below. These techniques are also very complementary and build off of each other to form a more complete picture of the formation and mineralization of tubular alteration features.

The FIB-TEM analyses provided very high-resolution images of the secondary phases in-filling the tubules and the contact between the tubules and the fresh basalt glass, as well as chemical analyses. These results showed the predominance of poorly-to highly ordered clays within the tubules and the presence of a thin leached rim around the tubule margins, reminiscent of incongruent dissolution. The consistency of these findings across samples that span over 100 million years in age and represent a variety of different alteration environments implies that the mechanisms involved in the formation and mineralization of tubular alteration features are common.

These results agree well with those of the synchrotron-based X-ray analyses. The hard X-ray analyses focused on the major elements Fe, Mn, Ca, and Ti in order to decipher their

distribution patterns and changes in oxidation and coordination states. Combining X-ray fluorescence microprobe mapping with μ-XANES, μ-XRD, and additional FIB-TEM analyses resulted in the identification of the secondary phases in-filling the alteration regions as primarily Fe^{3+}-bearing silicates, with secondary Fe- and Ti-oxides, a partially oxidized Mn-silicate phase, and zeolites. A comparison of the secondary mineralogies of the palagonite, tubules, and cracks showed that the mineralization of the alteration regions involves multiple successive stages of fluid flow, causing complex patterns of mineral dissolution and precipitation. The soft X-ray analyses mapped the distributions of Si, Al, Mg, O, Cl, P, and S, and focused on the oxidation state of S at key spots. These results provided more insight into the distributions of the secondary mineral phases, showing that the proportions of clays, zeolites, and oxides vary both between and within samples, and identified potential evidence of biological processing or possibly organic matter in the form of P and S enrichment hot spots. Qualitative comparisons of the sulfur μ-XANES spectra to model compound spectra showed the predominance of oxidized S in the hot spots, likely in a sulfate phase.

By putting all of these results together the major trends in geochemical characteristics of tubular alteration features emerge. Cumulatively, these analyses show that the mechanisms involved in the formation and mineralization of tubules are common throughout the ocean basins and throughout time. All of these analyses were performed on the same set of samples, which was carefully chosen to represent the biggest range in ages, collection depths, and alteration conditions available, and yet all of the alteration regions show similar textural and chemical characteristics. The common presence of the leached alteration rim implies that all tubules are initially formed by incongruent dissolution, which is consistent with microbial silicate dissolution mechanisms (see Section 1.4). While the distributions of secondary phases vary

somewhat across micron scales, in general tubular alteration features are in-filled with Fe^{3+}-bearing silicates, Fe- and Ti-oxides, and zeolites, with minor Cu, S^{6+}, and P-bearing phases in discrete hot spots. The similarities in secondary phases between the tubules and palagonite regions, which often differ from those in the cracks, implies that numerous episodes of fluid flow have occurred, with one stage replacing or overprinting another. The fact that different samples over 100 million years apart in age show the same complex mineral dissolution and precipitation patterns means that the original formation of the tubules happens early on and fluid flow continues until the cracks are sealed.

It's possible that if the tubules are in fact formed by endolithic microorganisms, they begin burrowing as soon as the crust is cool enough for occupation and fluids have penetrated the cracks and fissures. Obtaining metabolites and trace elements from the basalt is energy-expensive, as it requires production of appendages or extracellular enzymes to facilitate electron transfer and nutrient extraction and immobilization (see section 1.4.3). Since the likely chemolithoautotrophic metabolisms operating in these systems are relatively energy-poor, the microorganisms would have to live slowly, possibly taking hundreds to thousands of years to form a single 100 μm-long tubule. Fungal tunneling in feldspars, which is a good analog for tubule formation in basalt glass, has been shown to be an extremely slow process, taking up to 1000 years (Smits, 2006). The microorganisms would be able to actively metabolize as long as there was sufficient flow of oxidized seawater through the cracks, bringing the necessary electron acceptors and removing waste products. As soon as there is enough sediment and secondary phase deposition in the volcanic layers to limit permeability and cut off flow of oxidized seawater then the microbes would cease to function metabolically, although cellular integrity could potentially be preserved for far longer (see Section 1.5). With continued abiotic

mineralization the ultimate sealing off of the system the cells would eventually degrade *in situ*, or possibly become permineralized and entombed.

Stein and Stein (1994) estimate that the average "sealing age" of the oceanic crust – the age at which the sealing of fractures by sediment and secondary minerals cuts off hydrothermal flow – is 65±10 Ma for all of the ocean basins. While there may be continued "closed circulation" flow after the major fractures have sealed, there would likely be little chemical exchange between the fluids within the crust and seawater (Alt, 1995). Several studies of secondary minerals in subseafloor drill cores and the Troodos ophiolite estimate that the majority of the oxidative alteration of oceanic crust takes place within the first 5 to 10 million years and ceases by 15 to 20 million years (Hart and Staudigel, 1986; Peterson *et al*., 1986; Johnson and Semyan, 1994; Booij *et al*., 1995; Grevemeyer and Weigel, 1997; Bach and Edwards, 2003). Thus, the formation of the tubules would have to take place within the first few million years after cooling of the crust. After formation, continued closed circulation flow would cause the cyclic dissolution and re-precipitation of secondary phases within the alteration regions until the cracks became sealed. This model explains the commonalities seen between all of the samples examined, where formation of the tubules takes place early on, under comparable conditions, and the systems are sealed after 15-20 million years, preserving the mineralogy of the oxidative alteration period.

5.1.2 *Strengthening the Evidence for Biogenicity*

As discussed in section 1.6, the classification of a feature as an unambiguous biosignature requires that it can only be produced by life. In the case of trace fossils there often isn't one single piece of evidence that satisfies the biological argument, instead the combination of

multiple different lines of evidence tip the scales towards biogenicity. While some of these factors on their own may be ambiguous, for example minerals that could be formed biologically or abiotically, when multiple different characteristics that are consistent with biological presence or activity are put together the case can be very strong for classification of a feature as a biosignature. The analyses conducted in this work have resulted in a detailed visual and geochemical characterization of tubular alteration features, yielding insights into the mechanisms of formation and mineralization, but they have not provided a smoking gun of biogenicity. However, these results did revealed several different geochemical components that are consistent with biological activity.

It is hypothesized that tubular alteration features are formed either directly or indirectly as either a direct a result of the microbial extraction of metabolites and/or trace elements or indirectly from by-products of microbial metabolic processes (see Section 1.2). Both the direct and indirect mechanisms are expected to leave signs of microbial geochemical processing in the form of redox gradients, biominerals, and organic deposits. Chemical equilibrium in a microenvironment means that there is little energy to be exploited by cells, thus redox disequilibrium is favorable to life. One way this disequilibrium is established in the subsurface is through the contact of oxidized air or water with reduced rocks or minerals, which can be exploited by microbial metabolisms (see Section 1.5). Thus, *a priori* I expected to see depletions of the reduced metals Fe^{2+}, Mn^{2+}, and S^{2-}, the deposition of oxidized products, Fe^{3+}, Mn^{4+}, and S^{6+}, and the accumulation of C, and P. With the exception of Mn^{4+}, these are precisely the main results of the geochemical analyses, and in one sample there was also a Mn^{3+} phase (896A-11R1, see Chapter 3). The predominance of poorly-ordered clays mixed with an amorphous matrix in the tubules is also consistent with biomineralization (e.g. Schultze-Lam *et al*., 1996; Fortin and

Ferris, 1998; Konhauser and Urrutia, 1999). However, it is also possible to precipitate all of the oxidized secondary phases abiotically and, as shown in Chapter 3, most of these phases do in fact appear to be the result of successive stages of fluid flow.

In addition, the mineral phases identified in this work show no clear signs of the thermodynamic disequilibrium that often characterizes biominerals. For example, microbial activity can lead to the production of abundant Fe-oxides, far in excess of what would be produced by abiotic oxidation. The main factors involved in both the increased kinetic and thermodynamic favorability of Fe-oxide deposition are direct enzymatic oxidation of Fe^{2+}, decreased pH through excretion of organic acids, aqueous Fe immobilization via production of siderophores, and nucleation on bacterial surfaces (e.g. Douglas and Beveridge, 1998; Fortin and Ferris, 1998; Fortin *et al*., 1998; Banfield *et al*., 2001). The same factors apply to microbial deposition of Mn-oxides (e.g. Tebo *et al*., 2004). While some Fe-oxides were identified in the tubules, the concentrations were minimal compared to Fe-silicates, and only in one sample was a partially oxidized Mn-silicate identified. These results are consistent with both biological and abiotic mineralization, thus making the interpretation of these deposits ambiguous. The S^{6+} deposits could also be formed by either biological processing or by abiotic mineralization. However, unlike the oxidized Fe and Mn minerals, with the S-bearing deposits there is the potential to identify the chemical coordination and isotopic composition of the sulfur through further studies, which could possibly reveal evidence of its biogenic origin or metabolic processing, as discussed in Chapter 4.

The accumulations of C and P are harder to explain by purely abiotic mechanisms, and on their own are the strongest indicators of biological activity or presence. While it is possible that there could be some seawater input of particulate organic matter to the deep subseafloor volcanic

layers, it is likely very limited in concentration (Edwards *et al*., 2005), likely too low to build up measureable organic deposits. Thus, it would be difficult to invoke the input of organic matter to explain the C and P enrichments. In addition, phosphorus concentrations are very low in submarine basalt glass, typically on the order of 0.05 to 0.45 wt% (as P_2O_5) and tend to be significantly depleted in altered glass (Schramm *et al*., 2005; Walton *et al*., 2005). While no single one of these observations alone are enough to verify the biogenicity of the tubules beyond a doubt, put together they help to strengthen the argument for microbial formation, and at this point the weight of the evidence is on the biological side.

Putting together all of the observations from previous studies and the results of this work, is it easiest to explain the formation of tubular alteration features in subseafloor basalts as a result of the activity of endolithic microorganisms. As discussed above, chemolithoautotrophs are probably introduced to the system as soon as seawater penetrates the cracks. Once attached to the walls via extracellular polysaccharides and/or various appendages they begin to extract the reduced metals, sulfur, and trace elements from the basalt via production of organic acids, enzymes and direct extracellular electron transfer. This causes the instability of the silicate matrix leading to incongruent dissolution. As the initial etch pits (possibly granular alteration) deepen into tubules, the cells must either extend filaments or appendages, such as pili or nanowires, into the end of the tunnel, or occupy it themselves if there is sufficient fluid flow for exchange of metabolites and waste products. As the tubules extend further into the glass they will inevitably encounter phenocrysts; if they are plagioclase they will be avoided, while the olivine crystals will be sought out for their high Fe concentrations. This geochemical processing will lead to the authigenic precipitation of oxidized metals in the form of nano-aggregated clays and oxyhydroxide minerals, both on the surfaces of the cells and within the tubules. These

processes will proceed throughout the entire stage of oxidative alteration of the volcanic layers (10's to ~100 thousand years), possibly taking that whole period of time to form a single 100 μm-long tubule. Throughout this entire process there will likely be changes on the chemical and physical conditions of the fluids flowing through the cracks, including inputs of hydrothermal fluids, which could be catastrophic for the tubule-formers, depending on the temperatures and chemistries of the fluids. This could cause tubule formation in some regions to cease earlier than others. The fluids will also progressively alter the glass surrounding the tubules to palagonite, in some cases overprinting previous tubules. Ultimately the process will end once fluid flow ceases due to the sealing off of the cracks, preserving the morphologies of the mineralized tubules and possibly some traces of the biominerals and cellular material.

The results from this work support all of these steps in the tubule formation process; however, a few key pieces of additional evidence from further studies would lend even more support. For example, if the C, P, or S deposits could be conclusively identified as biological in origin, or younger samples were identified containing active microorganisms, the scales might finally be tipped towards clear classification of tubular alteration features as biosignatures. Such a result would indicate that this process has been operating since life first emerged on Earth, and would be very exciting for the prospects of finding life on another planet.

5.2. Further Studies

5.2.1 *Additional Micro-Analytical Techniques*

This study made use of a number of cutting-edge micro-analytical techniques, and helped to push the advancement of synchrotron beamline development (see Section 1.8). To the best of

my knowledge, at the time of this writing there are only a few additional techniques available that could potentially further our understanding of the geochemical characteristics of tubular alteration features and potentially add significant evidence to the argument for their biogenicity. First, as discussed in Chapter 4, the application of nano-scale secondary ion mass spectroscopy, or NanoSIMS, to these features could be quite revealing. By targeting the sulfur hotspots, a detailed NanoSIMS analysis might potentially show a clear signal of biological fractionation, which would strongly support the theory that sulfide-oxidizing organisms play an important role in tubule formation. Whether or not there is enough sulfur in the hot spots for a successful and accurate NanoSIMS analysis is unclear, as it is quite difficult to quantify the sulfur concentration. It is also possible that a NanoSIMS analysis could be conducted on carbon enrichments within the tubules. Previous studies of carbon deposits in altered glassy pillow rims have shown that they have low $\delta^{13}C$ values compared to carbonates in the crystalline interiors, indicating potential biological fractionation (Thorseth *et al*., 1995; Torsvik *et al*., 1998; Furnes *et al*., 2001a, 2004; Fliegel *et al*., 2010b). However, these studies have generally used much larger spot sizes than that available on most NanoSIMS instruments (100 nm or less), and may have overlapped with carbonate deposits. Whether or not there are high enough carbon concentrations to be able to use spots sizes less than 1 μm is also questionable. The major drawback to this technique is that NanoSIMS analyses of sulfur or carbon would be quite destructive to the tubules, as a large amount of material must be ablated in order to achieve reasonable counting statistics.

Second, the synchrotron-based technique of scanning transmission X-ray microscopy (STXM) could potentially provide more detailed geochemical and biological information than a soft X-ray fluorescence microprobe. STXM beamlines offer the ability to collect very high-

resolution quantitative soft X-ray element maps and fluorescence spectra, with spots sizes on the order of ~30 nm. This technique is particularly useful for the analysis of organic molecules. By mapping the distribution of low-Z elements and collecting near-edge X-ray absorption fine structure (NEXAFS) spectra one can identify particular functional groups (Templeton and Knowles, 2009). In the past several years this technique has been gaining popularity for many different applications, including investigations of biomineralization (e.g. Benzerara *et al*., 2011; Miot, J., *et al.* 2011; Couradeau *et al*. 2012) and microfossils (e.g. Benzerara *et al*., 2006; Galvez *et al*. 2012.). However, since STXM works in transmission mode it is not possible to use this technique on standard petrographic thin sections, thus it is necessary to mill ultra-thin sections using a FIB instrument.

Thus far, STXM has only been used a few times in the analysis of tubular alteration features. In their study of alteration features in drill cores samples from the Ontong Java Plateau, Benzerara *et al*. (2007) used STMX to show the presence of oxidized iron in the tubules and to identify carbon deposits, likely of an organic nature. Collaborator Daniel Fliegel and others used STXM on FIB-milled sections in two previous studies of tubular alteration features in ophiolites (Fliegel *et al*., 2010b, 2011), and one study of a sample from Hole 418A (Fliegel *et al*., in review), which is very similar to sample 418A-56-5 used in this work. These results also identified oxidized Fe and possible organic carbon deposits, as well as titanite within the tubules in the ophiolite samples. In further analyses of tubular alteration features, STXM analyses could potentially be very revealing when combined with synchrotron-based hard X-ray microprobe fluorescence mapping and the other synchrotron-based and FIB-TEM techniques used in this work.

An additional technique that could potentially be helpful in further analyses of these samples is micron-scale Raman spectroscopy. This technique works by measuring the inelastic or Raman scattering of light from a laser source. When the monochromatic laser beam interacts with a solid the molecular vibrations cause shifts in the photon energy – this is known as the Raman effect. The amplitude of the energy shift gives information about the system's vibrational modes (Smith and Dent, 2005). By focusing the laser through a lens this technique can be used for spot analyses of particular regions of interest, with spot sizes typically less than 1 μm, and to map the distributions of particular functional groups. Micro-Raman spectroscopy is becoming common in the study of both young and ancient microfossils, providing insight into the distributions of various mineral phases and organic groups (e.g. Schopf *et al*., 2002; Edwards *et al*., 2004; van Zuilen *et al*., 2005; Villar *et al*., 2005; Lepot *et al*., 2009; Wacey *et al*., 2011a,b).

In the fall of 2011 I had the opportunity to use the confocal laser Raman microscope in the Raman Lab at the University of Bergen (UiB), Norway, as a visiting scholar to the UiB Center for Geobiology. Using the argon laser source with an incident wavelength of 514 nm, I collected spectra from a number of spots within tubules, palagonite, cracks, and basalt glass in several different samples. The spectra for the different spots are clearly distinguishable from one another (Figure 1), however, in general the data are too noisy to fit to the model compound database. This noise is likely a due to both the heterogeneity and the partially amorphous nature of the secondary minerals in-filling the alteration regions. As with other spectroscopic techniques, it can be challenging to separate distinct peaks from different phases in heterogeneous environmental samples. In addition, in materials that strongly fluoresce the Raman scattering signal can be drowned out by fluorescence interference (Smith and Dent, 2005). In several of the samples I analyzed there was also interference from strong carbon peaks,

which was left over from previously carbon-coating the thin sections for electron microscopy (trace carbon was left even after re-polishing). So while the micro-Raman spectra are potentially useful for differentiating alteration regions within a sample, they are not useful for the identification of mineral species. It's possible that the resolution of the peaks could be improved with further polishing of the thin sections, on new sections that have never been carbon coated, or possibly on FIB-milled sections, however the generally poorly crystalline nature of the secondary phases limits the utility of micro-Raman spectroscopy for analysis of tubular alteration features.

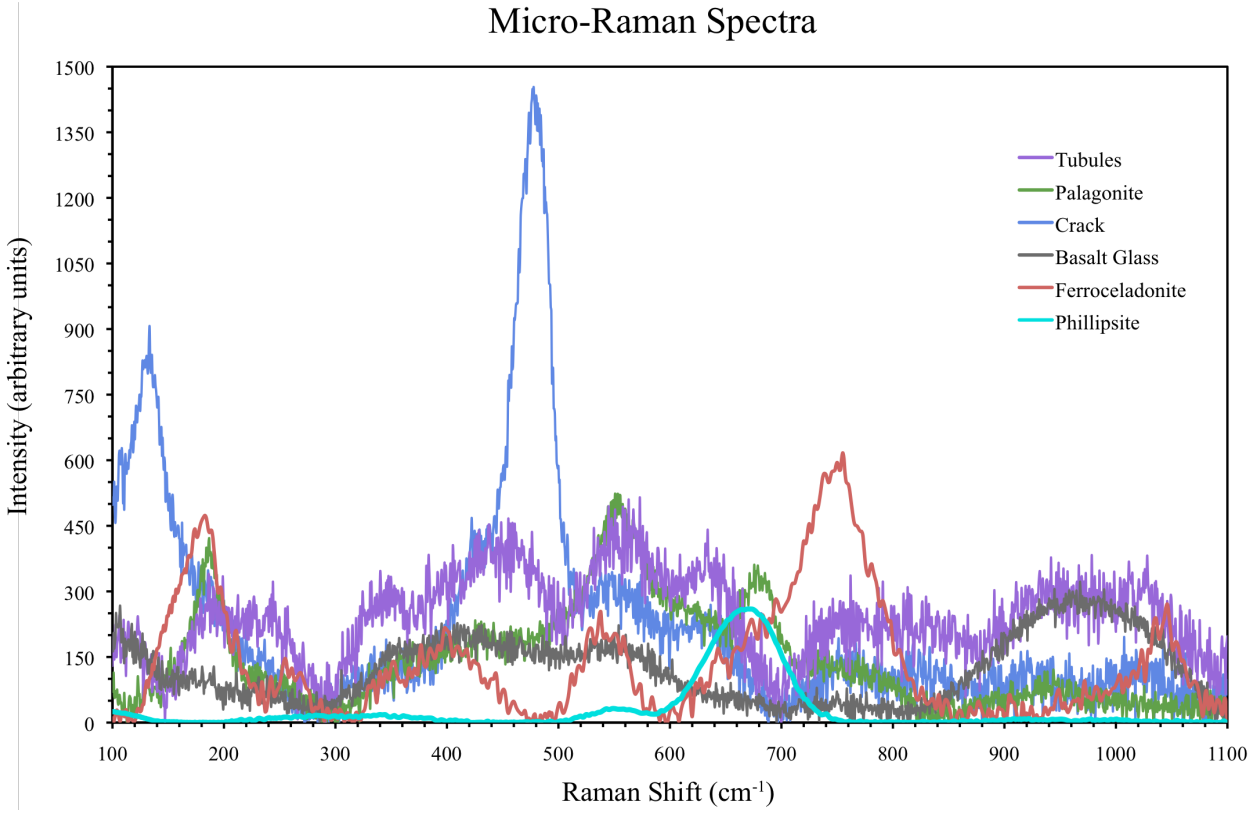

Figure 1. Micro-Raman spectra collected from a spot in the tubules (purple), palagonite (green), crack (blue), and basalt glass (gray) from sample 896A-11R1 and two relevant model compounds, ferroceladonite (red) and phillipsite (turquoise). The tubule spectrum was collected in the Raman Lab at the University of Bergen using an argon laser source at 514 nm incident wavelength. The spot size was difficult to measure, but was visibly less than the width of the tubule. The model compound spectra were obtained from the RRUFF database (http://rruff.info).

5.2.2 *Investigations of Young Seafloor Basalts*

The micron-scale analyses discussed above could potentially provide addition and possibly stronger geochemical evidence for the biogenicity of the tubules. Another way to significantly strengthen the case for microbial formation would be to find tubules in younger basalts, particularly those with viable, metabolically active intact cells still inside. Given that new seafloor is constantly forming, it can be assumed that tubule formation is still happening today, and that there are examples throughout the ocean basins of every different stage of the formation and mineralization process. If young basalt glass samples were found with intact cells in incipient or fully formed tubules, it could still be argued that these cells are simply occupying the tubules and were not involved in their formation. High-resolution imaging of the interactions of the cells with the glass and chemical analyses of the local microenvironment would be needed to settle this question and could potentially reveal strong enough evidence to put the biogenicity case to rest. If, for example, such analyses revealed attachment of a cellular appendage, such as pili or nanowires to the wall of the tubule, or the build up of organic acids and/or extracellular polysaccharides within the tubule and associated with the cells, there would be little doubt left as to the role of microorganisms in tubule formation. The discovery of intact cells in tubules from younger samples could also answer the question of which microorganisms are responsible for tubule formation. It is now possible to amplify and sequence the DNA of an organism from only a single cell (e.g. Lange, 2005; Ochman, 2007; Walker and Parkhill, 2008; Kalisky and Quake, 2011), which makes it possible to conduct genomic studies of low-biomass systems, such as the subseafloor.

In 2008 and 2009 I was provided the opportunity to collect and study young seafloor basalts as a member of the scientific party on two NSF-funded Iron Microbial Observatory

(FeMO) research cruises. The FeMO study site is the Lō‘ihi Seamount and vicinity on the flank of Mauna Loa off the southeastern coast of Hawaii, which has been an area of exciting biological and geological work for the past decade (Emerson and Moyer 2002; Templeton et al., 2005; Garcia et al., 2006; Santelli et al., 2008; Glazer and Rouxel, 2009; Edwards *et al*., 2011a), thus the ages of many of the flows are well known. Using the remote submersible Jason 2, I collected numerous pillow basalts of various ages (~150 – 4,000 years old) and alteration states from many different locations on the seamount. Collection of pillow basalts by a robotic submersible is much less destructive than drilling, thus there is the potential to observe intact cells within alteration features. At each site, one or more rocks were collected specifically for biological purposes in “bioboxes”, which were sealed containing the local sampling site water so they wouldn’t be contaminated on the return to the surface. Each rock sample was processed onboard in a stainless steel clean-box using sterile tools. Rock processing entailed chipping off surface glass and alteration rims and storing chips in sterile tubes for later processing and analyses. Larger fragments with alteration rims were also collected from each sample for later thin-sectioning and petrographic description.

In total, I returned to Colorado with more than 20 rock samples, each of which had been initially processed as above. Finding microbial alteration features in young basalts of known age would be a huge breakthrough, however, this presents a significant challenge. In order to identify alteration features it is necessary to make thin sections from the rock samples, but if the features are just beginning to form and/or are sparsely distributed then it’s like looking for a needle in a haystack. To start I chose a handful of rock samples that each had a layer of fresh glass, but represented a variety of different characteristics such as porosity, surface alteration, and from different locations on the seamount. I chose areas in each rock that represented a cross-section

through the alteration rind and into the glass and made polished thin-sections. After thoroughly examining each section for alteration features, I was unable to find any sign of tubular alteration features. It's possible that the seafloor conditions are not conducive to tubule formation (see section 5.2.3 below) and therefore a search for tubules in young seafloor basalts is fruitless. It's also possible that I simply missed the needle in the haystack and that further exhaustive examination of thin sections from young seafloor or subseafloor basalts could reveal incipient tubule formation.

5.2.3 *Are Laboratory Simulations Possible?*

The only way to clearly demonstrate the microbial formation of tubular alteration features in real time would be to reproduce them in the laboratory. Numerous researchers have demonstrated that microorganisms can grow in lab cultures containing only a minimal medium of basalt glass chips or powder and artificial or sterilized seawater (e.g. Thorseth *et al.*, 2001; Edwards *et al*., 2003; Kruber *et al.*, 2008), which often results in the formation of etch pits and other surface alteration features, but thus far no one has been able to induce the formation of tubules. As part of the FeMO research cruises, I also grew cultures in artificial seawater media with basalt glass chips and powder. I prepared biological samples from both the surface layers and chips of the underlying fresh glass from rocks collected at various locations on Lō‘ihi and surrounding seamounts. Small pieces of surface alteration layers were collected using sterile forceps and placed in both aerobic and anaerobic sterile culture tubes. I prepared the anaerobic tubes pre-cruise using minimal artificial seawater media with basalt powder and a small amount of iron oxides, and then bubbled the tubes to remove the oxygen. The tubes were inoculated with glass chips on board and kept anaerobic by bubbling the media with filtered nitrogen gas. Back

in the laboratory I kept the cultures in the dark at 4°C to simulate the *in situ* conditions. Over the next few years I periodically sampled the cultures to look for growth and removed a few of the glass chips to look for alteration via SEM imaging. The cultures did grow slowly and groups of cells were often visible attached to the surfaces of the glass pieces, but I observed little surface alteration and nothing resembling incipient tubules. This is likely due to the difficulty in accurately simulating the conditions in the subseafloor, or even at the seafloor.

In the subseafloor chemolithoautotrophic microorganisms are subjected to extreme pressures and possibly high temperatures, both of which are not well constrained. The chemistry of the fluids circulating within the cracks and fissures is also not well understood. In addition, in the cultures I used a small amount of basalt glass in a relatively large amount of seawater, resulting in a high water to rock ratio. In the subseafloor the situation is reversed: the system is mostly comprised of rock with only a small amount of fluid. The water to rock ratio has an important impact on the dissolution of the basalt glass and the availability of metabolites and removal of waste materials, which determines the possible metabolic processes and the rates at which they operate. Thus, a realistic simulation of the conditions under which tubular formation happens requires a set up that flows a small amount of fluid through a large amount of rock under high pressure and temperature for an extended period of time. Needless to say, this set up would be very difficult at best. Thus, with current technology an accurate laboratory simulation of the *in situ* conditions in the subseafloor is unreasonable.

5.3 A Broader Perspective on Biosignatures

The study of the formation and preservation of modern biosignatures forms the groundwork for examining ancient rocks on Earth and meteorites for signs of early life, and for designing future planetary missions, particularly those that involve sample return. As discussed in section 1.6, the unambiguous identification of a true biosignature is often very difficult; the results of this work show demonstrate just how challenging this distinction can be. When abiotic mineralization overlaps, overprints, or replaces biominerals then the potential evidence of biological geochemical processing may be lost, making the interpretation of the features more difficult. This is the case for tubular alteration features in subseafloor basalts and ophiolites. The multiple successive stages of fluid flow within the tubules implies that even if the tubules were in fact originally formed by microorganisms and there were once biomineral deposits in the tubules, the later abiotic mineralization stages make the mineral interpretation ambiguous. This work has demonstrated a mechanism by which mineralized alteration features in basalt glass that may have once been strong biosignatures are modified to ambiguity.

In any system characterized by fluid-rock interactions there is the potential for abiotic processes to compete with biomineralization and in some cases obscure potential biosignatures. In order to preserve any original biominerals and permineralized cells in subseafloor tubular alteration features the fluid flow would have to be abruptly and permanently arrested during the oxidative alteration stage, such as by quickly clogging the cracks with a rapid input of a large amount of sedimentary material. These findings should be considered when examining alteration features in other systems, in particular those potentially affected by aqueous abiotic modification and overprinting of biominerals. While these results do not clearly identify these features as

biosignatures, they do add significantly to our understanding of biosignatures in general. The ability to distinguish a biogenic feature from an abiotic one requires an understanding of both biological and abiotic alteration and mineralization processes, as well as insight into how features change and are erased through geological time. In the search for signs of life it is equally as important to understand what is a biosignature as it is to understand what is not.

COMPILED REFERENCES

Abramov, O., and Mojzsis, S.J. (2009) Microbial habitability of the Hadean Earth during the late heavy bombardment. *Nature* 459: 419-422.

Aitken, C.M., Jones, D.M., and Larter, S.R. (2004) Anaerobic hydrocarbon biodegradation in deep subsurface oil reservoirs. *Nature* 431: 291-294.

Allwood, A.C., Grotzinger, J.P., Knoll, A.H., Burch, I.W., Anderson, M.S., Coleman, M.L., and Kanik, I. (2009) Controls on development and diversity of Early Archean stromatolites. *Proceedings of the National Academy of Sciences of the United States of America* 106: 9548-9555.

Allwood, A.C., Walter, M.R., Burch, I.W., and Kamber, B.S. (2007) 3.43 billion-year-old stromatolite reef from the Pilbara Craton of western Australia: Ecosystem-scale insights to early life on Earth. *Precambrian Research* 158: 198-227.

Alt, J.C. (1995) Subseafloor Processes in Mid-Ocean Ridge Hydrothermal Systems. In *Seafloor Hydrothermal Systems: Physical, Chemical, Biological, and Geological Interactions*. Humphris, S.E., Zierenberg, R.A., Mullineaux, L.S., and Thomson, R.E. (eds): American Geophysical Union, pp. 85-114.

Alt, J.C. (1999) Very low-grade hydrothermal metamorphism of basic igneous rocks. In *Low Grade Metamorphism*. Frey, M., and Robinson, D. (eds). Oxford, UK: Blackwell, pp. 169-201.

Alt, J.C., Davidson, G.J., Teagle, D.A.H., and Karson, J.A. (2003) Isotopic composition of gypsum in the Macquarie Island ophiolite: Implications for the sulfur cycle and the subsurface biosphere in oceanic crust. *Geology* 31: 549-552.

Alt, J.C., and Honnorez, J. (1984) Alteration of the Upper Oceanic-Crust, DSDP Site-417 - Mineralogy and Chemistry. *Contributions to Mineralogy and Petrology* 87: 149-169.

Alt, J.C., Kinoshita, H., Stokking, L.B., Allerton, S., Bach, W., Becker, K. et al. (1993) Site 896. In *Proceedings of the Ocean Drilling Program; Initial reports, Leg 148*. College Station, TX: Ocean Drilling Program, p. 352.

Alt, J.C., and Mata, P. (2000) On the role of microbes in the alteration of submarine basaltic glass: a TEM study. *Earth and Planetary Science Letters* 181: 301-313.

Alt, J.C., Saltzman, E.S., and Price, D.A. (1985) Anhydrite in hydrothermally altered basalts: Deep Sea Drilling Project Hole 504B, Leg 83. In *Initial Reports of the Deep Sea Drilling Project Vol. 83* U.S. Government Printing Office, pp. 283–288.

Amend, J.P., and Teske, A. (2005) Expanding frontiers in deep subsurface microbiology.

Palaeogeography Palaeoclimatology Palaeoecology 219: 131-155.

Andrews, A.J. (1979) Effect of low-temperature seawater-basalt interaction on the distribution of sulfur in oceanic-crust, layer-2. *Earth and Planetary Science Letters* 46: 68-80.

Arrhenius, S. (1903) Die Verbreitung des Lebens im Weltenraum. *Die Umschau* 7: 481-485.

Bach, W., and Edwards, K.J. (2003) Iron and sulfide oxidation within the basaltic ocean crust: Implications for chemolithoautotrophic microbial biomass production. *Geochimica et Cosmochimica Acta* 67: 3871-3887.

Bajt, S., Sutton, S.R., and Delaney, J.S. (1994) X-ray microprobe analysis of iron oxidation-states in silicates and oxides using x-ray-absorption near-edge structure (XANES). *Geochimica et Cosmochimica Acta* 58: 5209-5214.

Balci, N., Mayer, B., Shanks Iii, W.C., and Mandernack, K.W. (2012) Oxygen and sulfur isotope systematics of sulfate produced during abiotic and bacterial oxidation of sphalerite and elemental sulfur. *Geochimica et Cosmochimica Acta* 77: 335-351.

Banerjee, N.R., Furnes, H., Muehlenbachs, K., and Staudigel, H. (2004) Microbial alteration of volcanic glass in modern and ancient oceanic crust as a proxy for studies of extraterrestrial material [abstract 1248]. *In 35th Lunar and Planetary Science Conference Abstracts* LPI Contribution No. 1197, Lunar and Planetary Institute, Houston, Texas.

Banerjee, N.R., Furnes, H., Muehlenbachs, K., Staudigel, H., and de Wit, M. (2006) Preservation of ~3.4-3.5 Ga microbial biomarkers in pillow lavas and hyaloclastites from the Barberton Greenstone Belt, South Africa. *Earth and Planetary Science Letters* 241: 707-722.

Banerjee, N.R., and Muehlenbachs, K. (2003) Tuff life: Bioalteration in volcaniclastic rocks from the Ontong Java Plateau. *Geochemistry Geophysics Geosystems* 4: doi:10.1029/2002GC000470.

Banerjee, N.R., Simonetti, A., Furnes, H., Muehlenbachs, K., Staudigel, H., Heaman, L., and Van Kranendonk, M.J. (2007) Direct dating of Archean microbial ichnofossils. *Geology* 35: 487-490.

Banerjee, N.R., Simonetti, A., Furnes, H., Muehlenbachs, K., Staudigel, H., and Van Kranendonk, M.J. (2006) Direct dating of Archean microfossils preserved in pillow basalts from the Pilbara Craton. *Geochimica et Cosmochimica Acta* 70: A33-A33.

Banfield, J.F., Moreau, J.W., Chan, C.S., Welch, S.A., and Little, B. (2001) Mineralogical biosignatures and the search for life on Mars. *Astrobiology* 1: 447.

Barker, W.W., Welch, S.A., and Banfield, J.F. (1997) Biogeochemical weathering of silicate minerals. In *Geomicrobiology: Interactions between Microbes and Minerals*, pp. 391-428.

Barker, W.W., Welch, S.A., Chu, S., and Banfield, J.F. (1998) Experimental observations of the effects of bacteria on aluminosilicate weathering. *American Mineralogist* 83: 1551-1563.

Baross, J.A., and Hoffman, S.E. (1985) Submarine hydrothermal vents and associated gradient environments as sites for the origin and evolution of life. *Origins of Life and Evolution of the Biosphere* 15: 327-345.

Bednarz, U., and Schmincke, H.U. (1989) Mass transfer during sub-seafloor alteration of the upper Troodos crust (Cyprus). *Contributions to Mineralogy and Petrology* 102: 93-101.

Bennett, P.C., Rogers, J.R., and Choi, W.J. (2001) Silicates, silicate weathering, and microbial ecology. *Geomicrobiology Journal* 18: 3-19.

Benzerara, K., Menguy, N., Banerjee, N.R., Tyliszczak, T., Brown, G.E., and Guyot, F. (2007) Alteration of submarine basaltic glass from the Ontong Java Plateau: A STXM and TEM study. *Earth and Planetary Science Letters* 260: 187-200.

Benzerara, K., Menguy, N., Guyot, F., Vanni, C., and Gillet, P. (2005) TEM study of a silicate-carbonate-microbe interface prepared by focused ion beam milling. *Geochimica et Cosmochimica Acta* 69: 1413-1422.

Benzerara, K., Menguy, N., Lopez-Garcia, P., Yoon, T.H., Kazmierczak, J., Tyliszczak, T. et al. (2006) Nanoscale detection of organic signatures in carbonate microbialites. *Proceedings of the National Academy of Sciences of the United States of America* 103: 9440-9445.

Benzerara, K., Miot, J., Morin, G., Ona-Nguema, G., Skouri-Panet, F., and Ferard, C. (2011) Significance, mechanisms and environmental implications of microbial biomineralization. *Comptes Rendus Geoscience* 343: 160-167.

Berger, G., Schott, J., and Loubet, M. (1987) Fundamental processes controlling the 1st stage of alteration of a basalt glass by seawater - An experimental-study between 200-degrees-C and 320-degrees-C. *Earth and Planetary Science Letters* 84: 431-445.

Bernard, S., Benzerara, K., Beyssac, O., Menguy, N., Guyot, F., Brown, G.E., and Goffe, B. (2007) Exceptional preservation of fossil plant spores in high-pressure metamorphic rocks. *Earth and Planetary Science Letters* 262: 257-272.

Berry, A.J., O'Neill, H.S.C., Jayasuriya, K.D., Campbell, S.J., and Foran, G.J. (2003) XANES calibrations for the oxidation state of iron in a silicate glass. *American Mineralogist* 88: 967-977.

Berry, A.J., Walker, A.M., Hermann, J., O'Neill, H.S., Foran, G.J., and Gale, J.D. (2007) Titanium substitution mechanisms in forsterite. *Chemical Geology* 242: 176-186.

Blum, A., and Lasaga, A. (1988) Role of surface speciation in the low-temperature dissolution of minerals. *Nature* 331: 431-433.

Böhlke, J.K., Honnorez, J., and Honnorez-Guerstein, B.M. (1980) Alteration of basalts from site 396 B, DSDP: Petrographic and mineralogic studies. *Contributions to Mineralogy and Petrology* 73: 341-364.

Booij, E., Gallahan, W.E., and Staudigel, H. (1995) Ion-exchange experiments and Rb/Sr dating on celadonites from the Troodos ophiolite, Cyprus. *Chemical Geology* 126: 155-167.

Boston, P.J., Ivanov, M.V., and McKay, C.P. (1992) On the Possibility of Chemosynthetic Ecosystems in Subsurface Habitats on Mars. *Icarus* 95: 300-308.

Brack, A. (1999) Life in the Solar System. *Advances in Space Research* 24: 417-433.

Brasier, M.D., Green, O.R., Lindsay, J.F., McLoughlin, N., Steele, A., and Stoakes, C. (2005) Critical testing of Earth's oldest putative fossil assemblage from the ~3.5 Ga Apex Chert, Chinaman Creek, western Australia. *Precambrian Research* 140: 55-102.

Brown, D.A., Kamineni, D.C., Sawicki, J.A., and Beveridge, T.J. (1994) Minerals associated with biofilms occurring on exposed rock in a granitic underground research laboratory. *Applied and Environmental Microbiology* 60: 3182-3191.

Buick, R. (1990) Microfossil recognition in Archean rocks; an appraisal of spheroids and filaments from a 3500 m.y. old chert-barite unit at North Pole, Western Australia. *PALAIOS* 5: 441-459.

Cady, S.L., Farmer, J.D., Grotzinger, J.P., Schopf, J.W., and Steele, A. (2003) Morphological biosignatures and the search for life on Mars. *Astrobiology* 3: 351-368.

Canfield, D.E. (2001) Biogeochemistry of Sulfur Isotopes. *Reviews in Mineralogy and Geochemistry* 43: 607-636.

Cann, J., and Gillis, K. (2004) Hydrothermal insights from the Troodos ophiolite, Cyprus. In *Hydrogeology of the Oceanic Lithosphere*. Davis, E.E., and Elderfield, H. (eds). Cambridge, UK: Cambridge University Press.

Cavalazzi, B. (2007) Chemotrophic filamentous microfossils from the Hollard Mound (Devonian, Morocco) as investigated by focused ion beam. *Astrobiology* 7: 402-415.

Chalmin, E., Farges, F., and Brown, G. (2009) A pre-edge analysis of Mn K-edge XANES spectra to help determine the speciation of manganese in minerals and glasses. *Contributions to Mineralogy and Petrology* 157: 111-126.

Chapelle, F.H., O'Neill, K., Bradley, P.M., Methe, B.A., Ciufo, S.A., Knobel, L.L., and Lovley, D.R. (2002) A hydrogen-based subsurface microbial community dominated by methanogens. *Nature* 415: 312-315.

Clark, B.C. (2001) Planetary interchange of bioactive material: probability factors and implications. *Origins of Life and Evolution of Biospheres* 31: 185-197.

Clayton, T., and Pearce, R.B. (2000) Alteration mineralogy of Cretaceous basalt from ODP Site 1001, Leg 165 (Caribbean Sea). *Clay Minerals* 35: 719-733.

Cockell, C.S., and Herrera, A. (2008) Why are some microorganisms boring? *Trends in Microbiology* 16: 101-106.

Cohen, P.A., Bradley, A., Knoll, A.H., Grotzinger, J.P., Jensen, S., Abelson, J. et al. (2009) Tubular compression fossils from the Ediacaran Nama Group, Namibia. *Journal of Paleontology* 83: 110-122.

Connell, L., Barrett, A., Templeton, A., and Staudigel, H. (2009) Fungal Diversity Associated with an Active Deep Sea Volcano: Vailulu'u Seamount, Samoa. *Geomicrobiology Journal* 26: 597 - 605.

Cottrell, E., Kelley, K.A., Lanzirotti, A., and Fischer, R.A. (2009) High-precision determination of iron oxidation state in silicate glasses using XANES. *Chemical Geology* 268: 167-179.

Couradeau, E., Benzerara, K., Gerard, E., Moreira, D., Bernard, S., Brown, G.E., and Lopez-Garcia, P. (2012) An early-branching microbialite cyanobacterium forms intracellular carbonates. *Science* 336: 459-462.

Cousins, C.R., Smellie, J.L., Jones, A.P., and Crawford, I.A. (2009) A comparative study of endolithic microborings in basaltic lavas from a transitional subglacial-marine environment. *International Journal of Astrobiology* 8: 37-49.

Cowen, J.P. (2004) The microbial biosphere of sediment-buried oceanic basement. *Research in Microbiology* 155: 497-506.

Cowen, J.P., Giovannoni, S.J., Kenig, F., Johnson, H.P., Butterfield, D., Rappe, M.S. et al. (2003) Fluids from aging ocean crust that support microbial life. *Science* 299: 120-123.

Crovisier, J.L., Honnorez, J., and Eberhart, J.P. (1987) Dissolution of basaltic glass in seawater - Mechanism and rate. *Geochimica et Cosmochimica Acta* 51: 2977-2990.

Crovisier, J.L., Thomassin, J.H., Juteau, T., Eberhart, J.P., Touray, J.C., and Baillif, P. (1983) Experimental seawater basaltic glass interaction at 50-degrees-C - Study of early developed phases by electron-microscopy and X-Ray photoelectron spectrometry. *Geochimica et Cosmochimica Acta* 47: 377-387.

D'Hondt, S., Jorgensen, B.B., Miller, D.J., Batzke, A., Blake, R., Cragg, B.A. et al. (2004) Distributions of microbial activities in deep subseafloor sediments. *Science* 306: 2216-2221.

Daughney, C.J., Rioux, J.P., Fortin, D., and Pichler, T. (2004) Laboratory investigation of the

role of bacteria in the weathering of basalt near deep sea hydrothermal vents. *Geomicrobiology Journal* 21: 21-31.

Dawson, J.B., and Smith, J.V. (1982) Upper-mantle amphiboles - a review. *Mineralogical Magazine* 45: 35-46.

Delaney, J.S., Dyar, M.D., Sutton, S.R., and Bajt, S. (1998) Redox ratios with relevant resolution: Solving an old problem by using the synchrotron microXANES probe. *Geology* 26: 139-142.

Dingwell, D.B., Paris, E., Seifert, F., Mottana, A., and Romano, C. (1994) X-Ray-Absorption Study of Ti-Bearing Silicate-Glasses. *Physics and Chemistry of Minerals* 21: 501-509.

Dmitriev, L., and Heirtzler, J., et al. (1978) Initial Reports of the Deep Sea Drilling Project 46. Washington, DC.: US Government Printing Office.

Donnelly, T., Francheteau, J., Bryan, W., Robinson, P.T., Flower, M.F.J., and Salisbury, M. (1979) Initial Reports of the Deep Sea Drilling Project, v. 51, 52, 53. In. Washington: U.S. Government Printing Office, pp. 1535-1555.

Douglas, S., and Beveridge, T.J. (1998) Mineral formation by bacteria in natural microbial communities. *FEMS Microbiology Ecology* 26: 79-88.

Drever, J.I. (1994) The effect of land plants on weathering rates of silicate minerals. *Geochimica et Cosmochimica Acta* 58: 2325-2332.

Drief, A., and Schiffman, P. (2004) Very low-temperature alteration of sideromelane in hyaloclastites and hyalotuffs from Kilauea and Mauna Kea volcanoes: Implications for the mechanism of palagonite formation. *Clays and Clay Minerals* 52: 622-634.

Dyar, M.D., Delaney, J.S., Sutton, S.R., and Schaefer, M.W. (1998) Fe3+ distribution in oxidized olivine: A synchrotron micro-XANES study. *American Mineralogist* 83: 1361-1365.

Edmond, J.M., Measures, C., McDuff, R.E., Chan, L.H., Collier, R., Grant, B. et al. (1979) Ridge crest hydrothermal activity and the balances of the major and minor elements in the ocean - Galapagos data. *Earth and Planetary Science Letters* 46: 1-18.

Edwards, H.G.M., Wynn-Williams, D.D., and Villar, S.E.J. (2004) Biological modification of haematite in Antarctic cryptoendolithic communities. *Journal of Raman Spectroscopy* 35: 470-474.

Edwards, K., Fisher, A., and Wheat, C.G. (2012a) The deep subsurface biosphere in igneous ocean crust: frontier habitats for microbiological exploration. *Frontiers in Microbiology* 3.

Edwards, K.J., Bach, W., and McCollom, T.M. (2005) Geomicrobiology in oceanography:

microbe-mineral interactions at and below the seafloor. *Trends in Microbiology* 13: 449-456.

Edwards, K.J., Becker, K., and Colwell, F. (2012b) The deep, dark energy biosphere: Intraterrestrial life on Earth. *Annual Review of Earth and Planetary Sciences* 40: 551-568.

Edwards, K.J., Glazer, B.T., Rouxel, O.J., Bach, W., Emerson, D., Davis, R.E. et al. (2011a) Ultra-diffuse hydrothermal venting supports Fe-oxidizing bacteria and massive umber deposition at 5000 m off Hawaii. *ISME Journal* 5: 1748-1758.

Edwards, K.J., McCollom, T.M., Konishi, H., and Buseck, P.R. (2003) Seafloor bioalteration of sulfide minerals: Results from in situ incubation studies. *Geochimica et Cosmochimica Acta* 67: 2843-2856.

Edwards, K.J., Rogers, D.R., Wirsen, C.O., and McCollom, T.M. (2003) Isolation and characterization of novel psychrophilic, neutrophilic, Fe-oxidizing, chemolithoautotrophic alpha- and, gamma-Proteobacteria from the deep sea. *Applied and Environmental Microbiology* 69: 2906-2913.

Edwards, K.J., Wheat, C.G., and Sylvan, J.B. (2011b) Under the sea: microbial life in volcanic oceanic crust. *Nature Reviews Microbiology* 9: 703-712.

Eggleton, R.A., Foudoulis, C., and Varkevisser, D. (1987) Weathering of basalt: changes in Rock chemistry and mineralogy. *Clays and Clay Minerals* 35: 161-169.

Ehret, G., Crovisier, J.L., and Eberhart, J.P. (1986) A new method for studying leached glasses: Analytical electron microscopy on ultramicrotomic thin sections. *Journal of Non-Crystalline Solids* 86: 72-79.

Einen, J., Kruber, C., Øvreås, L., Thorseth, I.H., and Torsvik, T. (2006) Microbial colonization and alteration of basaltic glass. *Biogeosciences Discussions* 3: 273-307.

Emerson, D., and Moyer, C.L. (2002) Neutrophilic Fe-oxidizing bacteria are abundant at the Loihi Seamount hydrothermal vents and play a major role in Fe oxide deposition. *Applied and Environmental Microbiology* 68: 3085-3093.

Engel, A.S., Lichtenberg, H., Prange, A., and Hormes, J. (2007) Speciation of sulfur from filamentous microbial mats from sulfidic cave springs using X-ray absorption near-edge spectroscopy. *FEMS Microbiology Letters* 269: 54-62.

Fairén, A.G. (2010) A cold and wet Mars. *Icarus* 208: 165-175.

Farges, F. (1999) A Ti K-edge EXAFS study of the medium range environment around Ti in oxide glasses. *Journal of Non-Crystalline Solids* 244: 25-33.

Farges, F., and Brown, G.E. (1997) Coordination chemistry of titanium(IV) in silicate glasses

and melts .4. XANES studies of synthetic and natural volcanic glasses and tektites at ambient temperature and pressure. *Geochimica et Cosmochimica Acta* 61: 1863-1870.

Farges, F., Rossano, S., Lefrere, Y., Wilke, M., and Brown, G.E. (2005) Iron in silicate glasses: a systematic analysis of pre-edge, XANES and EXAFS features. *Physica Scripta* T115: 957-959.

Farmer, J.D. (1999) Taphonomic modes in microbial fossilization. In *Size Limits of Very Small Microorganisms: Proceedings of a Workshop*. Space Studies Board, N.R.C. (ed). Washington DC: National Academy Press, pp. 94-102.

Farmer, J.D., and Des Marais, D.J. (1999) Exploring for a record of ancient Martian life. *Journal of Geophysical Research-Planets* 104: 26977-26995.

Ferris, F.G., Fyfe, W.S., and Beveridge, T.J. (1987) Bacteria as nucleation sites for authigenic minerals in a metal-contaminated lake sediment. *Chemical Geology* 63: 225-232.

Fisher, A.T., Davis, E.E., and Becker, K. (2008) Borehole-to-borehole hydrologic response across 2.4 km in the upper oceanic crust: Implications for crustal-scale properties. *Journal of Geophysical Research-Solid Earth* 113: 15.

Fisk, M.R., and Giovannoni, S.J. (1999) Sources of nutrients and energy for a deep biosphere on Mars. *Journal of Geophysical Research-Planets* 104: 11805-11815.

Fisk, M.R., Giovannoni, S.J., and Thorseth, I.H. (1998) Alteration of oceanic volcanic glass: Textural evidence of microbial activity. *Science* 281: 978-980.

Fisk, M.R., Popa, R., Mason, O.U., Storrie-Lombardi, M.C., and Vicenzi, E.P. (2006) Iron-magnesium silicate bioweathering on Earth (and Mars?). *Astrobiology* 6: 48-68.

Fleet, M.E. (2005) XANES spectroscopy of sulfur in Earth materials. *The Canadian Mineralogist* 43: 1811-1838.

Fletcher, I.R., Kilburn, M.R., and Rasmussen, B. (2008) NanoSIMS u-scale in situ measurement of C-13/C-12 in early Precambrian organic matter, with permil precision. *International Journal of Mass Spectrometry* 278: 59-68.

Fliegel, D., Knowles, E., Wirth, R., Templeton, A., Staudigel, H., Muehlenbachs, K., and Furnes, H. (in press) Characterization of alteration textures in Cretaceous oceanic crust from the N-Atlantic (DSDP Hole 418A) by spatially-resolved spectroscopy.

Fliegel, D., Kosler, J., McLoughlin, N., Simonetti, A., de Wit, M.J., Wirth, R., and Furnes, H. (2010) In-situ dating of the Earth's oldest trace fossil at 3.34 Ga. *Earth and Planetary Science Letters* 299: 290-298.

Fliegel, D., Wirth, R., Simonetti, A., Furnes, H., Staudigel, H., Hanski, E., and Muehlenbachs, K. (2010) Septate-tubular textures in 2.0-Ga pillow lavas from the Pechenga Greenstone Belt: a

nano-spectroscopic approach to investigate their biogenicity. *Geobiology* 8: 372-390.

Fliegel, D., Wirth, R., Simonetti, A., Schreiber, A., Furnes, H., and Muehlenbachs, K. (2011) Tubular textures in pillow lavas from a Caledonian west Norwegian ophiolite: A combined TEM, LA-ICP-MS, and STXM study. *Geochemistry Geophysics Geosystems* 12.

Foriel, J., Philippot, P., Susini, J., Dumas, P., Somogyi, A., Salome, M. et al. (2004) High-resolution imaging of sulfur oxidation states, trace elements, and organic molecules distribution in individual microfossils and contemporary microbial filaments. *Geochimica et Cosmochimica Acta* 68: 1561-1569.

Fortin, D., and Ferris, F.G. (1998) Precipitation of iron, silica, and sulfate on bacterial cell surfaces. *Geomicrobiology Journal* 15: 309-324.

Fortin, D., Ferris, F.G., and Scott, S.D. (1998) Formation of Fe-silicates and Fe-oxides on bacterial surfaces in samples collected near hydrothermal vents on the Southern Explorer Ridge in the northeast Pacific Ocean. *American Mineralogist* 83: 1399-1408.

Fry, J.C., Parkes, R.J., Cragg, B.A., Weightman, A.J., and Webster, G. (2008) Prokaryotic biodiversity and activity in the deep subseafloor biosphere. *FEMS Microbiology Ecology* 66: 181-196.

Furnes, H. (1984) Chemical changes during progressive subaerial palagonitization of a subglacial olivine tholeiite hyaloclastite - A microprobe study. *Chemical Geology* 43: 271-285.

Furnes, H., Banerjee, N.R., Muehlenbachs, K., and Kontinen, A. (2005) Preservation of biosignatures in metaglassy volcanic rocks from the Jormua ophiolite complex, Finland. *Precambrian Research* 136: 125-137.

Furnes, H., Banerjee, N.R., Muehlenbachs, K., Staudigel, H., and de Wit, M. (2004) Early life recorded in Archean pillow lavas. *Science* 304: 578-581.

Furnes, H., Banerjee, N.R., Staudigel, H., Muehlenbachs, K., McLoughlin, N., De Wit, M., and Van Kranendonk, M. (2007) Comparing petrographic signatures of bioalteration in recent to Mesoarchean pillow lavas: Tracing subsurface life in oceanic igneous rocks. *Precambrain Research*: 156-176.

Furnes, H., McLoughlin, N., Muehlenbachs, K., Banerjee, N.R., Staudigel, H., Dilek, Y. et al. (2008) Oceanic pillow lavas and hyaloclastites as habitats for microbial life through time - A review. In *Links Between Geological Processes, Microbial Activities & Evolution of Life*. Dilek, Y., Furnes, H., and Muehlenbachs, K. (eds): Springer.

Furnes, H., Muehlenbachs, K., Torsvik, T., Thorseth, I.H., and Tumyr, O. (2001a) Microbial fractionation of carbon isotopes in altered basaltic glass from the Atlantic Ocean, Lau Basin and Costa Rica Rift. *Chemical Geology* 173: 313-330.

Furnes, H., Muehlenbachs, K., Torsvik, T., Tumyr, O., and Shi, L. (2002) Bio-signatures in metabasaltic glass of a Caledonian ophiolite, West Norway. *Geological Magazine* 139: 601-608.

Furnes, H., Muehlenbachs, K., Tumyr, O., Torsvik, T., and Thorseth, I.H. (1999) Depth of active bio-alteration in the ocean crust: Costa Rica Rift (Hole 504B). *Terra Nova* 11: 228-233.

Furnes, H., Muehlenbachs, K., Tumyr, O., Torsvik, T., and Xenophontos, C. (2001b) Biogenic alteration of volcanic glass from the Troodos ophiolite, Cyprus. *Journal of the Geological Society* 158: 75-82.

Furnes, H., Staudigel, H., Thorseth, I.H., Torsvik, T., Muehlenbachs, K., and Tumyr, O. (2001c) Bioalteration of basaltic glass in the oceanic crust. *Geochemistry Geophysics Geosystems* 2: doi:10.1029/2000GC000150.

Gadd, G.M., Rhee, Y.J., Stephenson, K., and Wei, Z. (2011) Geomycology: metals, actinides and biominerals. *Environmental Microbiology Reports* 4: 270-296.

Galvez, M.E., Beyssac, O., Benzerara, K., Bernard, S., Menguy, N., Cox, S.C. et al. (2012) Morphological preservation of carbonaceous plant fossils in blueschist metamorphic rocks from New Zealand. *Geobiology* 10: 118-129.

Giorgetti, G., Marescotti, P., Cabella, R., and Lucchetti, G. (2001) Clay mineral mixtures as alteration products in pillow basalts from the eastern flank of Juan de Fuca Ridge: a TEM-AEM study. *Clay Minerals* 36: 75-91.

Glazer, B.T., and Rouxel, O.J. (2009) Redox Speciation and Distribution within Diverse Iron-dominated Microbial Habitats at Loihi Seamount. *Geomicrobiology Journal* 26: 606-622.

Gold, T. (1992) The Deep, Hot Biosphere. *Proceedings of the National Academy of Sciences of the United States of America* 89: 6045-6049.

Golden, D.C., Ming, D.W., Morris, R.V., Brearley, A., Lauer, H.V., Treiman, A.H. et al. (2004) Evidence for exclusively inorganic formation of magnetite in Martian meteorite ALH84001. *American Mineralogist* 89: 681-695.

Golden, D.C., Ming, D.W., Schwandt, C.S., Lauer, H.V., Jr., Socki, R.A., Morris, R.V. et al. (2001) A simple inorganic process for formation of carbonates, magnetite, and sulfides in Martian meteorite ALH84001. *American Mineralogist* 86: 370-375.

Golubic, S., Radtke, G., and Campion-Alsumard, T.L. (2005) Endolithic fungi in marine ecosystems. *Trends in Microbiology* 13: 229-235.

Gorby, Y.A., Yanina, S., McLean, J.S., Rosso, K.M., Moyles, D., Dohnalkova, A. et al. (2006) Electrically conductive bacterial nanowires produced by Shewanella oneidensis strain MR-1

and other microorganisms. *Proceedings of the National Academy of Sciences of the United States of America* 103: 11358-11363.

Grassle, J.F. (1985) Hydrothermal vent animals: distribution and biology. *Science* 229: 713-717.

Grevemeyer, I., and Weigel, W. (1997) Increase of seismic velocities in upper oceanic crust: The "superfast" spreading East Pacific Rise at 14 degrees 14'S. *Geophysical Research Letters* 24: 217-220.

Griffith, L.L., and Shock, E.L. (1995) A geochemical model for the formation of hydrothermal carbonates on Mars. *Nature* 377: 406-408.

Harder, J. (1997) Species-independent maintenance energy and natural population sizes. *FEMS Microbiology Ecology* 23: 39-44.

Hart, S.R., Blusztajn, J., Dick, H.J.B., and Lawrence, J.R. (1994) Fluid circulation in the oceanic-crust - Contrast between volcanic and plutonic regimes. *Journal of Geophysical Research-Solid Earth* 99: 3163-3173.

Hart, S.R., and Staudigel, H. (1986) Ocean Crust Vein Mineral Deposition - Rb/Sr Ages, U-Th-Pb Geochemistry, and Duration of Circulation at DSDP Sites 261, 462 and 516. *Geochimica et Cosmochimica Acta* 50: 2751-2761.

Haskin, L.A., Wang, A., Jolliff, B.L., McSween, H.Y., Clark, B.C., Des Marais, D.J. et al. (2005) Water alteration of rocks and soils on Mars at the Spirit rover site in Gusev crater. *Nature* 436: 66-69.

Hay, R.L., and Iijima, A. (1968) Nature and origin of palagonite tuffs of the Honolulu Group on Oahu, Hawaii. In *Studies in Volcanology - A Memoir in Honor of Howel Williams*. Boulder, CO: Geological Society of America, pp. 331-376.

Heaney, P.J., Vicenzi, E.P., Giannuzzi, L.A., and Livi, K.J.T. (2001) Focused ion beam milling: A method of site-specific sample extraction for microanalysis of Earth and planetary materials. *American Mineralogist* 86: 1094-1099.

Henderson, G.S., Liu, X., and Fleet, M.E. (2002) A Ti L-edge X-ray absorption study of Ti-silicate glasses. *Physics and Chemistry of Minerals* 29: 32-42.

Herkenhoff, K.E., Squyres, S.W., Arvidson, R., Bass, D.S., Bell, J.F., Bertelsen, P. et al. (2004) Evidence from Opportunity's microscopic imager for water on Meridiani Planum. *Science* 306: 1727-1730.

Hernandez, M.E., and Newman, D.K. (2001) Extracellular electron transfer. *Cellular and Molecular Life Sciences* 58: 1562-1571.

Hersman, L., Maurice, P., and Sposito, G. (1996) Iron acquisition from hydrous Fe(III)-oxides

by an aerobic Pseudomonas sp. *Chemical Geology* 132: 25-31.

Hoehler, T., and Westall, F. (2010) Mars exploration program analysis group goal one: Determine if life ever arose on Mars. *Astrobiology* 10: 859-867.

Hoehler, T.M. (2004) Biological energy requirements as quantitative boundary conditions for life in the subsurface. *Geobiology* 2: 205-215.

Hoehler, T.M., Alperin, M.J., Albert, D.B., and Martens, C.S. (2001) Apparent minimum free energy requirements for methanogenic Archaea and sulfate-reducing bacteria in an anoxic marine sediment. *FEMS Microbiology Ecology* 38: 33-41.

Hofmann, B.A. (2008) Morphological biosignatures from subsurface environments: Recognition on planetary missions. *Space Science Reviews* 135: 245-254.

Huber, J.A., Butterfield, D.A., and Baross, J.A. (2003) Bacterial diversity in a subseafloor habitat following a deep-sea volcanic eruption. *FEMS Microbiology Ecology* 43: 393-409.

Hullebusch, E. van., Rossano, S., Farges, F., Lenz, M., Labanowski, J., Lagarde, O. et al. (2009) Sulfur K-edge XANES spectroscopy as a tool for understanding sulfur chemical state in anaerobic granular sludge. In *14th International Conference on X-Ray Absorption Fine Structure (XAFS14)*: Journal of Physics: Conference Series, pp. 1-4.

Humphris, S.E., and Thompson, G. (1978) Trace element mobility during hydrothermal alteration of oceanic basalts. *Geochimica et Cosmochimica Acta* 42: 127-136.

Izawa, M.R.M., Banerjee, N.R., Flemming, R.L., and Bridge, N.J. (2010) Preservation of microbial ichnofossils in basaltic glass by titanite mineralization. *Canadian Mineralogist* 48: 1255-1265.

Jannasch, H.W., and Mottl, M.J. (1985) Geomicrobiology of deep-sea hydrothermal vents. *Science* 229: 717-725.

Jeanthon, C. (2000) Molecular ecology of hydrothermal vent microbial communities. *Antonie van Leeuwenhoek* 77: 117-133.

Johnson, H.P., and Semyan, S.W. (1994) Age variation in the physical-properties of oceanic basalts - Implications for crustal formation and evolution. *Journal of Geophysical Research-Solid Earth* 99: 3123-3134.

Johnston, C.G., and Vestal, J.R. (1993) Biogeochemistry of oxalate in the Antarctic cryptoendolithic lichen-dominated community. *Microbial Ecology* 25: 305-319.

Jongmans, A.G., Van Breemen, N., Lundström, U.S., Van Hees, P.A.W., Finlay, R.D., Srinivasan, M. et al. (1997) Rock eating fungi. *Nature* 389.

Jørgensen, B.B., and D'Hondt, S. (2006) Ecology - A starving majority deep beneath the seafloor. *Science* 314: 932-934.

Jugo, P.J., Wilke, M., and Botcharnikov, R.E. (2010) Sulfur K-edge XANES analysis of natural and synthetic basaltic glasses: Implications for S speciation and S content as function of oxygen fugacity. *Geochimica et Cosmochimica Acta* 74: 5926-5938.

Kalisky, T., and Quake, S.R. (2011) Single-cell genomics. *Nature Methods* 8: 311-314.

Kempe, A., Wirth, R., Altermann, W., Stark, R.W., Schopf, J.W., and Heckl, W.A. (2005) Focused ion beam preparation and in situ nanoscopic study of Precambrian acritarchs. *Precambrian Research* 140: 36-54.

Kim, S.S., Bargar, J.R., Nealson, K.H., Flood, B.E., Kirschvink, J.L., Raub, T.D. et al. (2011) Searching for biosignatures using electron paramagnetic resonance (EPR) analysis of manganese oxides. *Astrobiology* 11: 775-786.

Knoll, A.H., Javaux, E.J., Hewitt, D., and Cohen, P. (2006) Eukaryotic organisms in Proterozoic oceans. *Philosophical Transactions of the Royal Society B-Biological Sciences* 361: 1023-1038.

Knowles, E., Wirth, R., and Templeton, A. (in review) A comparative analysis of potential biosignatures in basalt glass by FIB-TEM.

Konhauser, K. (2007) *Introduction to Geomicrobiology*. Malden, MA: Blackwell Publishing.

Konhauser, K.O. (1997) Bacterial iron biomineralisation in nature. *FEMS Microbiology Reviews* 20: 315-326.

Konhauser, K.O., and Urrutia, M.M. (1999) Bacterial clay authigenesis: a common biogeochemical process. *Chemical Geology* 161: 399-413.

Kopp, R.E., and Kirschvink, J.L. (2008) The identification and biogeochemical interpretation of fossil magnetotactic bacteria. *Earth-Science Reviews* 86: 42-61.

Kruber, C., Thorseth, I.H., and Pedersen, R.B. (2008) Seafloor alteration of basaltic glass: Textures, geochemistry, and endolithic microorganisms. *Geochemistry Geophysics Geosystems* 9.

Labrenz, M., Druschel, G.K., Thomsen-Ebert, T., Gilbert, B., Welch, S.A., Kemner, K.M. et al. (2000) Formation of sphalerite (ZnS) deposits in natural biofilms of sulfate-reducing bacteria. *Science* 290: 1744-1747.

Lange, B.M. (2005) Single-cell genomics. *Current Opinion in Plant Biology* 8: 236-241.

Lanzirotti, A., Tappero, R., and Schulze, D.G. (2010) Practical Application of Synchrotron-

Based Hard X-Ray Microprobes in Soil Sciences. In *Developments in Soil Science*. Singh, B., and Gräfe, M. (eds): Elsevier, pp. 27-72.

Laverne, C., Belarouchi, A., and Honnorez, J. (1996) Alteration mineralogy and chemistry of the upper oceanic crust from Hole 896A, Costa Rica Rift. In *Proceedings of the Ocean Drilling Program, Scientific Results*. College Station, TX: Ocean Drilling Program, pp. 151-170.

Lee, M.R. (2010) Transmission electron microscopy (TEM) of Earth and planetary materials: A review. *Mineralogical Magazine* 74: 1-27.

Lee, M.R., Bland, P.A., and Graham, G. (2003) Preparation of TEM samples by focused ion beam (FIB) techniques: applications to the study of clays and phyllosilicates in meteorites. *Mineralogical Magazine* 67: 581-592.

Lee, M.R., Brown, D.J., Smith, C.L., Hodson, M.E., Mackenzie, M., and Hellmann, R. (2007) Characterization of mineral surfaces using FIB and TEM: A case study of naturally weathered alkali feldspars. *American Mineralogist* 92: 1383-1394.

Lee, Y.J., Prange, A., Lichtenberg, H., Rohde, M., Dashti, M., and Wiegel, J. (2007) In situ analysis of sulfur species in sulfur globules produced from thiosulfate by Thermoanaerobacter sulfurigignens and Thermoanaerobacterium thermosulfurigenes. *Journal of Bacteriology* 189: 7525-7529.

Lemelle, L., Labrot, P., Salome, M., Simionovici, A., Viso, M., and Westall, F. (2008) In situ imaging of organic sulfur in 700-800 My-old Neoproterozoic microfossils using X-ray spectromicroscopy at the SK-edge. *Organic Geochemistry* 39: 188-202.

Lepot, K., Benzerara, K., and Philippot, P. (2011) Biogenic versus metamorphic origins of diverse microtubes in 2.7 Gyr old volcanic ashes: Multi-scale investigations. *Earth and Planetary Science Letters* 312: 37-47.

Lepot, K., Philippot, P., Benzerara, K., and Wang, G.Y. (2009) Garnet-filled trails associated with carbonaceous matter mimicking microbial filaments in Archean basalt. *Geobiology* 7: 393-402.

Link, L., Jakosky, B., and Thyne, G. (2005) Biological potential of low-temperature aqueous environments on Mars. *International Journal of Astrobiology* 4: 155-164.

Lovely, D.R. (1995) Deep subsurface microbial processes. *Reviews of Geophysics* 33: 365-381.

Lovley, D.R. (1991) Dissimilatory Fe(III) and Mn(IV) reduction. *Microbiological Reviews* 55: 259-287.

Lundström, U., and Öhman, L.O. (1990) Dissolution of feldspars in the presence of natural, organic solutes. *Journal of Soil Science* 41: 359-369.

Luther, G.W., Rozan, T.F., Taillefert, M., Nuzzio, D.B., Di Meo, C., Shank, T.M. et al. (2001) Chemical speciation drives hydrothermal vent ecology. *Nature* 410: 813-816.

Lutz, R.A., and Kennish, M.J. (1993) Ecology of deep-sea hydrothermal vent communities: A review. *Reviews of Geophysics* 31: 211-242.

Lysnes, K., Thorseth, I.H., Steinsbu, B.O., Ovreas, L., Torsvik, T., and Pedersen, R.B. (2004) Microbial community diversity in seafloor basalt from the Arctic spreading ridges. *FEMS Microbiology Ecology* 50: 213-230.

Magnuson, T.S., Hodges-Myerson, A.L., and Lovley, D.R. (2000) Characterization of a membrane-bound NADH-dependent Fe3+ reductase from the dissimilatory Fe3+-reducing bacterium Geobacter sulfurreducens. *FEMS Microbiology Letters* 185: 205-211.

Maher, K.A., and Stevenson, D.J. (1988) Impact frustration of the origin of life. *Nature* 331: 612-614.

Malpas, J., Moores, E.M., Panayiotou, A., and Xenophontos, C. (1990) *Ophiolites: Oceanic Crustal Analogs. Proceedings of the Symposium 'Troodos 1987'*. Nicosia, Cyprus: The Geological Survey Department, Ministry of Agriculture and Natural Resources.

Manceau, A., Tommaseo, C., Rihs, S., Geoffroy, N., Chateigner, D., Schlegel, M. et al. (2005) Natural speciation of Mn, Ni, and Zn at the micrometer scale in a clayey paddy soil using X-ray fluorescence, absorption, and diffraction. *Geochimica et Cosmochimica Acta* 69: 4007-4034.

Mason, O.U., Di Meo-Savoie, C.A., Van Nostrand, J.D., Zhou, J.Z., Fisk, M.R., and Giovannoni, S.J. (2009) Prokaryotic diversity, distribution, and insights into their role in biogeochemical cycling in marine basalts. *ISME Journal* 3: 231-242.

Mason, O.U., Nakagawa, T., Rosner, M., Van Nostrand, J.D., Zhou, J., Maruyama, A. et al. (2010) First investigation of the microbiology of the deepest layer of ocean crust. *PLoS ONE* 5: e15399.

Mason, O.U., Stingl, U., Wilhelm, L.J., Moeseneder, M.M., Di Meo-Savoie, C.A., Fisk, M.R., and Giovannoni, S.J. (2007) The phylogeny of endolithic microbes associated with marine basalts. *Environmental Microbiology* 9: 2539-2550.

Mathez, E.A. (1976) Sulfur solubility and magmatic sulfides in submarine basalt glass. *Journal of Geophysical Research* 81: 4269-4276.

Mayhew, L.E., Webb, S.M., and Templeton, A.S. (2011) Microscale imaging and identification of Fe speciation and distribution during fluid-mineral reactions under highly reducing conditions. *Environmental Science & Technology* 45: 4468-4474.

McCollom, T.M. (2000) Geochemical constraints on primary productivity in submarine

hydrothermal vent plumes. *Deep-Sea Research Part I-Oceanographic Research Papers* 47: 85-101.

McCollom, T.M., and Bach, W. (2009) Thermodynamic constraints on hydrogen generation during serpentinization of ultramafic rocks. *Geochimica et Cosmochimica Acta* 73: 856-875.

McCollom, T.M., and Shock, E.L. (1997) Geochemical constraints on chemolithoautotrophic metabolism by microorganisms in seafloor hydrothermal systems. *Geochimica et Cosmochimica Acta* 61: 4375-4391.

McEwen, A.S., Hansen, C.J., Delamere, W.A., Eliason, E.M., Herkenhoff, K.E., Keszthelyi, L. et al. (2007) A closer look at water-related geologic activity on Mars. *Science* 317: 1706-1709.

McKay, D.S., Clemett, S.J., Thomas-Keprta, K.L., Wentworth, S.J., Gibson, E.K., Robert, F. et al. (2006) Observation and analysis of in situ carbonaceous matter in Nakhla: Part I [abstract 2251]. *Lunar and Planetary Science Conference Abstracts* 37.

McKay, D.S., Gibson, E.K., Thomas-Keprta, K.L., Vali, H., Romanek, C.S., Clemett, S.J. et al. (1996) Search for past life on Mars: Possible relic biogenic activity in Martian meteorite ALH84001. *Science* 273: 924-930.

McLoughlin, N., Brasier, M.D., Wacey, D., Green, O.R., and Perry, R.S. (2007) On biogenicity criteria for endolithic microborings on early earth and beyond. *Astrobiology* 7: 10-26.

McLoughlin, N., Furnes, H., Banerjee, N.R., Muehlenbachs, K., and Staudigel, H. (2009) Ichnotaxonomy of microbial trace fossils in volcanic glass. *Journal of the Geological Society, London* 166: 159-169.

McLoughlin, N., Wacey, D., Kruber, C., Kilburn, M.R., Thorseth, I.H., and Pedersen, R.B. (2011) A combined TEM and NanoSIMS study of endolithic microfossils in altered seafloor basalt. *Chemical Geology* 289: 154-162.

Melosh, H.J. (1988) The rocky road to panspermia. *Nature* 332: 687-688.

Ménez, B., Pasini, V., and Brunelli, D. (2012) Life in the hydrated suboceanic mantle. *Nature Geoscience*.

Mével, C. (2003) Serpentinization of abyssal peridotites at mid-ocean ridges. *Comptes Rendus Geoscience* 335: 825-852.

Miot, J., Maclellan, K., Benzerara, K., and Boisset, N. (2011) Preservation of protein globules and peptidoglycan in the mineralized cell wall of nitrate-reducing, iron(II)-oxidizing bacteria: a cryo-electron microscopy study. *Geobiology* 9: 459-470.

Moody, J.B. (1976) Serpentinization - Review. *Lithos* 9: 125-138.

Morita, R. (2000) Is H2 the universal energy source for long-term survival? *Microbial Ecology* 38: 307-320.

Nealson, K.H., Belz, A., and McKee, B. (2002) Breathing metals as a way of life: Geobiology in action. *Antonie Van Leeuwenhoek International Journal of General and Molecular Microbiology* 81: 215-222.

Nealson, K.H., and Saffarini, D. (1994) Iron and manganese in anaerobic respiration - Environmental significance, physiology, and regulation. *Annual Review of Microbiology* 48: 311-343.

Neilands, J.B. (1995) Siderophores - Structure and function of microbial iron transport compounds. *Journal of Biological Chemistry* 270: 26723-26726.

Newberry, C.J., Webster, G., Cragg, B.A., Parkes, R.J., Weightman, A.J., and Fry, J.C. (2004) Diversity of prokaryotes and methanogenesis in deep subsurface sediments from the Nankai Trough, Ocean Drilling Program Leg 190. *Environmental Microbiology* 6: 274-287.

Newman, D.K., and Kolter, R. (2000) A role for excreted quinones in extracellular electron transfer. *Nature* 405: 94-97.

Nigro, L., Harris, K., Orcutt, B., Hyde, A., Clayton-Luce, S., Becker, K., and Teske, A. (2012) Microbial communities at the borehole observatory on the Costa Rica Rift flank (Ocean Drilling Program Hole 896A). *Frontiers in Microbiology* 3.

O'Day, P.A., Rivera, N., Jr., Root, R., and Carroll, S.A. (2004) X-ray absorption spectroscopic study of Fe reference compounds for the analysis of natural sediments. *American Mineralogist* 89: 572-585.

Ochman, H. (2007) Single-cell genomics. *Environmental Microbiology* 9: 7-7.

Oehler, D.Z., Robert, F., Chaussidon, M., and Gibson, E.K. (2008) Bona fide biosignatures: Insights from combined NanoSIMS-SIMS. *Geochimica et Cosmochimica Acta* 72: A698-A698.

Oehler, D.Z., Robert, F., Mostefaoui, S., Meibom, A., Selo, M., and McKay, D.S. (2006) Chemical mapping of Proterozoic organic matter at submicron spatial resolution. *Astrobiology* 6: 838-850.

Orcutt, B.N., Sylvan, J.B., Knab, N.J., and Edwards, K.J. (2011) Microbial ecology of the dark ocean above, at, and below the seafloor. *Microbiology and Molecular Biology Reviews* 75: 361-422.

Parkes, R.J., Cragg, B.A., Bale, S.J., Getliff, J.M., Goodman, K., Rochelle, P.A. et al. (1994) Deep bacterial biosphere in Pacific-Ocean sediments. *Nature* 371: 410-413.

Pearce, J.A., Lippard, S.J., and Roberts, S. (1984) Characteristics and tectonic significance of supra-subduction zone ophiolites. In *Marginal Basin Geology: Volcanic and Associated Sedimentary and Tectonic Processes in Modern and Ancient Marginal Basins*. Kokelaar, B.P., and Howells, M.F. (eds). London, UK: Geological Society London, pp. 77-94.

Pedersen, K. (1993) The deep subterranean biosphere. *Earth-Science Reviews* 34: 243-260.

Perry, R.S., McLoughlin, N., Lynne, B.Y., Sephton, M.A., Oliver, J.D., Perry, C.C. et al. (2007) Defining biominerals and organominerals: Direct and indirect indicators of life. *Sedimentary Geology* 201: 157-179.

Peterson, C., Duncan, R., and Scheidegger, K.F. (1986) Sequence and longevity of basalt alteration at Deep Sea Drilling Project Site 597. In *Initial Reports of the Deep Sea Drilling Project 92*. M. Leinen, et al. (ed): U.S. Government Printing Office, pp. 505-515.

Petit, P.E., Farges, F., Wilke, M., and Sole, V.A. (2001) Determination of the iron oxidation state in Earth materials using XANES pre-edge information. *Journal of Synchrotron Radiation* 8: 952-954.

Philippot, P., Foriel, J., Susini, J., Khodja, H., Grassineau, N., and Fouquet, Y. (2003) High-resolution imaging of transition metal and sulfur-redox distribution in individual microfossils. *Journal De Physique IV* 104: 381-384.

Pickering, I.J., George, G.N., Yu, E.Y., Brune, D.C., Tuschak, C., Overmann, J. et al. (2001) Analysis of sulfur biochemistry of sulfur bacteria using X-ray absorption spectroscopy. *Biochemistry* 40: 8138-8145.

Poulet, F., Bibring, J.P., Mustard, J.F., Gendrin, A., Mangold, N., Langevin, Y. et al. (2005) Phyllosilicates on Mars and implications for early martian climate. *Nature* 438: 623-627.

Prange, A., Chauvistre, R., Modrow, H., Hormes, J., Truper, H.G., and Dahl, C. (2002) Quantitative speciation of sulfur in bacterial sulfur globules: X-ray absorption spectroscopy reveals at least three different species of sulfur. *Microbiology-SGM* 148: 267-276.

Prange, A., Dahl, C., Truper, H.G., Behnke, M., Hahn, J., Modrow, H., and Hormes, J. (2002) Investigation of S-H bonds in biologically important compounds by sulfur K-edge X-ray absorption spectroscopy. *European Physical Journal D* 20: 589-596.

Preston, L.J., Izawa, M.R.M., and Banerjee, N.R. (2011) Infrared spectroscopic characterization of organic matter associated with microbial bioalteration textures in basaltic glass. *Astrobiology* 11: 585-599.

Price, P.B., and Sowers, T. (2004) Temperature dependence of metabolic rates for microbial growth, maintenance, and survival. *Proceedings of the National Academy of Sciences of the United States of America* 101: 4631-4636.

Rasmussen, B. (2000) Filamentous microfossils in a 3,235-million-year-old volcanogenic massive sulphide deposit. *Nature* 405: 676-679.

Robinson, P.T., Flower, M.F.J., Swanson, D.A., and Staudigel, H. (1979) Lithology and eruptive stratigraphy of Cretaceous oceanic crust, western Atlantic Ocean. In *Initial Reports DSDP LI, LII, LIII*. Donnelly, T., Francheteau, J., Bryan, W., Robinson, P., Flower, M., and Salisbury, M. (eds). College Station, TX: Ocean Drilling Program, pp. 1535-1555.

Robinson, P.T., Malpas, J., and Xenophontos, C. (2003) The Troodos Massif of Cyprus: Its role in the evolution of the ophiolite concept. *Geological Society of America Special Papers* 373: 295-308.

Robinson, P.T., Melson, W.G., Ohearn, T., and Schmincke, H.U. (1983) Volcanic glass compositions of the Troodos Ophiolite, Cyprus. *Geology* 11: 400-404.

Romano, C., Paris, E., Poe, B.T., Giuli, G., Dingwell, D.B., and Mottana, A. (2000) Effect of aluminum on Ti-coordination in silicate glasses: A XANES study. *American Mineralogist* 85: 108-117.

Rompel, A., Cinco, R.M., Latimer, M.J., McDermott, A.E., Guiles, R.D., Quintanilha, A. et al. (1998) Sulfur K-edge x-ray absorption spectroscopy: A spectroscopic tool to examine the redox state of S-containing metabolites in vivo. *Proceedings of the National Academy of Sciences of the United States of America* 95: 6122-6127.

Rouxel, O., Ono, S.H., Alt, J., Rumble, D., and Ludden, J. (2008) Sulfur isotope evidence for microbial sulfate reduction in altered oceanic basalts at ODP Site 801. *Earth and Planetary Science Letters* 268: 110-123.

Sand, W., and Bock, E. (1991) Biodeterioration of mineral materials by microorganisms - Biogenic sulfuric and nitric-acid corrosion of concrete and natural stone. *Geomicrobiology Journal* 9: 129-138.

Sansone, F.J. (1986) Depth distribution of short-chain organic-acid turnover in Cape Lookout Bight sediments. *Geochimica et Cosmochimica Acta* 50: 99-105.

Santelli, C.M., Banerjee, N., Bach, W., and Edwards, K.J. (2010) Tapping the subsurface ocean crust biosphere: Low biomass and drilling-related contamination calls for improved quality controls. *Geomicrobiology Journal* 27: 158-169.

Santelli, C.M., Edgcomb, V.P., Bach, W., and Edwards, K. (2009) The diversity and abundance of bacteria inhabiting seafloor lavas positively correlate with rock alteration. *Environmental Microbiology* 11: 86-98.

Santelli, C.M., Orcutt, B.N., Banning, E., Bach, W., Moyer, C.L., Sogin, M.L. et al. (2008) Abundance and diversity of microbial life in ocean crust. *Nature* 453: 653-657.

Schiffbauer, J.D., and Xiao, S.H. (2009) Novel application of focused ion beam electron microscopy (FIB-EM) in preparation and analysis of microfossil ultrastructures: A new view of complexity in early eukaryotic organisms. *PALAIOS* 24: 616-626.

Schmincke, H.-U., and Bednarz, U. (1990) Pillow, sheet flow and breccia flow volcanics and volcano-tectonic hydrothermal cycles in the Extrusive Series of the northeastern Troodos ophiolite (Cyprus). In *Ophiolites: Oceanic Crustal Analogs. Proceedings of the Symposium 'Troodos 1987'*. Malpas, J., Moores, E.M., Panayiotou, A., and Xenophontos, C. (eds). Nicosia, Cyprus: The Geological Survey Department, Ministry of Agriculture and Natural Resources, pp. 185-206.

Schmincke, H.U., Rautenschlein, M., Robinson, P.T., and Mehegan, J.M. (1983) Troodos extrusive series of Cyprus: A comparison with oceanic crust. *Geology* 11: 405-409.

Schopf, J.W. (1993) Microfossils of the early Archean Apex Chert - New evidence of the antiquity of life. *Science* 260: 640-646.

Schopf, J.W. (2004) Earth's earliest biosphere: status of the hunt. In *The Precambrian Earth*. Eriksson, P.G., Altermann, W., Nelson, D.R., Mueller, W.U., and Catuneanu, O. (eds). New York, NY: Elsevier, pp. 516-539.

Schopf, J.W., Kudryavtsev, A.B., Agresti, D.G., Wdowiak, T.J., and Czaja, A.D. (2002) Laser-Raman imagery of Earth's earliest fossils. *Nature* 416: 73-76.

Schott, J., Pokrovsky, O.S., and Oelkers, E.H. (2009) The Link Between Mineral Dissolution/Precipitation Kinetics and Solution Chemistry. In *Thermodynamics and Kinetics of Water-Rock Interaction*. Chantilly: Mineralogical Society of America, pp. 207-258.

Schramm, B., Devey, C.W., Gillis, K.M., and Lackschewitz, K. (2005) Quantitative assessment of chemical and mineralogical changes due to progressive low-temperature alteration of East Pacific Rise basalts from 0 to 9 Ma. *Chemical Geology* 218: 281-313.

Schulte, M., Blake, D., Hoehler, T., and McCollom, T. (2006) Serpentinization and its implications for life on the early Earth and Mars. *Astrobiology* 6: 364-376.

Schultze-Lam, S., Fortin, D., Davis, B.S., and Beveridge, T.J. (1996) Mineralization of bacterial surfaces. *Chemical Geology* 132: 171-181.

Seewald, J.S., and Seyfried, W.E. (1990) The effect of temperature on metal mobility in subseafloor hydrothermal systems - constraints from basalt alteration experiments. *Earth and Planetary Science Letters* 101: 388-403.

Seewald, J.S., and Seyfried, W.E. (1990) The effect of temperature on metal mobility in subseafloor hydrothermal systems: constraints from basalt alteration experiments. *Earth and Planetary Science Letters* 101: 388-403.

Shock, E.L. (1997) High-temperature life without photosynthesis as a model for Mars. *Journal of Geophysical Research-Planets* 102: 23687-23694.

Sleep, N.H., Meibom, A., Fridriksson, T., Coleman, R.G., and Bird, D.K. (2004) H2-rich fluids from serpentinization: Geochemical and biotic implications. *Proceedings of the National Academy of Sciences of the United States of America* 101: 12818-12823.

Sleep, N.H., and Zahnle, K. (1998) Refugia from asteroid impacts on early Mars and the early Earth. *Journal of Geophysical Research-Planets* 103: 28529-28544.

Smith, E., and Dent, G. (2005) *Modern Raman Spectroscopy: A Practical Approach*. West Sussex, England: Wiley.

Smits, M.M. (2006) Mineral tunneling by fungi. In *Fungi in Biogeochemical Cycles*. Gadd, G.M. (ed). Cambridge: Cambridge University Press, pp. 681–717.

Souza-Egipsy, V., Wierzchos, J., Ascaso, C., and Nealson, K.H. (2005) Mg-silica precipitation in fossilization mechanisms of sand tufa endolithic microbial community, Mono Lake (California). *Chemical Geology* 217: 77-87.

Squyres, S.W., Grotzinger, J.P., Arvidson, R.E., Bell, J.F., Calvin, W., Christensen, P.R. et al. (2004) In situ evidence for an ancient aqueous environment at Meridiani Planum, Mars. *Science* 306: 1709-1714.

Stakes, D.S., and Oneil, J.R. (1982) Mineralogy and stable isotope geochemistry of hydrothermally altered oceanic rocks. *Earth and Planetary Science Letters* 57: 285-304.

Stakes, D.S., Taylor, H.P., and Fisher, R.L. (1984) Oxygen-isotope and geochemical characterization of hydrothermal alteration in ophiolite complexes and modern oceanic crust. *Geological Society, London, Special Publications* 13: 199-214.

Staudigel, H., Chastain, R.A., Yayanos, A., and Bourcier, W. (1995) Biologically mediated dissolution of glass. *Chemical Geology* 126: 147-154.

Staudigel, H., Furnes, H., Banerjee, N.R., Dilek, Y., and Muehlenbachs, K. (2006) Microbes and volcanoes: A tale from the oceans, ophiolites, and greenstone belts. *GSA Today* 16: 4-10.

Staudigel, H., Furnes, H., McLoughlin, N., Banerjee, N.R., Connell, L.B., and Templeton, A. (2008) 3.5 billion years of glass bioalteration: Volcanic rocks as a basis for microbial life? *Earth-Science Reviews* 89: 156-176.

Staudigel, H., and Hart, S.R. (1983) Alteration of basaltic glass - Mechanisms and significance for the oceanic-crust seawater budget. *Geochimica et Cosmochimica Acta* 47: 337-350.

Staudigel, H., Hart, S.R., Schmincke, H.U., and Smith, B.M. (1989) Cretaceous ocean crust at

DSDP site-417 and site-418 - carbon uptake from weathering versus loss by magmatic outgassing. *Geochimica et Cosmochimica Acta* 53: 3091-3094.

Staudigel, H., Yayanos, A., Chastain, R., Davies, G., Verdurmen, E.A.T., Schiffman, P. et al. (1998) Biologically mediated dissolution of volcanic glass in seawater. *Earth and Planetary Science Letters* 164: 233-244.

Stein, C.A., and Stein, S. (1994) Constraints on hydrothermal heat flux through the oceanic lithosphere from global heat flow. *Journal of Geophysical Research* 99: 3081-3095.

Stetter, K.O., Huber, R., Blochl, E., Kurr, M., Eden, R.D., Fielder, M. et al. (1993) Hyperthermophilic archaea are thriving in deep North-Sea and Alaskan oil-reservoirs. *Nature* 365: 743-745.

Stevens, T. (1997) Lithoautotrophy in the subsurface. *FEMS Microbiology Reviews* 20: 327-337.

Stevens, T.O., and McKinley, J.P. (1995) Lithoautotrophic microbial ecosystems in deep basalt aquifers. *Science* 270: 450-454.

Stöffler, D., Horneck, G., Ott, S., Hornemann, U., Cockell, C.S., Moeller, R. et al. (2007) Experimental evidence for the potential impact ejection of viable microorganisms from Mars and Mars-like planets. *Icarus* 186: 585-588.

Stöhr, J. (1992) *NEXAFS Spectroscopy*. New York: Springer-Verlag.

Storrie-Lombardi, M.C., and Fisk, M.R. (2004) Elemental abundance distributions in suboceanic basalt glass: Evidence of biogenic alteration. *Geochemistry Geophysics Geosystems* 5.

Stroncik, N.A., and Schmincke, H.U. (2001) Evolution of palagonite: Crystallization, chemical changes, and element budget. *Geochemistry Geophysics Geosystems* 2.

Stroncik, N.A., and Schmincke, H.U. (2002) Palagonite - a review. *International Journal of Earth Sciences* 91: 680-697.

Summit, M., and Baross, J.A. (2001) A novel microbial habitat in the mid-ocean ridge subseafloor. *Proceedings of the National Academy of Sciences of the United States of America* 98: 2158-2163.

Tazaki, K. (1997) Biomineralization of layer silicates and hydrated Fe/Mn oxides in microbial mats: An electron microscopical study. *Clays and Clay Minerals* 45: 203-212.

Tebo, B.M., Bargar, J.R., Clement, B.G., Dick, G.J., Murray, K.J., Parker, D. et al. (2004) Biogenic manganese oxides: Properties and mechanisms of formation. *Annual Review of Earth and Planetary Sciences* 32: 287-328.

Tebo, B.M., Ghiorse, W.C., van Waasbergen, L.G., Siering, P.L., and Caspi, R. (1997)

Bacterially mediated mineral formation: Insights into manganese (II) oxidation from molecular genetic and biochemical studies. In *Geomicrobiology: Interactions between Microbes and Minerals*. Banfield, J.F., and Nealson, K.H. (eds). Washington, DC: Mineralogical Society of America, pp. 225-266.

Templeton, A.S., Knowles, E.J., Eldridge, D.L., Arey, B.W., Dohnalkova, A.C., Webb, S.M., et al. (2009) A seafloor microbial biome hosted within incipient ferromanganese crusts. *Nature Geoscience* 2: 872-876.

Templeton, A.S., and Knowles, E.J. (2009) Microbial transformations of minerals and metals: Recent Advances in Geomicrobiology Derived from Synchrotron-Based X-ray Spectroscopy and X-ray Microscopy. *Annual Review of Earth and Planetary Sciences* 37: 367-391.

Templeton, A.S., Staudigel, H., and Tebo, B.M. (2005) Diverse Mn(II)-oxidizing bacteria isolated from submarine basalts at Loihi Seamount. *Geomicrobiology Journal* 22: 127-139.

Thorseth, I.H., Fumes, H., and Tumyr, O. (1995) Textural and chemical effects of bacterial-activity on basaltic glass - An experimental approach. *Chemical Geology* 119: 139-160.

Thorseth, I.H., Furnes, H., and Heldal, M. (1992) The importance of microbiological activity in the alteration of natural basaltic glass. *Geochimica et Cosmochimica Acta* 56: 845-850.

Thorseth, I.H., Furnes, H., and Tumyr, O. (1991) A textural and chemical study of Icelandic palagonite of varied composition and its bearing on the mechanism of the glass-palagonite transformation. *Geochimica et Cosmochimica Acta* 55: 731-749.

Thorseth, I.H., Pedersen, R.B., and Christie, D.M. (2003) Microbial alteration of 0-30-Ma seafloor and sub-seafloor basaltic glasses from the Australian Antarctic Discordance. *Earth and Planetary Science Letters* 215: 237-247.

Thorseth, I.H., Torsvik, T., Furnes, H., and Muehlenbachs, K. (1995) Microbes play an important role in the alteration of oceanic crust. *Chemical Geology* 126: 137-146.

Thorseth, I.H., Torsvik, T., Torsvik, V., Daae, F.L., and Pedersen, R.B. (2001) Diversity of life in ocean floor basalt. *Earth and Planetary Science Letters* 194: 31-37.

Tijhuis, L., Vanloosdrecht, M.C.M., and Heijnen, J.J. (1993) A thermodynamically based correlation for maintenance Gibbs energy-requirements in aerobic and anaerobic chemotropic growth. *Biotechnology and Bioengineering* 42: 509-519.

Toner, B.M., Santelli, C.M., Marcus, M.A., Wirth, R., Chan, C.S., McCollom, T. et al. (2009) Biogenic iron oxyhydroxide formation at mid-ocean ridge hydrothermal vents: Juan de Fuca Ridge. *Geochimica et Cosmochimica Acta* 73: 388-403.

Toporski, J.K.W., Steele, A., Westall, F., Thomas-Keprta, K.L., and McKay, D.S. (2002) The

simulated silicification of bacteria - New clues to the modes and timing of bacterial preservation and implications for the search for extraterrestrial microfossils. *Astrobiology* 2: 1-26.

Torsvik, T., Furnes, H., Muehlenbachs, K., Thorseth, I.H., and Tumyr, O. (1998) Evidence for microbial activity at the glass-alteration interface in oceanic basalts. *Earth and Planetary Science Letters* 162: 165-176.

Van Baleen, M.R. (1993) Titanium mobility in metamorphic systems: a review. *Chemical Geology* 110: 233-249.

van Zuilen, M.A., Mathew, K., Wopenka, B., Lepland, A., Marti, K., and Arrhenius, G. (2005) Nitrogen and argon isotopic signatures in graphite from the 3.8-Ga-old Isua Supracrustal Belt, Southern West Greenland. *Geochimica et Cosmochimica Acta* 69: 1241-1252.

Villar, S.E.J., Edwards, H.G.M., and Cockell, C.S. (2005) Raman spectroscopy of endoliths from Antarctic cold desert environments. *Analyst* 130: 156-162.

Wacey, D., Kilburn, M.R., McLoughlin, N., Parnell, J., Stoakes, C.A., Grovenor, C.R.M., and Brasier, M.D. (2008) Use of NanoSIMS in the search for early life on Earth: ambient inclusion trails in a c. 3400 Ma sandstone. *Journal of the Geological Society* 165: 43-53.

Wacey, D., Kilburn, M.R., Saunders, M., Cliff, J., and Brasier, M.D. (2011a) Microfossils of sulphur-metabolizing cells in 3.4-billion-year-old rocks of Western Australia. *Nature Geosciences* 4: 698–702.

Wacey, D., Saunders, M., Brasier, M.D., and Kilburn, M.R. (2011b) Earliest microbially mediated pyrite oxidation in ~3.4 billion-year-old sediments. *Earth and Planetary Science Letters* 301: 393-402.

Walker, A., and Parkhill, J. (2008) Single-cell genomics. *Nature Reviews Microbiology* 6: 176-177.

Wallace, P., and Carmichael, I.S.E. (1992) Sulfur in basaltic magmas. *Geochimica et Cosmochimica Acta* 56: 1863-1874.

Wallace, P.J., and Carmichael, I.S.E. (1994) S-speciation in submarine basaltic glasses as determined by measurements of S K-alpha X-ray wavelength shifts. *American Mineralogist* 79: 161-167.

Walton, A.W. (2008) Microtubules in basalt glass from Hawaii Scientific Drilling Project #2 phase 1 core and Hilina slope, Hawaii: evidence of the occurrence and behavior of endolithic microorganisms. *Geobiology* 6: 351-364.

Walton, A.W., and Schiffman, P. (2003) Alteration of hyaloclastites in the HSDP 2 Phase 1 Drill Core - 1. Description and paragenesis. *Geochemistry Geophysics Geosystems* 4.

Walton, A.W., Schiffman, P., and Macpherson, G.L. (2005) Alteration of hyaloclastites in the HSDP 2 Phase 1 Drill Core: 2. Mass balance of the conversion of sideromelane to palagonite and chabazite. *Geochemistry Geophysics Geosystems* 6.

Watteau, F., and Berthelin, J. (1994) Microbial dissolution of iron and aluminum from soil minerals - Efficiency and specificity of hydroxamate siderophores compared to aliphatic-acids. *European Journal of Soil Biology* 30: 1-9.

Welch, S.A., and Ullman, W.J. (1993) The effect of organic-acids on plagioclase dissolution rates and stoichiometry. *Geochimica et Cosmochimica Acta* 57: 2725-2736.

Westall, F. (1999) The nature of fossil bacteria: A guide to the search for extraterrestrial life. *Journal of Geophysical Research-Planets* 104: 16437-16451.

Westall, F. (2008) Morphological biosignatures in early terrestrial and extraterrestrial materials. *Space Science Reviews* 135: 95-114.

Wetzel, L.R., and Shock, E.L. (2000) Distinguishing ultramafic- from basalt-hosted submarine hydrothermal systems by comparing calculated vent fluid compositions. *Journal of Geophysical Research-Solid Earth* 105: 8319-8340.

Wierzchos, J., and Ascaso, C. (2002) Microbial fossil record of rocks from the Ross Desert, Antarctica: implications in the search for past life in Mars. *International Journal of Astrobiology* 1: 51-59.

Wierzchos, J., Ascaso, C., Sancho, L.G., and Green, A. (2003) Iron-rich diagenetic minerals are biomarkers of microbial activity in Antarctic rocks. *Geomicrobiology Journal* 20: 15-24.

Wierzchos, J., Sancho, L.G., and Ascaso, C. (2005) Biomineralization of endolithic microbes in rocks from the McMurdo Dry Valleys of Antarctica: implications for microbial fossil formation and their detection. *Environmental Microbiology* 7: 566-575.

Wilke, M., Farges, F., Petit, P.E., Brown, G.E., and Martin, F. (2001) Oxidation state and coordination of Fe in minerals: An Fe K-XANES spectroscopic study. *American Mineralogist* 86: 714-730.

Wilke, M., Klimm, K., and Kohn, S.C. (2011) Spectroscopic Studies on Sulfur Speciation in Synthetic and Natural Glasses. In *Sulfur in Magmas and Melts: Its Importance for Natural and Technical Processes*. Chantilly: Mineralogical Society of America, pp. 41-78.

Wilke, M., Partzsch, G.M., Bernhardt, R., and Lattard, D. (2004) Determination of the iron oxidation state in basaltic glasses using XANES at the K-edge. *Chemical Geology* 213: 71-87.

Wirth, R. (2004) Focused Ion Beam (FIB): A novel technology for advanced application of

micro- and nanoanalysis in geosciences and applied mineralogy. *European Journal of Mineralogy* 16: 863-876.

Wirth, R. (2009) Focused Ion Beam (FIB) combined with SEM and TEM: Advanced analytical tools for studies of chemical composition, microstructure and crystal structure in geomaterials on a nanometre scale. *Chemical Geology* 261: 217-229.

Xenophontos, C., and Malpas, J.G. (1987) Sheeted dikes and their relationships to pillow lavas and plagiogranite. In *Ophiolites and oceanic lithosphere: field excursion guidebook*. Xenophontos, C., and Malpas, J.G. (eds). Nicosia, Cyprus: Geological Survey Department, pp. 80-87.

Zerkle, A.L., Farquhar, J., Johnston, D.T., Cox, R.P., and Canfield, D.E. (2009) Fractionation of multiple sulfur isotopes during phototrophic oxidation of sulfide and elemental sulfur by a green sulfur bacterium. *Geochimica et Cosmochimica Acta* 73: 291-306.

Zhang, G., Dong, H., Jiang, H., Kukkadapu, R.K., Kim, J., Eberl, D., and Xu, Z. (2009) Biomineralization associated with microbial reduction of Fe3+ and oxidation of Fe2+ in solid minerals. *American Mineralogist* 94: 1049-1058.

Zhou, W.M., Peacor, D.R., Alt, J.C., Van der Voo, R., and Kao, L.S. (2001) TEM study of the alteration of interstitial glass in MORB by inorganic processes. *Chemical Geology* 174: 365-376.

Zhou, Z., and Fyfe, W.S. (1989) Palagonitization of basaltic glass from DSDP site-335, leg-37 - textures, chemical-composition, and mechanism of formation. *American Mineralogist* 74: 1045-1053.

APPENDIX A

Chapter 2

A comparative analysis of potential biosignatures in basalt glass by FIB-TEM

Supporting Information

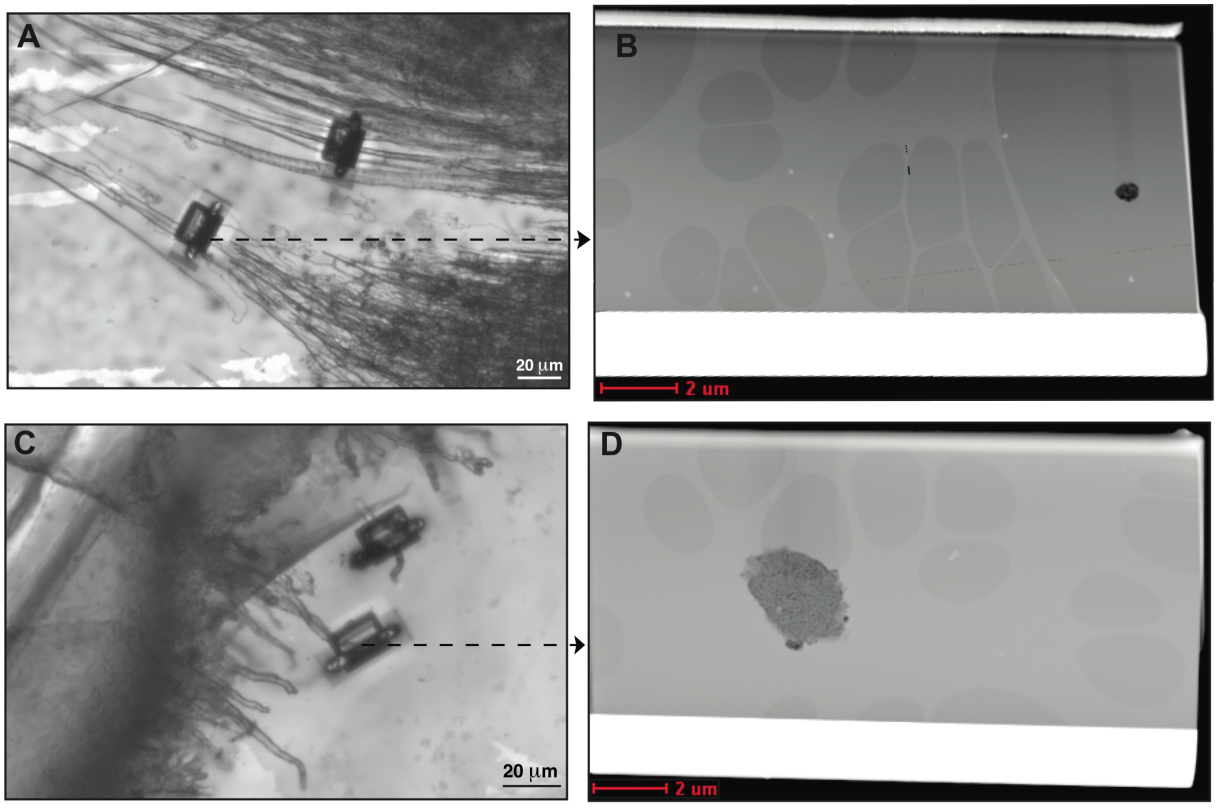

Figure A1. Thin-section photomicrographs (left) of the sample thin sections showing the locations of FIB milling. The finished FIB lamellae are shown on the right, corresponding to the milling location denoted by the arrows. The white strips on the top of the lamellae are the protective Pt layers and the white bands on the bottom are deposited Ga ions. A) and B) Sample 418A-56-5, Foil #2815. C) and D) Sample 896A-11R1, Foil #2817.

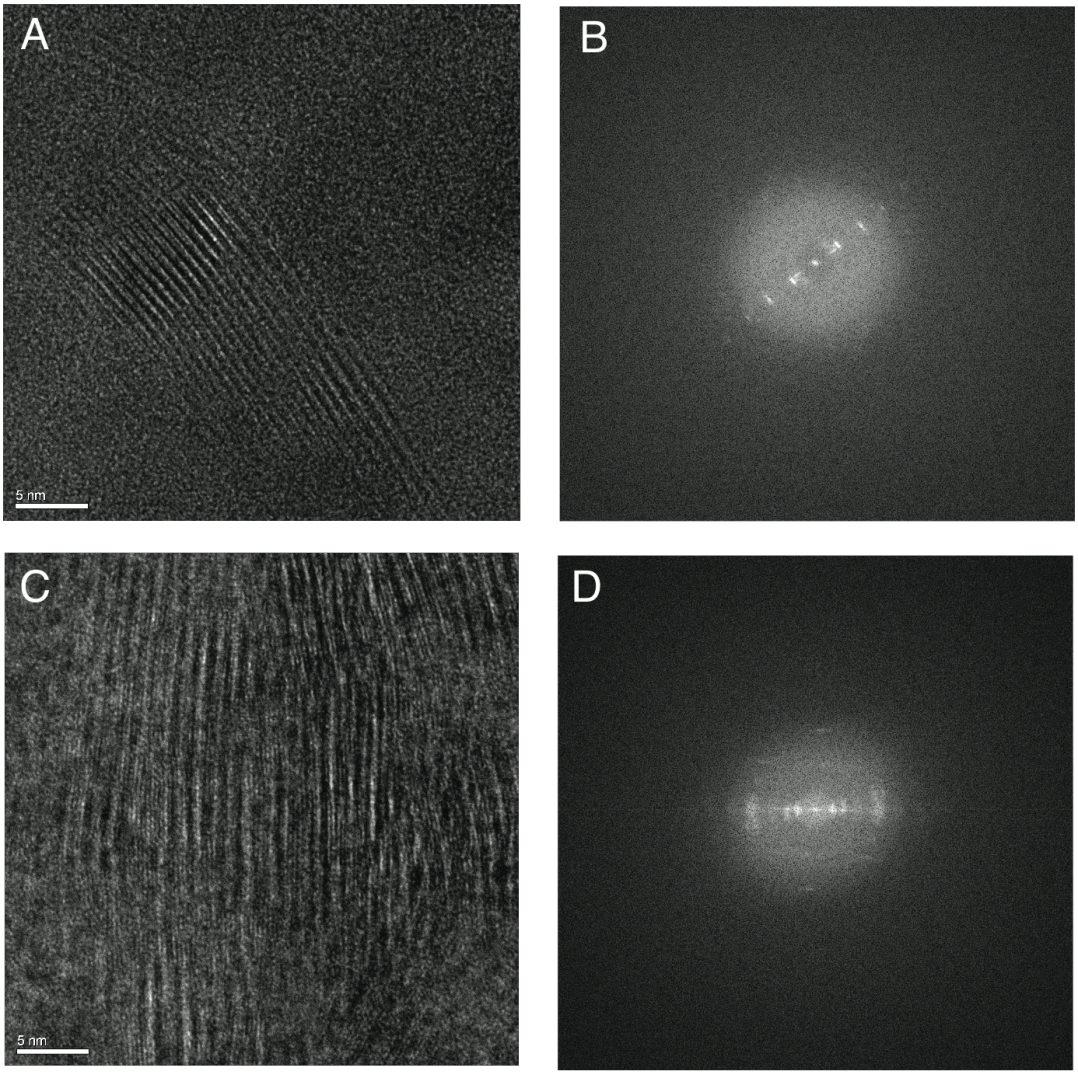

Figure A2. High-resolution images of the lattice fringes and associated fast Fourier transform (FFT), showing the partially crystalline nature of the phyllosilicates. A) and B) Sample 896A-11R1, Foil #2814. C) and D) Sample 418A-56-5, Foil #2813.

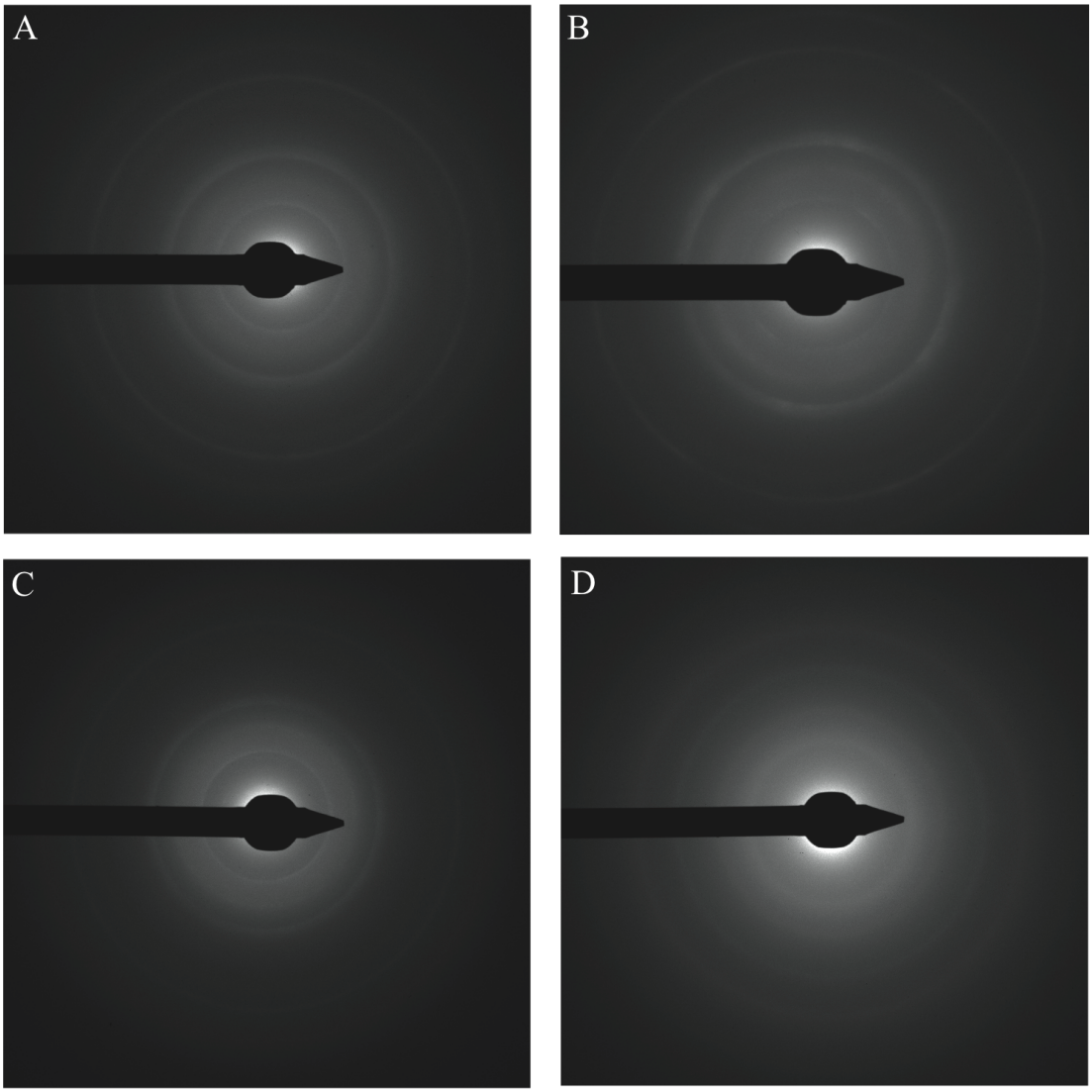

Figure A3. Diffraction patterns from each of the samples analyzed. A) Sample 896A-11R1 Foil #2817. The main d-spacings are 4.47, 2.57, and 1.53Å. B) Sample 418A-56-5 Foil #2813. The main d-spacings are 4.52, 2.60, and 1.52Å. C) Sample CY-1-34A Foil #2818. The main d-spacings are 6.77, 4.46, 2.58, and 1.49Å. D) Sample 46-396B-20 Foil #2996. The main d-spacings are 3.58, 2.53, and 1.85Å.

APPENDIX B

Chapter 3

Geochemical Characterization of Putative Biosignatures in Subseafloor Basalt Glass

Supporting Information

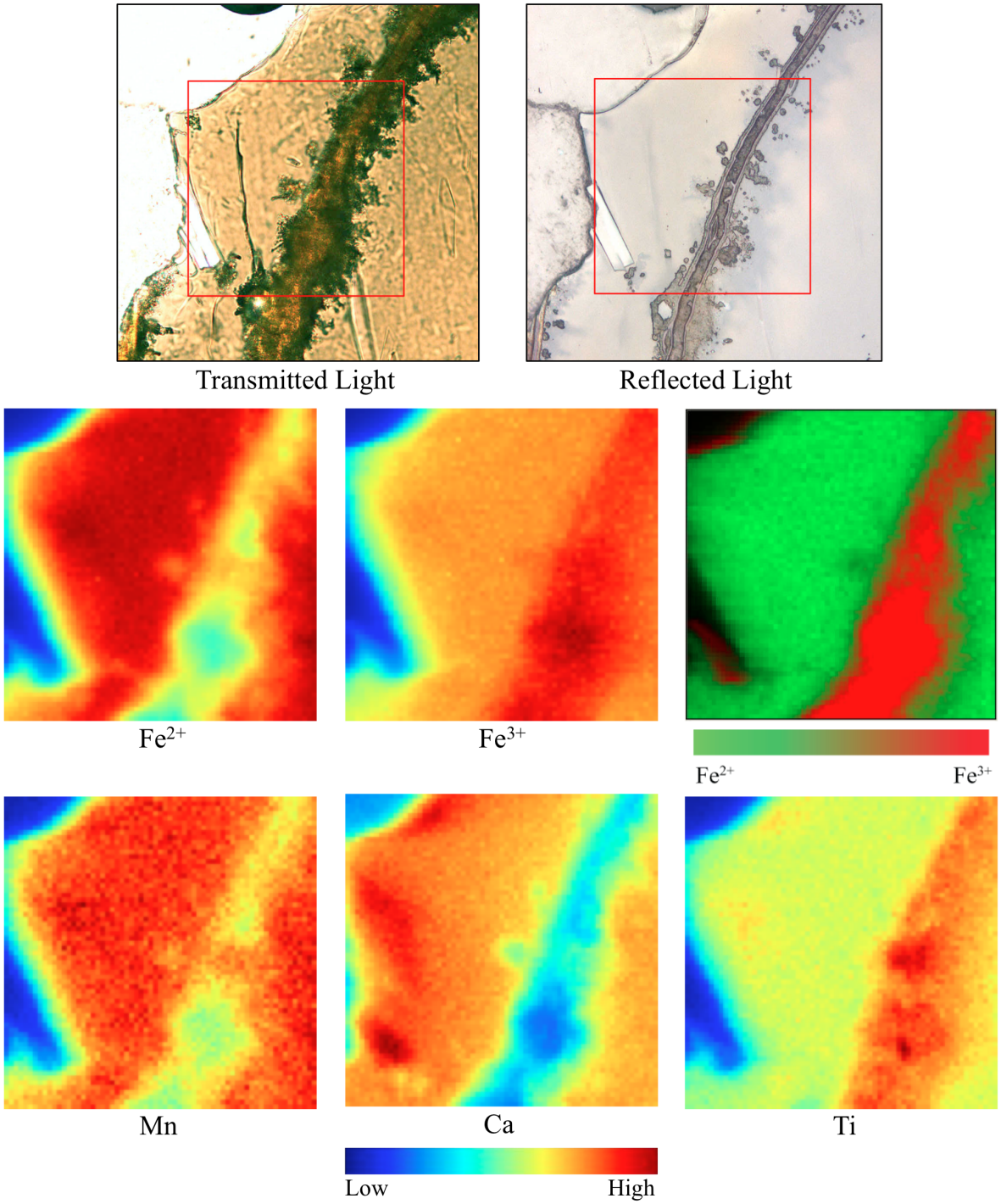

Figure B1. Upper: transmitted and reflected light photomicrographs of an alteration region in a thin section from sample 409-13. A crack runs through the center of the images, and a layer of crack-filling material can be seen in the middle. Clumps of tubules extend from the crack into the glass. Lower: element maps corresponding the area outlined by the red box in the photomicrographs. The colorscale for the relative intensities of the individual element maps is shown on the bottom, where blue corresponds to lower concentration and red to higher. The colorscale for the Fe oxidation state maps is shown on the right.

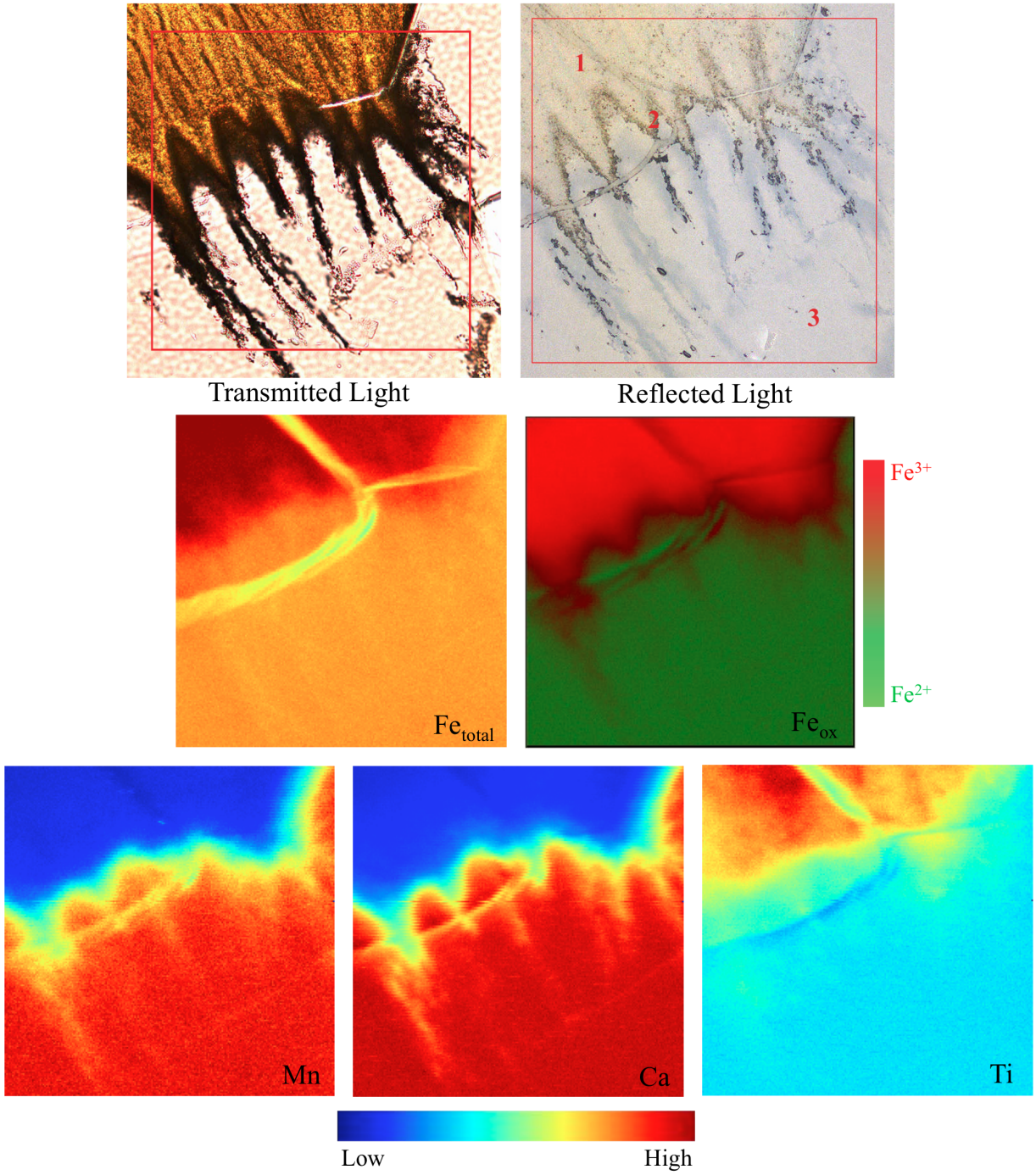

Figure B2. Upper: transmitted and reflected light photomicrographs of an alteration region in a thin section from sample 46-396B-16. A large zone of palagonite can be seen in the upper left, from which extend several clumps of tubules towards the lower right. The Fe μ-XANES spots analyzed are shown on the reflected light image. Lower: element maps corresponding the area outlined by the red box in the photomicrographs. The colorscale for the relative intensities of the individual element maps is shown on the bottom, where blue corresponds to lower concentration and red to higher. The colorscale for the Fe oxidation state map is shown on the right.

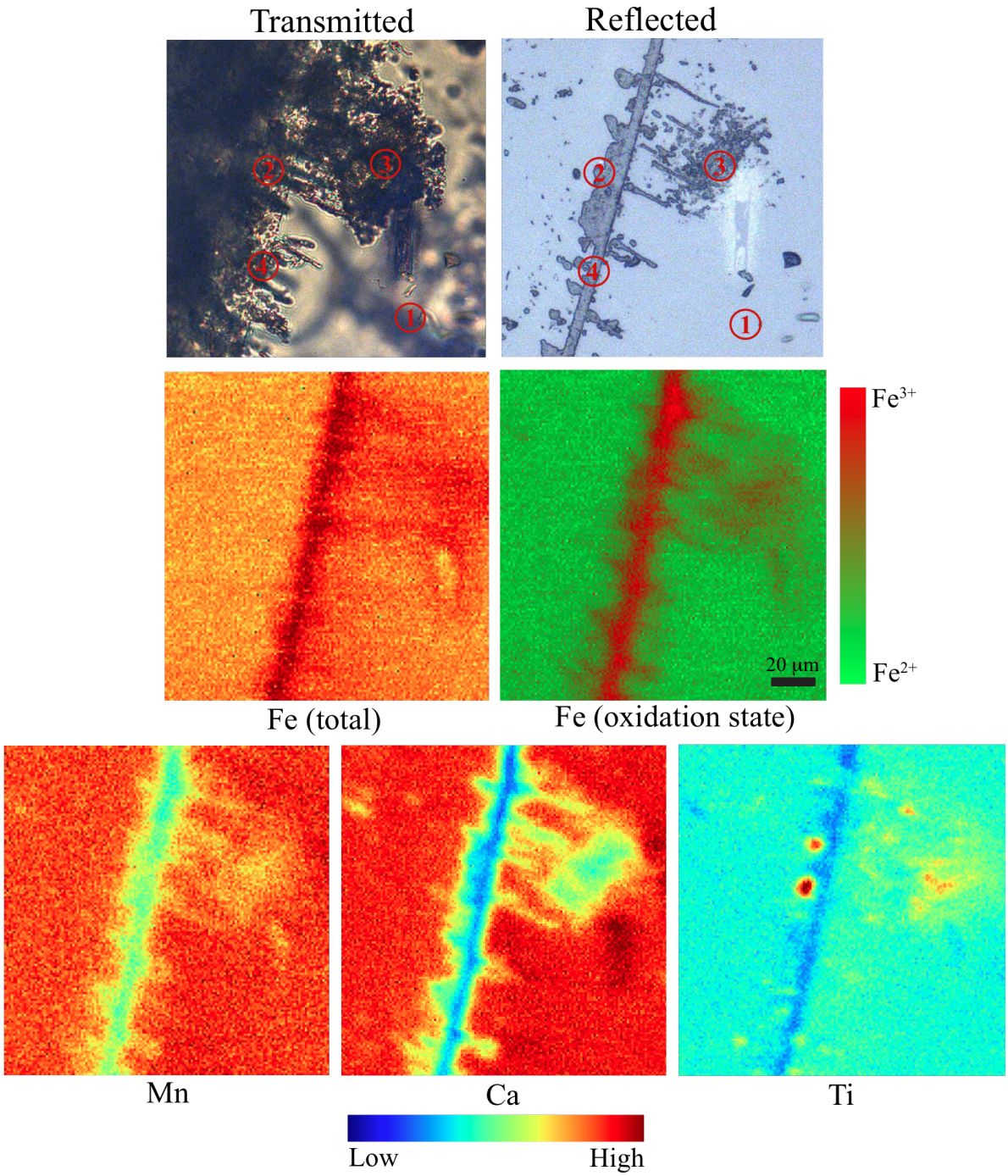

Figure B3. Top: Transmitted and reflected light photomicrographs of sample 418A-43-1. Numerous tubules can be seen branching off the crack running through the center of the images. The Fe XANES spots analyzed are shown in red circles. Bottom: X-ray fluorescence microprobe maps of the same region show the distributions of total Fe, Fe2+ versus Fe3+, Mn, Ca and Ti. The color scales indicate the relative intensities. In the Fe oxidation state map Fe2+ is shown as green and Fe3+ is red. For the element maps, blue is low concentration and dark red is high. The scale bar in the iron oxidation state map is 20 µm and applies to all of the maps and the photomicrographs. (Note: this figure is included in Fliegel *et al*., in press)

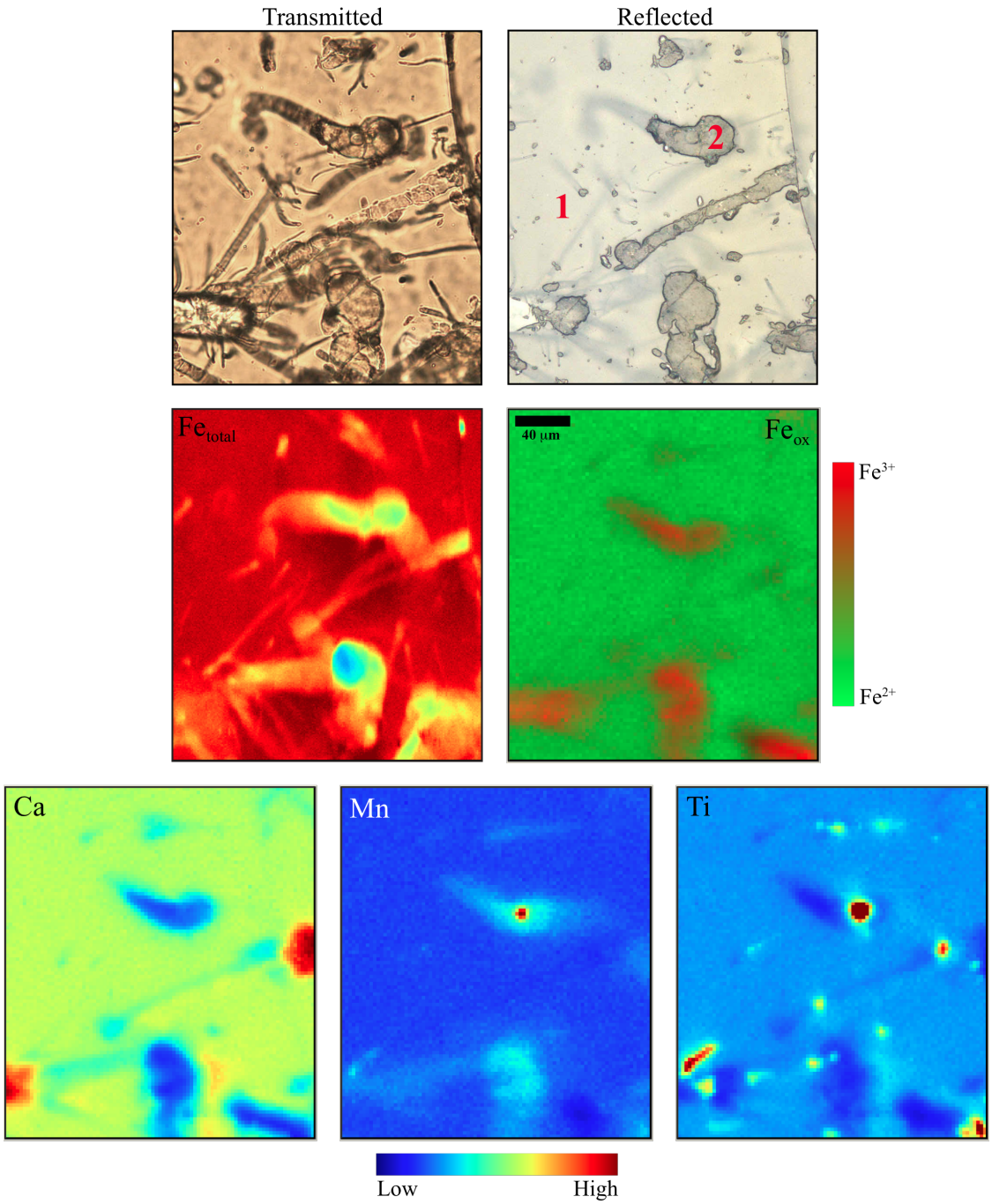

Figure B4. Upper: transmitted and reflected light photomicrographs of sample CY-1-31. Several tubules are visible throughout the region, some of which extend from the crack in the upper right corner. The locations of the Fe μ-XANES spots are shown on the reflected light image. Lower: X-ray microprobe maps showing the distributions of total Fe, Fe oxidation state, Ca, Mn, and Ti. The scale bar in the Fe oxidation state map is 40 mm and applies to all of the element maps and photomicrographs. The colorscale for the individual element maps is shown on the bottom, where blue corresponds to lower concentration and red to higher. The colorscale for the Fe oxidation state map is shown to the right.

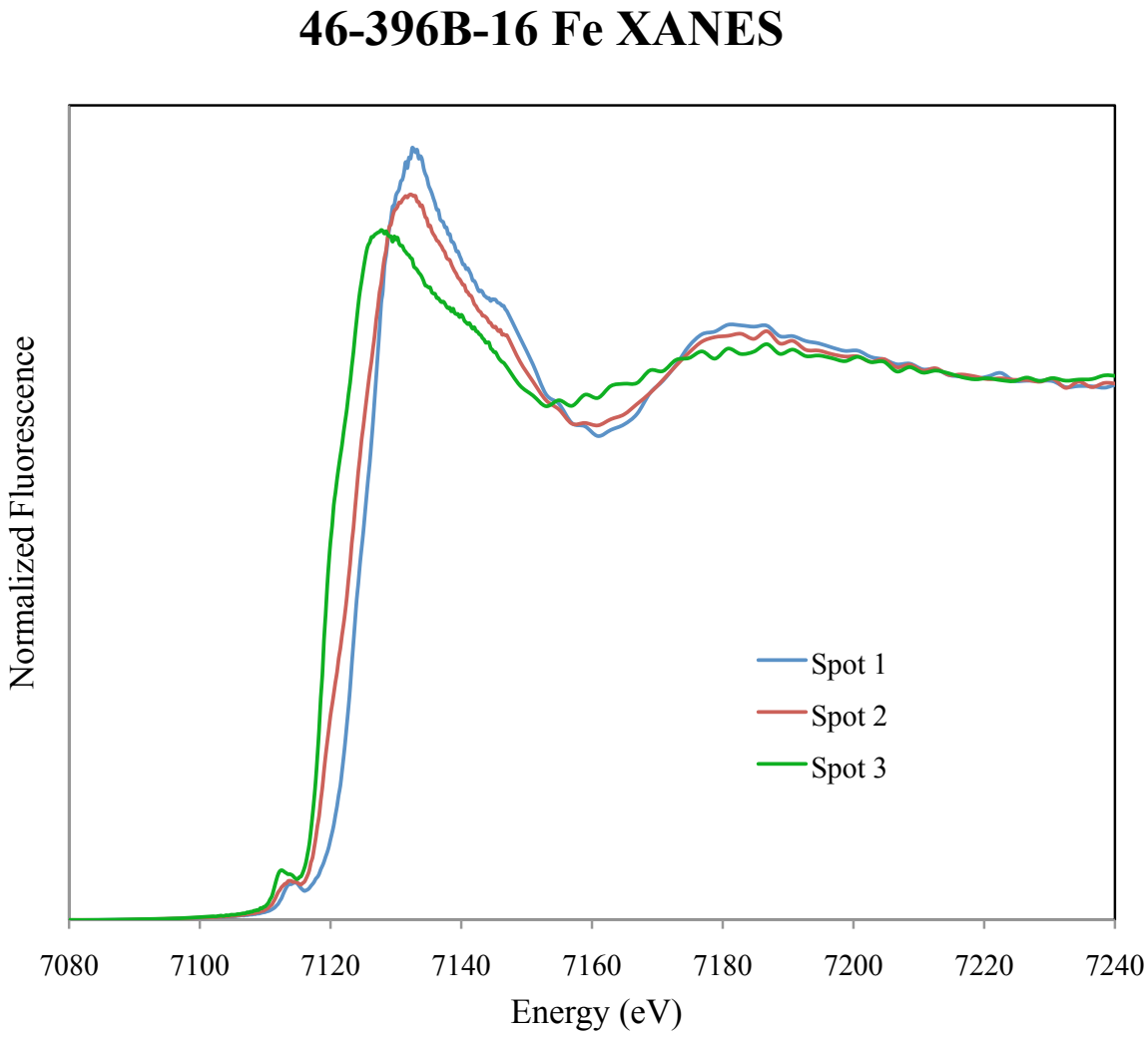

Figure B5. Fe μ-XANES spectra from the spots shown in the reflected light photomicrograph for sample 46-396B-16 (Figure B2). Spot 1 (blue) is in the palagonite and shows the most oxidized Fe compared to spots 2 (red), which is on the edge of the tubules, and spot 3 (green), which is in the glass.

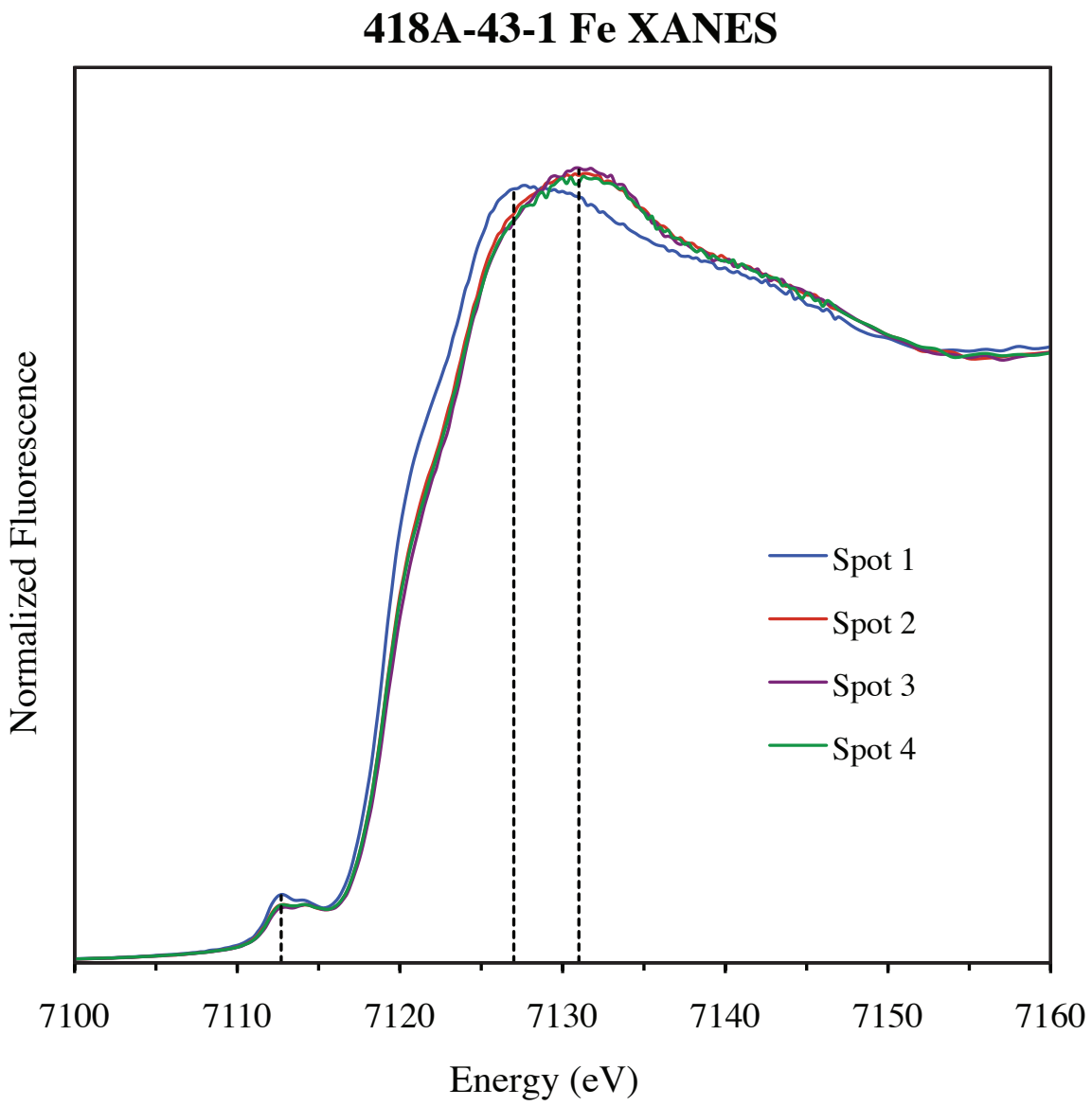

Figure B6. Fe K-edge μ-XANES spectra corresponding to spots 1-4 in the photomicrographs for sample 418A-43-1 (Figure B3). The peak maximum for spot 1 (blue line, 7127 eV), which is in fresh glass, is at lower energy than for spots 2-4 (red, green and purple, respectively, 7131 eV), which are targeting the alteration region. This shows that tubular alteration has significantly more Fe3+ than the fresh glass.

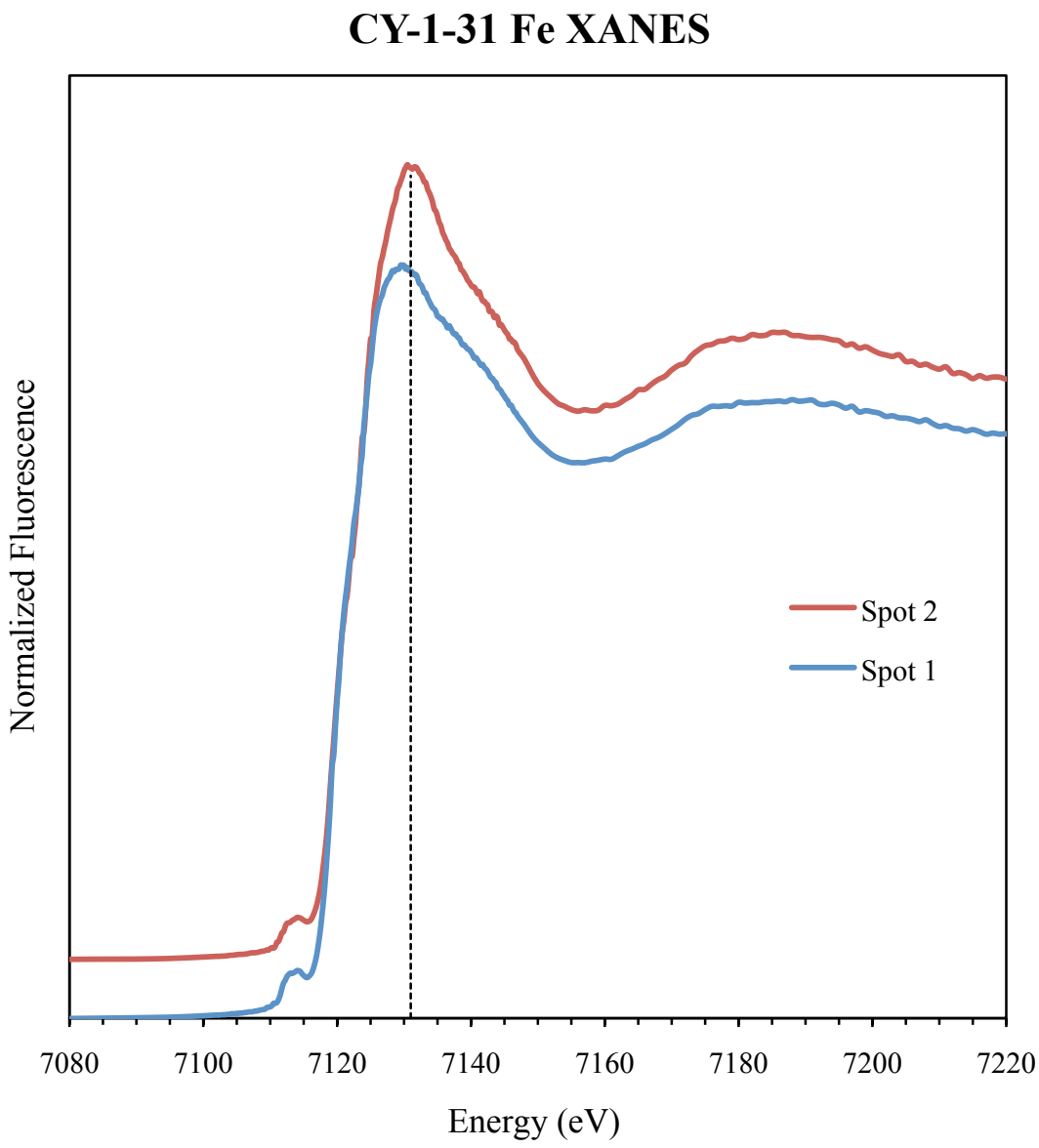

Figure B7. Fe μ-XANES spectra from the spots shown in the reflected light photomicrograph for sample CY-1-31 (Figure B4). Spot 2 (red) was collected from the exposed end of a tubule and is shifted slightly to the right of spot 1 (blue), indicating that the Fe is at least partially oxidized.

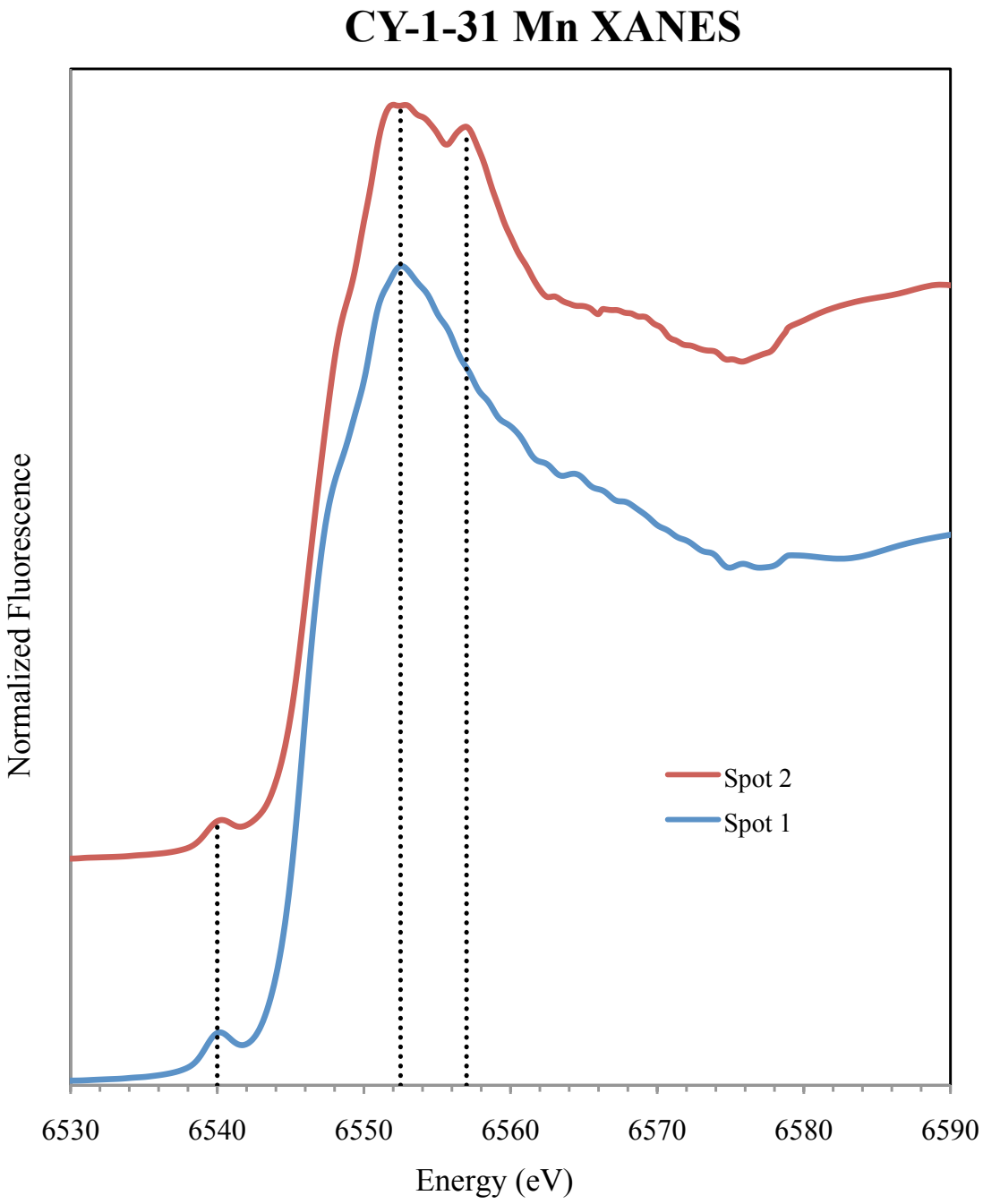

Figure B8. Mn μ-XANES spectra from the spots shown in the reflected light photomicrograph for sample CY-1-31 (Figure 4). Spot 1 (blue) was collected from a region of unaltered glass and shows only the Mn^{2+} peak. Spot 2 (red) was collected from the exposed end of a Mn enriched tubule (see Figure B7), and shows two main peaks, implying a mix of Mn^{2+} and Mn^{3+}.

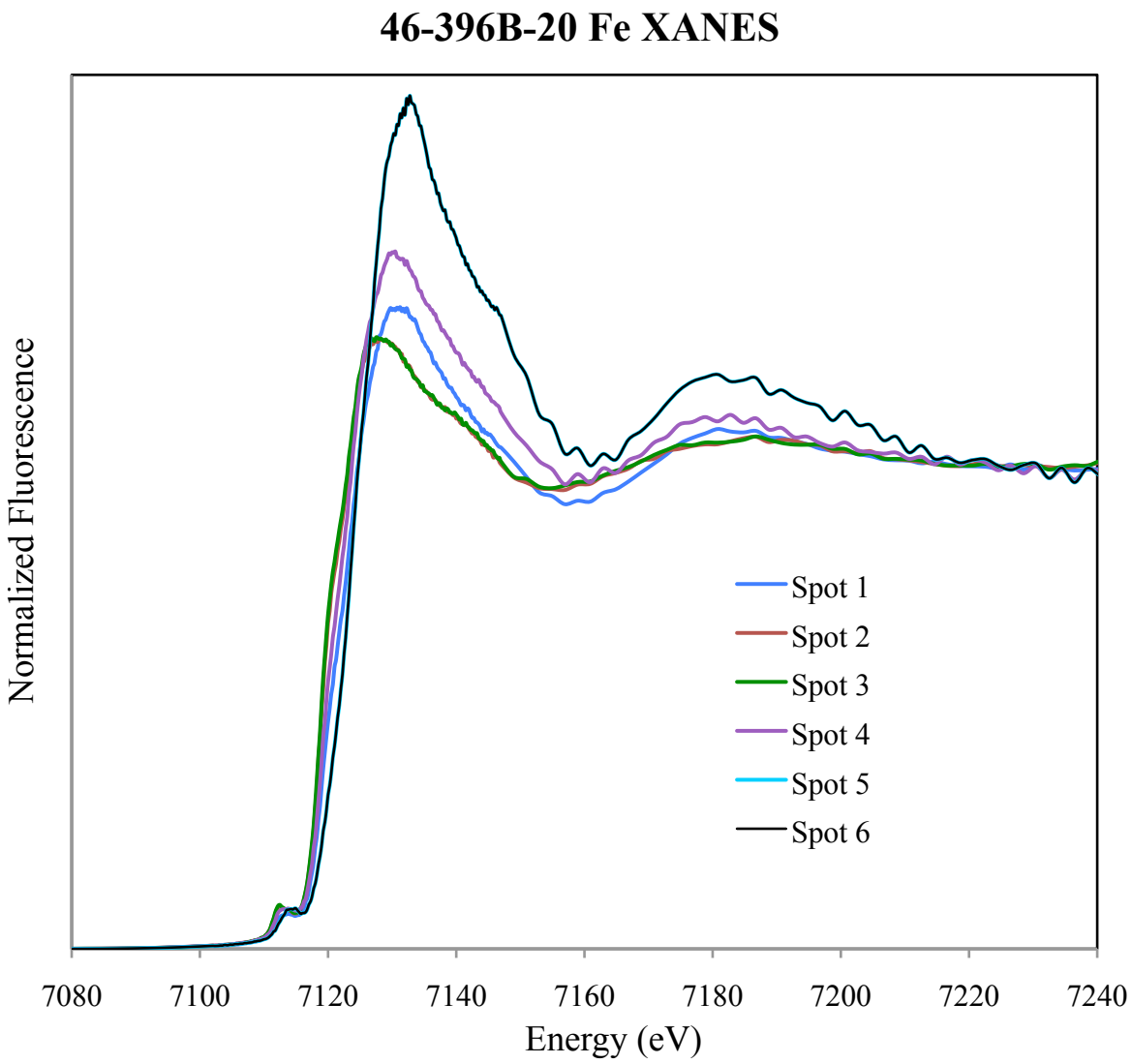

Figure B9. Fe μ-XANES spectra from the spots shown in the reflected light photomicrograph for sample 46-396B-20 (Chapter 3 Figure 3). Spot 2 (red), which is right on the edge of the alteration region, overlaps perfectly with spot 3 (green), which is in the glass. Both show that the Fe is reduced. Spots 1 and 4 show a mix of oxidized and reduced Fe, while spots 5 and 6 (overlapping) show primarily oxidized Fe.

The end.